

# Patterns of groundwater quality

PAGE 2

Nederlands Geographical Studies 335

**Patterns of Groundwater quality**  
in sandy aquifers under environmental pressure  
**Patronen van grondwaterkwaliteit**  
in zandige aquifers onder milieudruk

M.J.M. Vissers

Utrecht 2005

Koninklijk Nederlands Aardrijkskundig Genootschap/  
Faculteit Geowetenschappen, Universiteit Utrecht

Deze publicatie werd verdedigd als academisch proefschrift aan de universiteit Utrecht op 9 januari 2006

Supervisor (promotor): prof. dr. Peter A. Burrough  
Daily supervisor (co-promotor): dr. Paulien F.M. van Gaans  
Daily supervisor (co-promotor): dr. Marcel van der Perk

Assessment Committee (Promotiecommissie)  
Prof. dr. M.F.P. Bierkens (Utrecht University)  
Prof. W.M. Edmunds (University of Oxford)  
Prof. dr. ir. A. Leijnse (Wageningen University)  
Prof. dr. ir. T.N. Olsthoorn (Delft University of Technology)  
Prof. dr. P.J. Stuyfzand (Free University Amsterdam)

ISBN-10: 90-6809-375-4  
ISBN-13: 978-90-6809-375-9

Copyright © M.J.M. Vissers, p/a Faculteit Geowetenschappen  
Universiteit Utrecht 2005

Niets uit deze uitgave mag worden vermenigvuldigd en/of openbaar gemaakt door middel van druk, fotokopie of op welke wijze dan ook zonder voorafgaande schriftelijke toestemming van de uitgevers.

All rights reserved. No part of this publication may be reproduced, by print or photoprint, microfilm or any other means, without the written permission by the publishers.

*“If sustainable development is to mean anything, such development must be based on an appropriate understanding of the environment — an environment where knowledge of water resources is basic to virtually all endeavours.”*

Report on Water Resources Assessment, WMO/UNESCO, 1991



# CONTENTS

1	INTRODUCTION 11
1.1	Context 11
1.1.1	Societal context 11
1.1.2	Scientific context 12
1.2	Theoretical Framework 13
1.2.1	Input 13
1.2.2	Geochemical processes 15
1.2.3	Groundwater flow 17
1.3	So What's The Problem? 19
1.4	Research Questions 20
1.5	Research Areas 21
1.6	Thesis Outline 22
1.7	References 23
2	USING GROUNDWATER MODEL RESULTS FOR MAPPING GROUNDWATER FLOW AND QUALITY 31
2.1	Introduction 31
2.2	Study Area 33
2.3	Groundwater Flow Model 35
2.4	Post-Processing Representation Methods 36
2.4.1	Mapping groundwater flow and groundwater flow systems 36
2.4.2	Relating hydrology to groundwater quality 37
2.4.3	Quantitative vulnerability 37
2.4.4	Transit time distribution 38
2.5	Results And Interpretation 38
2.6	Discussion 42
2.6.1	Use of particle tracking 43
2.6.2	Groundwater flow systems 43
2.6.3	Application of the method presented 44
2.7	Conclusions 44
2.8	References 45
3	THE STABILITY OF GROUNDWATER FLOW SYSTEMS IN UNCONFINED SANDY AQUIFERS IN THE NETHERLANDS 47
3.1	Introduction 47
3.2	Study Area 49
3.3	Methods 51
3.3.1	Groundwater flow model 51
3.3.2	Sensitivity analysis 53
3.3.3	Automatic derivation of groundwater flow systems 54
3.4	Results 55
3.4.1	Model calibration 55
3.4.2	Groundwater flow and flow systems 56
3.4.3	Sensitivity analysis 59
3.5	Discussion 61
3.5.1	Assessment of the model 61
3.5.2	Implications for groundwater flow system theory 62

3.5.3	Groundwater flow patterns	63
3.5.4	Stability of groundwater flow systems	63
3.5.5	Implications for groundwater quality and contaminant transport	64
3.6	Conclusions	65
3.7	References	65
4	A CONCEPTUAL FRAMEWORK FOR PATTERNS AND CHANGES IN THE HYDROCHEMISTRY OF A SANDY AQUIFER	69
4.1	Introduction	69
4.2	Theory	70
4.2.1	Hydrological boundaries	70
4.2.2	Input boundaries: the streamtube concept	71
4.2.3	Geochemical boundaries	72
4.2.4	Changes	72
4.3	Characteristics Of The Study Area	73
4.3.1	Geomorphology	74
4.3.2	Mineralogy	75
4.3.3	Geohydrology	75
4.3.4	Land use history	76
4.4	Methods	76
4.4.1	Field sampling and laboratory analysis	76
4.4.2	Identification of water quality boundaries	77
4.4.3	Identification of water quality changes	77
4.5	Results	78
4.5.1	Hydrological boundaries	78
4.5.2	Geochemical boundaries	78
4.5.3	Streamtube boundaries	79
4.5.4	Changes	81
4.6	Detailed Interpretation Of Patterns And Changes In The Wells	82
4.7	Conclusions	86
4.8	References	86
5	THE CONTROLS AND SOURCES OF MINOR AND TRACE ELEMENTS IN GROUNDWATER IN SANDY AQUIFERS	89
5.1	Introduction	89
5.2	Theory	91
5.2.1	Pure phase thermodynamic equilibrium approach (EQ)	91
5.2.2	Codissolution - coprecipitation approach (CD-CP)	91
5.2.3	Sorption equilibrium through steady state input approach (SEQSSI)	93
5.3	Materials, Field And Laboratory Methods	96
5.3.1	Geography, geology and geohydrology	96
5.3.2	Available geochemical information	97
5.3.3	Groundwater sampling and analysis, quality control	100
5.4	Results And Discussion	102
5.4.1	Pure phase thermodynamic equilibrium approach (EQ)	102
5.4.2	Codissolution - coprecipitation approach (CD-CP)	103
5.4.3	Sorption equilibrium through steady state input approach (SEQSSI)	111
5.5	Conclusions And Summary	116
5.6	References	118



6	SYNTHESIS	123
6.1	Introduction	123
6.2	The Spatial Distribution Of Groundwater Quality	123
6.2.1	Flow	123
6.2.2	Input	124
6.2.3	Geochemical processes	125
6.3	The Temporal Distribution Of Groundwater Quality	126
6.4	Discussion	126
6.4.1	Modelling and verification of groundwater flow patterns	126
6.4.2	Characterization of groundwater quality patterns	127
6.4.3	Groundwater sampling and monitoring	128
6.5	References	129

SUMMARY 131

SAMENVATTING 133

CURICULUM VITAE 137

DANKWOORD 139

## FIGURES

1.1	Conceptual model of phreatic groundwater flow	18
1.2	Different conceptual models explaining a simple water quality pattern	20
1.3	Transmissivity distribution in the Netherlands, and the position of the study areas	23
2.1	Model area, Hengelo area of interest, streams, observation wells, and land use	33
2.2	Cross-section of the model area at y=475300	34
2.3	Schematic diagram of a groundwater flow system	37
2.4	Seepage- infiltration map and isohypse map of the second model layer	39
2.5	Transit distance and -time maps with subdivision in groundwater flow systems	40
2.6	Transit distance map at -10m gl and quantitative vulnerability map with subdivision in groundwater flow systems	41
2.7	Cumulative volumetric and areal transit time distribution	42
3.1	Salland land use, topography of the study area, and observation wells	48
3.2	Geological E-W cross-section trough the study area	50
3.3	Fixed drainage level areas and catchment areas, and streams	50
3.4	Yearly recharge from 1966-2003 in the Netherlands (1 and 2 year averages)	52
3.5	Four generated drainage level profiles in a discharge area	54
3.6	Groundwater flow system boundaries as derived from the Monte Carlo analysis superimposed on transit time and transit distance	57
3.7	Deep infiltration areas derived from the calibrated model	58
3.8	Groundwater age in three cross-sections across some groundwater flow systems	58
3.9	Transit distance for the historic, natural groundwater flow in the Salland area	59
3.10	Groundwater flow system membership map from sensitivity analysis of: (a) anisotropy, (b) drainage resistance, (c) recharge, and (d) drainage level	60
3.11	Identification the groundwater flow systems as the water volume defined by the set of fully adjacent flow lines	62

4.1	Schematical overview of the basic groundwater flow system	71
4.2	Types of changes in groundwater chemistry in the basic groundwater flow system	73
4.3	Land use in the Salland area, location of the borings, with modelled recharge lines towards the miniscreen wells	74
4.4	Schematical view of the geology	75
4.5	Transit time map of the well-section area and groundwater flow system boundaries	78
4.6	E-W cross section of geology, geochemical preconditions, land use, and wells	79
4.7	Histograms of the lognormalized SO <sub>4</sub> , NO <sub>3</sub> , Fe, and HCO <sub>3</sub> concentrations in 1996	80
4.8	SCD, TCD, Cl, SO <sub>4</sub> , HCO <sub>3</sub> , and NO <sub>3</sub> - depth profiles of boring A1	80
4.9	Electrical conductivity - depth profiles in the Salland section	81
4.10	Chloride, SO <sub>4</sub> , HCO <sub>3</sub> , Si, Mn, and Fe - depth profiles of boring A3	83
4.11	Chloride, SO <sub>4</sub> , HCO <sub>3</sub> , Fe, Ca, and Mg - depth profiles of boring A5	84
4.12	Chloride, Fe, and HCO <sub>3</sub> - depth profiles of boring A10	85
5.1	Graphical view of the conceptual model as defined in the SEQSSI approach	91
5.2	Map of the Salland study area, landuse, the borings and their recharge lines	96
5.3	Cross section showing the multilevel well transect with major hydrogeochemical zones, pollution grade, geology, and land use	98
5.4	Pie diagrams of cations in the average water types found in the well section	99
5.5	Scatterplots of (a) Be-Al, (b) La-Al, and (c) Sr-Ca in sediments	99
5.6	Scatterplots of (a) Sr-Ca, (b) Mg-Ca, (c) Ba-Ca, and (d) Mn-Fe	105
5.7	Concentration – Depth profiles of Fe, Mn, As, Mo, U, Co, Ni, Cu, Na, and P for borings A3, A5, A7, and A10	107
5.8	Surplus concentrations of Ca, Sr, Na, Mg, K, Rb, concentrations of Ba, Tl, Li, Si, and pH, and Na and Cl evapotranspiration (E.T.) factors in boring A1	108
5.9	Scatterplots of: (a) Hf-Zr, (b) Ga-Al, (c) Be-Al, and (d) La-Al	110
5.10	Scatterplots of Co, Ni, Cu, V, B, Rb, Cd, Li, and Cs against Na with seawater and rainwater ratio estimates	112
5.11	Scatterplots of Co, Ni, and Cu against Ca with seawater and rainwater ratios	113
5.12	Scatterplots of Al, Ca, and As against Na with seawater and rainwater ratios	114
5.13	Sodium normalized TE-Depth profiles of Rb, Li, Co, Ni, and Cu (weight basis) for all borings	115

## TABLES

1.1	Characteristics of the typical Dutch sandy phreatic aquifer	21
2.1	Summarized characteristics of the groundwater flow model	35
3.1	Parameters and variables varied in the sensitivity analysis	53
3.2	Formations and their calibrated hydraulic conductivities	55
5.1	Summary statistics and analytical precision of the trace elements analysed	101
5.2	Possible and observed saturation phases of TE	103
5.3	Summary of the governing controls of TE concentrations	117

# 1 INTRODUCTION

## 1.1 CONTEXT

This thesis is concerned with mapping, in its broadest sense, of groundwater quality in sandy phreatic aquifers, where water quality is simply defined as its chemical composition. As such, it does not consider suitability of groundwater for a specific purpose such as drinking water, livestock watering, irrigation, or industry. The motivation for this research comes from both the societal demand for environmental protection and regulation as from renewed scientific interest in the relations between processes and activities at the earth' surface and groundwater quality. This renewed scientific interest has been fed by recent advances in hydrological modelling, enabling focus on flow rather than just on groundwater heads, and by recent advances in hydrochemical analysis, enabling a more integrated, multivariate, truly geochemical approach towards groundwater quality mapping.

This introductory chapter starts with a brief sketch of the societal and scientific contexts of groundwater quality mapping, followed by a more elaborate discussion of the theoretical framework portraying the autonomous factors that together define the spatio-temporal distribution of groundwater quality. It then proceeds with the formulation of the research questions, and a characterization of sandy aquifers in general and the specific research areas in particular that were selected for this study. It concludes with marking the contours of how these research questions will be addressed in the following chapters.

### 1.1.1 Societal context

Groundwater quality and its spatio-temporal distribution are important for drinking, irrigation, and industrial water supply, and for sustaining the ecology of streams and wetlands (IAH, 2000). Increase and changes in environmental pressure threaten groundwater quality and complicate the assessment of its present and future spatial distribution. This is especially the case in populated areas with sandy, phreatic aquifers that are intimately linked to these changing conditions. The main stresses with adverse effects on the quality of the groundwater system can be summarized as being related to agricultural practices including groundwater level management, to air pollution and acid rain, and to overabstraction. Recognition by policy makers of the importance of, and the problems related to, protecting and assessing groundwater quality is evidenced by e.g. EU and international directives to protect groundwater from agricultural and other pollutants (EU, 1980; 1991; 1996; UNECE, 1979; 1998), global concern about sustainable water use (UN/WWAP, 2003), and of course the recent European Water Framework Directive (EU, 2000).

From a societal or policy point of view groundwater quality mapping should ideally provide a map displaying the current and future 3D distribution of all constituents considered relevant. Recent developments towards 'system-specific groundwater management' (Stuurman and Griffioen, 2003), indicate that not just a factual map but also, more importantly, a good understanding of groundwater quality appears crucial

from an environmental point of view. Water is the main transport medium for most substances, both from point source and from diffuse-source pollution. Groundwater is an important environmental compartment that plays an active role in the spreading of pollutants. Groundwater quality mapping in this broader sense corresponds to assessing and accounting for this role.

Large parts of the Netherlands consist of sandy phreatic aquifers. Groundwater is the major source of drinking water, and the high population density causes a mixture of land uses exerting considerable environmental pressure. Studying the role of the groundwater compartment in the redistribution of pollutants, and mapping and understanding the resulting patterns is thus especially relevant here. An example of the practical use of groundwater quality mapping in legislation is that more vulnerable areas can be subject to specific environmental legislation (Staatsblad, 1995; 1997).

### 1.1.2 Scientific context

From a geochemical point of view, groundwater is important in the distribution and redistribution of chemical components, as it is a major terrestrial compartment in the water cycle and hence most biogeochemical cycles. Groundwater quality mapping is thus equally important for understanding the distribution and abundance of elements, and the changes in their global or local cycles due to the spreading of contaminants.

Since the earliest assessments of groundwater quality, graphical representations of water compositions, of which piperdiagrams and stiffdiagrams are the most well known (Piper, 1944; Stiff, 1951), were abundantly used. In addition there exist classification schemes to subdivide water types on the basis of e.g. hardness, salinity, redox stages or combinations thereof (e.g. Stuyfzand, 1986; Lyngkilde and Christensen, 1992). The results are then drawn on maps or cross sections, to interpret them in spatial context.

Following developments in computer modeling (e.g. geographical information systems), the field of spatio-temporal mapping of groundwater quality saw its advent. This relatively young field is characterized by its multidisciplinary nature (Falkenmark and Mikulski, 1994). So far, this field has mainly aimed at groundwater protection. Results are usually presented in the form of aquifer vulnerability maps (Aller et al. 1987; Worall and Kolpin, 2003 and references therein). Though there is no consensus on the exact definition of groundwater quality mapping and aquifer vulnerability mapping (Gogu and Dassargues, 2000; Worrall et al. 2002), according to USEPA (1993) both aim at predicting the future distribution of groundwater quality. This essentially means that a proper understanding of all processes leading to the current groundwater quality is needed (as the present is the key to the future).

In aquifer vulnerability mapping, Focazio et al. (2002) distinguished subjective rating methods from objective methods. Subjective rating methods mainly comprise map overlay techniques, while objective methods are more closely tied to scientific questions, and may comprise geostatistical and multivariate methods, as well as process-simulating modelling. Often hybrid methods combine 'soft' information such as land use and population density with process-based methods.

A first example of groundwater quality mapping in the Netherlands is the study by Oude Munnick and Geirnaert (1991), who used overlay techniques to assess the groundwater vulnerability for the Noord Holland province. They distinguished sandy

from clayey areas. At a national scale, Frapporti et al. (1993a, 1993b) used multivariate statistical analysis to map different water types. The basic pattern includes higher salinities near coastal zones (see also Post, 2004; Oude Essink, 1996), river water types near the larger rivers (that are infiltrating rather than draining in large parts of the Netherlands), clean and unbuffered water types in the ice-pushed ridges and coastal dunes (see also Meinardi et al. 1999; Appelo, 1994; Stuyfzand, 1999), polluted water in the sandy agricultural areas (see also Oenema et al. 1998; Broers, 2002), and reduced water types in the peat and clay lowlands in the western part of the Netherlands.

Pebesma and De Kwaadsteniet (1997) used geostatistics to map the Dutch groundwater quality, and showed that incorporating land use and soil types improved interpolation results. Reijnders et al. (1998) directly used land use and soil type to calculate class average concentrations and ranges. Later studies aimed at the explicit use of more factors, such as geology and groundwater age, which were implicitly present in the studies mentioned above. This adding up of variables to better predict groundwater quality is, however, a scientifically risky method, as the factors commonly used are often mutually correlated, as e.g. depth and age, or soil type and geology. This leads to induced and spurious correlations (Brett, 2004; Jackson and Somers, 1991) that may result in a statistically better prediction, but clearly violate the scientific principle of parsimony.

The reason that factors such as land use, population density, or soil type, are so often correlated is that they are not truly single factors. They already represent a complex interaction between geologic, climatic, socio-economic, and historic-cultural circumstances. When used in aquifer vulnerability mapping, sandy phreatic aquifers are then merely identified as specifically vulnerable. A more detailed prediction of groundwater quality, both in spatial detail and in compositional terms, within a typical area such as the sandy phreatic aquifers, requires an understanding of, and knowledge concerning the true underlying factors that define groundwater quality. Essentially, the spatio-temporal distribution of groundwater quality depends on three factors only: input, geochemical processes, and groundwater flow (Engelen, 1981; Vissers et al. 1999). Schot (1990) already attributed changes in groundwater quality to these factors.

## 1.2 THEORETICAL FRAMEWORK

With input, geochemical processes, and groundwater flow being identified as the fundamental factors defining groundwater quality, this section will elaborate upon what is already known about these factors, both within their own merits and with respect to their role in defining groundwater quality. The aim here is not to give an exhaustive overview of the past and present state of the art, but to describe the aspects most relevant for the distribution of groundwater quality and present some historical landmarks that will aid in putting the current research into perspective.

### 1.2.1 Input

The input water quality is generally considered as the most important factor determining groundwater quality, especially from an environmental and risk assessment perspective. The input water quality at the phreatic water level could be defined simply as the sum of

the recharging water (usually rain water), and substances actively added on the land surface (mainly manure or fertilizer) or dissolved in the unsaturated zone. However, the plant-soil system influences the input in various ways. Removal of mineral substances through harvesting, temporary storage of elements in the biotic and organic soil compartments through plant-vascular pumping (Berthelsen et al. 1995), differences in evaporative concentration, and chemical processes such as oxidation of manure and sorption that occur in the unsaturated zone all influence the initial concentrations.

The most thorough approach to quantitatively assess and predict input water quality is by performing full mass-balance studies. Such mass-balance studies, however, are mainly performed in agriculture focussing on nutrients. Because of the high variability in e.g. sewage and manure application and composition as well as in evaporative concentration, that considerably complicate the performance of mass balances, other, minor substances, are usually ignored. These complications are the main reason why the assessment of input water quality mostly proceeds using a backward approach, where observed groundwater quality is used to establish relations with input related factors such as land use as e.g. in the study of Reijnders et al. (1998). In this way, various types of input have been identified in groundwater, e.g. rainwater, ubiquitous atmospheric pollution, or average agricultural pollution.

Rainwater is expected to determine the 'natural' groundwater quality. Its composition is actually highly variable in both time and space. In the Netherlands, for example, rainwater concentrations of sea salt constituents depend on the distance to the coast (Appelo and Postma, 1993). Furthermore, the terrestrial source contribution to both wet and dry deposition for soluble substances varies. Concentrations in groundwater subsequently depend on evapotranspiration, hence vegetation.

Nowadays the quality of rainwater and shallow groundwater in the Netherlands is dominated by pollution for many constituents. Diffuse atmospheric pollution is foremost visible in sulphate and nitrate concentrations (e.g. Stuyfzand, 1999). Non-seasalt sulphate concentrations increased due to the use of sulphur-containing fossil fuels, and reached their peak in 1965. Desulphurization of oil and the use of low-sulphur coal and natural gas led to a decrease (Stoddard et al. 1999). Diffuse atmospheric pollution of nitrogen is, except for the exhaust of nitrogen oxides due to fuel burning, due to indirect effects of manure spreading and can be very high in populated areas (Emmett et al. 1998; Van Breemen and Van Dijk, 1988). Both sulphate and nitrogen cause acidification, whereas nitrogen also results in eutrophication (Houdijk and Roelofs, 1991).

Diffuse agricultural pollution results from the excess application of fertilizer and manure. Apart from enhanced nitrogen concentrations, it also results in elevated concentrations of salt, potassium and phosphorous. Furthermore, magnesium and calcium are often applied to agricultural fields for optimal pH and base cation conditions (Böhlke, 2002). Indirect effects of manure application, resulting from its acid load, are an increase in hardness of groundwater.

Diffuse sources from roads and built-up areas can also be of importance for groundwater quality. Especially from smaller roads without dewatering system, considerable amounts of roadsalts can be expected (Huling and Hollocher, 1973). Urban water is characterized not only by vast amounts of point-source pollution plumes (Lloyd et al. 1991), diffuse pollution from gardening and leaking sewage systems often result in high concentrations of nutrients in groundwater as well (Trauth and Xanthopoulos, 1997).

For trace elements, the same processes play a role. In fact, man is dominating the trace element cycle on earth (Klee and Graedel, 2004; Nriagu, 1989), and atmospheric enrichment factors of many trace elements can be orders of magnitude higher than in the natural situation. However, making predictions for trace element input is even more difficult as it is for major elements and nutrients, as atmospheric input is hardly known and highly variable over short distances. Furthermore, estimations of trace element input are complicated because the form of the input, dissolved or particulate, is unknown. The effects of long-range atmospheric transport (Steinnes, 2001), which are observed even in polar ice caps (Boutron et al. 1984), have not yet been quantified (Rasmussen, 1998).

Agricultural trace element pollution can also be expected (Dach and Starmans, 2005; Senesi et al. 1999). These trace elements originate from constituents of swine and poultry food and food additives (As, Cu, and Zn; Bolan et al. 2004), and of phosphate fertilizers (e.g. Cd, Nicholson and Jones, 1994, and U, Guimond, 1990). The effects of such diffuse pollution of trace elements on the groundwater system are still poorly quantified.

### **1.2.2 Geochemical processes**

Geochemical processes can both be beneficial and harmful for groundwater quality. The high reactivity of the subsurface, both as a substrate for bacteria that may break down pollutants and as an immobilizing agent for pollutants, bacteria, and viruses, is also referred to as the geocleaning capacity or natural attenuation capacity in case of point source pollution. Natural attenuation and its enhancement receive a high amount of scientific interest for its possibilities as a cheap and efficient sanitation strategy. The geocleaning characteristic of aquifers has in fact long been recognized, and when actively put to use for purification of water it is called soil aquifer treatment (Pyne, 1995). The Amsterdam Water Supply has used infiltration of river water in the coastal dunes since 1957. Harmful effects of geochemical processes also happen. The most well known example is the high concentration of arsenic found in groundwater wells in Bangladesh (Nickson et al. 1998), where groundwater wells were installed to decrease the occurrence of waterborne diseases.

Groundwater – sediment interaction along the flow path includes a wide variety of processes, such as buffering, redox processes, sorption, dissolution, precipitation, and degradation. The resulting evolution of groundwater composition along flow paths was first described by Back (1966), who defined the principle of hydrochemical facies to describe the formation of distinct water types. For major element hydrochemistry, buffering and redox processes are considered the most important (Thorenson et al. 1979; Frapporti et al. 1993a; 1995; Vissers et al. 1999, Van Sambeek et al. 2000).

Buffering occurs mainly by calcite, which is common in most aquifers. When present, the carbonate equilibrium determines the near-neutral pH of the groundwater. If no calcite is present, other mineral phases such as clays and feldspars buffer to a pH of 5.5-6.5, which was first shown using a mass balance approach by Garrels and Mackenzie (1967). In a non steady-state situation, buffering also occurs by the exchangeable cations in the sediment (Hansen and Postma, 1995). Natural infiltration water has a pH of approximately 4.5, its acid load depending on evaporative concentration and the CO<sub>2</sub> pressure in the unsaturated zone. Enhanced acidification due to atmospheric and

agricultural pollution leads to increased weathering, and subsequently to enhanced concentrations of major and associated trace elements. The aquifer sediment buffering capacity both in terms of availability as in terms of reaction kinetics then determines how fast the acidification front progresses. Few studies are known that identify the main buffering minerals in Dutch groundwater (Mol et al. 2003).

Natural redox conditions include the range of oxic to methanogenic water (Champ et al. 1979). Redox processes were linked to the presence of microorganisms in aquifer sediments only recently (Wilson et al. 1983), which led to a large shift in paradigm until then determined by the inorganic equilibrium concept (Lindberg and Runnels, 1984; Barcelona et al. 1989). Pedersen et al. (1991) and Barcelona and Holm (1991) linked observed redox conditions to sediment characteristics, and defined the Total Reduction Capacity of sediment, which is the capacity of the sediment to reduce oxygen, nitrate, and sulphate. Major reducing components of aquifer sediments are organic matter, pyrite, siderite, and reduced metals in the primary mineral fraction. Later the Oxidation Capacity of sediments, primarily provided by iron and manganese oxyhydroxides, was defined (Heron et al. 1994). Both determine the ability of the aquifer to naturally attenuate oxidizing or reducing pollution compounds (Christensen et al. 2000). Similar parameters can be defined for groundwater; quantifying its oxidation and reduction capacity facilitates mass-balance modelling of redox processes (Tesoriero et al. 2000; Engesgaard and Kipp, 1992).

Further progress in the past decades was made by multicomponent kinetic approaches used in reactive transport modelling (Furrer et al. 1996; Parkhurst and Appelo, 1999). More and more is known about the reactivity of important aquifer constituents such as organic matter and iron oxyhydroxides, and their dependence on depositional environment and diagenesis (Hartog et al. 2004; Postma, 1993; Van Helvoort, 2003). Reactive transport modelling in more dimensions emerged soon after groundwater flow modelling became common use (Frind et al. 1989). At present a large amount of 3D multicomponent reactive transport models are available (Van der Lee and De Windt, 2001).

Somewhat similar to the change in thinking about redox and kinetic processes, organic hydrogeochemistry became recognized as being important in contaminant transport in general. The inorganic thermodynamical equilibrium assumption made in speciation modelling (Parkhurst et al. 1980; Reed, 1982; Turner et al. 1981; Van Gaans, 1989), has proven very valuable, but in many cases explains the observations in the natural environment insufficiently well. The realization that organic matter and colloids may increase metal solubility has long been known (Bloom, 1981). Binding of metals to organic matter generally follows the Irving-Williams order; Hg (II), Cu, Pb, and Sn (II) are very tightly bound by organic matter as compared to other trace elements. Organic complexation also is of major importance for otherwise insoluble elements such as aluminium (Mulder and Stein, 1994). Many models have subsequently been developed to describe organic complexation (Christensen et al. 1999; Benedetti et al. 1996).

Particulate matter as an important contributor to groundwater hydrogeochemistry was also early recognized (Stumm and Bilinski, 1972). Attention to suspended particulates and colloids has risen in recent decades with the developments in ultrafiltration (Dupré et al. 1999; Nelson et al. 2003), in situ techniques (Lead et al. 1997), and trace element analytical techniques (Ivahnenco et al. 2001).



In recent decades, a better understanding of the processes as well as of their interactions has been achieved. Interactions are for example changes in the sorption capacity due to redox alteration of mineral surfaces (Knapp et al. 2002) or to specific mobilization of cations by DOC or colloids (Buerge-Weirich et al. 2002). In addition, mineralogy receives increasing attention; both composition and reactivity of clay and hydroxide minerals are very important to model groundwater quality (Wood, 2000, Zhu and Burden, 2001). Their role especially becomes visible where the aquifer system is perturbed due to enhanced input of acid, oxidant, or reductant (Edmunds et al. 1992; Larsen and Postma, 1997; Bennett et al. 1993; Van Breukelen et al. 2003). Because of the complex interactions between aquifer materials and groundwater, chemical heterogeneity of aquifers is expected to be even larger than hydrological heterogeneity, and thus may be at least as important for the spreading of contaminants.

### **1.2.3 Groundwater flow**

Falkenmark and Allard (1991) defined a framework for relating groundwater flow to groundwater quality, for which two complementary perspectives exist. The first perspective is where at one moment in time the observed water quality in streams, discharge areas, and wells is related to recharge areas in terms of past land-use history. The second perspective is where the future and past pathways of point-source pollution are delineated, indicating where and when pollution problems can be expected. These two perspectives are more or less exemplified respectively by capture zone modelling and point source pollution / reactive transport modelling.

The understanding of groundwater flow commenced with the recognition of its relation with topography (Hubbert, 1940). Analytical solutions leading to the definition of hydrological systems and their hierarchical configuration (Tóth, 1963), as well as the observation that discharge is not limited to valley bottoms in a relatively flat topography led to further understanding of the chorological relations of groundwater in the landscape. These findings were later followed by numerical solutions of more complicated situations (Freeze and Witherspoon, 1966; 1967; 1968). Later progress includes the interactions with surface water and lakes (Winter, 1978; De Vries, 1977).

With the introduction of MODFLOW (McDonald and Harbaugh, 1988), three-dimensional groundwater flow modelling became common (Karssenberg et al. 2005). Since then groundwater flow in sedimentary aquifers could adequately be modelled for most purposes, barring restrictions with respect to computer power. Scientific focus shifted towards capture zone modelling and uncertainty assessment of modelled capture zones (Gomez-Hernandez and Gorelick, 1989; Varljen and Shafer, 1991; Bair et al. 1991; Bhatt, 1993), towards modelling multiphase transport and density and temperature driven groundwater flow (Abriola, 1989; Simmons et al. 2001), and towards characterizing flow in heterogeneous and fractured rock aquifers (Bierkens, 1996; Scheibe and Yabusaki, 1998; Berkowitz, 2002). These aspects are particularly relevant for wellhead protection and sanitation.

Groundwater flow systems analysis as defined by Tóth (1963) facilitates the establishment of the relation between the observed water quality in streams, discharge areas, and wells and the past land-use history in their respective recharge areas (Falkenmark and Allard, 1991). Engelen et al. (1986) and Engelen and Kloosterman

(1996) recognized this, and used 3D systems analysis and the new possibilities of groundwater flow modelling in an ecohydrological analysis to explain the decline in phreatophytic vegetation in the Netherlands. However, the subjectivity of the methods developed by Engelen et al. (1986), as well as the problems associated with their interpretation and extension of Tóths' definitions (Van Buuren, 1991), may have impeded widespread use of their methods.

Yet, the possibilities of regional groundwater flow systems analysis for nature planning, well protection, or simply the understanding of groundwater quality patterns, are sweeping. The recent developments in surface water quality modelling illustrate the need for this type of information from the groundwater system both from a quantitative and qualitative point of view. Information on the transit time distribution (or 'apparent age') of groundwater and water of gaining streams in relation to eutrophication and spreading of contaminants in the environment are crucial from both a legislative and preventive viewpoint. Such information can also be used for nature planning for restoration of fens and phreatophytic vegetation (Batelaan et al 2002). This is recognized in detailed studies performed in riparian zones in similar environments as in the Netherlands (Böhlke and Denver, 1995; Lowrance et al. 1997; Puckett and Cowdery, 2002), but in the Netherlands studies have regrettably only addressed the horizontal and temporal dimension (Pedroli, 1990; Hefting and De Klein, 1998; Hefting et al. 2003). In the above-described fields, hydrogeochemical information often is the only means to verify model calculations of ground- and surface water interaction.

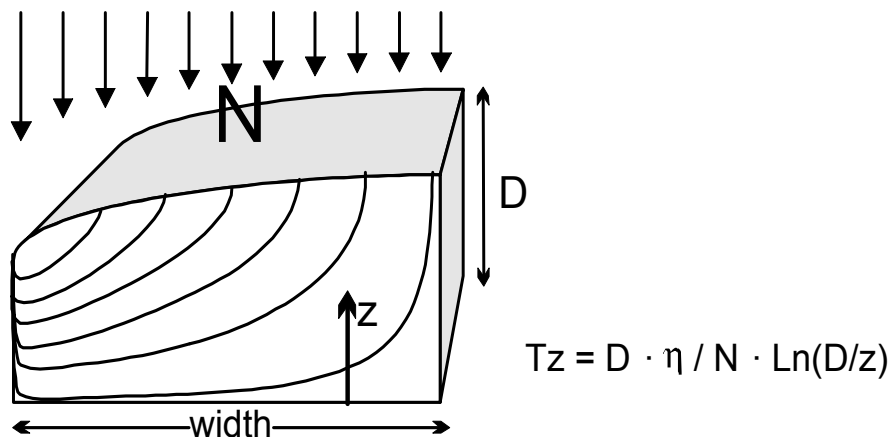


Figure 1.1 Conceptual model of phreatic groundwater flow, where  $T_z$  is the age at distance  $z$  from the base of the aquifer,  $D$  is the aquifer thickness, and  $N$  is the net recharge rate, and  $\eta$  the porosity (Vogel, 1967; Eldor and Dagan 1972; Appelo and Postma, 1993)

For the spatio-temporal distribution of groundwater quality, one of the main insights that regional groundwater flow systems analysis can give is insight in the position within such a system. In the vertical direction, age increases approximately linearly with depth depending on the recharge rate, or approximately logarithmically if the hydrological base is shallow (Vogel, 1967; Eldor and Dagan 1972; Appelo and Postma, 1993). This is visualized in Figure 1.1. This conceptual model that consists of a phreatic aquifer with a partially or fully penetrating discharge area is often used to describe groundwater quality patterns (Philips, 2003; Böhlke, 2002; Broers, 2002). This age-depth relation has been

confirmed in many studies using environmental isotopes and tracers such as tritium and CFC's (Eriksson, 1958; Allison and Huges, 1978; Robertson and Cherry, 1989; Meinardi, 1994; Böhlke and Denver, 1995). However, the use of this conceptual model has implications for the horizontal dimension as well. Vertical compression of flow lines towards the discharge area occurs (Frapporti et al. 1995); meaning near a discharging stream the full recharge area is reflected in a depth profile. With an aquifer thickness of 50-100 m and a 5 km long recharge area (as in Frapporti et al. 1995; Broers, 2002), parcels with a length of 200 m would be transformed into 2-4 m thick streamtubes. At the divide of the groundwater flow system (right side of Figure 1.1), vertical flow causes the complete history of one parcel to be reflected in the depth profile. As opposed to the many possibilities for verifying the vertical flow component through dating, verification of the horizontal groundwater flow and of the precise location of the recharge area is difficult. Tracer experiments may provide one means, but a clever use of multivariate hydrochemistry also offers great opportunities to identify flow in the horizontal direction.

### 1.3 SO WHAT'S THE PROBLEM?

While it is easy to see that the manifestations and interactions of the three factors elaborated above (input, geochemical processes, flow) result in the observed groundwater quality distribution, it is much more difficult to decide on which process actually causes an observed groundwater quality pattern. Consider for example the situations shown in Figure 1.2, where in each case the upper well screen displays a high nitrate concentration, and a deeper screen shows a near-zero nitrate concentration. Such a decrease is actually ubiquitously observed, as it follows the natural evolution in redox conditions (section 1.2.2; Back, 1966).

The observed pattern could simply be explained by kinetic reduction of the nitrate, with the removal rate proportional to the nitrate concentration (Uffink, 2003). This would result in an exponential decrease of nitrate with age, hence depth (Figure 1.2a). An apparent kinetic reduction may also be induced by the heterogeneous presence of reducing sediment pockets (Pedersen et al. 1991), as shown in Figure 1.2b. The observed pattern could also be due to the groundwater flow pattern; in Figure 1.2c the deeper screen is situated in an old, regional groundwater flow system, explaining low concentrations. The presence and absence of nitrate might also be linked to input water (Andersen and Kristiansen, 1984; Ronen et al. 1987; Figure 1.2d) or to sediment characteristics (Heron and Christensen, 1995; Böhlke et al. 2002; Figure 1.2e).

Any of the above explanations in any combination could thus describe the nitrate concentration pattern construed from the limited amount of actual observations. In addition, if the true process would be known, an accurate and complete description of the present state of a groundwater system is hampered by the fact that it would require the collection of an impractically large amount of data. Moreover, information, such as historical rainwater quality, historic input quantities and composition, and original sediment composition, cannot be determined anymore. This problem, common in geosciences, is that of underdetermination. In such cases, the true causes can only be inferred to the best explanation (Kleinhans and Buskes, 2002). Yet, in groundwater

quality issues, knowing the true cause is mandatory for taking the right legislative and preventive actions.

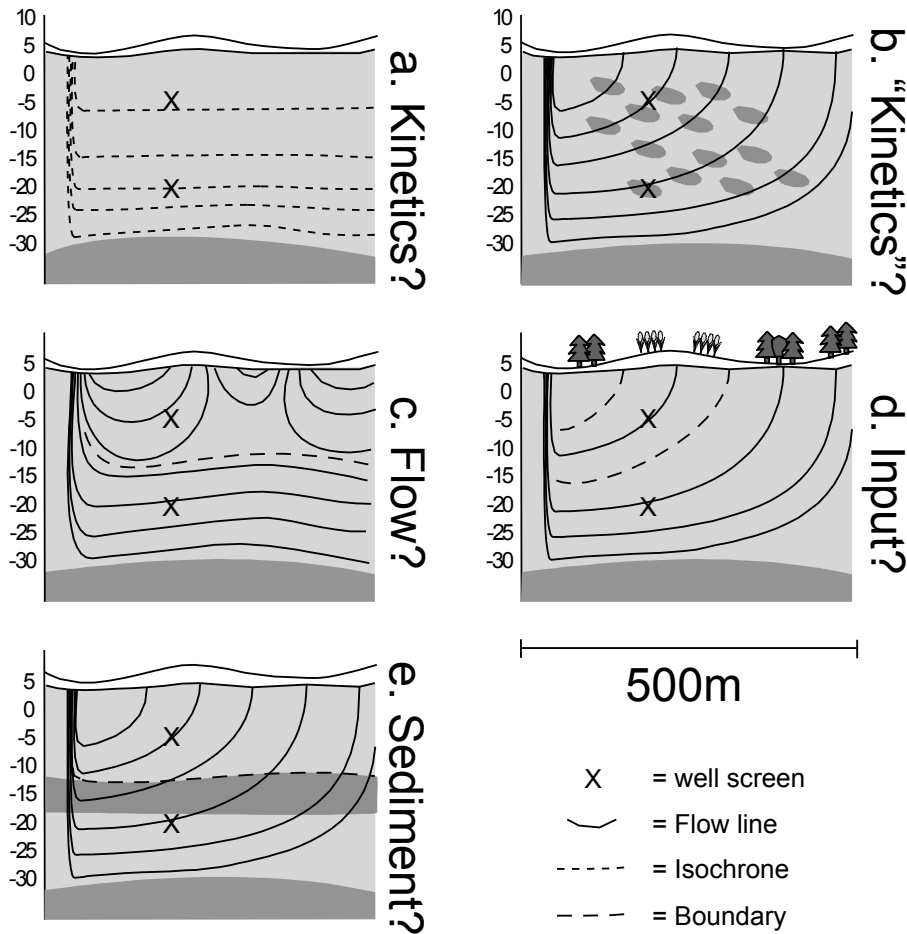


Figure 1.2 Different conceptual models explaining a simple water quality pattern of high concentrations in an upper sample, and near-zero concentrations in a lower sample in a phreatic aquifer

## 1.4 RESEARCH QUESTIONS

This thesis addresses the problem identified by developing smart strategies for optimal use of obtainable information on groundwater hydrology and geochemistry. In line with the societal and scientific context and theoretical framework as outlined above, this thesis aims at the following questions:

1. What is the spatio-temporal distribution of groundwater quality in phreatic aquifers and how can it best be characterized in terms of groundwater flow, input, geochemical processes, and their interaction?
2. What is the influence and impact of the recent environmental changes in these three factors?
3. What are the opportunities for using this information to better predict the future distribution of groundwater quality in phreatic aquifers?

*Table 1.1* Characteristics of the typical Dutch sandy phreatic aquifer

Aquifer thickness	The thickness of the phreatic aquifer averages 50 m, and varies from very shallow (<10 m) to more than 100 m (Figure 1.3).
Aquifer hydraulic conductivity	A layer of fine eolian sand of up to 10 m thick with lower conductivity (~5 m/d) is present in most of the Netherlands. The sandy deposits below are usually river sands with higher conductivities (10-20 m/d).
Precipitation and evapotranspiration	During the summer half-year the precipitation and evaporation more or less counterbalance; the precipitation surplus of about 275 mm prevails during the winter period (Ernst, 1962; Van der Sluijs and De Gruijter, 1985)
Gradients	The topographical slopes perpendicular to the stream channels (transversal slopes) are remarkably uniform and close to 1:500 for the smaller as well as for the larger streams. The same applies to the stream gradients (longitudinal slopes), which vary from 1:1500 for the steepest areas to 1:2500 for the most level areas (De Vries, 1994; Ernst, 1978)
Drainage density and network	In most areas the natural drainage pattern is intensified both by increasing capacities by channel enlargement (Ernst, 1978), as well as by creating artificial drainage networks. The first order drainage network consists of streams and ditches only active in high groundwater level conditions, while the second order network (stream spacing 1350 – 4000 m, De Vries, 1977) is more deeply incised and drains groundwater more permanently (De Vries, 1995)
Topography	Undulating topography with height differences up to 3 m
Land use	70% agriculture, 15% forest/nature, and 15% built-up/roads (CBS, 2000)
Geochemistry/mineralogy	Sandy, often calcareous, with alkali-feldspars, clay, and ironhydroxides as major phases besides quartz, often with trace amounts of organic carbon, pyrite, glauconite, and heavy minerals

## 1.5 RESEARCH AREAS

As mentioned before, sandy phreatic aquifers make up a large part of the Netherlands, and the population density and land use intensity are such that the Dutch sandy aquifers are ideally suited to study the groundwater quality in response to increased environmental pressure. The characteristics of the ‘typical Dutch phreatic aquifer’ are summarized in Table 1. Of course these characteristics apply equally well to many other parts of the world.

Two study areas in particular were selected to explore the research questions (see Figure 1.3). The first study area is situated in the Twente region, and focuses on the area around the city of Hengelo. Societal aspects of this study were part of a project ‘Groundwater quality maps of the city of Hengelo’ (Schipper and Vissers, 2003; Vissers et al. 2004). In this urbanized area, characterized by large differences in topographic gradient, abundant clay layers, the presence of drinking, industrial, and water-level management abstractions, a canal, and many changes with respect to the natural drainage system, the effects of these features can be assessed and described, as well as their influence on the expected and observed groundwater quality.

The second study area situated in Salland was chosen because of the presence of a section of multilevel wells, that offers a unique opportunity for detailed observation of the spatio-temporal distribution of groundwater quality. The area has been under study since 1989 (Hoogendoorn, 1990; Frapporti et al. 1995; Van Uden and Vissers, 1998; Vissers et al. 1999). In this area especially the large regional differences in aquifer

thickness, gradients, sediment reactivity, and land use allow for a direct assessment of the impact of the factors identified.

## 1.6 THESIS OUTLINE

Groundwater flow provides the spatial connection between input water quality and observed groundwater quality patterns, and without flow there would be no continued aquifer buffering. In *chapters 2 and 3* of this thesis specific attention is therefore given to flow as the primary groundwater quality-distributing factor. Using hydrological modelling, insight in groundwater quality patterns is expected to improve. For the urbanized Hengelo study area I studied how groundwater flow modelling helps to answer the two complementary perspectives of water-quality related questions (paragraph 1.2.2). The resulting flow patterns are considered in terms of the spreading of diffuse and point source pollution, and in terms of the local groundwater management and use.

In *chapter 3* a similar approach was applied for the Salland research area, where effort was put in assessing the uncertainty in flow patterns, important when interpreting observations at the point scale and for the potential spreading of pollutants. Where most research focuses on uncertainties in aquifer parametrization and heterogeneity, in this chapter variables that actually display a high degree of temporal variability and spatial uncertainty: precipitation and water level management are specifically considered.

In *chapter 4* the hydrogeochemistry of the Salland aquifer is investigated in terms of the three factors determining the spatial distribution of groundwater quality: hydrology, input, and geochemical processes. Using the geohydrological and hydrochemical information from the multilevel well section, a hydrochemical streamtube general framework is developed, to describe the spatial patterns and changes observed.

*Chapter 5* discusses the controls and sources of trace elements. A process-based, sequential approach was used to test both the sources and controls. Firstly, equilibrium modelling was used to test for pure phase solid saturation and dissolution. Secondly, a codissolution - coprecipitation approach was used to test for sedimentary sources and controls resulting from mixed phase solid saturation and dissolution. Thirdly, a new approach, the sorption equilibrium through steady-state input approach (SEQSSI), was developed to test groundwater trace element concentrations for surficial input and cation exchange as controlling factors.

As each of the chapters two to five was written as a separate paper, there is some inevitable overlap in the introductions and area descriptions.

The synthesis in *chapter 6* summarizes and integrates the main results of this thesis. The implications for the proper perception of the spatial distribution of groundwater quality, for predicting the future groundwater quality, and for monitoring are discussed.

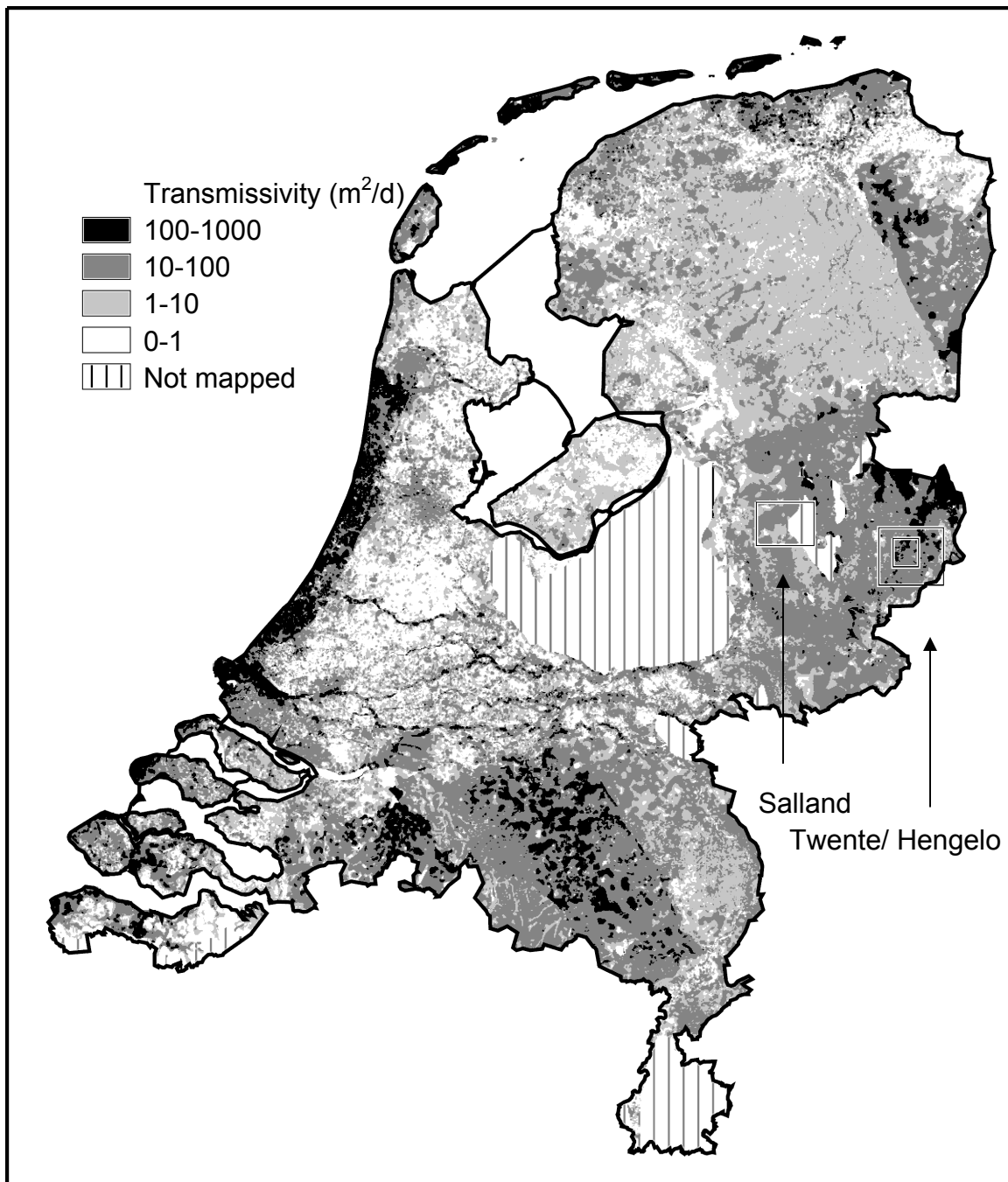


Figure 1.3 Transmissivity distribution in the Netherlands (after Van der Linden et al. 2002), and the position of the study areas

## 1.7 REFERENCES

Abriola, L.M. (1989), Modeling multiphase migration of organic-chemicals in groundwater systems - a review and assessment. *Environmental Health Perspectives* 83, pp 117-143

- Aller, L., Bennett, T., Lehr, J.H., Petty, R.J. (1987), DRASTIC: A standardized system for evaluating ground water pollution potential using hydrogeologic settings. U.S. EPA/600/2-87/035, 455p
- Allison, G.B., Hughes, M.W. (1978), The use of environmental chloride and tritium to estimate total recharge to an unconfined aquifer. *Australian Journal of Soil Research* 16, pp 181-195
- Andersen, L.J., Kristiansen, H. (1984), Nitrate in groundwater and surface water related to land use in the Karup basin, Denmark. *Environmental geology* 5, pp 207-212
- Appelo, C.A.J., Postma, D. (1993), *Geochemistry, Groundwater, and Pollution*. Balkema, Rotterdam
- Appelo, C.A.J. (1994), Cation and proton exchange, pH variations, and carbonate reactions in a freshening aquifer. *Water Resources Research* 30, pp 2793-2805
- Back, W. (1966), Hydrochemical facies and groundwater flow patterns in northern part of Atlantic Coastal Plain. US Geological Survey Professional Paper 498-A, 42p
- Bair, S.E., Safreed, C.M., Stasny, E.A. (1991), A Monte Carlo approach for determining traveltime-related capture zones of wells using convex hulls a confidence regions. *Ground water* 29, pp 849-855
- Barcelona, M.J., Holm, T.R., Schock, M.R., George, G.K. (1989), Spatial and temporal gradients in aquifer oxidation-reduction conditions. *Water Resources Research* 25, pp 991-1003
- Barcelona, M.J., Holm, T.R. (1991), Oxidation-reduction capacities of aquifer solids. *Environmental Science and Technology* 25, pp 1565-1572
- Batelaan, O., De Smedt, F., Triest, L. (2003), Regional groundwater discharge: phreatophyte mapping, groundwater modelling and impact analysis of land-use change. *Journal of Hydrology* 275, pp 86-108
- Benedetti, M.F., van Riemsdijk, W.H., Koopal, L.K., Kinniburgh, D.G., Gooddy, D.C., Milne, C.J. (1996), Metal ion binding by natural organic matter: From the model to the field. *Geochimica et Cosmochimica Acta* 60, pp 2503-2513
- Bennett, P.C., Siegel, D.E., Baedecker, M.J., Hult, M.F. (1993), Crude oil in a shallow sand and gravel aquifer - I. Hydrogeology and inorganic geochemistry. *Applied Geochemistry* 8, pp 529-549
- Berkowitz, B. (2002), Characterizing flow and transport in geological media: A review. *Advances in Water Resources* 25, pp 861-884
- Berthelsen, B.O., Steinnes, E., Solbert, W., Jingsen, L. (1995), Heavy metal concentrations in plants in relation to atmospheric heavy metal deposition. *Journal of Environmental Quality* 24, pp 1018-1026
- Bhatt, K (1993), Uncertainty in wellhead protection area delineation due to uncertainty in aquifer parameter values. *Journal of Hydrology* 149, pp 1-8
- Bierkens, M.F.P. (1996), Modeling hydraulic conductivity of a complex confining layer at various spatial scales. *Water Resources Research* 32, pp 2369-2382
- Bloom, P.R. (1981), Phosphorus adsorption by an Aluminium-peat complex. *Soil Science Society of America Journal* 45, pp 267-72
- Bolan, N.S., Adriano, D.C., Mahimairaja, S. (2004), Distribution and bioavailability of trace elements in livestock and poultry manure by-products. *Critical Reviews in Environmental Science and Technology* 34, pp 291-338
- Boutron, C. Leclerc, M., Lorius, C. (1984), Atmospheric trace elements in Antarctic prehistoric ice collected at a coastal ablation area. *Atmospheric Environment* 18, pp 1947-1953
- Böhlke, J.K., Denver, J.M. (1995), Combined use of groundwater dating, chemical and isotopic analyses to resolve the history and fate of nitrate contamination in two agricultural watersheds, Atlantic coastal plain, Maryland. *Water Resources Research* 31, pp 2319-2339
- Böhlke, J.K. (2002), Groundwater recharge and agricultural contamination. *Hydrogeology Journal* 10, pp 153-179
- Böhlke, J.K., Wanty, R., Tuttle, M., Delin, G., Landon, M. (2002), Denitrification in the recharge area and discharge area of a transient agricultural nitrate plume in a glacial outwash sand aquifer, Minnesota. *Water Resources Research* 38, 1105
- Broers, H.P. (2002), Strategies for regional groundwater quality monitoring. *Netherlands Geographical Studies NGS 306*, Utrecht University
- Brett, M.T. (2004), When is a correlation between non-independent variables 'spurious'? *OIKOS* 105, pp 647-656
- Buerge-Weirich, D., Hari, B., Xue, H., Behra, P., Sigg, L. (2002), Adsorption of Cu, Cd, and Ni on goethite in the presence of natural groundwater ligands. *Environmental Science and Technology* 36, pp 328-336
- CBS (2000), Land use in the Netherlands, CBS



- Champ, D.R., Gulens, J., Jackson, R.E. (1979), Oxidation-reduction sequences in ground water flow systems. *Canadian Journal of earth sciences* 16, pp 12-23
- Christensen, J.B., Botma, J.J., Christensen, T.H. (1999), Complexation of Cu and Pb by DOC in polluted groundwater: a comparison of experimental data and predictions by computer speciation models (WHAM and MINTEQA2). *Water Research* 33, pp 3231-3238
- Christensen, T.H., Bjerg, P.L., Banwart, S.A., Jakobsen, R., Heron, G., Albrechtsen, H-H. (2000), Characterization of redox conditions in groundwater contaminant plumes. *Journal of Contaminant Hydrology* 45, pp 165-241
- Dach, J., Starmans, D. (2005), Heavy metal balance in Polish and Dutch agronomy: actual state and provisions for the future. *Agriculture, Ecosystems & Environment* 107, pp 309-316
- De Vries, J.J. (1977), The stream network in the Netherlands as a groundwater discharge phenomenon. *Netherlands Journal of geosciences* 56, pp 103-122
- De Vries, J.J. (1994), Dynamics of the interface between streams and groundwater systems in lowland areas, with reference to stream net evolution. *Journal of Hydrology* 155, pp 39-56
- De Vries, J.J. (1995), Seasonal expansion and contraction of stream networks in shallow groundwater systems. *Journal of Hydrology* 170, pp 15-26
- Dupré, B., Viers, J., Dandurand, J-L., Polve, M., Benézéth, P., Vervier, P., Braun, J-J. (1999), Major and trace elements associated with colloids in organic-rich river waters: ultrafiltration of natural and spiked solutions. *Chemical Geology* 160, pp 63-80
- Edmunds, W.M., Kinniburgh, D.G., Moss, P.D. (1992), Trace metals in interstitial waters from sandstones: Acidic inputs to shallow groundwaters. *Environmental Pollution* 77, pp 129-141
- Eldor, M., Dagan, G. (1972), Solutions of hydrodynamic dispersion in porous media. *Water Resources Research* 8, pp 1316-1331
- Emmett, B.A., Boxman, D., Bredemeier, M., Gundersen, P., Kjønaas, O.J., et al. (1998), Predicting the Effects of Atmospheric Nitrogen Deposition in Conifer Stands: Evidence from the NITREX Ecosystem-Scale Experiments. *Ecosystems* 1, pp 352-360
- Engelen, G.B. (1981), A systems approach to groundwater quality – Methodological aspects. *The Science of the Total Environment* 21, pp 1-15
- Engelen, G.B., de Ruiter-Peltzer, J.C., Oude-Munnink, J.E. (1986), Water systems in the Netherlands. In: Engelen, G.B., Jones, G.P. (eds), *Developments in the analysis of groundwater flow systems*, IAHS Publication no. 163
- Engelen, G.B., Kloosterman, F.H. (1996), *Hydrological systems analysis, methods and applications*. Water Science and Technology Library, 20, Kluwer academic publishers
- Engesgaard, P., Kipp, K.L. (1992), A geochemical transport model for redox-controlled movement of mineral fronts in groundwater flow systems: A case of nitrate removal by oxidation of pyrite. *Water resources research* 28, pp 2829-2843
- Eriksson, E. (1958), The possible use of tritium for estimating groundwater storage. *Tellus* 10, pp 472-478
- Ernst, L.F. (1962), Grondwaterstromingen in de verzadigde zone en hun berekeningen bij aanwezigheid van horizontale evenwijdige open leidingen. PhD. thesis, Universiteit Utrecht
- Ernst, L.F. (1978), Drainage of undulating sandy soils with high groundwater tables 1: A drainage formula based on a constant hydraulic head ratio. *Journal of Hydrology* 39, pp 1-30
- EU (1980), Council Directive 80/68/EEC of 17 December 1979 on the protection of groundwater against pollution caused by certain dangerous substances
- EU (1991), Council Directive 91/676/EEC of 12 December 1991 concerning the protection of waters against pollution caused by nitrates from agricultural sources. L 375, 31.12.1991
- EU (1996), Council Directive 96/62/EC of 27 September 1996 on ambient air quality assessment and management. L 296, 21/11/1996
- EU (2000), Water Framework Directive. L 327, 22.12.2001
- Falkenmark, M., Allard, B. (1991), Water quality genesis and disturbances of natural freshwaters. In: Hutzinger, O. (ed), *The handbook of environmental chemistry, Volume 5 Part A: Water Pollution*, Springer-Verlag, Heidelberg-Berlin
- Falkenmark, M., Mikulski, Z. (1994), The key role of water in the landscape system. *Geochemical Journal* 33, pp 355-363

- Focazio, M.J., Reilly, T.E., Rupert, M.G., Helsel, D.R. (2002), Assessing ground water vulnerability to contamination: providing scientifically defensible information for decision makers. USGS Circular 1224
- Frapporti, G., Vriend, S.P., van Duijvenbooden, W. (1993a), Hydrogeochemistry of Dutch groundwater: classification into natural homogeneous groupings with fuzzy c-means clustering. *Applied Geochemistry* 8, pp 273-276
- Frapporti, G., Vriend, S.P., Van Gaans, P.F.M. (1993b), Hydrogeochemistry of the shallow Dutch groundwater: interpretation of the national Groundwater Quality Monitoring Network. *Water Resources Research* 29, pp 2993-3004
- Frapporti, G., Hoogendoorn, J.H., Vriend, S.P. (1995), Detailed hydrochemical studies as a useful extension of national ground-water monitoring networks. *Ground water* 33, pp 817-828
- Freeze, R.A., Witherspoon, P.A. (1966), Theoretical analyses of regional groundwater flow 1. Analytical and numerical solutions to the mathematical model. *Water Resources Research* 2, pp 641-656.
- Freeze, R.A., Witherspoon, P.A. (1967), Theoretical analysis of regional groundwater flow 2. Effect of water-table configuration and subsurface permeability variation. *Water Resources Research* 3, pp 623-634
- Freeze, R.A., Witherspoon, P.A. (1968), Theoretical analysis of regional groundwater flow 3. Quantitative interpretation. *Water Resources Research* 4, pp 581-590
- Frind, E.O., Duynisveld, W.H.M., Strebel, O., Boettcher, J. (1989), Simulation of nitrate and sulphate transport and transformation in the Fuhrberger aquifer, Hannover, Germany. In: Kobus H.E., Kinzelbach, W. (eds), *Contaminant transport in groundwater*, Balkema, Rotterdam, pp 97-104
- Furrer, G., von Gunten, U., Zobrist, J. (1996), Steady-state modelling of biogeochemical processes in columns with aquifer material 1: speciation and mass balances. *Chemical Geology* 133, pp 15-28
- Garrels, R.M., Mackenzie, F.T. (1967), Origin of the chemical composition of some springs and lakes, In: *Equilibrium concepts in natural water systems: Advances in Chemistry Series. no. 67*, American Chemical Society, Washington, D.C., p 222-242
- Gogu, R.C., Dassargues, A. (2000), Current trends and future challenges in groundwater vulnerability assessment using overlay and index methods. *Environmental geology* 39, pp 549-559
- Gomez-Hernandez, J.J., Gorelick, S.M. (1989), Effective groundwater model parameter values: Inference of spatial variability of hydraulic conductivity, leakance, and recharge. *Water Resources Research* 25, pp 405-419.
- Guimond, R.J. (1990), Radium in fertilizers: the environmental behavior of radium. *International Atomic Energy Agency, Technical Reports Series* 310, pp 113-128
- Hansen, B.K., Postma, D. (1995), Acidification, buffering and salt effects in the unsaturated zone of a sandy aquifer, Klosterhede, Denmark. *Water Resources Research* 31, pp 2795-1809
- Hartog, N., van Bergen, P.F., de Leeuw, J.W., Griffioen, J. (2004), Reactivity of organic matter in aquifer sediments: geological and geochemical controls. *Geochimica et Cosmochimica Acta* 68, pp 1281-1292
- Hefting, M.M., Bobbink, R., De Caluwe, H. (2003), Nitrous oxide emission and denitrification in chronically nitrate-loaded riparian buffer zones. *Journal of Environmental Quality* 32, pp 1194-1203
- Hefting, M.M., de Klein, J.J.M. (1998), Nitrogen removal in buffer strips along a lowland stream in the Netherlands: a pilot study. *Environmental Pollution* 102, pp 521-526
- Heron, G., Christensen, T.H. (1995), Impact of sediment-bound iron on redox buffering in a landfill leachate polluted aquifer (Vejen, Denmark). *Environmental Science and Technology* 29, pp 187-192
- Heron, G., Christensen, T.H., Tjell, J.Cr. (1994), Oxidation capacity of aquifer sediments. *Environmental Science and Technology* 28, pp 153-158
- Hoogendoorn, J.H. (1990), *Grondwatersysteemonderzoek Salland I en II*. DGV-TNO, Oosterwolde
- Houdijk, A.L.F.M., Roelofs, J.G.M. (1991), Deposition of acidifying and eutrophating substances in Dutch forests. *Acta Botanica Neerlandica* 40, pp 245-255
- Hubbert, K.M. (1940), The theory of ground-water motion. *The Journal of Geology* 48, pp 785-944
- Huling, E.E., Hollocher, T.C. (1973), Groundwater contamination by road salt: Steady state concentrations in east-central Massachusetts. *Science* 176, pp 288-290
- IAH, 2000, Creation of an International Groundwater Resources Assessment Centre (INGRACE) - an information note

- Ivahnenko, T., Szabo, Z., Gibs, J. (2001), Changes in sample collection and analytical techniques and effects on retrospective comparability of low-level concentrations of trace elements in ground water. *Water Research* 35, pp 3611-3624
- Jackson, D.A., Somers, K.M. (1991), The spectre of 'spurious' correlations, *Oecologia*, 86, pp 147
- Karssenberg, D., Pfeffer, K., Vissers, M.J.M. (2005), Software tools for hydrological modelling, In: Giupponi, C., Jakman, A.J., Karssenberg, D., Hare, M.P. (eds), *Sustainable management of water resources: An integrated approach*, Edward Elgar publishing, pp 235-265
- Klee, R.J., Graedel, T.E. (2004), *Elemental cycles: A Status Report on Human or Natural Dominance*, *Annu. Rev. Environ. Resour.* 29, pp 69–107
- Kleinhans, M.G., and Buskes, C.J.J. (2002), *Philosophy of earth science; just sloppy physics?*, Netherlands Centre for River research symposium, October 2002, Nijmegen
- Knapp, E.P., Herman, J.S., Mills A.L., Hornberger, G.M. (2002), Changes in the sorption capacity of Coastal Plain sediments due to redox alteration of mineral surfaces. *Applied Geochemistry* 17, pp 387–398
- Larsen, F., Postma, D. (1997), Nickel mobilization in a groundwater well field: Release by pyrite oxidation and desorption from manganese oxides. *Environmental Science and Technology* 31, pp 2589-2595
- Lead, J.R., Davidson, W., Hamilton-Taylor, J., Buffle, J. (1997), Characterizing Colloidal Material in Natural Waters. *Aquatic Geochemistry* 3, pp 213–232
- Lindberg, R.D., Runnels, D.D. (1984), Ground water redox reactions: An analysis of equilibrium state applied to Eh measurements and geochemical modeling. *Science* 225, pp 925-927
- Lloyd, J.W., Williams, G.M., Foster, S.S.D., Ashley, R.P., Lawrence, A.R. (1991), Urban and industrial groundwater pollution, In: Downing, R.A., Wilkinson, W.B. (eds), *Applied groundwater hydrology a British perspective*, Clarendon press, Oxford, pp 134-148
- Lowrance, R., Altier, L.S., Newbold, J.D., Schnabel, R.R., Groffmann, P.M. (1997), Water Quality Functions of Riparian Forest Buffers in Chesapeake Bay Watersheds, *Environmental Management*, 21, pp 687–712
- Lyngkilde, J., Christensen, T.H. (1992), Redox zones of a landfill leachate pollution plume (Vejen, Denmark). *Journal of Contaminant Hydrology* 10, pp 273-289
- McDonald M.G., Harbaugh, A.W. (1988), A Modular-Three Dimensional Finite Difference Ground-water Flow Model. *Techniques of Water Resources Investigations of the USGS. Book 6, Chapter A1.*
- Meinardi, C.R. (1994), *Ground water recharge and travel times in the sandy regions of the Netherlands*, Phd thesis Vrije Universiteit Amsterdam, Amsterdam, the Netherlands
- Meinardi, C.R., Rolf, A., Klaver, G., van Os, B. (1999), Results of field measurements at groundwater and sprengen of the Veluwe, RIVM Report 714851003
- Mol, G., Vriend, S.P., van Gaans, P.F.M. (2003), Feldspar weathering as the key to understanding soil acidification monitoring data; a study of acid sandy soils in the Netherlands. *Chemical Geology* 202, pp 417-441
- Mulder, J., Stein, A. (1994), The solubility of aluminium in acidic forest soils: Long-term changes due to acid deposition. *Geochimica et Cosmochimica acta* 58, pp 85-94
- Nelson, B.J., Wood, S.A., Osiensky, J.L. (2003), Partitioning of REE between solution and particulate matter in natural water: a filtration study. *Journal of Solid State Chemistry* 171, pp 51-56
- Nicholson, F.E., Jones, K.C. (1994), Effects of phosphate fertilizers and atmospheric deposition on long-term changes in the cadmium content of soils and crops. *Environmental Science and Technology* 28, pp 2170-2175
- Nickson, R., McArthur, J., Burgess, W., et al. (1998), Arsenic poisoning of Bangladesh groundwater. *Nature* 395, pp 338-338
- Nriagu, J.O. (1989), A global assessment of natural sources of atmospheric trace metals. *Nature* 338, pp 47-49
- Oenema, O., et al. (1998), Leaching of nitrate from agriculture to groundwater: the effect of policies and measures in the Netherlands. *Environmental Pollution* 102, pp 471-478
- Oude Essink, G.H.P. (1996), *Impact of sea level rise on groundwater flow regimes. A sensitivity analysis for the Netherlands*. PhD thesis Delft University of Technology. Delft Studies in Integrated Water Management 7, 428 p
- Oude Munnick, J.M.E., Geirnaert, W. (1991), GIS assisted design of a monitoring network for non-point groundwater pollution in the province of North-Holland. *Hydrogeology* 1, pp 91-104

- Parkhurst, D.L., Thorstenson, D.C., Plummer, L.N. (1980), PHREEQE a computer program for geochemical calculations. US Geol Survey Water Resources Investigations 80-96
- Parkhurst, D.L., Appelo, C.A.J. (1999), User's guide to phreeqc (version 2) – a computer program for speciation, batch-reaction, one-dimensional transport, and inverse geochemical calculations. USGS Water Resources Investigation Report 99-4259, 310p
- Pebesma, E.J., De Kwaadsteniet, J.W. (1997), Mapping groundwater quality in the Netherlands. *Journal of Hydrology* 200, pp 364-386
- Pedersen, J.K., Bjerg, P.L., Christensen, T.H. (1991), Correlation of nitrate profiles with groundwater and sediment characteristics in a shallow sandy aquifer. *Journal of Hydrology* 124, pp 263-277
- Pedroli, B. (1990), Ecohydrological parameters indicating different types of shallow groundwater. *Journal of Hydrology* 120, pp 381-403
- Philips, O.M. (2003), Groundwater flow patterns in extensive shallow aquifers with gentle relief: Theory and application to the Galena/Locust Grove region of eastern Maryland. *Water Resources Research* 39, pp 1149
- Piper, A.M. (1944), A graphic procedure in the geochemical interpretation of water analyses. *Transactions of the American Geophysical Union* 25, pp 914-928
- Post, V.E.A. (2004), Groundwater salinization processes in the coastal areas of the Netherlands due to transgressions during the Holocene, PhD Thesis, Vrije Universiteit Amsterdam
- Postma, D. (1993), The reactivity of iron oxides in sediments: a kinetic approach. *Geochimica et Cosmochimica Acta* 57, pp 5027-5034
- Puckett, L.J., Cowdery, T.K. (2002), Transport and fate of nitrate in a glacial outwash aquifer in relation to ground water age, land use practices, and redox reactions. *Journal of Environmental Quality* 31, pp 782-796
- Pyne, R.D. (1995), Groundwater recharge and wells: A guide to aquifer storage recovery, CRC press
- Rasmussen, P.E. (1998), Long-range atmospheric transport of trace metals: the need for geoscience perspectives. *Environmental geology* 33, pp 96-108
- Reed, M.H. (1982), Calculation of multicomponent chemical equilibria and reaction processes in systems involving minerals, gases and an aqueous phase. *Geochimica et Cosmochimica Acta* 46, pp 513-528
- Reijnders, H.F.R., Van Drecht, G., Prins, H.F., Boumans, L.J.M. (1998), The quality of the groundwater in the Netherlands. *Journal of Hydrology* 207, pp 179-188
- Robertson, W.D., Cherry, J.A. (1989), Tritium as an indicator of recharge and dispersion in a groundwater system in central Ontario. *Water Resources Research* 25, pp 1097-1109
- Ronen, D., Magaritz, M., Almon, E., Amiel, A.J. (1987), Anthropogenic anoxification ('eutrophication') of the water table region of a deep phreatic aquifer. *Water Resources Research* 23, pp 1554-1560
- Scheibe, T., Yabusaki, S. (1998), Scaling of flow and transport behavior in heterogeneous groundwater systems. *Advances in Water Resources* 22, pp 223-238
- Schipper, P.N.M., Vissers, M.J.M. (2003), Ground water quality maps of Hengelo (In Dutch), SKB project report, SV-60, SKB Gouda
- Schot, P.P. (1990), Groundwater systems analyses of the Naardermeer wetland, the Netherlands, In: Simpson, E.S., Sharp, J.M. (eds) Selected papers from the 28th International Geological Congress, Washington, Hannover, 1, 257-269
- Senesi, G.S., Baldassarre, G., Senesi, N., Radina, B. (1999), Trace element inputs into soils by anthropogenic activities and implications for human health. *Chemosphere* 39, pp 343-377
- Simmons, C.T., Fenstemaker, T.R., Sharp, Jr. J.M. (2001), Variable-density groundwater flow and solute transport in heterogeneous porous media: approaches, resolutions, and future challenges. *Journal of Contaminant Hydrology* 52, pp 245-275
- Steinnes, E. (2001), Metal contamination of the natural environment in Norway from long range atmospheric transport. *Water, Air, and Soil Pollution: Focus* 1, pp 449-460
- Staatsblad (1995), Grondwaterwet; wijziging mbt voor het onttrekken van grondwater te stellen algemene regels e.a., Stb 268
- Staatsblad (1997), Besluit gebruik dierlijke meststoffen 1998, Stb 601
- Stiff, H.A. Jr. (1951), The interpretation of chemical water analysis by means of patterns. *Journal of Petroleum Technology* 3, 10, technical note 84
- Stoddard, J.L., Jeffries, D.S., Lükewille, A., Clair, T.A., Dillon, P.J., et al. (1999), Regional trends in aquatic recovery from acidification in North America and Europe. *Nature* 401, pp 575-578

- Stumm, W., Bilinski, H.I. (1972), Trace element patterns in natural waters: difficulties in interpretation arising from our ignorance of their speciation. In: Jenkins, S.H. (ed), *Advances of Water Pollution Research. Proceedings of the 6th international conference*. Pergamon Press, pp 39-52
- Stuurman, R.J., Griffioen, J. (2003), *Systeemgericht grondwaterbeheer; drie praktijkgevallen van problemen in grondwaterbeheer*. TCB R18(2003), Den Haag.
- Stuyfzand, P.J. (1986), A new hydrogeochemical classification of watertypes: principles and application to the coastal dunes aquifer system of the Netherlands. *Proceedings 9th SWIM, Delft (The Netherlands)*, pp. 641-656
- Stuyfzand, P.J. (1999), Patterns in groundwater chemistry resulting from groundwater flow. *Hydrogeology Journal* 7, pp 15-27
- Tesoriero, A.J., Liebscher, H., Cox, S.E. (2000), Mechanism and rate of denitrification in an agricultural watershed: Electron and mass balance along groundwater flow paths. *Water Resources Research* 36, pp 1545-1559
- Thorstenson, D.C., Fisher, D.W., Croft, M.G. (1979), The geochemistry of the Fox Hills-Basal Hell Creek aquifer in southwestern North Dakota and northwestern South Dakota. *Water Resources Research* 15, pp 1479-1498
- Tóth, J. (1963), A theoretical analysis of groundwater flow in small drainage basins. *Journal of Geophysical Research* 68, pp 4795-4812
- Trauth, R., Xanthopoulos, C. (1997), Non-point pollution of groundwater in urban areas. *Water Research* 31, pp 2711-2718
- Turner, D.R., Whitfield, M., Dickson, A.G. (1981), The equilibrium speciation of dissolved components in freshwater and seawater at 25°C and 1 atm pressure. *Geochimica et Cosmochimica Acta* 45, pp 855-881
- Uffink, G.J.M. (2003), Determination of denitrification parameters in deep groundwater, RIVM report 703717011
- UNECE (1979), *Geneva Convention on Long-range Transboundary Air Pollution*
- UNECE (1998), *Aarhus Protocol on Heavy Metals, Aarhus Protocol on Persistent Organic Pollutants (POPs)*
- UN/WWAP (United Nations/World Water Assessment Programme) (2003), *UN World Water Development Report: Water for People, Water for Life*. Paris, New York and Oxford, UNESCO (United Nations Educational, Scientific and Cultural Organization) and Berghahn Books.
- USEPA (1993), *A review of methods for assessing aquifer sensitivity and ground water vulnerability to pesticide contamination*, USEPA, Office of Water, Washington DC.
- Van Breemen, N., van Dijk, H.F.G. (1988), Ecosystem effects of atmospheric deposition of nitrogen in the Netherlands. *Environmental Pollution* 54, pp 249-274
- Van Breukelen, B.M., Roling, W.F.M., Groen, J., Griffioen, J., Verseveld, H.W. (2003), Biogeochemistry and isotope geochemistry of a landfill leachate plume. *Journal of Contaminant Hydrology* 65, pp 245-268
- Van Buuren, M. (1991), A hydrological approach to landscape planning: the framework concept elaborated from a hydrological perspective. *Landscape and Urban Planning* 21, pp 91-107
- Van der Lee J., De Windt L. (2001), Present state and future directions of modeling of geochemistry in hydrogeological systems. *Journal of Contaminant Hydrology* 47, pp265-282
- Van der Linden, W., Kremers, A.H.M., Weerts, H.J.T. (2002), *Landelijke karakterisatie topsysteem*, in opdracht van Droogtestudie Nederland RIZA, RIVM en Alterra. Eindrapport. NITG 02-112-B
- Van der Sluijs, P., De Gruijter, J.J. (1985), Water table classes: a method to describe seasonal fluctuation and duration of water tables on Dutch soil maps. *Agricultural Water Management* 10, pp 109-125
- Van Gaans, P.F.M. (1989), WATEQX-A restructured, generalized, and extended fortran 77 computer code and database format for the wateq aqueous chemical model for element speciation and mineral saturation, for use on personal computers or mainframes. *Computers & Geosciences* 15, 843-887
- Van Helvoort, P.J. (2003), *Complex Confining Layers*. Netherlands Geographical Studies NGS 321, Utrecht University
- Van Sambeek, M.H.G., Eggenkamp, H.G.M., Vissers, M.J.M. (2000), The groundwater quality of Aruba, Bonaire and Curacao: a hydrogeochemical study. *Netherlands Journal of geosciences* 79, pp 459-466
- Van Uden, J.G., Vissers, M.J.M. (1998), *A hydrochemical study in Salland (in Dutch)*, MSc. thesis, Utrecht University, Department of Geochemistry, Utrecht

- Varljen, M.D., Shafer, J.M. (1991), Assessment of uncertainty in time-related capture zones using conditional simulation of hydraulic conductivity. *Ground Water* 29, pp 737-748
- Vissers, M.J.M., Frapporti, G., Hoogendoorn, J.H., Vriend, S.P. (1999), The dynamics of groundwater chemistry in unconsolidated aquifers: The Salland section. *Physics and Chemistry of the Earth (B)* 24, pp 529-534
- Vissers, M.J.M., Schipper, P.N., Van Gaans, P.F.M. (2004), Stromingen in grondwaterkwaliteitskaarten. *Stromingen* 10, pp 5-16
- Vogel, J.C. (1967), Investigation of groundwater flow with radiocarbon. *Isotopes in hydrology*. International Atomic Energy Agency, Vienna, pp 355-368
- Wilson, J.T., McNabb, J.F., Balkwill, D.L., Ghiorse, W.C. (1983), Enumeration and characterization of bacterial indigenous to a shallow water-table aquifer. *Ground Water* 21, pp 134-142
- Winter, T.C. (1978), Numerical simulation of steady-state, threedimensional ground-water flow near lakes. *Water Resources Research* 14, pp 245-254
- Wood, W.W. (2000), It's the heterogeneity! *Ground Water* 38, pp 1-1
- Worrall, F., Kolpin, D.W. (2003), Direct assessment of groundwater vulnerability from single observations of multiple contaminants. *Water Resources Research* 39, pp 1345
- Worrall, F., Besien, T., Kolpin, D.W. (2002), Groundwater vulnerability: interactions of chemical and site properties, *The Science of the Total Environment* 299, pp 131-143
- Zhu, C., Burden, D.S. (2001), Mineralogical compositions of aquifer matrix as necessary initial conditions in active contaminant transport models. *Journal of Contaminant Hydrology* 51, pp 145-161

## 2 USING GROUNDWATER MODEL RESULTS FOR MAPPING GROUNDWATER FLOW AND QUALITY

M.J.M. Vissers, P.N.M. Schipper<sup>+</sup>, P.F.M. Van Gaans

<sup>+</sup> Grontmij Advies & Techniek bv, Water division, Houten

**Abstract.** A method for describing groundwater flow that gives detailed insight in groundwater flow and subsequently in groundwater quality is presented. Groundwater flow is the key factor that determines the spatial distribution of groundwater of different composition, and it can be modelled relatively easily. Yet groundwater flow modelling is not often used in the context of water quality, mainly because the standard output of hydrological models is not easily interpreted in terms of groundwater composition. This paper introduces a technique using MODPATH to get detailed 3D maps of groundwater flow patterns, complemented by representations of the model results specifically suitable for groundwater quality mapping. The conventional maps of net groundwater recharge and path-lines are combined with maps of transit distance, transit time and travel distance at various specified depths. A fifth map depicts a combination of transit time and recharge. It identifies the areas most susceptible to pollution from a quantitative perspective. The combination of all maps is used to deduce the configuration of groundwater flow systems, which are, in turn, projected on these maps. To this end, the hydrological system analysis as developed by Tóth (1963) is expanded towards three dimensions.

*Keywords: Systems analysis, particle tracking, groundwater flow, the Netherlands*

### 2.1 INTRODUCTION

Knowledge of the spatial distribution of groundwater composition can be useful for spatial planning, protection, sanitation, and risk assessment. For example, knowledge of current and future groundwater composition in discharge areas may help to plan nature areas (Batelaan et al. 2003). Knowledge of the redox state of the groundwater and aquifer sediments and its distribution is essential for contaminant plume remediation (Christensen et al. 2000). In addition, knowledge on groundwater flow helps to determine the position and propagation of contaminant plumes, and thereby the determination of sanitation strategies.

For predictive mapping of groundwater composition, the factors that determine it must be modelled. Even though many mathematical models have been developed to simulate all known processes that determine the chemical composition of groundwater (Van der Lee and De Windt, 2001), few are actually used in groundwater protection programs. This is due to difficulties in data collection, model selection, and model implementation (Wang, 1997). Furthermore, computing time limits the application of such models at the regional scale (MacQuarrie et al. 2001). In most cases, however, limited data availability hinders the use of 3D reactive transport models. This is because the ambient groundwater composition (which will be called groundwater quality from hereon), which is also input for these models, is unknown. The unknown ambient groundwater quality has led to approaches other than the process-based approach to groundwater quality mapping, but at the cost of limiting the model to one component or group of components, or restricting it to a qualitative answer.

For groundwater quality mapping, Focazio et al. (2002) distinguished subjective rating methods from statistical and process-based methods. They classified statistical methods together with the process-based approach as both are closely tied to objective scientific purposes. When a subjective rating method is used, groundwater quality mapping is usually called aquifer vulnerability mapping. Though there is little consensus on the terminology (Gogu and Dassargues, 2000; Worrall et al. 2002), here the definition of USEPA (1993) is used. In this definition, aquifer vulnerability mapping, like groundwater quality mapping, aims to predict the future spatial distribution of groundwater quality, which essentially means a proper understanding of all processes leading to the current groundwater quality. Both aquifer vulnerability and groundwater quality mapping include land-use management and contaminant characteristics. Subjective rating methods produce categories of vulnerability, which are quantified or even verified using water quality data (Nolan et al. 1997). The term groundwater quality mapping is mostly used when objective, (geo)statistical methods are used to map the spatial distribution of groundwater quality (Frapporti et al. 1995; Pebesma and De Kwaadsteniet, 1997; Sánchez-Martos et al. 2001). In a process-based approach, the basic factors that determine groundwater quality must be identified and modelled. The two basic factors that determine groundwater quality at a specified point (Engelen, 1981; Vissers et al. 1999) are:

- Quality of the infiltrated water. This includes recharging water (rain, dry deposition, evapotranspiration, surface water) as well as added substances (manure, fertilizers, dry deposition, and organic contaminants).
- Post-infiltration reactive processes. These can be split up into various geochemical processes, such as sorption, redox reactions, buffering, degradation, dissolution, etc.

When the spatial distribution of groundwater quality is taken into account, the third factor is:

- Groundwater flow.

Estimating the first two factors is often complicated. It is difficult to predict the input water quality by for example relating input to land-use. Especially in populated areas input is highly variable, and its history mostly unknown. To predict which post-infiltration geochemical processes can be expected, knowledge of sediment characteristics is important. Especially in sandy and heterogeneous aquifers with limited buffering capacity, redox and pH conditions are hard to predict, and usually insufficient observations are available to discriminate between the geochemical processes spatially.

The third process, groundwater flow, can more easily be predicted and modelled and is, at least in the Netherlands, less hampered by data availability and process knowledge. Like knowledge of groundwater quality, knowledge of groundwater flow is essential for groundwater protection, sanitation, and risk assessment, and can be related to groundwater quality. Groundwater flow path analysis and recharge area mapping can be an important tool for water resources management through land use planning (Harris et al. 1988; Robinson and Reay, 2002; Batelaan et al. 2003).

There are two complementary perspectives for relating groundwater flow to groundwater quality (Falkenmark and Allard, 1991). The first is where at one moment in time the observed water quality in streams, discharge areas, and wells is related to recharge areas in terms of past land-use history. The second perspective is where the



future and past pathways of point-source pollution are delineated, indicating where and when pollution problems can be expected. This paper demonstrates how results from groundwater models can be used for mapping groundwater quality using the approach of Falkenmark and Allard (1991). Stationary groundwater flow is modelled using MODFLOW (McDonald and Harbaugh, 1988). The particle-tracking program MODPATH (Pollock, 1994) is then used to investigate the unconfined and semi-confined groundwater flow in the area. The interpretation of the maps resulting from this method is an extension of the hydrological systems analysis as put forward by Tóth (1963) and Engelen and Kloosterman (1996). These two-dimensional views of groundwater flow are extended towards an integrated set of maps describing the flow pattern and groundwater flow systems in three dimensions as well as their temporal characteristics. In addition, a parameter defined as quantitative vulnerability is mapped, highlighting the areas most important for the overall aquifer groundwater quality.

## 2.2 STUDY AREA

Groundwater flow in the study area is topography-driven. This means that groundwater flow and flow systems (Tóth, 1963) are determined by the ratio between horizontal and vertical conductivity ( $K_H/K_V$ ), the thickness of the aquifer, and topographic relief of the study area (Zijl, 1999). These and other features of the study area important for hydrology are described below.

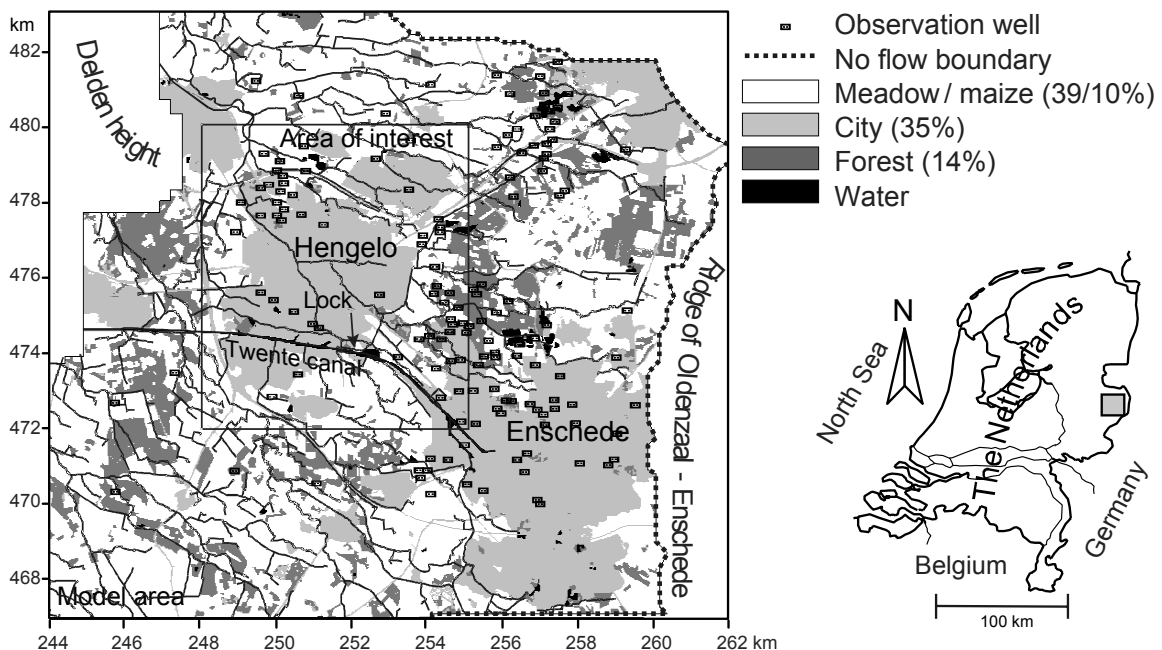


Figure 2.1 Model area, Hengelo area of interest, streams, observation wells, main features and land use, with coordinates in km RDS (Dutch ordnance datum)

The study area is situated in the east of the Netherlands, in an urban agglomeration of the cities Hengelo (80,000 inhabitants) and Enschede (150,000 inhabitants). Locations of

observation wells are shown in Figure 2.1, which also shows the area of interest; the city of Hengelo and its surroundings.

The eastern side of the study area is bounded by an ice-pushed ridge, which forms a natural groundwater divide, with heights of 50 - 70 m OD (Dutch ordnance datum). In the northwest, the 'Delden height' (30 m OD), a small core of ice-pushed material covered by eolian sands is found. The Hengelo Basin is situated in between these ridges, with elevations of 10 - 20 m OD. From the ridge in the east towards the northwest the elevation decrease is accompanied by a decrease in gradient from 2.5 m/km near the groundwater divide to less than 1 m/km. An east west directed dense network of streams, forming the natural drainage system of the ice-pushed ridge since the last ice age, characterizes the relatively flat area. In total the area contains more than 500 km of streams (Figure 2.1), which equals a drainage density of 1.69 km/km<sup>2</sup>. These streams are the main form of drainage, and are in some wet areas complemented by artificial drainage systems. Within the cities the streams were filled in and streams reaching the cities were diverted towards the 'Twente canal', causing high groundwater levels in urban areas, especially where high hydraulic gradients are found together with clay layers or thin aquifers. In these locations extraction wells were placed to reduce the inconvenience associated with high groundwater levels.

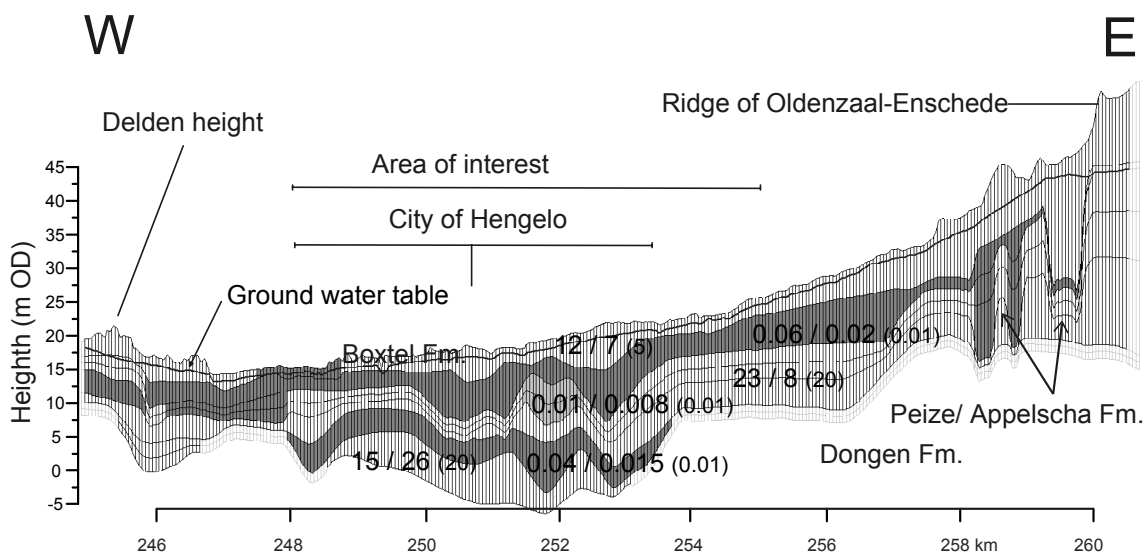


Figure 2.2 Cross-section of the model area at  $y=475300$ . Grey bounded cells are inactive cells in the lowest layers, dark coloured cells indicate aquitards, and calibrated conductivities are given as  $K_H / K_V$  values, followed by the initial values between brackets (in m/d)

Figure 2.2 shows the hydrological schematization and geology of an east – west transect of the study area. The 'Dongen formation' (De Mulder et al. 2003), a marine Eocene formation consisting of clay, fine sand, and sandstone, forms the hydrological base on top of which the ice-pushed ridge is found. Early Pleistocene river deposits of the rivers Elbe and Weser (the Peize formation) consisting of gravels and coarse sands occur at the foot of the ridge.

The largest part of the aquifer is made up by the Drenthe formation, consisting both of clays and of sandy glacio-fluvial and glacio-lacustrine deposits that filled up

channels that formed in the basement during the Saalien ice age. The ice-pushed deposits are covered by moraine deposits (gravel containing loamy sand). In the lower parts of the aquifer, periglacial deposits of the Boxtel formation are found, consisting of fluvioglacial sands and clays (Weichselien) with eolian fine sands on top. Along the streams, Holocene stream deposits consisting of finer-grained material are found.

## 2.3 GROUNDWATER FLOW MODEL

The size of the study area is 16 x 18 km, to ensure no boundary effects will be present within the Hengelo area of interest. The east side of the study area forms a natural groundwater divide, which is modelled as a no-flow boundary (Figure 2.1). In the northwest, the very clayey ‘Delden height’ caused model instability and has been left out of the model. A fixed-head boundary was used in the west.

*Table 2.1* Summarized characteristics of the groundwater flow model

MODFLOW PACKAGE	Explanation
BCF	7 layers, 50 x 50 m grid cells, (93896 x 7 cells), 18 x 16 km <sup>a</sup>
BASIC: No Flow	Groundwater divide in the east of the study area <sup>b</sup>
BASIC: Constant Head	Minimal 1 m –groundwater level, interpolation of DINO-data, only in bottom 4 layers in sandy deposits <sup>c</sup>
WELLS	Average of period 1991 – 1998 was taken, and wells were only included when this average > 50.000 m <sup>3</sup> /y
DRAIN	Level: 1 m –ground level
RIVERS	Interpolation of weir heights (average of up- and downstream water level), 300 data points
RECHARGE	KNMI (1991-1998): local weather stations for precipitation, resulting in the following net recharge: Grass 0.85 (0.83), forest 1.00 (1.06), Urban 0.42, heathland 1.20. in mm/d <sup>d</sup>
Ground level	From recently updated digital elevation model 2002 (25 x 25 m) <sup>e</sup>
Observation wells	Only considered when > 100 measurements in period 1991 – 1998 are available, with standard deviation < 1.5 m. This resulted in 210 observation wells in the area

a Method used for implementation of discontinuous layers comparable with Jones et al. (2002)

b No-flow east of coordinate x = 254000, constant head west of coordinate x=254000 (see Figure 2.1)

c TNO REGIS (100 x 100 m) and TNO DINO form the Dutch databases of borings and groundwater head measurements

d Field values in the study area found by Meinardi (1994) between brackets

e AHN (Algemeen Hoogtemodel Nederland) elevation model provided by the Ministry of Transport, Public Works and Water Management

The complex geology of the Drenthe Formation and the accompanying large variations in hydraulic conductivities required the use of 7 model layers. The area was discretized using a model grid size of 50 x 50 m, as at larger cell size interpolation problems could occur which would negatively influence the estimation of the diffuse drainage elevation that is related to the surface level in the model (Table 1). This was recognized in the stream drainage levels, which were interpolated using true weir heights. The change from an initial model with 100 x 100 m grid size to the final model 50 x 50 m grid resulted in a decrease of the average stream level from –2.04 m ground level to -1.06 m ground level.

This was due to a strong over-generalization of the topography at the larger grid size (see Bryan, 2003). Further details are listed in Table 1. The mean absolute model error decreased from an initial 1.39 m to 1.02 m when incorporating true stream drainage levels instead of linking them to surface elevation. A further decrease of 0.19 m was obtained by changing the mostly ‘dry’ river cells on the ridges into drainage cells. Subsequently automatic parameter estimation (PEST; Doherty et al. 1994) was used to calibrate horizontal and vertical conductivities of the seven model layers. Results of this calibration are graphically depicted in Figure 2.2, and led to a further decrease in the mean absolute model error to 0.72 m. Not considering the ridge above 35 m where the absolute error is greatest, the mean absolute model error is 0.39 m.

Net recharge in the upper active cell was calculated by subtracting the Makkink crop-reference evapotranspiration values (Makkink, 1957, Winter et al. 1995) from precipitation data, as calculated by the KNMI (1991-1998). For pine forest the actual evaporation was adjusted to 80% of the potential evapotranspiration, according to Meinardi (1994).

## 2.4 POST-PROCESSING REPRESENTATION METHODS

### 2.4.1 Mapping groundwater flow and groundwater flow systems

First a conventional map showing isohypses and net recharge of the area of interest was constructed directly from the MODFLOW output, where seepage and infiltration rates were estimated by calculating the flux between the upper two model layers.

To visualize the transit time and transit distance of groundwater from the location of infiltration, two additional maps were made after flow path analysis using MODPATH. Particles were released in the modelled flow field at the water table in the 50 m model grid, using one particle per model cell, and an effective porosity of 0.35. Particles were tracked forward until a strong sink, i.e. a cell that drains all incoming water, was reached. The tabular output was recalculated and exported to a GIS for visualization of the flow paths. The endpoint file that contains the starting and end points of the particle tracking analysis was used to calculate transit times and distances, which are visualized in a GIS.

Subsequently, these maps were used to delineate groundwater flow systems. Tóth (1963) defined groundwater flow systems for cross-sectional views as ‘a set of flow lines in which any two flow lines adjacent at one point of the flow region remain adjacent through the whole region; they can be intersected anywhere by an uninterrupted surface in which flow takes place in one direction only’. The extension of this definition towards three dimensions implies that the set of adjacent flow lines can be curved, for example around a seepage area. This is shown in Figure 2.3, where a top view of flow lines towards a discharge area is displayed. In this 3D flow example it follows that the ‘uninterrupted surface’ must be curved around the seepage area as well. The figure displayed thus consists of one groundwater flow system, as may not directly be concluded from a cross-sectional view.

The definition of a groundwater flow system would thus suffice as ‘a water volume defined by the set of adjacent flow lines’. This is for example the case when all

flow lines are directed towards a single continuous discharge area, and implies that a groundwater flow system can be identified by a continuous field of transit distances around a continuous discharge area. The definition and identification of groundwater flow systems is thus analogous to that of a stream catchment area. The limits of the groundwater flow systems thus specified were manually drawn in a GIS and projected over the maps created.

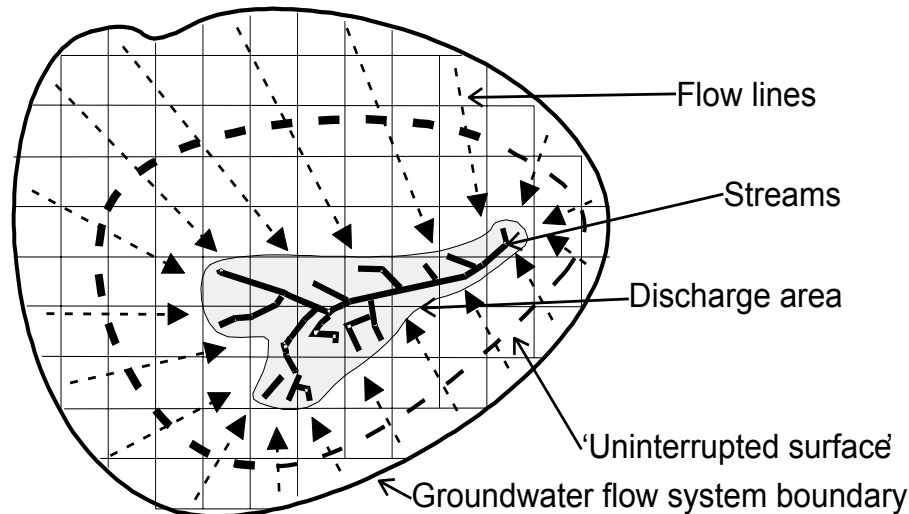


Figure 2.3 Schematic diagram of a groundwater flow system

#### 2.4.2 Relating hydrology to groundwater quality

The first approach of Falkenmark and Allard (1991) is the possibility to assess the expected groundwater quality in discharge areas or wells by knowing the recharge areas and historic land use and water quality. In the approach used here, flow and groundwater quality are related to each other by using groundwater flow systems analysis. Groundwater flow system boundaries also help to indicate the limits of pollution pathways.

In the second approach one should be able to predict the tracks of pollution. For this, not only the projected horizontal flow direction is needed, but also flow in the third dimension. Therefore, a set of maps was made to enable the prediction of travel distance and time at specified depths below ground level. For these maps backtracking was used: for each location on the 50 m grid at a given depth below ground level, the travel distance from the initial point of infiltration was calculated and plotted in a GIS.

#### 2.4.3 Quantitative vulnerability

Because the product of transit time and recharge rate at each model grid cell determines the contribution of each model cell to the overall groundwater volume of the aquifer, it can be considered as an adequate indicator for the vulnerability of the grid cell from a groundwater-quantitative perspective. This indicator can be interpreted as an imaginary

vertical water column from each grid cell, which, if divided by the net porosity, approximately equals the maximum depth the water will travel after infiltration:

$$QV = n(x,y) \cdot T(x,y) / \eta \quad (1)$$

where  $n$  [L/T] is the local net recharge rate at  $(x,y)$ ,  $\eta$  is the effective porosity, and  $T$  [T] is the transit time of the particle recharged at this point. Only areas where recharge is larger than 0 m/y are considered. Mapping this indicator identifies areas that make large contributions to the overall groundwater quality in the aquifer. On the other hand, mapping this indicator reveals the areas with short travel times and depths, which are more vulnerable from a surface water quality perspective (Osborne and Kovacic, 1993; Engelen, 1981).

#### 2.4.4 Transit time distribution

The residence time or turnover time, which is also defined as the average transit time of the water entering a compartment, is often used in reservoir theory (Eriksson, 1971; Bolin and Rodhe, 1973). In many cases the *distribution* of transit time is more convenient to describe a reservoir. It provides a measure to compare recharge zones (Robinson and Reay, 2002). The distribution of groundwater transit times is often very skewed due to the groundwaters' short-circuited behaviour. Median transit times are therefore a more appropriate, robust indicator of the age of the groundwater than the residence time. Furthermore, transit times have been often related to the percentage of total watershed area (e.g. Robinson and Reay, 2002), while in fact they should be related to recharge volume. Both the cumulative transit distribution expressed as proportion of the area and as proportion of recharge volume were derived from the MODPATH-simulation.

## 2.5 RESULTS AND INTERPRETATION

*Traditional model output:* Figure 2.4 shows the traditional model output of the hydrological model, consisting of hydraulic heads represented by isohypses, and net recharge to the aquifer. From this map it is clear that flow is generally directed to the west-northwest, and that upward seepage areas can be found in many different zones. However, decimetre scale differences in heads can have a major influence on groundwater flow. These small differences are concealed by the large differences in heads found in the area, and therefore not visible in Figure 2.4. Furthermore, no estimations of age, groundwater flow systems, or groundwater quality can be made from this map.

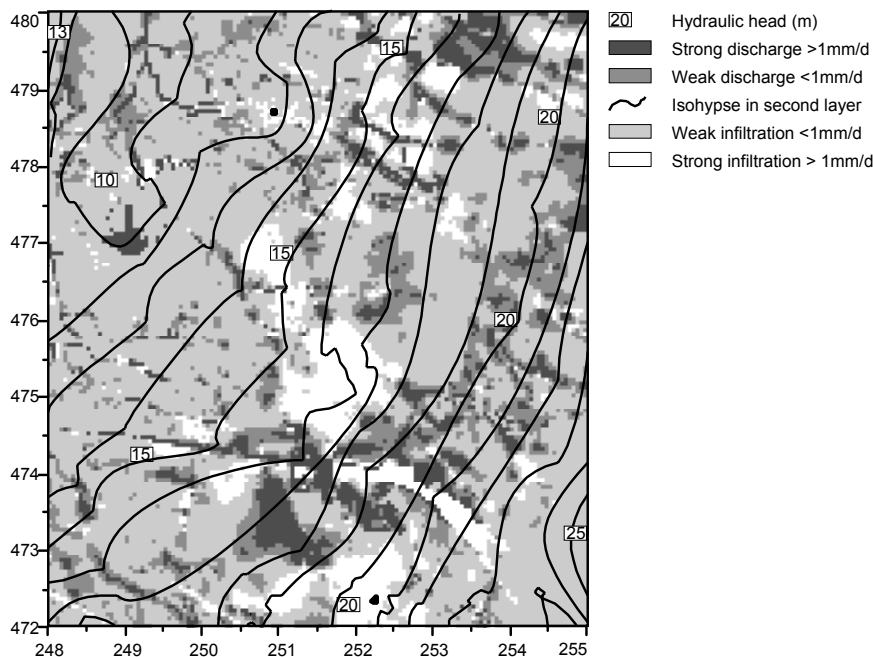


Figure 2.4 Conventional seepage- infiltration map of the area of interest and isohypse map of the second model layer

*Transit distance:* Figure 2.5a shows the transit distance in combination with the calculated flow paths. Only a quarter of the calculated paths are shown for clarity. The effect of the large difference in surface elevation that is visible in the isohypses disappears because only horizontal flow distance is visualized. This map provides a different perspective on the groundwater flow than the pattern shown in Figure 2.4. The recharge areas of abstraction wells and upward seepage areas can easily be deduced from the map, enabling the identification of groundwater flow systems at a very detailed level. In the study area the recharge areas of regional groundwater flow systems that comprise only a few percent of the area can also be recognized. They are located on groundwater flow system boundaries and have transit distances larger than the size of the groundwater flow systems they bound.

*Transit times:* Figure 2.5b shows the transit times. Because groundwater travels a much shallower and hence faster pathway near groundwater discharge areas than in areas near groundwater flow system boundaries, the groundwater travel times were mapped using a logarithmic classification. In this figure, the influence of geology is visible, which is not the case for the transit distance map (Figure 2.5a). Groundwater passing through clay layers reaches higher ages than groundwater only passing through sandy sediments. Especially in areas where shallow clay layers are present, recharge rates become very low. Here, transit times typically exceed 1000 years. However, these large transit times at shallow depths may be subject to considerable uncertainty, given the complex geology of the topsoil, as clay layers may be discontinuous in the top layer. The 10- and 25- year zones of e.g. drinking water wells can be derived directly from the maps.

*Groundwater flow systems:* The groundwater flow system boundaries are projected on Figures 2.5 and 2.6, and on a topographical map for location reference (not shown). As is evident from the maps, the calculated groundwater flow directions within

the study area are highly variable and the derived groundwater flow systems are variable in size. Some groundwater flow systems consist of one large system with few or no local systems superimposed, other systems completely consist of small systems, sometimes with sizes as small as few model cells. A fully automated deduction of groundwater flow systems is therefore difficult in this area, and boundaries were discerned manually. Only the larger and most important groundwater flow systems have been discerned. However, objectiveness is largely maintained, as the maps from which they are derived are still shown. Discerning the flow systems improves map readability and aids in mutual and topographical location reference.

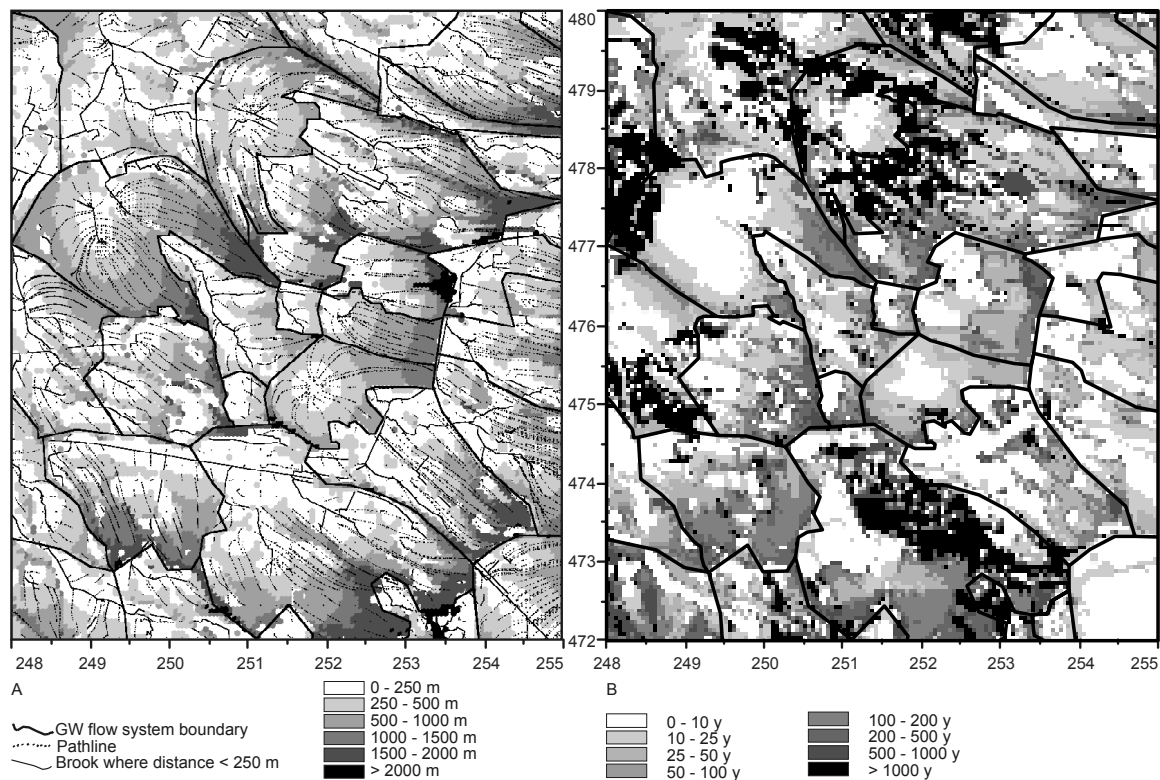


Figure 2.5 (a) Subdivision into groundwater flow systems and transit distance in the area of interest. The black colours on system boundaries indicate recharge areas of deeper ground water systems. Streams are only shown where transit distance < 250m, and (b) Transit times from infiltration points with 10-years zones (white), 25-years zones, and 50, 100, 200, 500, and 1000 years zones (up to black) and groundwater flow system boundaries

Four different types of groundwater flow systems can be discerned:

- Abstraction systems, where all water recharging the aquifer will reach a certain well or well field. They show circular transit distance patterns around the pumping area.
- Upward seepage area systems, where groundwater will discharge into a seepage area or wetland. They are characterized by their large discharge area (see Figure 2.4).
- Stream systems, where one or more streams form an elongated discharge area, fed by contiguous recharge areas.



- Clay- and flat systems, which form fine-scale flow systems with long transit times, due to low relief and slow groundwater flow.

The groundwater flow system boundaries often form the recharge areas of regional systems, and are recognized by having the longest transit times and distances.

*Travel distance at specified depths:* In Figure 2.6a, the 10 -metre depth travel distance map is shown as an example. In combination with Figure 2.5a, from which flow horizontal direction can be derived, a good estimation of the location of the infiltration point of groundwater found at any location and depth can be made. This helps to determine pollution tracks, and helps to identify the recharge area when a groundwater sample is considered. Furthermore, the ‘deeper’ maps, like the ordinary transit distance map, directly show the configuration of the deeper groundwater flow systems.

*Quantitative vulnerability:* For the calculation a maximum transit time of 1000 years was defined for the area, to eliminate the influence of extreme transit times at groundwater flow system boundaries. The resulting map is shown in Figure 2.6b, and shows high vulnerabilities in some places not directly surmised from comparing Figures 2.4 and 2.5. In general the clay areas and areas near discharge areas are found not to be vulnerable, as very little water infiltrates or very short transit times exist. Most vulnerable are sandy infiltration areas and well capture areas.

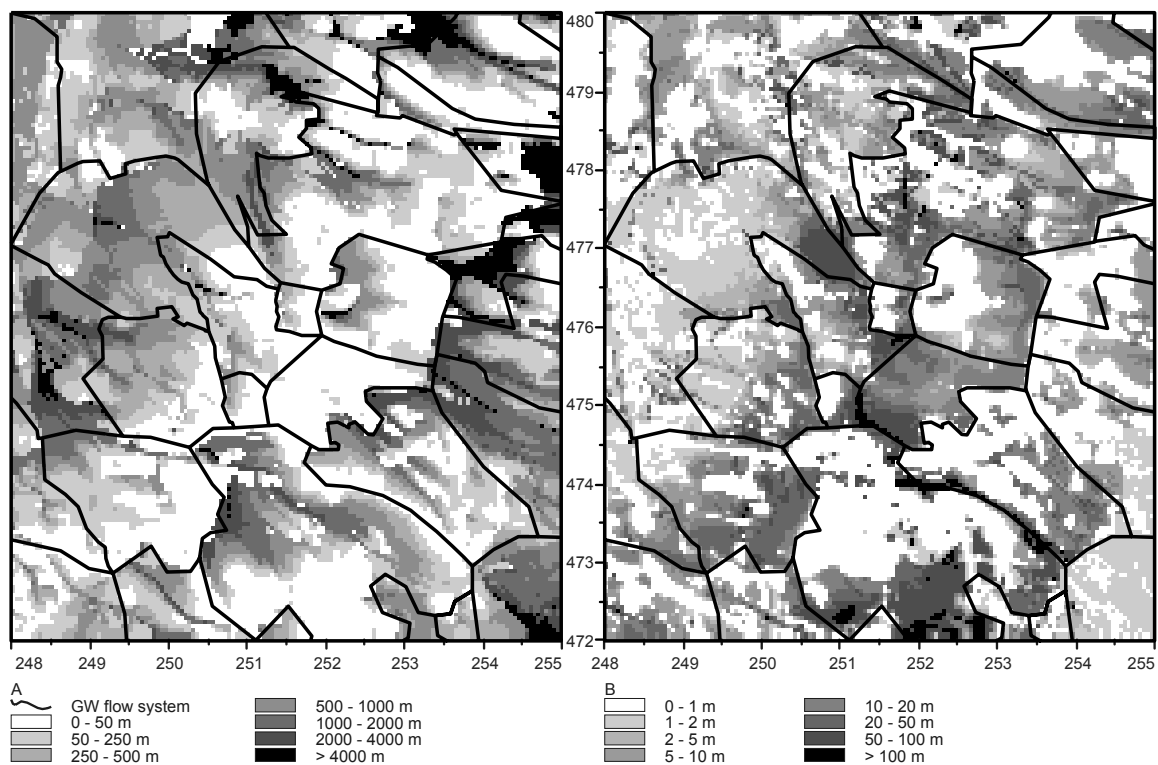


Figure 2.6 (a) Depth – transit distance map, here at 10m –ground level and (b) Quantitative vulnerability map of the area of interest, both in combination with subdivision in groundwater flow systems

*Transit time distribution:* Both the volumetric and areal cumulative transit time distribution derived from the MODPATH-simulation are presented in Figure 2.7. The median volumetric transit time of the groundwater is 33 years and 80 % of the

groundwater is less than 100 years old. The median areal transit time is 50 years, and in 65% of the area recharges water that becomes less than 100 years old. The flat clayey areas that have very long transit times, but very low recharge rates, are responsible for the difference between the areal cumulative transit time distribution and the volumetric transit time distribution.

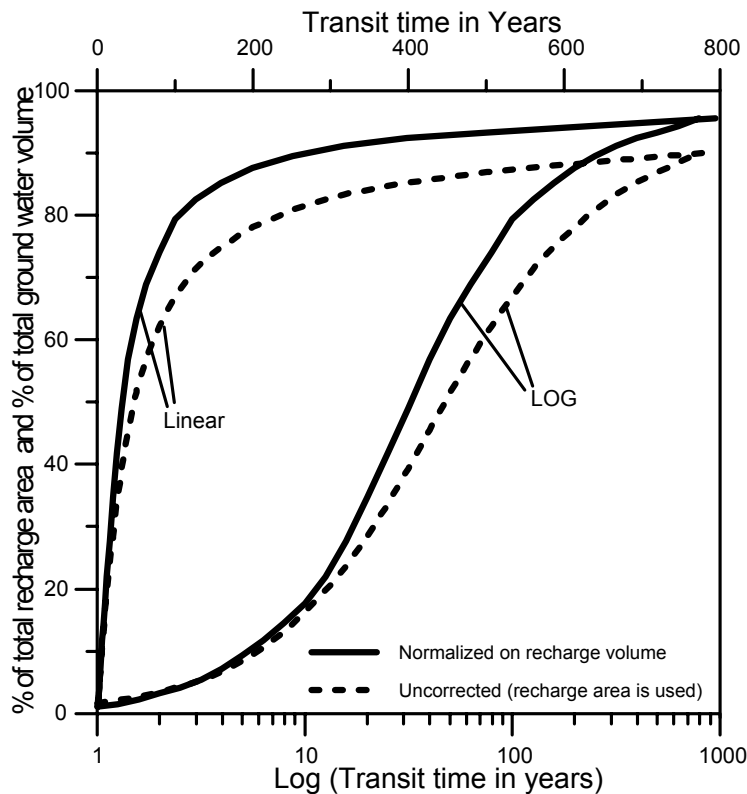


Figure 2.7 Cumulative transit time distribution of the whole model area, showing the difference between values as % recharge area and % recharge volume on a linear and log scale

## 2.6 DISCUSSION

This study shows a new application of mapping groundwater flow using MODPATH. Groundwater flow and groundwater flow systems were analyzed using a combination of the following maps: (1) isohypses and net recharge, (2) path lines and transit distance, (3) transit time, (4) a set of depth maps with travel distance, and (5) quantitative vulnerability, in combination with a topographical map with the derived groundwater flow systems acting as a reference. In fact the way model output is displayed may be viewed as an alternative way to present the output of hydrological models in addition to the traditional approaches that focus on hydraulic heads and the water balance.

The maps created are meant to be understandable for end-users, who can deduce age, recharge areas, flow direction, and flow distances at a certain depths. The use of different colours for different maps may further increase user-friendliness. The information obtained from the maps may help to interpret the possible effects of

interventions in input water quality, and observations of groundwater quality can directly be interpreted in terms of flow paths and recharge areas.

### **2.6.1 Use of particle tracking**

Several other studies have used MODPATH for purposes similar to those shown here. For example Blair et al. (1990) mapped zones of equal travel time to analyse the influence of different pumping rates. By using transit time and distance maps as shown in this study, the same information can be derived. Buxton et al. (1991) used particle tracking on Long Island to identify recharge areas of a deeper aquifer. More recently, Batelaan et al. (2003) mapped recharge rates of a large area with well-distinguished catchment areas, and used MODPATH to subdivide the area into groundwater flow systems and to map transit times towards the different discharge areas for phreatophyte mapping and land use planning. In a similar way, Robinson and Reay (2002) used MODPATH to analyze flow by using land use in recharge areas and the distribution of transit times in a single groundwater flow system for better land use management purposes with respect to nitrogen loads. By comparing the groundwater flow systems and transit time maps a similar analysis can be performed.

The choice of using only strong particle sinks in MODPATH was based on the assumption that the presence of weak sinks (drainage) leads to a lower net recharge only (Batelaan and De Smedt, 2004). These lower recharge rates are already visualized in Figure 2.4, and are reflected by the groundwater flow in general, and thus by the maps. Furthermore the use of strong sinks reduces the amount of discharge cells, making the deduction of groundwater flow systems more straightforward.

In order to prevent pathline errors, the model cell-size should be small enough (Haitjema et al. 2001). In the Hengelo groundwater flow model, cell sizes are much smaller than the characteristic leakage length. Conversely, path lines should not be interpreted at scales smaller than the scale necessary to accurately describe field features. In the study area this type of error are mainly due to small variations in ground level that may cause a small groundwater flow system to arise. These very small (few model cells) groundwater flow systems were therefore not discerned separately.

### **2.6.2 Groundwater flow systems**

The delineation of groundwater flow systems in this study resulted in more and smaller groundwater flow systems than in a previous study performed in the same area (Engelen and Kloosterman, 1996). This is mainly because of the much larger cell-size (250 x 250 m) in their study, which also meant streams were not explicitly represented by that model; they used areal drainage instead. The predicted locations of discharge areas are very similar in both models, just like the hydraulic head distribution, indicating the importance of topographical relief for groundwater flow. The smaller model cell-size in this study also enabled a more detailed geological schematization. This resulted in more deformed groundwater flow systems in the current study. The main reason for the differences in size, shape, and definition of groundwater flow systems however, is caused by the difference in technique to derive the groundwater flow system boundaries. When done based on particle paths and net recharge maps, only the largest, most obvious

systems will be identified. In this study these boundaries are deduced from the maps created from the particle tracking analysis, giving more objective and more detailed results.

### **2.6.3 Application of the method presented**

The method presented is generic; it can be applied in any situation that requires insight into the spatio-temporal distribution of groundwater. However, application specifics may depend on the characteristics of the aquifer under study. For example, when large differences in depth to groundwater table are found, it might be better to relate the depth intervals to the groundwater table. One may be more interested in travel distance in a specified aquifer when a multiple aquifer system is considered.

Also, application of the method used in this study in natural stream networks may result in complex and large discharge areas, a problem also encountered in defining stream catchment and subcatchment areas and boundaries (Strahler, 1952), which is analogous to the delineation of groundwater flow systems. In the field of stream catchment delineation solutions are being developed for such scale problems (e.g. Jones, 2002; Lacroix et al. 2002).

## **2.7 CONCLUSIONS**

Even though hydrological models have been available for several decades, assessment of groundwater flow and its relation to groundwater quality and aquifer vulnerability through hydrological modelling has not been optimal. It was shown that with relatively simple postprocessing of the hydrological model results, direct insight in regional groundwater flow patterns can be obtained. This is especially helpful when aquifers with complex geology and drainage are considered, and where the configuration of groundwater flow systems is very sensitive to the fine-scale variations in topography, or where human interventions in the system may have had a large influence on groundwater flow i.e. in aquifers where flow directions are not evident.

The application of the groundwater flow systems analysis was expanded towards three dimensions. This means the recharge areas for streams, discharge areas, and wells, can directly be derived, and can be interpreted in terms of historical and future diffuse input of contaminants by also considering transit times. The delineation of future and past pathways of point source pollution is achieved by using pathline maps in combination with 'travel distance at specified depth' maps. This can give support for determining background values, to bound diffuse and point source pollution, to identify areas vulnerable to pollution, to determine options for sanitation, and for 'water sensible planning' in general, for example by managing land-use on recharge areas of valuable wetlands. The method presented in this paper can be readily implemented for any existing groundwater flow model.

## 2.8 REFERENCES

- Batelaan, O., De Smedt, F., Triest, L. (2003), Regional ground water discharge: phreatophyte mapping, ground water modelling, and impact analysis of land-use change. *Journal of Hydrology* 275, pp 86-108
- Batelaan, O., De Smedt, F. (2004), SEEPAGE, a new MODFLOW DRAIN package. *Ground Water* 42, pp 576-588
- Blair, E.S., Sheets, R.A., Eberts, S.M. (1990), Particle-tracking analysis of flow paths and traveltimes from hypothetical spill sites within the capture area of a wellfield. *Ground Water* 28, pp 884-892
- Bolin, B., Rodhe, H. (1973), A note on the concepts of age distribution and transit time in natural reservoirs, *Tellus*, 25, pp 58-62
- Bryan, B.A. (2003), Physical environmental modeling, visualization and query for supporting landscape planning decisions. *Landscape and Urban Planning* 65, pp 237-259
- Buxton, H.T., Reilly, T.E., Pollock, D.W., Smolensky, D.A. (1991), Particle tracking analysis of recharge areas on long island, New York. *Ground Water* 29, pp 63-71
- Christensen, T.H., Bjerg, P.L., Banwart, S.A., Jakobsen, R., Heron, G., Albrechtsen, H-H. (2000), Characterization of redox conditions in ground water contaminant plumes. *Journal of Contaminant Hydrology* 45, pp 165-241
- De Mulder, E.F.J., Geluk, M.C., Ritsema, I.L., Westerhoff, W.E., Wong, Th.E. (2003), De ondergrond van Nederland, Wolters-Noordhoff bv Groningen/Houten, The Netherlands
- Doherty J., Brebber, L., Whyte, P. (1994), PEST: Model Independent Parameter estimation. *Watermark Computing*, TIC: 240719, Oxley, Australia
- Engelen, G.B. (1981), A systems approach to groundwater quality – Methodological aspects. *The Science of the Total Environment* 21, pp 1-15
- Engelen, G.B., Kloosterman, F.H. (1996), Hydrological systems analysis, methods and applications. *Water Science and Technology Library* 20, Kluwer academic publishers
- Eriksson, E. (1971), Compartment models and reservoir theory. *Annual Reviews in Ecosystems and Systematics* 2, pp 67-84
- Falkenmark, M., Allard, B. (1991), Water quality genesis and disturbances of natural freshwaters, In: Hutzinger, O. (ed) *The handbook of environmental chemistry* 5, part A: Water pollution. Springer-Verlag, Heidelberg-Berlin, pp 45-78
- Focazio, M.J., Reilly, T.E., Rupert, M.G., Helsel, D.R. (2002), Assessing ground water vulnerability to contamination: providing scientifically defensible information for decision makers. *USGS Circular* 1224
- Frapporti, G., Hoogendoorn, J.H., Vriend, S.P. (1995), Detailed hydrochemical studies as a useful extension of national ground-water monitoring networks. *Ground Water* 33, pp 817-828
- Gogu, R.C., Dassargues, A. (2000), Current trends and future challenges in ground water vulnerability assessment using overlay and index methods. *Environmental geology* 39, pp 549-559
- Haitjema, H., Kelson, V., De Lange, W. (2001), Selecting MODFLOW cell sizes for accurate flow fields, *Ground Water* 39, pp 931-938
- Harris, G., Clary, M.B., Hatzinger, P., Root, K. (1988), Mapping ground water recharge areas for land use planning, a case study in northern New York, USA. *Land Use Policy* July 1988, pp 329-340
- Jones, N.L., Budge, T.J., Lemon, A.M., Zundel, A.K. (2002), Generating MODFLOW grids from boundary representation solid models. *Ground Water* 40, pp 194-200
- Jones, R. (2002), Algorithms for using a DEM for mapping catchment areas of stream sediment samples. *Computers & Geosciences* 28, pp 1051-1060
- KNMI (Royal Dutch Meteorological Institute), 1991-1998, Maandoverzicht van de Neerslag en Verdamping in Nederland (Monthly recharge and Evapotranspiration in the Netherlands), De Bilt, the Netherlands
- Lacroix, M.P., Martz, L.W., Kite, G.W., Garbrecht, J. (2002), Using digital terrain analysis modeling techniques for the parameterization of a hydrologic model. *Environmental Modelling & Software* 17, pp 127-136
- MacQuarrie, K.T.B., Sudicky, E.A., Robertson, W.D. (2001), Multicomponent simulation of wastewater-derived nitrogen and carbon in shallow unconfined aquifers II. Model application to a field site. *Journal of Contaminant Hydrology* 47, pp 85-104

- Makkink, G.F., 1957, Testing the Penman formula by means of lysimeters. *International Journal of Water Engineering* 11, pp 277-288
- McDonald, M.G., Harbaugh, A.W. (1988), A Modular-Three Dimensional Finite Difference Ground-water Flow Model, *Techniques of Water Resources Investigations of the USGS. Book 6, Chapter A1.*
- Meinardi, C.R. (1994), Ground water recharge and travel times in the sandy regions of the Netherlands. Phd thesis Vrije Universiteit Amsterdam, Amsterdam, the Netherlands
- Nolan, B.T., Ruddy, B.C., Hitt, K.J., Helsel, D.R. (1997), Risk of nitrate in ground waters of the United States - a national perspective. *Environmental Science and Technology* 31, pp 2229-2236
- Osborne, L.L., Kovacic, D.A. (1993), Riparian Vegetated Buffer Strips in Water-Quality Restoration and Stream Management. *Freshwater Biology* 29, pp 243-258
- Pebesma, E.J., De Kwaadsteniet, J.W. (1997), Mapping ground water quality in the Netherlands. *Journal of Hydrology* 200, pp 364-386
- Pollock, D.W. (1994), User's Guide for MODPATH / MODPATH-PLOT, Version 3: A particle tracking post-processing package for MODFLOW, the U. S. Geological Survey finite-difference ground-water flow model. USGS Open File Report 94-464
- Robinson, M.A., Reay, W.G. (2002), Ground water flow analysis of a mid-atlantic outer coastal plain watershed, Virginia, U.S.A. *Ground Water* 40, pp 123-131
- Sánchez-Martos, F., Jiménez-Espinosa, R., Pulido-Bosch, A. (2001), Mapping ground water quality variables using PCA and geostatistics: a case study of Bajo Andarax, southeastern Spain. *Hydrological Sciences* 46, pp 227-241
- Strahler, A.N. (1952), Hypsometric (area-altitude) analysis of erosional topography. *Bulletin of the Geological Society of America* 63, pp 1117-1142
- Tóth, J. (1963), A theoretical analysis of ground water flow in small drainage basins. *Journal of Geophysical Research* 68, pp 4795-4812
- USEPA (1993), A review of methods for assessing aquifer sensitivity and ground water vulnerability to pesticide contamination. USEPA, Office of Water, Washington DC
- Van der Lee, J., De Windt, L. (2001), Present state and future directions of modeling of geochemistry in hydrogeological systems. *Journal of Contaminant Hydrology* 47, pp 265-282
- Vissers, M.J.M., Frapporti, G., Hoogendoorn, J.H., Vriend, S.P. (1999), The dynamics of ground water chemistry in unconsolidated aquifers: The Salland section. *Phys. Chem. Earth (B)* 24, pp 529-534
- Wang, X. (1997), Conceptual design of a system for selecting appropriate ground water models in ground water protection programs, *Environmental Management*, 21, pp 607-615
- Winter, T.C., Rosenberry, D.O., Sturrock, A.M. (1995), Evaluation of 11 equations for determining evapotranspiration for a small lake in the north central United States. *Water Resources Research* 31, pp 983-993
- Worrall, F., Besien, T., Kolpin, D.W. (2002), Ground water vulnerability: interactions of chemical and site properties. *The Science of the Total Environment* 299, pp 131-143
- Zijl, W. (1999), Scale aspects of ground water flow and transport systems. *Hydrogeology Journal* 7, pp 139-150

# 3 THE STABILITY OF GROUNDWATER FLOW SYSTEMS IN UNCONFINED SANDY AQUIFERS IN THE NETHERLANDS

M.J.M. Vissers, M. van der Perk

**Abstract.** Groundwater flow patterns are temporally variable and uncertain, due to climatologically or anthropogenically induced variation in boundary conditions, and uncertainties in hydraulic model parameters. The quantification and mapping of uncertainty in flow patterns is especially essential in relatively flat areas where flow direction is sensitive to centimetre-scale head variations. In this study we aim to quantify and map the sensitivity of shallow groundwater flow patterns to uncertainties in anisotropy, drainage resistance, variations in drainage level and groundwater recharge for a sandy unconfined aquifer in the Salland region, the Netherlands. For this purpose, the most probable configuration of current groundwater flow systems was mapped using particle tracking and Monte Carlo analysis. Sensitivity was represented by the membership of each model cell to the defined groundwater flow systems given the uncertainties and variations in the hydraulic parameters and boundary conditions. In addition, the current configuration of groundwater flow systems was compared to the historical situation without artificial drainage. The average groundwater flow system size was found to be in the order of a few square kilometres, with a relatively stable configuration. In contrast to the intrinsic and temporally invariant hydraulic parameters, which were shown to have a minor influence on the spatial configuration of groundwater flow systems, natural variation in recharge and variations in drainage level management exert a large influence.

*Keywords: Systems analysis, Drainage, Anisotropy, Flow Paths, the Netherlands, Monte Carlo analysis*

## 3.1 INTRODUCTION

In the past decade, there has been a growing interest in information on groundwater flow for land use planning and the conservation and management of ecosystems in addition to the traditional fields of groundwater sanitation and well capture zone delineation (Harris et al. 1988; Van Buuren, 1991; Robinson and Reay; 2002, Batelaan et al. 2003). The analysis of groundwater flow systems (Tóth, 1963; Engelen and Kloosterman, 1996) provides valuable insight in flow patterns, which, when combined with knowledge on contaminant input and geochemical processes, provides detailed insight in the spatio-temporal distribution of groundwater quality. The groundwater flow systems analysis provides an answer to an important water quality related issue, which is to relate observed water quality in streams, discharge areas, and wells at one moment in time to their recharge areas in terms of past land use and water quality (Falkenmark and Allard, 1991).

Mapping groundwater flow is usually performed using particle tracking, as isohypses conceal most details of groundwater flowpaths. In capture zone modelling, backward particle tracking analysis is frequently used (Bair et al. 1991; Frind et al. 2002), but also forward procedures are used to assess the probability of capture (Hunt et al. 2001; Van Leeuwen et al. 1999). In assessments of free groundwater systems forward tracking procedures are also used. Modica et al. (1997) used detailed forward particle tracking analysis to investigate the influence of streams in a generic aquifer, combined

with parametric analysis of aquifer parameters. Buxton et al. (1991), and later Robinson and Reay (2002) and Batelaan et al. (2003) mapped groundwater residence times in a region or catchment using forward particle tracking. In *chapter 2* it was demonstrated that results from forward particle tracking analyses can be rendered into comprehensible two-dimensional maps of three-dimensional groundwater flow. These include map representations of groundwater flow systems combined with transit time, transit distance, travel distance at specified depths, net groundwater recharge, and piezometric heads.

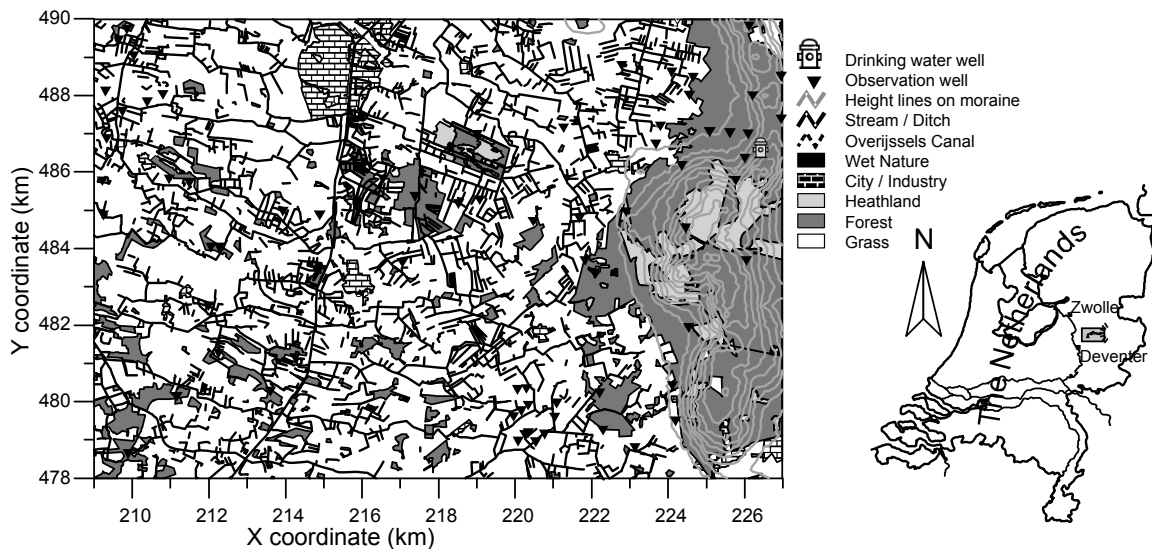


Figure 3.1 Location of the Salland study area in the Netherlands, land use, and topography of the study area (Coordinates in km RDS, Dutch ordnance datum), observation wells, the location of the groundwater abstraction well, as well as the full drainage network (streams and ditches) and main canal

However, the delineation of groundwater flow systems is not unambiguous, even in aquifers with relatively simple geometry (Frapporti et al. 1995). Zijl (1999) showed that the hydraulic anisotropy and the ‘wavelength’ of the topography, which often corresponds to the distance between streams, are the critical parameters that determine the penetration depth of groundwater flow systems and thus their hierarchical configuration. However, uncertainties in hydraulic parameters that determine this anisotropy and wavelength, i.e. horizontal and vertical hydraulic conductivity and drainage level and resistance, give rise to uncertainties in the size and spatial configuration of the groundwater flow systems. Furthermore, the boundaries of flow systems may be unstable or move due to climatologically or anthropogenically induced changes in boundary conditions. Seasonal and inter-annual variations in groundwater recharge may lead to contraction and expansion of the stream network (De Vries, 1995), and thus in changes in the flow pattern. Human interventions in the drainage system, groundwater extraction, or artificial recharge can have substantial, but often unknown, effects on the spatial configuration of groundwater flow systems.

Up to date studies of uncertainties in groundwater flow modelling have largely been focused on the assessment of the influence of uncertainty and heterogeneity in model parameter values and boundary conditions on groundwater flow (e.g. Gomez-Hernandez and Gorelick, 1989; Varljen and Shafer, 1991; Vassolo et al. 1998) and the



quantification of uncertainty of well-capture zones (e.g. Bair et al. 1991; Bhatt, 1993; Van Leeuwen et al. 1999; Wheeler et al. 2000). Uncertainties in free groundwater flow patterns have not been quantified. These uncertainties and variations in groundwater flow pattern may impede the determination of past and future groundwater flowpaths and, consequently, hamper the solution to the above stated water quality related issue. Therefore, quantification of the uncertainties and variations in groundwater flow patterns is essential in the analysis and interpretation of spatial and temporal patterns in groundwater quality.

The aim of this study is to quantify and map the sensitivity of shallow groundwater flow patterns in a relatively flat, sandy unconfined aquifer, to variations in anisotropy in hydraulic conductivity, drainage level, drainage resistance, and groundwater recharge. For this purpose, the Salland region, the Netherlands, was chosen as study area, because this area is typical for sandy areas in the Netherlands with respect to topography and aquifer properties. A three-dimensional hydrological model was set up using MODFLOW (McDonald and Harbaugh, 1988) and calibrated against observed piezometric heads. Groundwater flow paths were computed using MODPATH (Pollock, 1989) and were used to map groundwater flow. A Monte Carlo analysis was performed to automatically map the spatial configuration of groundwater flow systems. To assess the stability of the flow patterns the following steps were undertaken. First, the current spatial configuration of groundwater flow systems was compared to the natural pattern without artificial drainage. Second, a sensitivity analysis was performed to assess the hydraulic parameters and model boundary conditions to which groundwater flow patterns are most sensitive.

### 3.2 STUDY AREA

The study area comprises an area of 12 km x 18 km situated in the Salland region in the eastern part of the Netherlands (Figure 3.1). The area stretches across a cover sand plain with undulating topography in the western part of the study area towards the 'Holterberg' ice-pushed ridge (ice-displaced local deposits), which reaches +75 m OD, in the eastern part (Figure 3.1 and 3.2). The cover sand (Boxtel Formation, Wierden Member; De Mulder et al. 2003) is a few meters thick and covers coarser fluvial sands (Kreftenheye Formation). These sandy deposits, that formed during the late Saalian, Eemian and Weichselian (~150 – 11 ka BP) comprise the studied aquifer with a base typically at –30 m OD. In the far west fine-grained floodbasin deposits locally occur within the Kreftenheye sands at approximately –10 m OD. The western half of the study area is underlain by impermeable fluvio-glacio-lacustrine clays (Kreftenheye Formation, Twello Member) (see Figure 3.2).

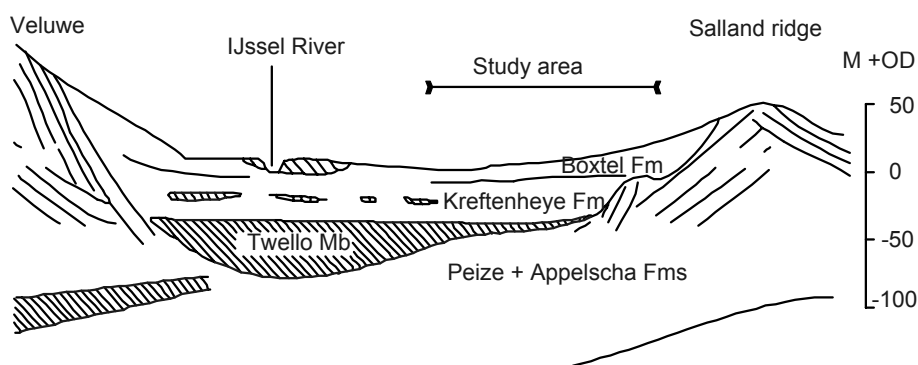


Figure 3.2 Geological E-W cross-section trough the study area

Until the mid 19<sup>th</sup> century, there were hardly any streams present in the area and groundwater was discharged through evapotranspiration in wetlands. In 1858 AD the Overijssels Canal crossing the model area from south to north was excavated. As the population increased in the 19th century, the poor sandy soils near the ridge were locally cultivated and drained by canals and ditches. Most of the sandy soils east of the canal remained vegetated by heather. With the introduction of artificial fertilizers after 1900 much of the heather was rapidly removed and the land was drained and cultivated. The drainage pattern follows the low-lying areas between the cover sand ridges. The stream density is 1.7 km/km<sup>2</sup>, which means that the average stream distance is 580 m (not including the small ditches). Current land use is mainly grassland with some patches of forest. Most people live in small villages.



Figure 3.3 Fixed drainage level areas and catchment areas (grey shades), and streams maintained by the water board (dotted lines); random areas for the Monte Carlo analysis are indicated by 'X', extend is the same as in Figure 3.1

Groundwater levels in the low-lying, western part of the study area are currently managed in 'fixed drainage level areas' by the local water board. In these areas, the drainage levels

are maintained by means of weirs in the artificial streams (Figure 3.3). During summertime the drainage levels are about 0.20 m higher than in winter to retain water for agricultural use. There are two drinking water abstraction wells in the area, One is located beneath the base of the phreatic aquifer, and does not affect the phreatic water table. The other well is situated in the northeast of the area, beneath the ridge (Figure 3.1). The pumping rate of this 'Nijverdal' well is  $5 \cdot 10^6 \text{ m}^3/\text{y}$ . In addition, farmers use local wells for crop irrigation during dry summers.

### 3.3 METHODS

#### 3.3.1 Groundwater flow model

A stationary groundwater flow model of the study area was set up in MODFLOW (McDonald and Harbaugh, 1988) with  $50 \times 50 \text{ m}$  cell size and six layers, as derived from the REGIS database (REgional Geohydrological Information System) provided by TNO-NITG (Dutch Institute of Applied Geoscience). The  $50 \times 50 \text{ m}$  cell size was chosen based on the average distance between the streams and was considered sufficiently small to accurately track flow paths (Haitjema et al. 2001). Surface elevation was taken from the  $25 \times 25 \text{ m}$  AHN (Algemeen Hoogtemodel Nederland) elevation model provided by the Ministry of Transport, Public Works and Water Management. Fixed-level head boundaries were used to conceptualize the sides of the model. The eastern model boundary coincides approximately with the groundwater divide on the ice-pushed ridge, but since the influence of the groundwater extraction (see Figure 3.1) on the location of the groundwater divide was not a priori known, a fixed-level head boundary was used here as well. The fixed heads at the model boundaries were derived and optimized using interpolated observed piezometric heads in and around the area.

Net recharge was estimated from precipitation and evapotranspiration data provided by the meteorological institute (KNMI, 1966-2003). Average annual rainfall in the period 1966 - 2003 amounts to 782 mm. Reference evapotranspiration (KNMI, 1966 - 2003) is provided according to Penman (1948) for the period 1966-1988 (open-water  $E_o$ ) and according to Makkink (1957) afterwards (reference grassland evapotranspiration  $E_r$ ; where  $E_r = E_o \cdot 0.8$ ). The average value of reference evapotranspiration for grassland over the entire period is 528 mm/yr, and is relatively constant. This would lead to an average grassland net recharge of 255 mm/yr. However, net recharge shows a seasonal pattern of shortage in summer and a surplus in winter. Also between different years large differences exist, which is illustrated in Figure 3.4. A correction for evaporation depletion in summer of 70 mm/yr on average (Meinardi, 1994) leads to a groundwater recharge rate of approximately 325 mm/yr for grassland. Crop factors were used for heather (0.9) and forest (0.7) to estimate evaporation relative to reference grassland evaporation, though it may be larger in areas with a shallow water table (*chapter 4*). For built-up areas the net recharge was assumed to be 0.5 times net recharge for grassland.

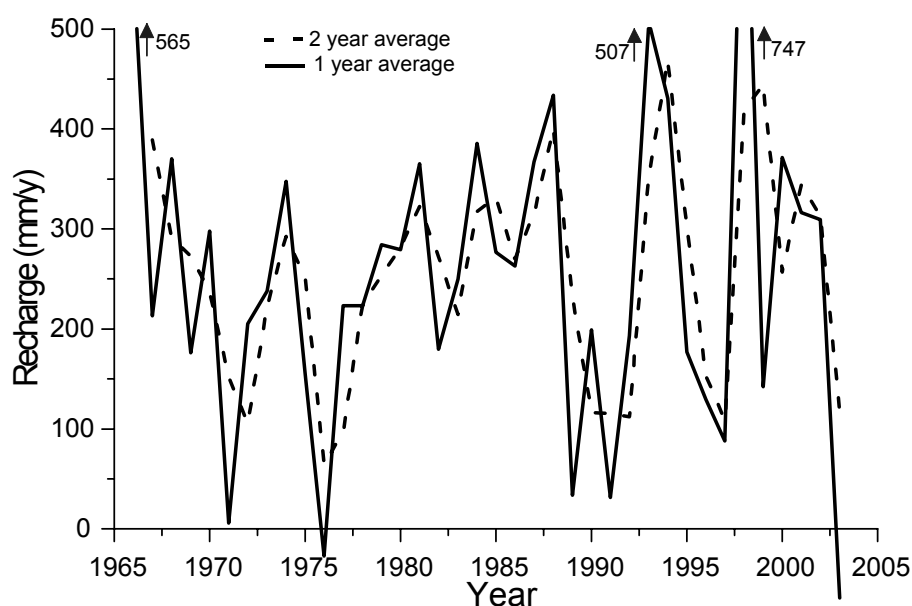


Figure 3.4 Yearly recharge from 1966-2003 in the Netherlands (1 and 2 year averages)

Drainage levels were taken from the data on winter drainage levels provided by the local water board. A good match between the minimum elevation minus 0.60 m and the drainage level was found which provided a check on the data obtained from the water board. Large deviations from this rule of thumb were examined and where necessary adapted. Such large deviations occurred mostly at the foot of the ridge, where weir levels in the low parts of the fixed drainage level areas do not represent the drainage level in the tributary ditches in the upstream parts of the drainage area. In these cases, the fixed drainage level areas were divided into two or more subareas, for which different drainage levels were established. Drainage resistance was calculated assuming a stream width of 1 m, and a streambed conductance of 5 m/d. The drainage network data were incorporated in the model in the form of drainage cells rather than river cells, because in summer many streams and ditches are dry, and the influence of infiltrating streams is considered to be very minor (see De Vries, 1994).

Previous transient and steady state modelling efforts (Van Uden and Vissers, 1998; Hoogendoorn, 1990) provided initial values for hydraulic conductivity. The hydraulic conductivities were further calibrated manually using average values of biweekly measured groundwater heads in observation wells from the DINO database (Data and Information of the Dutch Subsurface, TNO-NITG). Only wells for which more than 100 measurements in the period 1991-1998 are available (71 wells) were used for model calibration. Three observation wells were omitted; one because it displayed heads above ground level, the others because they are situated on the ridge, and displayed high (>2 m) deviations from the calculated pattern, probably due to tilted clay layers in the ice-pushed ridge. The hydraulic conductivities of the layers were further optimized using automatic parameter estimation using PEST (Doherty, 1994) assuming isotropy.

To estimate the effect of the artificial drainage pattern, the historic situation was simulated by removing the artificial streams and ditches in the model area. Instead, a diffuse drainage level of 0.5 m beneath the surface level was used. The diffuse drainage

was combined with a layer of very high hydraulic conductivity on top of the surface level, similar to Batelaan et al. (2003), to ensure a constant head boundary when groundwater rises above the surface level. The drainage resistance was optimized manually, so that a maximum similarity between modelled wetlands and those depicted on a historical map from 1848 of the area (Wolters-Noordhof Atlasproducties, 1990) was achieved.

The results from the calibrated groundwater flow model were analyzed using MODPATH (Pollock, 1989) following the method explicated in *chapter 2*. Transit distance and transit time maps of the area were derived using forward particle tracking. In the centre of each cell, a particle was placed at the water table and all particles were traced to their respective discharge area. For each particle, the horizontal transit distance and transit time in years were recorded and stored as attribute values of the initial location of the particles. The resulting maps depict the time and distance groundwater will travel from the point of infiltration. In addition, the recharge areas of deep groundwater were identified using backtracking from each cell at 0.8 times the depth of the shallowest clay layers. Vertical cross-sections of groundwater age and transit distance were generated by backward particle tracking. In each cell, particles were placed at an interval of 1 m down to -30 m OD, an interval of 2 m between -30 m and -50 m OD, and an interval of 5 m further downwards. These particles were traced backwards to their point of infiltration. Also in this case the travel time (i.e. groundwater age) and transit distance were stored and linked to their initial location.

### 3.3.2 Sensitivity analysis

A sensitivity analysis was performed to identify to which model parameters or boundary conditions the current pattern of groundwater flow is most sensitive. For this purpose, an approach similar to that by Frapporti et al. (1995) and De Mars and Garritsen (1997), who analyzed changes in two-dimensional, vertical flow patterns in response to differences in anisotropy, was followed. Four factors, namely anisotropy, recharge, drainage resistance, and drainage elevations were varied independently. Table 1 lists the values and the number of model runs for each model parameter. The model results were presented as zones of membership to the groundwater flow systems that were automatically derived as described below.

*Table 3.1* Parameters and variables varied in the sensitivity analysis

Parameter	# of simulations	Values
Anisotropy	5	Vertical conductivities 0.5, 1, 2, 4, 8 times the initial anisotropy (= 1)
Drainage Resistance	15	Stepwise variation by a factor of 1.25, from 0.21 times to 4.77 times the drainage resistance as in the calibrated model
Recharge	37	Two-year moving average recharge for the 1966-2003 period (see Figure 3.4)
Drainage Level	25	Gaussian white noise with mean 0 and standard deviation of 0.25 m on the current drainage level areas.

The anisotropy was varied in five consecutive steps of a factor of two and drainage resistance in 15 steps of a factor of 1.25 (see Table 1). For recharge, the model was run for two-year moving average recharges for 1966-2003 (37 model runs, see Figure 3.4). Preliminary model calculations showed that two-year averaged recharge steady state models simulated the temporal variation in observed heads better than annual average recharge. Moreover, the use of two-year average recharge values avoided negative recharge values, because in some years a negative net annual average recharge occurred.

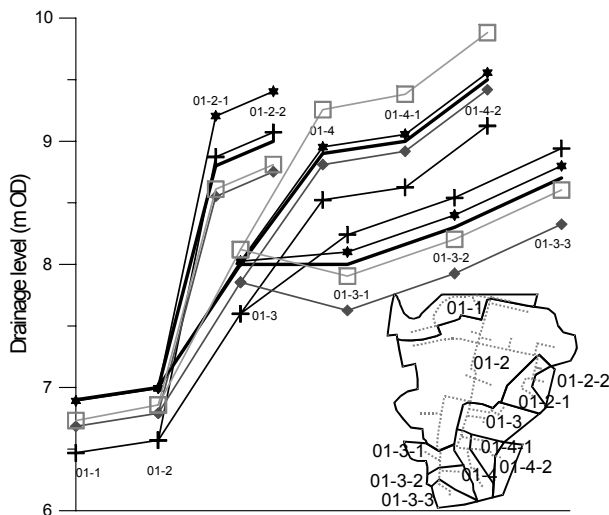


Figure 3.5 Four generated drainage level profiles in a discharge area, which is situated in the north-west of the study area (see Figure 3.3); the original (solid line) levels are also shown

Winter drainage levels of the streams were varied by adding Gaussian white noise with zero mean and 0.25 m standard deviation up- and downstream each stream and upstream large tributaries (Figure 3.5). In between the changed ‘fixed drainage level areas’, drainage levels were interpolated according to the existing topology of the streams. Because drainage level differences in different fixed drainage level areas are often in the order of tens of centimetres, the addition of variation may lead to topologically incorrect water levels in the stream network in a few cases (also visible in Figure 3.5). The variation imposed on the drainage levels is relatively large compared to current variations in water levels, but the variation resembles the changes in drainage level over the past 25 years and possible changes due to spatial planning and nature conservation measures in the near future.

### 3.3.3 Automatic derivation of groundwater flow systems

In order to facilitate the automatic mapping of groundwater flow systems, the continuous discharge areas that define them (Tóth, 1963, *chapter 2*) were identified. For this purpose, a Monte Carlo analysis was performed to derive the most probable configuration of groundwater flow systems under natural and humanly induced variations. These variations concerned model variables that are not inherent to the aquifer, i.e. drainage level and recharge. Drainage level is the only parameter that can change and has significantly changed due to human interventions and recharge is highly variable in time

(Figure 3.4). One hundred generated drainage input files were combined with a two-year average recharge file randomly chosen from the 37 files used in the sensitivity analysis (Table 1). The recharge data were rounded off to tenths of mm per day. This resulted in a total of 100 model simulations and, accordingly a set of 100 realizations of groundwater flow patterns generated by MODPATH.

All endpoint files from the Monte Carlo simulation were put into a database, resulting in 100 (number of model runs)  $\times$  86,400 (number of cells) records with cell coordinates of starting and endpoints. The continuous discharge areas were derived by buffering the endpoint cell coordinates with a 150 m (3 model cells) radius circle in a geographical information system (GIS). The spatial delineation of the groundwater flow systems was subsequently achieved by determining the discharge area to which each cell discharges in the majority of the simulations. However, many small continuous discharge areas never constitute the most occurring discharge area of any source cell, and thus the groundwater flow system has zero size. In addition, very small systems are not mappable. Therefore, groundwater flow systems were discarded if their size was smaller than 50 model cells (approximately 175 x 175 m). The cells originally belonging to these small systems were assigned to the next most probable, large groundwater flow system.

## 3.4 RESULTS

### 3.4.1 Model calibration

Table 2 lists the calibrated hydraulic conductivities for the different geological formations in the study area. The apparently low calibrated conductivity for the ice-pushed ridge is probably due to the pushed layers that cause high anisotropy and resistance in unknown directions. The calibrated stationary model showed a mean error of -0.06 m, a mean absolute error of 0.19 m, and a root mean square error of 0.23 m. The good results of the calibration are mainly due to the accurate information on drainage levels in the area. Using a no-flow boundary instead of a fixed head boundary at the sides of the deep aquifer beneath the Twello Member clay layer had no visible effect on groundwater flow and recharge areas of deeper groundwater. For the historical model, a drainage conductance of 5000 m<sup>2</sup>/d yielded the closest resemblance between the locations of wetted cells (i.e. cells where water levels exceed surface elevation) and the locations of wetlands as derived from historical maps for 1850 AD.

*Table 3.2* Formations and their calibrated hydraulic conductivities

Formation	Calibrated K
Ice-Pushed Ridge	1 m/d
Boxtel Formation	5 m/d
Kreftenheye Formation	12 m/d
Eemian Clays	0.001 m/d
Twello (Clay) Member	0.001 m/d
Peize / Appelscha Formation	20 m/d
Oosterhout Basement	-

### 3.4.2 Groundwater flow and flow systems

Figure 3.6 shows the automatically derived groundwater flow system boundaries on top of the transit time and transit distance maps according to the calibrated stationary model. The maps show a complex groundwater flow pattern with 201 groundwater flow systems (average size approximates 1 km<sup>2</sup>, median size = 0.4 km<sup>2</sup> not counting the systems east of the ridge). The general groundwater flow direction is towards the west but is highly variable especially near discharge areas that are small compared to their recharge areas. In the eastern part of the model area elongated systems are prevailing, mostly originating from the ice-pushed ridge. Towards the west, where the topography is flattening, the flow systems become more round in shape. Some elongated groundwater flow systems are also present in the western part of the area, but these are shaped by their elongated discharge areas: streams. In the eastern part of the area, the recharge area of the well abstraction is also clearly visible by the circular transit distance pattern around the pumping location, shifting the groundwater divide of the ridge to the west (compare the height lines in Figure 3.1). Some flow systems do not have a discharge area at first sight and are entirely black in both figures. These systems are 'recharge windows' of regional groundwater flow systems. The groundwater infiltrating in these areas ends up in or beneath the Twello Member clay layer or surpasses other groundwater flow systems before it is discharged. They have very long transit times and distances, and are often discharged at the model boundaries. The influence of the fixed head boundary is locally seen at the model boundaries in the eastern part of the model area.

The boundaries of the groundwater flow systems indicate recharge areas of deep groundwater (Figure 3.6). Water infiltrated near the groundwater flow system boundaries travels a much deeper path than water recharging the centre of these systems that follows a superficial path until reaching the same discharge area. Deeper flow paths are accompanied by longer transit times. This effect was also described by Modica et al. (1997).

The result of the backward tracking simulation, used to identify recharge areas of deep groundwater, is shown in Figure 3.7. The observed recharge areas are mainly determined by the drainage pattern. The recharge areas of deep groundwater are in all cases groundwater flow system boundaries (compare Figure 3.6), and are in that way helpful to derive the fully penetrating groundwater flow systems. Some areas are very wide, and can be considered as significantly recharging the deeper parts of the aquifer, whereas others are very narrow, meaning that these areas are not substantially recharging deep groundwater, but merely indicate the presence of a groundwater flow system boundary.



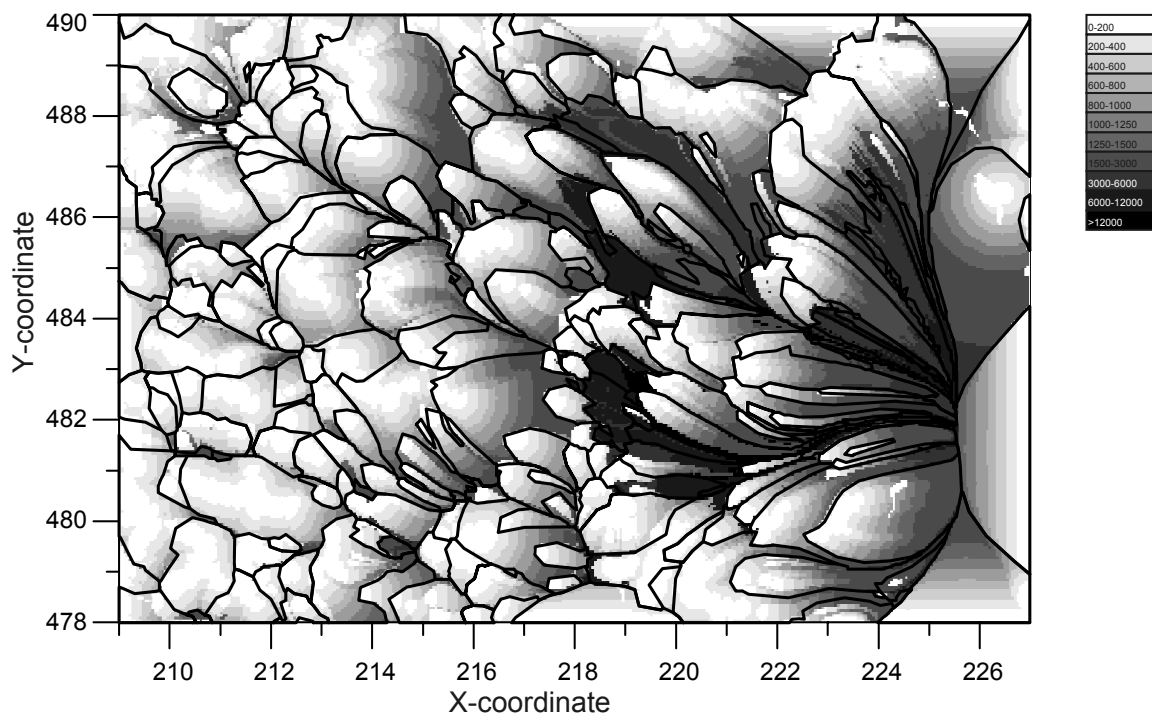


Figure 3.6 Groundwater flow system boundaries as derived from the Monte Carlo analysis superimposed on (a) Transit time in years and (b) Transit distance in meters derived from the calibrated model

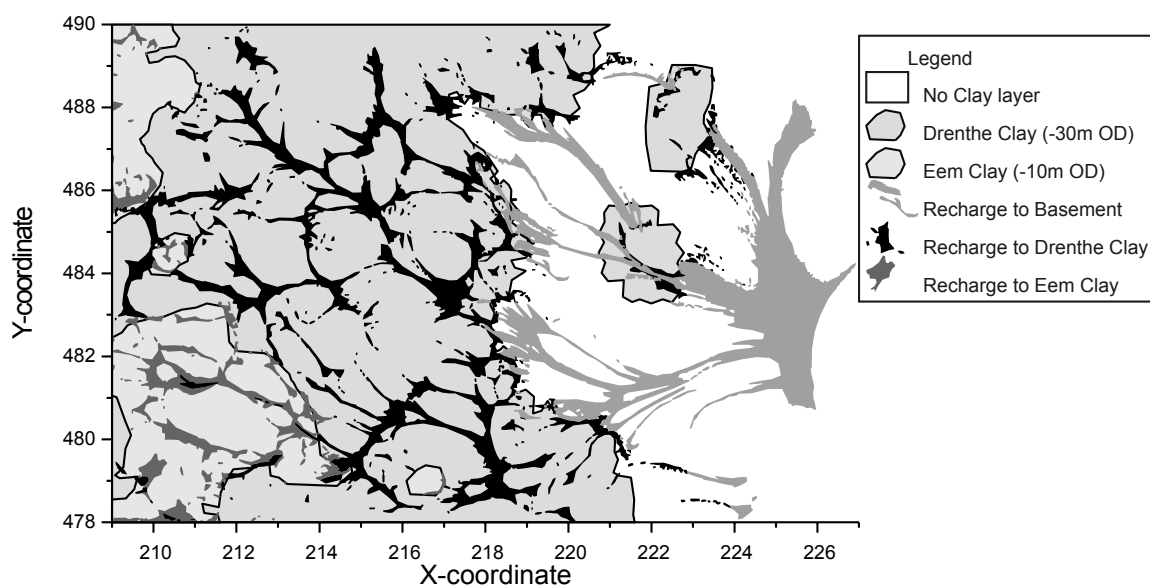


Figure 3.7 Deep infiltration areas derived from the calibrated model, where particles reach 0.8x the depth of the clay layers or 0.8x the base of the aquifer in m OD

Figure 3.8 shows the groundwater age in three cross-sections across some groundwater flow systems. As can be expected in recharge areas, i.e. the largest part of the study area, the age of the groundwater increases with depth and is approximately constant at a given depth. The age-depth relation remains constant across the flow system boundaries. Only in discharge areas and below clay layers a different, more variable, age-depth relation is found. In a transit distance cross section flow direction can be obtained and groundwater flow system boundaries would be visible as water divides with zero transit distance.

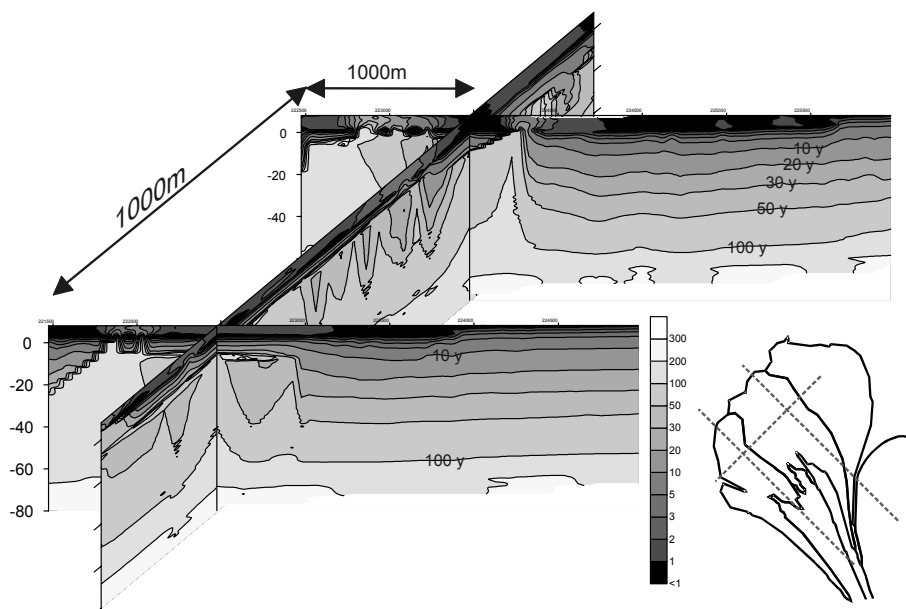
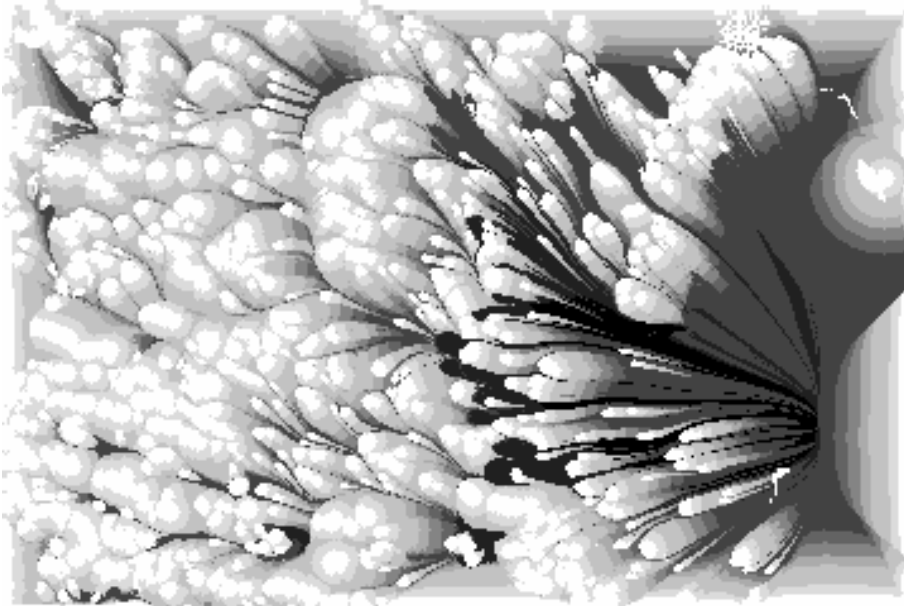


Figure 3.8 Groundwater age in three cross-sections across some groundwater flow systems in the northeast of the study area and the locations of these cross-sections (no clay layers in these sections)



*Figure 3.9* Transit distance for the historic, natural groundwater flow in the Salland area. The legend and extend are the same as in Figure 3.6

Figure 3.9 shows the transit distance map for the natural, historic situation, where the abstraction is still incorporated to enable better mutual comparison. At the foot of the ice-pushed ridge in the north-eastern part of the study area, the natural flow pattern does not deviate much from the current pattern (see Figure 3.6b). However, at the foot of the ice-pushed ridge in the central and south-eastern part of the area, the transit distances and the recharge area of deep groundwater are much larger than at present. Especially in this area and in the low-lying western part of the study area, artificial drainage has caused major shifts in the flow pattern. Compared to the current flow pattern, the historic situation shows expanded discharge areas due to the higher water tables.

### **3.4.3 Sensitivity analysis**

Figure 3.10 shows the results of the sensitivity analysis, in terms of membership intervals to the groundwater flow system as derived from the Monte Carlo analysis (see above). Five classes of probability that the infiltrating water is discharged within the same flow system as indicated by the black lines are discerned. The 0-40% class means that the water may end up in at least three different discharge areas. The 40-60% class is often encountered between two adjoining flow systems, which means that the probability that infiltrating water is discharged in the same system or the adjoining system is approximately equal. The 80-100 % class indicates that it is likely that the infiltrated water is discharged within the same system.

Figure 3.10a shows that the flow pattern is relatively insensitive to changes in anisotropy, important for the penetration depth of local systems. Even if the vertical conductivities are 1/8th of the original (horizontal) conductivities, the effect is generally minor. The recharge areas of deep groundwater were found to contract at higher

anisotropy, as more groundwater is recycled at shallower depths. The ‘recharge windows’ of the regional system (the black areas in Figure 3.6a and 3.6b) are particularly sensitive to this effect. Some small subsystems become larger at higher anisotropy, and some small systems change their discharge area completely (arrow in Figure 3.10a), but only for an anisotropy ratio of 8, which is unrealistically high for this area.

Figure 3.10b shows that also sensitivity to drainage resistance is relatively small in most areas. However, at very high conductivities the drainage cells start acting as a fixed head boundary, and discharge more water. This may lead to inactivation or size reduction of other groundwater flow systems (see arrows in Figure 3.10b). This only happens at a resistance of less than half of the calibrated value.

Figure 3.10c shows the sensitivity of the groundwater flow systems to recharge fluctuations. In periods of low recharge, the water table is lower, which causes groundwater to cease flowing towards drainage areas or streams opposite to the general westward flow direction. This effect is mainly visible at the fringes of the flow system westerly from the drainage areas (see arrows in Figure 3.10c). In low-recharge periods, also the recharge areas of deep groundwater become slightly smaller.

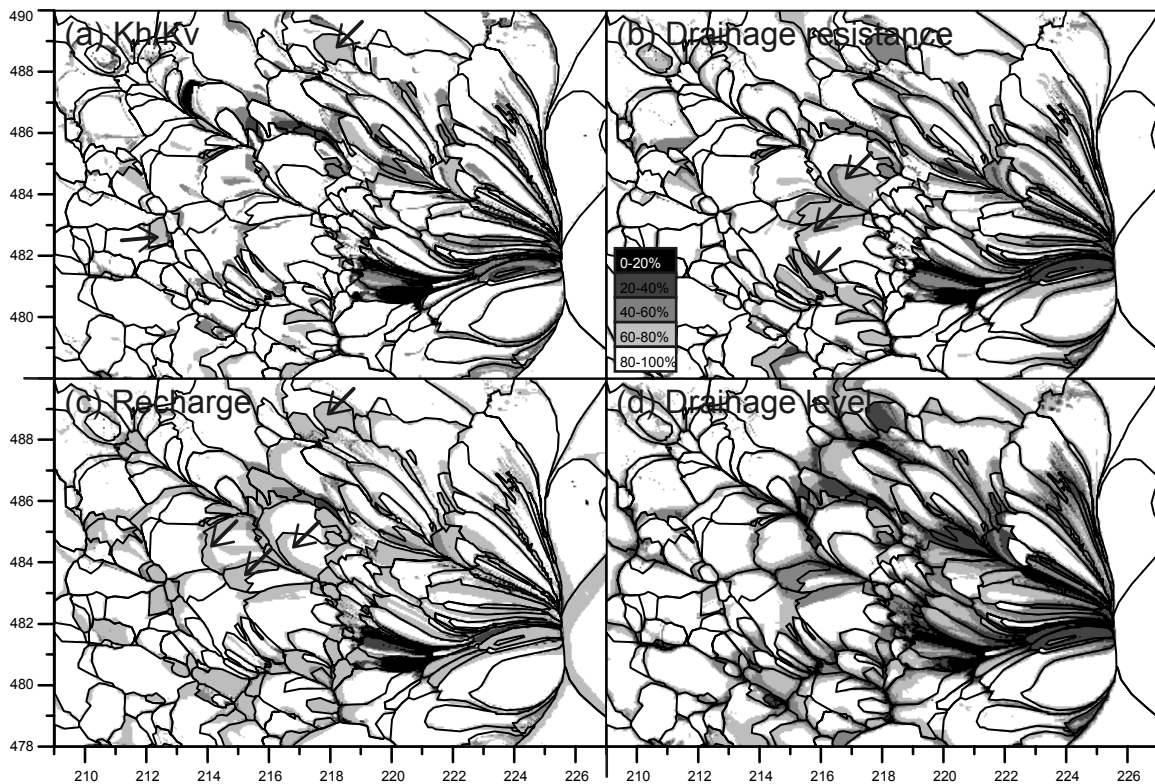


Figure 3.10 Comparison of model results as indicated by a 20% interval of membership to a predefined groundwater flow system with the most probable groundwater flow systems from the Monte Carlo simulation: (a) differences in anisotropy for calibrated groundwater model. Note that higher anisotropy causes a slight reduction in the area of deep recharge. (b) Influence of drainage resistance (c) differences in recharge, and (d) drainage level of the streams and ditches. The arrows indicate areas discussed in the text

Figure 3.10d shows the sensitivity to differences in drainage level. The effects of changes in drainage level are relatively large, and imply considerable displacements in the

position of groundwater flow systems. The areas where the effect of drainage level is largest correspond to the areas where the largest differences occurred between the historical and current situation (compare Figure 3.6b and Figure 3.9).

The sensitivity analysis demonstrates that most groundwater flow systems are quite stable, especially in the western, low-lying part of the model area, whereas systems near the ice-pushed ridge in the eastern part of the area are more sensitive to changes in the boundary conditions and hydraulic parameters. In general, smaller systems are more sensitive. The 'recharge window' of the regional system in the eastern part is particularly sensitive. Variations in drainage resistance and anisotropy are relatively unimportant for the configuration, shape and size of the groundwater flow systems in the Salland aquifer. Drainage level of the canals and ditches, which is determined by the management of fixed drainage level areas, and the fluctuations in effective recharge are most important for groundwater flow.

## 3.5 DISCUSSION

### 3.5.1 Assessment of the model

We examined the sensitivity of the shape, size, and position of groundwater flow systems in the Salland area, the Netherlands, to changes in hydraulic parameters and boundary conditions. We also presented a novel method to derive automatically the most probable configuration of groundwater flow systems by means of a Monte Carlo analysis. The automated mapping of the groundwater flow systems, the calculations of groundwater transit times and distances, and the sensitivity analysis were performed using particle tracking for stationary flow fields. The main reason for the use of a stationary model was that it is very effective in terms of computation time. To simulate a full water cycle with residence times of hundreds of years is very time consuming and would take millions of particles to be tracked (Rock and Kupfersberger, 2002). The residence times in the aquifer are much larger than could reasonably be achieved by a transient model run. However, the use of stationary model runs needs caution, as a calculated stationary flow pattern may deviate from the actual transient situation at a specific point in time. The largest part of the aquifer has a thin unsaturated zone, and a relatively constant characteristic response time (Kraaijenhof-van de Leur, 1958; Goode and Konikow, 1990) of 3-4 months. Only beneath the ice-pushed ridge the characteristic response time is larger; approximately 8 months not taking into account the unsaturated zone. The use of a steady-state model is admissible from that perspective; times are short enough to assume steady-state model runs to approximate transient conditions. In the Monte Carlo analysis, the variations in recharge and drainage level corresponded approximately to the long-term temporal variation and distribution of these variables. Therefore, it is likely that the stationary model results are a good representation of the average pattern of and variations in the transient groundwater flow in the study area.

### 3.5.2 Implications for groundwater flow system theory

In our analysis we encountered problems with existing definitions of groundwater flow systems. Tóth (1963) defined a groundwater flow system in a 2D cross-sectional view as ‘a set of flow lines in which any two flow lines adjacent at one point of the flow region remain adjacent throughout the whole region; it can be intersected anywhere by an uninterrupted surface across which flow takes place in one direction only’. Engelen and Kloosterman (1996) gave a different definition of a groundwater flow system: ‘a geographically distinct domain of the subsoil, which is filled with a pattern of flow lines from one coherent recharge area to one or more discharge areas’. They redefined the definition of Tóth’s groundwater flow system as a ‘flow branch’. Although the definition by Engelen and Kloosterman (1996) works well in a vertical cross section, it is ill-defined in a planar two-dimensional or three-dimensional view of groundwater systems. In most cases, also in this study, there is only one continuous recharge area in which many discharge areas are located, so according to the definition by Engelen and Kloosterman (1996) the entire study area is comprised of just one groundwater flow system. Therefore, we took the definition of Tóth as a starting point to analyze the flow pattern.

Nevertheless, we had to refine the definition by Tóth (1963) as stated above. The extension of this definition towards three dimensions implies that the set of adjacent flow lines can be curved, for example around a seepage area. For example, Figure 3.11 shows a schematic groundwater flow system in a stream with two tributaries. From this 3D flow example it follows that the intersecting uninterrupted surface must be curved around the seepage area. The figure displayed thus consists of one groundwater flow system, as may not directly be evident from a cross-sectional view.

The definition of a groundwater flow system would suffice as ‘a water volume defined by a set of adjacent flow lines’. This is for example the case when all flow lines are directed towards a single continuous discharge area; the characteristic used in this study. The definition in this way is analogous to that of surface water catchment areas.

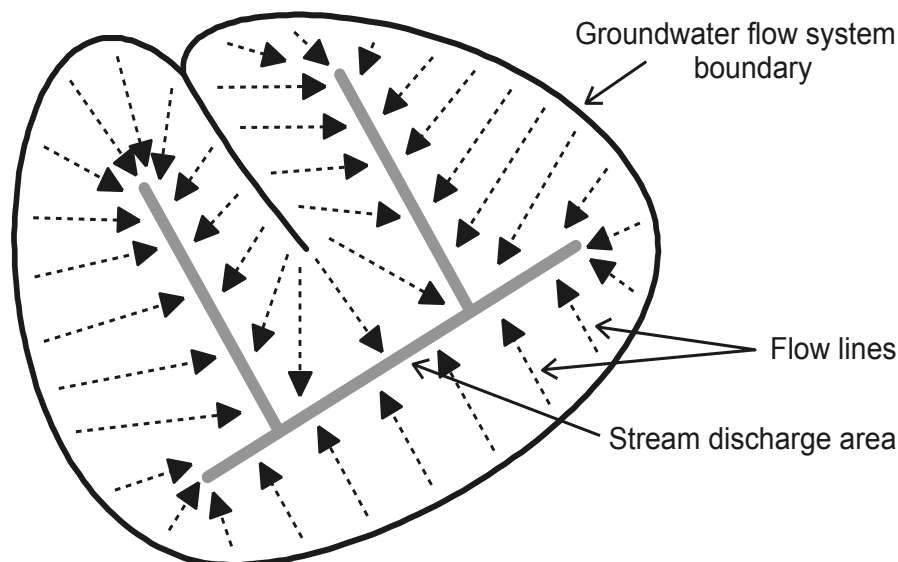


Figure 3.11 Identification the groundwater flow systems as the water volume defined by the set of fully adjacent flow lines

### 3.5.3 Groundwater flow patterns

The model results show that the groundwater flow pattern is largely controlled by the drainage pattern of the streams and ditches, and thus by the topography of the area. As a consequence, the transit distances are mostly less than one kilometre and the size of the groundwater flow systems is 1.0 km<sup>2</sup> on average when not accounting for the systems east of the ridge. Such relatively small-sized flow systems were also found for another aquifer around Hengelo town situated approximately 30 km east-south-east from the Salland area (*chapter 2*). Most flow patterns are local, except for a few regional systems fed by 'recharge windows' depicted in Figure 3.6 as black recharge areas without accompanying white discharge areas within the same system. The regional recharge areas comprise approximately 6% of the study area. This means 94% of the recharge is discharged in local groundwater flow systems and resurfaces within approximately 1 km.

The discharge areas are small compared to the recharge areas, which is in accordance with the findings by Puckett et al. (2002). Based on the wavelength and anisotropy of the area, the groundwater penetration depths can be expected to reach several hundreds of meters (Zijl, 1993). Therefore, the groundwater flow systems in most cases reach the base of the aquifer. In intensively drained areas (that may have about one ditch every 50 m) shallow, local systems may exist, as the penetration depth is much shallower (Zijl, 1999). Since these intensively drained areas are located in upward seepage areas, it is expected these will only display shallow rainwater lenses present in winter (Schot et al. 2004). In the study area, local systems never extend beneath the clay layers. Recharge of groundwater beneath clay layers is often located at the fringes of the clay layer, as is indicated in Figure 3.7.

### 3.5.4 Stability of groundwater flow systems

Comparison of the current flow pattern with the historical flow pattern (Figure 3.9) shows that the artificial drainage pattern has primarily led to larger, more distinct flow patterns in the present situation than in the past, more 'natural' situation. However, it also has caused discharge area contraction, i.e. smaller isolated discharge areas with intense discharge (hydrological fragmentation).

To analyze the stability of the current groundwater flow systems, a sensitivity analysis was performed in which anisotropy, drainage resistance, recharge rate and drainage level were varied. Anisotropy affects the horizontal position of the groundwater flow systems only to a minor extent. However, it influences the penetration depth of the groundwater, which causes the effect to be more pronounced in the recharge areas of deep groundwater. Variations in drainage resistance and groundwater recharge rates lead mostly to a change in convexity of the groundwater table. More pronounced convexities of the groundwater table were found for high recharge and high drainage resistance. These higher convexities cause more drainage areas to be active and more water to be attracted from downstream areas as backflow. Consequently, the variations in drainage resistance and recharge differences mainly influence the longitudinal shape of the groundwater flow systems. Variations in drainage levels in the stream network have the largest effect on the position of the groundwater flow systems, especially at the foot of

the ice-pushed ridge. This area corresponds to the area that showed the largest changes compared to the historical situation without artificial drainage.

From the sensitivity analysis, it can be concluded that the current groundwater flow systems are relatively stable. This implies that uncertainties in the hydraulic model parameters have only little impact on the spatial configuration of the flow systems. It also implies that recent and future interventions in the drainage levels have had and will have limited impact on the size and position of the flow systems. The largest changes in groundwater flow pattern occurred as a result of the construction of the artificial drainage network in the mid 19th century.

### **3.5.5 Implications for groundwater quality and contaminant transport**

Previous studies (e.g. Frapporti et al. 1995; Vissers et al. 1999) have shown that considerable volumes of the unconfined aquifer in the study area are affected by contaminants from agricultural sources. To identify the contaminant source areas and to assess the future contaminant dispersion, knowledge of the current groundwater flow pattern is especially valuable, since widespread diffuse pollution commenced in the 1950s, after the construction of the artificial drainage networks. Because the groundwater flow systems were found to be quite stable, contaminants advectively transported by groundwater flow, in principle, remain within the flow system in which they infiltrate. The transit time and transit distance maps (Figure 3.6) help to interpret how far contaminants will travel and how long it takes before they reach the groundwater discharge areas (see *chapter 2*). Conversely, these maps may thus also help to determine whether a contaminant plume has reached a discharge area. Together with Figure 3.7, the maps may identify recharge areas of deep groundwater, which could be considered particularly sensitive to contamination. Knowledge of the historic groundwater flow pattern may not be directly useful for the interpretation of current contaminant transport in the aquifer. However, if the historical groundwater flow patterns have been stable for thousands of years, knowledge of these patterns can be used to better understand the position of chemical boundaries, such as calcite dissolution fronts and redox boundaries between oxic and anoxic groundwater. Such boundaries have important implications for the chemical behaviour of contaminants, and thus for their dispersal in the aquifer (Christensen et al. 2000).

The sensitivity analysis showed that climate-induced variations in recharge and human interventions in the drainage levels can cause slight displacements of the groundwater flow system boundaries as depicted in Figs 3.10c and 3.10d. These displacements of the system boundaries cause the flow direction of the shallow groundwater to change at the fringes of the groundwater flow systems during the seasons. Such temporal variation in flow direction may contribute significantly to the aquifer dispersivity. Key factors for enhanced dispersion are changes in flow direction and heterogeneity of the aquifer (Gelhar et al. 1992; Kim et al. 2000). This was also shown by Goode and Konikow (1990), who calculated especially large apparent dispersivities at short characteristic response times of the order of months. The characteristic response time to cyclic stress period ratio (Goode and Konikow, 1990), which is less than 1, suggests transience is of importance for dispersivity in the study area. Because the groundwater that infiltrates at the fringes of the groundwater flow system often feed the



deeper groundwater, the fluctuations in groundwater flow direction and the resulting enhanced dispersion imply that the zone potentially contributing to contamination of the deep groundwater is broader than the fields situated above the flow system boundary. This particularly applies also to the 'recharge window' of deep groundwater, whose surface area is very sensitive to changes in recharge and drainage level.

### 3.6 CONCLUSIONS

For an unconsolidated, sandy phreatic aquifer, detailed insight into the groundwater flow pattern and its uncertainty was generated by using a combination of groundwater flow modelling and particle tracking. Quantification of this uncertainty was attained by applying the groundwater flow system theory and extending it towards three dimensions, followed by probabilistic mapping of groundwater flow system boundaries from Monte Carlo analysis. From these analyses it was shown that the groundwater flow pattern depends on the mainly artificial drainage pattern and on recharge variability. In general, the groundwater flow systems are small sized and the groundwater transit distances rarely exceed one kilometre. In contrast to the intrinsic and temporally invariant aquifer parameters, which were shown to have a minor influence on the spatial configuration of groundwater flow systems, natural variation in recharge and variations in drainage level management exert a relatively large influence, and may lead to activation or inactivation of parts of the drainage system. As a consequence, both patterns and uncertainties were shown to be highly variable throughout the area.

Groundwater flow system boundaries bound pollution plumes as well. Flow directions and the membership to a defined groundwater flow system are highly certain and invariable near discharge areas. Near the groundwater flow system boundaries flow directions are highly uncertain and variable, and dispersivities are expected to be relatively large. This type of information may help to improve sanitation strategies. The information and knowledge on both the spatial pattern of groundwater flow system boundaries and their uncertainties should be used for protection or restoration of recharge areas of stream and wetland ecosystems.

### 3.7 REFERENCES

- Bair, S.E., Safreed, C.M., Stasny, E.A. (1991), A Monte Carlo approach for determining traveltime-related capture zones of wells using convex hulls as confidence regions. *Ground Water* 29, pp 849-855
- Batelaan, O., De Smedt, F., Triest, L. (2003), Regional ground water discharge: phreatophyte mapping, ground water modelling, and impact analysis of land-use change. *Journal of Hydrology* 275, pp 86-108
- Bhatt, K. (1993), Uncertainty in wellhead protection area delineation due to uncertainty in aquifer parameter values. *Journal of Hydrology* 149, pp 1-8
- Buxton, H.T., Reilly, T.E., Pollock, D.W., Smolensky, D.A. (1991), Particle tracking analysis of recharge areas on Long Island, New York. *Ground Water* 29, pp 63-71
- Christensen, T.H., Bjerg, P.L., Banwart, S.A., Jakobsen, R., Heron, G., Albrechtsen, H-H. (2000), Characterization of redox conditions in groundwater contaminant plumes. *Journal of Contaminant Hydrology* 45, pp 165-241
- De Mars, H., Garritsen, A.C. (1997), Interrelationship between water quality and groundwater flow dynamics in a small wetland system along a sandy hill ridge. *Hydrological Processes* 11, pp 335-351

- De Mulder, E.F.J., Geluk, M.C., Ritsema, I.L., Westerhoff, W.E., Wong, Th.E. (2003), De ondergrond van Nederland. Wolters-Noordhoff bv Groningen/Houten, The Netherlands
- De Vries, J.J. (1995), Seasonal expansion and contraction of stream networks in shallow groundwater systems. *Journal of Hydrology* 170, pp 15-26
- De Vries, J.J. (1994), Dynamics of the interface between streams and groundwater systems in lowland areas, with reference to stream net evolution. *Journal of Hydrology* 155, pp 39-56
- Doherty, J., Brebber, L., Whyte, P. (1994), PEST: Model Independent Parameter estimation. Watermark Computing, TIC: 240719, Oxley, Australia
- Engelen, G.B., Kloosterman, F.H. (1996), Hydrological systems analysis, methods and applications. Water Science and Technology Library 20, Kluwer academic publishers
- Falkenmark, M., Allard, B. (1991), Water quality genesis and disturbances of natural freshwaters. In: Hutzinger, O. (ed) *The handbook of environmental chemistry* 5, part A: Water pollution. Springer-Verlag, Heidelberg-Berlin, pp 45-78
- Frapporti, G., Hoogendoorn, J.H., Vriend, S.P. (1995), Detailed hydrochemical studies as a useful extension of national ground water monitoring networks. *Ground Water* 33, pp 817-828
- Frind, E.O., Muhammad, D.S., Molson, J.W. (2002), Delineation of three-dimensional well capture zones for complex multi-aquifer systems. *Ground Water* 60, pp 586-598
- Gelhar, L.W., Welty, C., Rehfeldt, K.R. (1992), A critical review of data on field-scale dispersion in aquifers. *Water Resources Research* 28, pp 1955-1974
- Gomez-Hernandez, J.J., Gorelick, S.M. (1989), Effective groundwater model parameter values: Inference of spatial variability of hydraulic conductivity, leakance, and recharge. *Water Resources Research* 25, pp 405-419.
- Goode, D.J., Konikow, L.F. (1990), Apparent dispersion in transient groundwater flow. *Water Resources Research* 26, pp 2339-2351
- Haitjema, H., Kelson, V., de Lange, W. (2001), Selecting MODFLOW cell sizes for accurate flow fields. *Ground water* 39, pp 931-938
- Harris, G., Clary, M.B., Hatzinger, P., Root, K. (1988), Mapping ground water recharge areas for land use planning, a case study in northern New York, USA. *Land Use Policy* 329-340
- Hoogendoorn, J.H. (1990), Grondwatersysteemonderzoek Salland I en II. DGV-TNO, Oosterwolde.
- Hunt, R.J., Steuer, J.J., Mansor, M.T.C., Bullen, T.D. (2001), Delineating a recharge area for a spring using numerical modeling, Monte Carlo techniques, and geochemical investigation. *Ground Water* 39, pp 702-712
- Kim, K., Anderson, M.P., Bowser, C.J. (2000), Enhanced dispersion in groundwater caused by temporal changes in recharge rate and lake levels. *Advances in Water Resources* 23, pp 625-635
- KNMI (Royal Dutch Meteorological Institute), 1966-2003, Maandoverzicht van de Neerslag en Verdamping in Nederland (Monthly recharge and Evapotranspiration in the Netherlands), De Bilt, the Netherlands
- Kraaijenhof-van de Leur, D.A. (1958), A study of non-steady groundwaterflow with special reference to a reservoir-coefficient'. *De Ingenieur* 70, pp 87-94
- Makkink, G.F. (1957), Testing the Penman formula by means of lysimeters. *International Journal of Water Engineering* 11, pp 277-288
- McDonald, M.G., Harbaugh, A.W. (1988), A Modular-Three Dimensional Finite Difference Ground-water Flow Model. *Techniques of Water Resources Investigations of the USGS. Book 6, Chapter A1.*
- Meinardi, C.R. (1994), Groundwater recharge and travel times in the sandy regions of the Netherlands. RIVM Rep 715501004, PhD thesis, Vrije Universiteit, Amsterdam.
- Modica, E., Reilly, T.E., Pollock, D.W. (1997), Patterns and age distribution of ground-water flow to streams. *Ground Water* 35, pp 523-537
- Penman, H.L., 1948, Natural evaporation from open water, bare soil and grass. *Royal Society, London Proc. Series A*, 193, pp 120-146
- Pollock, D.W. (1989), Documentation of computer programs to compute and display pathlines using results from the U.S. Geological Survey modular three-dimensional finite-difference ground-water flow model: U.S. Geological Survey Open-File Report 89-381, 188 p.
- Puckett, L.J., Cowdery, T.K., McMahon, P.B., Tornes, L.H., Stoner, J.D. (2002), Using chemical, hydrologic, and age dating analysis to delineate redox processes and flow paths in the riparian zone of a glacial outwash aquifer-stream system. *Water Resources Research* 38, pp 1134

- Robinson, M.A., Reay, W.G. (2002), Ground water flow analysis of a mid-atlantic outer coastal plain watershed, Virginia, U.S.A. *Ground Water* 40, pp 123-131.
- Rock, G., Kupfersberger, H. (2002), Numerical delineation of transient capture zones. *Journal of Hydrology* 269, pp 134-149
- Schot, P.P., Dekker, S.C., Poot, A. (2004), The dynamic form of rainwater lenses in drained fens. *Journal of Hydrology* 293, pp 74-84
- Tóth, J. (1963), A theoretical analysis of groundwater flow in small drainage basins. *Journal of Geophysical Research* 68, pp 4795-4812
- Van Buuren, M. (1991), A hydrological approach to landscape planning: the framework concept elaborated from a hydrological perspective. *Landscape and Urban Planning* 21, pp 91-107
- Van Uden, J.G., Vissers, M.J.M. (1998), A hydrochemical study in Salland (in Dutch), M.Sc. thesis, Utrecht University, Department of Geochemistry, Utrecht
- Van Leeuwen, M., te Stroet, C.B.M., Butler, A.P., Tompkins, J.A. (1999), Stochastic determination of the Wierden (Netherlands) capture zones. *Ground Water* 35, pp 8-17
- Varljen, M.D., Shafer, J.M. (1991), Assessment of uncertainty in time-related capture zones using conditional simulation of hydraulic conductivity. *Ground Water* 29, pp 737-748
- Vassolo, S., Kinzelbach, W., Schäfer, W. (1998), Determination of a well head protection zone by stochastic inverse modeling. *Journal of Hydrology* 206, pp 268-280
- Vissers, M.J.M., Frapporti, G., Vriend, S.P., Hoogendoorn, J.H. (1999), The dynamics of groundwater chemistry in unconsolidated aquifers: the Salland section. *Physics and Chemistry of the Earth (B)* 24, pp 529-534
- Wheater, H.S., Tompkins, J.A., van Leeuwen, M., Butler, A.P. (2000), Uncertainty in groundwater flow and transport modelling - a stochastic analysis of well-protection zones. *Hydrological Processes* 14, pp 2019-2029
- Wolters-Noordhof Atlasproducties 1990. Grote historische atlas van Nederland 1:50 000, deel 3 Oost-Nederland 1830-1855, Groningen: Wolters-Noordhof
- Zijl, W. (1993), Schaalanalyse met behulp van fourier-analyse: Toepassing op grondwaterstroming ten gevolge van ruimtelijke variaties in de grondwaterspiegel en putonttrekkingen (in English), In: CHO Commissie voor Hydrologisch onderzoek TNO, Schaalproblemen in de hydrologie, Rapporten en Nota's 31, pp 51-76
- Zijl, W. (1999), Scale aspects of ground water flow and transport systems. *Hydrogeology Journal* 7, pp 139-150



# 4 A CONCEPTUAL FRAMEWORK FOR PATTERNS AND CHANGES IN THE HYDROCHEMISTRY OF A SANDY AQUIFER

M.J.M. Vissers, G. Frapporti<sup>+</sup>, S.P. Vriend, P.F.M. Van Gaans, M. van der Perk

<sup>+</sup> Environment Agency, UK

**Abstract.** High-resolution chemical data of multilevel wells provide detailed insight into groundwater quality patterns in space and time. The description, interpretation, and prediction of these spatial patterns and their changes, is provided via a consistent framework for water quality boundaries that includes the concept of streamtubes. The use and differentiation of streamtubes is illustrated in a section of multilevel wells in an unconsolidated aquifer in the eastern part of the Netherlands, which was sampled in 1989, 1996, and 2002. First, observed patterns are related to the horizontal and vertical position within the groundwater flow system and to geochemical, hydrological, and input-induced boundaries as observed from hydrochemical and borehole data. Secondly, by using the streamtube concept changes in groundwater quality can be explained by changes in hydrology, pollution intensity, and chemical reactions within the sediment. Short-term trends in water chemistry were predicted, and changes along a flow path were related to land use changes and to diffuse atmospheric pollution.

*Keywords:* Groundwater quality, streamtube approach, redox, buffering, phreatic aquifer

## 4.1 INTRODUCTION

As directly usable groundwater resources become increasingly limited in the Netherlands, there is a growing demand for a detailed assessment of groundwater quality. Where regional monitoring networks provide general information on base line status and trends in groundwater quality, detailed surveys of the groundwater quality reveal complex patterns, even at a local scale. These patterns may be related to varying composition of the water at the time of infiltration, or to geochemical and/ or to changes in the hydrological flow pattern. Uncertainties and changes in e.g. the hydrology make it difficult to unravel the spatio-temporal distribution of groundwater chemistry in a given area. Especially when identifying the causes of groundwater quality deterioration, insight into how these patterns evolve is crucial.

Sections of multilevel wells may bring clarity into the complex patterns of groundwater quality, particularly if the wells are positioned parallel to the flow direction. At present such well sections are, mostly installed for modelling water quality near point sources of pollution. They are used to provide information on specific hydrogeochemical responses to aquifer pollution (e.g. Hansen and Postma, 1995; Rödelberger, 1989; Smith et al. 1991), or are used for reactive transport parameter estimation (e.g. Ceazan et al. 1989; DeSimone and Howes, 1998) and for calibration of hydrochemical models (Frind et al. 1990; Stollenwerk, 1996). In these kinds of studies hydrogeochemical information is mostly used to delineate the position and propagation of a single plume, whereas regional hydrological system information is often not considered.

The aim of this chapter is to present a consistent conceptual framework for the local to regional scale description of local scale observed groundwater quality patterns in

unconfined sandy aquifers, as well as for the changes therein. This conceptual framework combines hydrogeological modeling and is based on defining streamtubes, the use and identification of which is illustrated for a multilevel well section in Salland, a rural area in the eastern part of the Netherlands.

## 4.2 THEORY

Frapporti et al. (1993, 1995) showed, by clustering hydrochemical data of the Dutch groundwater quality-monitoring network into homogeneous water types, that the hydrochemical processes of calcite-dissolution, nitrate reduction, and pollution (mainly by manure) govern the groundwater composition distribution in the Dutch groundwater in general. They roughly indicated where each water type discerned was most likely to occur. In more detail, the pattern of groundwater quality, i.e. the spatial distribution of groundwater with differing composition, can also be described in terms of the configuration of water type *boundaries*. As already mentioned in *chapter 1*, the three basic factors determining groundwater quality are groundwater flow, input, and geochemical processes. With water type boundaries forming the basic delineators, they must then also be subdivided into hydrological boundaries, input boundaries, and geochemical boundaries. Within this concept, changes in the groundwater quality pattern are described as movements or displacements of boundaries caused by changes in flow, input, or geochemical processes.

### 4.2.1 Hydrological boundaries

The basic element of groundwater flow to be considered is a single groundwater flow system (Tóth, 1963; *chapter 2, 3*). A 2-D representation of this basic element is shown in Figure 4.1 for free flow from a groundwater divide towards a draining watercourse or discharge area, in a homogeneous, isotropic aquifer with constant thickness. Age increases with depth depending on the recharge rate and porosity, initially almost linear but obviously approximately logarithmically towards the hydrological base (Böhlke, 2002). Flow line density clearly increases towards the discharge area. Groundwater flow system boundaries, especially those between a local and regional groundwater flow system, can be expected to also represent water quality boundaries, due to the difference in recharge area and age. Also, physical hydrological boundaries such as clay layers usually represent groundwater flow system boundaries. Whereas the vertical groundwater divide is less likely to represent a shift in groundwater quality, the confluence of flow lines in the discharge area is expected to be related to quality differences.

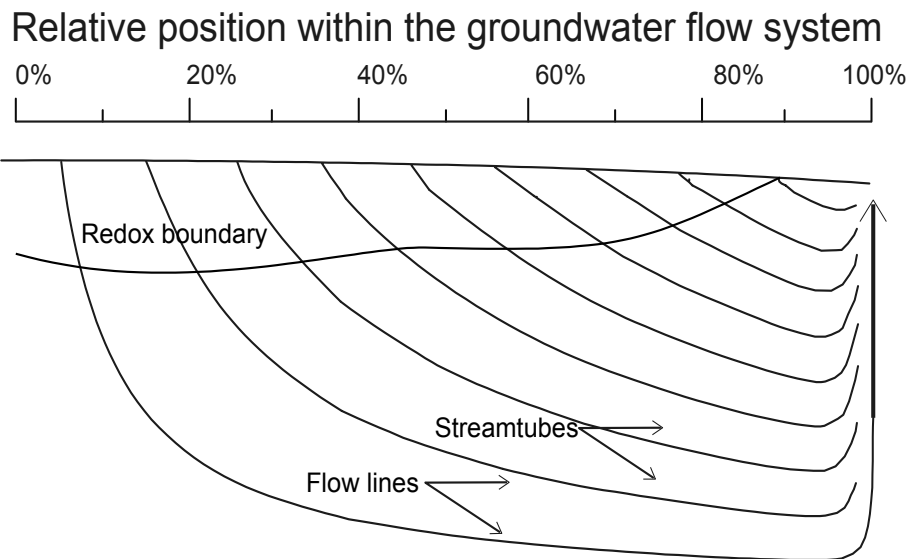


Figure 4.1 Schematic overview of flow lines and streamtubes in the basic groundwater flow system

#### 4.2.2 Input boundaries: the streamtube concept

The streamtube concept was initially introduced to describe transport in heterogeneous porous media (Thiele, 1994, Datta-Gupta and King, 1995) based on its original use in flow net construction (e.g. Engelen, 1981). In this context the heterogeneous subsurface of flow systems is subdivided into streamtubes that are near homogeneous from a physico-chemical perspective such that (Feyen et al. 1998):

- The total land surface can be characterized as a collection of streamtubes.
- There is no exchange of water and solutes between the streamtubes.
- Within each streamtube, water flow and solute transport can be described by specific model parameters.

Here, we define a streamtube as a groundwater volume recharged in an area that is homogeneous with respect to input water quality, hence land use. Flow is described as piston flow with negligible transversal dispersion between the streamtubes, as can be expected in steady transport systems (Zijl, 1999). In a vertical cross-section or multilevel well, streamtube boundaries should then be recognizable by a chemical difference between vertically adjacent mini screens. The flow lines in Figure 4.1 might thus also be viewed as streamtube boundaries.

The relative horizontal position in the groundwater flow system and its size are crucial for the observed water quality patterns with depth, as well as their changes. Near the groundwater divides (0% in Figure 4.1), subvertical groundwater flow implies that only one streamtube can be observed in all vertical screens. Closer to the discharge area, more streamtubes can be observed depending on the groundwater flow system size and land use scale. The latter information can be obtained from hydrological modelling and geographical analysis.

### 4.2.3 Geochemical boundaries

Geochemical boundaries are caused by water-sediment interaction. They comprise redox, buffering, and sorption boundaries. Natural redox conditions include the range from oxic to methanogenic water (Champ et al. 1979) resulting from the sequence of inorganically or bacterially mediated terminal electron accepting processes (TEAPS; Chapelle, 2003). In the natural situation, the occurrence of such zones is principally related to sediment reduction capacities (Pedersen, 1991; Barcelona and Holm, 1991) and to the input water quality (Lyngkilde and Christensen, 1992). Depending on how reaction kinetics and groundwater flow velocities relate to the sampling scale, these boundaries may appear as sharp or gradual. The same is true for buffering and sorption, where the occurrence of carbonate in combination with input acidity, or the sediment exchange capacity in combination with input metal load, primarily determine the location of the geochemical boundaries.

In as far as geochemical boundaries are related to sediment properties, they can also be identified from boring descriptions. They may coincide with primary geological boundaries; in the case of clay and peat layers these are likely to be hydrological boundaries as well. Geochemical boundaries lead to variations of water quality within streamtubes and normally will cross over through adjacent streamtubes (see Figure 4.1).

### 4.2.4 Changes

When the groundwater quality at a certain point, e.g. a well-screen, has changed, this can be due to three different processes (adapted from Schot, 1990; Figure 4.2):

- Changes in the groundwater flow pattern (type 1 change)
- Changes in the chemical composition of the infiltrated water (type 2 change)
- Changes caused by hydrogeochemical processes (type 3 change)

This means increased concentrations of a pollutant in a well screen are not necessarily caused by increasing pollution of the infiltrated water over the time period considered. To differentiate between the causes of water quality changes, again the streamtube concept can be applied. Using this concept, the different types of change are characterized as follows:

*Type 1 changes:* Hydrological changes cause either permanent or oscillating vertical movements or changes in thickness of a streamtube. A cause of such a change can be that groundwater observed at a certain depth is recharged in another area. Hydrological changes can be expected from the occurrence of wet and dry years, while seasonal effects are expected to have a marginal effect on the flow pattern (*chapter 3*; Reilly and Pollock, 1995). Similarly, changes in land use that bring about changes in net infiltration rate affect the groundwater flow pattern (Portniaguine and Solomon, 1998). From Figure 4.2 it is evident that such a change in recharge only affects flow downstream of the change, and the vertical displacement of the streamtube boundaries needs not be unidirectional within one vertical profile. More permanent type 1 changes may be caused by changes in the configuration of the drainage network (see *chapter 3*).



*Type 2 changes:* Changes in the composition at the primary source result in water quality differences *within* the streamtube, hence in a water quality change at some moment in time at the observation point. In unpolluted waters, such a change will mainly reflect changes in the rainwater composition and its evaporative concentration. It can be expected that large-scale land use changes such as cultivation of heathlands and deforestation may cause large type 2 changes in groundwater quality. More recent changes include the introduction of maize and accompanying overfertilization which will result in a change towards heavily polluted groundwater (Böhlke, 2002).

In a vertical cross-section or multilevel well, type 2 changes in groundwater chemistry will be noted first in the shallower well screen within a streamtube, as the deeper groundwater is older. Increasing pollution of the input water will thus result in a decreasing concentration-depth profile across one streamtube. The opposite occurs if input concentrations are decreasing.

*Type 3 changes:* Geochemical changes are caused by water-sediment interaction that eventually results in the displacement of geochemical boundaries. Typically, these boundaries move slowly compared to groundwater flow. For example, the consumption of sedimentary organic carbon through denitrification causes a downward movement of the nitrate reduction boundary. Likewise, the calcite dissolution front moves as calcite is leached. Also cation exchange processes such as the breakthrough of K can bring about changes in groundwater quality, without the need for a change in input composition over the time-period considered. Because of its association with pollution and a moderate retardation factor of about two in very coarse sediments (Ceazan et al. 1989), the latter could also be seen as a type 2 change. However, for trace elements with much larger retardation factor, breakthrough is considered as a type 3 change.

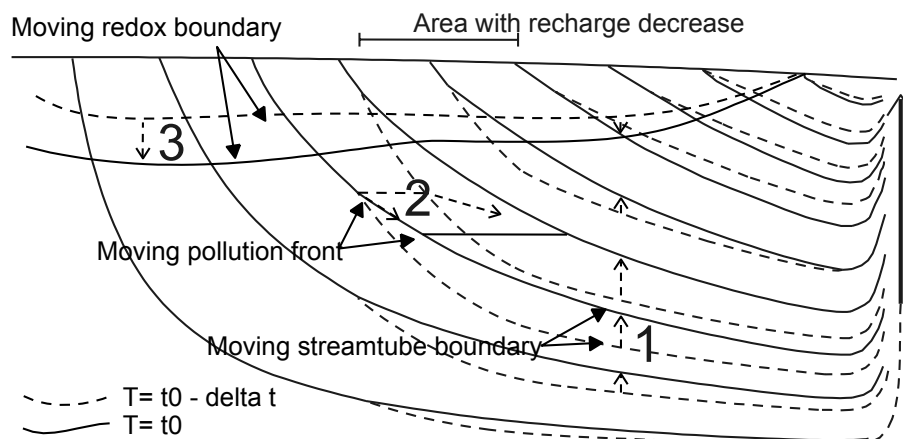


Figure 4.2 Schematic overview of streamtubes, and the types of changes in groundwater chemistry that can cause groundwater quality change at a certain point

### 4.3 CHARACTERISTICS OF THE STUDY AREA

The Salland multilevel well section is situated in a sandy, unconfined, unconsolidated aquifer in the eastern part of the Netherlands (Figure 4.3 and 4.4). It was set up in 1987

by Hoogendoorn (1990) in order to assess the presence of hierarchical flow patterns according to the concept as introduced by Tóth (1963), by using a combination of hydrological modelling and interpretation of hydrochemical information. The area and well-locations were chosen based on hydrological systems analysis (see Engelen and Kloosterman, 1996). The well section consists of 10 borings (A1 – A11; Figure 4.3) to a depth of -30 to -50 m OD with 0.15 m long mini well screens. The upper 10 to 12 mini screens were placed every meter, and the deeper ones every two meters, down to the base of the phreatic aquifer. Hoogendoorn (1990) and Frapporti et al. (1995) showed that groundwater flow and chemistry in the Salland area are complex with local and regional systems, and hydrological modelling alone is not sufficient to unambiguously describe the flow. These first studies were based on a sampling campaign in 1989. In 1996 the Salland section was resampled to investigate the changes in groundwater chemistry that had occurred over the seven-year period (Vissers et al. 1999) and in 2002 the section was sampled for the third time.

As discussed, hydrogeochemistry is basically determined by the hydrological situation, the composition of the recharging water, and processes that have occurred along the flow path. Geomorphology, mineralogy, geohydrology, and history of land use in the Salland area are therefore pertinent to this study.

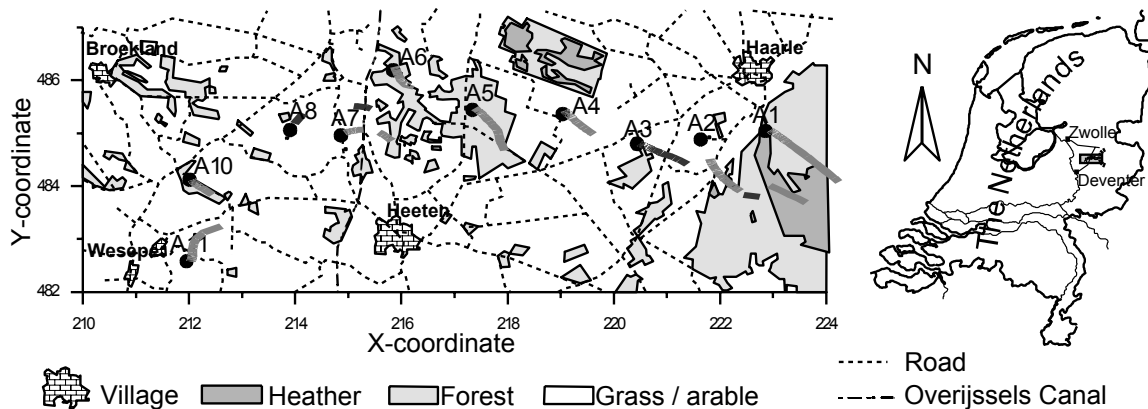


Figure 4.3 Land use in the Salland area, location of the borings, and their geographical position in the Netherlands, with coordinates in km RDS (Dutch ordnance datum). Lines indicate modelled recharge lines towards the miniscreen wells (chapter 3). Recharge lines of boring A3 and A8 are in black, others are given in grey

#### 4.3.1 Geomorphology

The basic geomorphology of the area was shaped during the Saalian (~150 ka ago, De Mulder et al. 2003). The well section starts at the ‘Holterberg’ ice-pushed ridge in the east (ice-displaced local deposits flanking the glacial tongue basin), which reaches +75 m OD (Figures 4.3 and 4.4). Towards the west, the well section runs across a cover sand plain, with undulating topography. The cover sand (Boxtel Formation, Wierden Member, Lithostragraphy cf. De Mulder et al. 2003) is a few meters thick and covers coarser fluvial sands (Kreftenheye Formation). These deposits, that formed in the late Saalian, Eemian and Weichselian (~150 – 11 ka BP) comprise the studied aquifer with a base

typically at -30 m OD. In the western part of the well section, the aquifer is underlain by impermeable fluvio-glacio-lacustrine clays that filled the Saalian tongue basin following deglaciation (Kreftenheye Formation, Twello Member). In the eastern part the poor river sands of the Peize and Appelscha Formations are found. The Peize Formation consists of very poor grey to white coloured sands and gravels from Baltic rivers; the Appelscha Formation contains grey or light yellow medium to very coarse sands and gravel, and is of slightly different origin. No shallow impermeable layer is present, and marine deposits form the hydrological base at -80 m OD here. In the profiles of borings A10 and A11 the Zutphen Member (organic rich fine grained sediments) is found at approximately -7 m OD. It can be expected that the phreatic aquifer has had active rainwater-fed groundwater flow since the start of the Holocene, as before permafrost and depositional river flow conditions prevailed in the area.

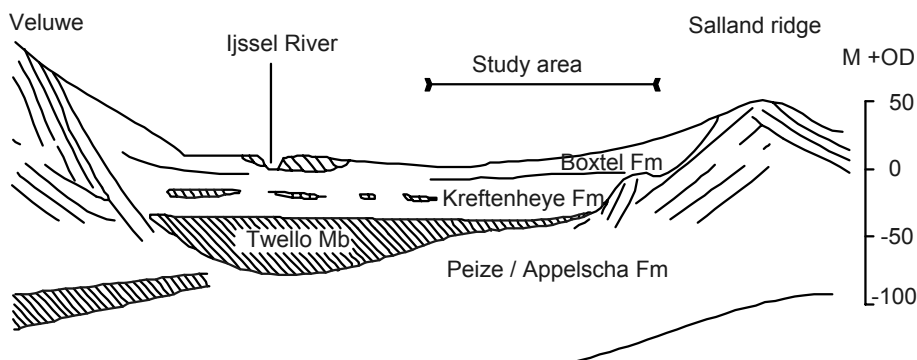


Figure 4.4 Schematic view of the geology

### 4.3.2 Mineralogy

Frapporti et al. (1995) determined the mineralogy of the aquifer. The sediments of the aquifer contain mainly quartz (up to 95 wt %) and 0-10 wt % feldspar. The clay fraction mainly consists of illites, with lesser amounts of smectites and kaolinites. Calcite is absent in the shallow part of the ice-pushed ridge; low concentrations (up to 1%) are found in the deeper parts of borings A2-A5. The other parts of the well section contain 2-20 wt % of calcite (coarse sands 2-5 wt %, fine sands 5-20 wt %), and occasionally contain trace amounts of pyrite of up to 0.4 wt %. Organic matter contents are commonly less than 0.05 wt %, but in some deeper sediments 0.5 wt % organic carbon is found.

### 4.3.3 Geohydrology

Average annual rainfall is about 770 mm (KNMI, 1966-2003). The climate is temperate, with a precipitation deficit in summer. Based on tritium measurements, Meinardi (1994) calculated a net infiltration of approx. 340 mm/yr on grassland. A dense network of ditches drains the area, to make it suitable for agriculture. The flow pattern was modelled in 2-D by FLOWNET (Elburg et al. 1987) by Hoogendoorn (1990), 3-D with Microfem (Hemker and Van Elburg, 1990) by van Uden and Vissers (1998), and for this thesis (*chapter 3*) using MODFLOW (McDonald and Harbaugh, 1988). The calculated recharge

lines of the well screens are shown in Figure 4.3. Figure 4.5 shows the occurrence of many small groundwater flow systems within the area (see also *chapter 3*), superimposed upon a general east to west groundwater flow. Groundwater ages of up to 120-150 years were estimated.

#### **4.3.4 Land use history**

The area around the Salland section was first inhabited in the 13th century. Small areas with poor sandy soils were artificially elevated with manure, straw, heath and all types of human waste; the so-called 'enk-soils'. As a consequence, the original groundwater flow and chemistry has already been anthropogenically influenced for centuries in these areas. Using the calculated groundwater age, especially the land use history and the hydrological interventions of the last century are relevant for the temporal and spatial variations in groundwater quality as presently observed.

In 1858 AD the Overijsselsch Canal that crosses the well section was dug. As the population increased in the 19th century, the poor sandy soils near the ice-pushed ridge were first cultivated on a local scale. Most of the sandy soils east of the canal remained vegetated by heath. With the advent of fertilizers after 1900 much of the heath was rapidly removed and the land was drained and cultivated; forests on the ridge disappeared due to felling of trees. Before the 1950's most of the arable land was concentrated in the 'enk-soils'. Afterwards the cultivated lands were used in rotations for crop and pasture. By 1970 almost all the heathlands on the ice-pushed ridge had been reforested, and maize was introduced. With the recent introduction of intensive indoor cattle-breeding units nearby, large quantities of manure are applied mainly to the fodder-maize, which can take high manure doses, and to a lesser extent to grassland. Figure 4.3 shows the current land use. Today 54% of the land consists of meadows (dairy farming), 22% of forest/heath, 8% of roads/built-up areas, and 18% of arable land (mostly maize).

## **4.4 METHODS**

### **4.4.1 Field sampling and laboratory analysis**

Sampling was done using vacuum hand pumps, flushing each mini well system with at least 3 volumes. In 1989 the samples were analyzed by TNO (Hoogendoorn, 1990). In 1996, Ec and pH were measured in the field, whereas alkalinity (by Gran-titration) was measured within 12 hours at a field lab. Eh was measured using a standard electrode. Samples were filtered (0.45  $\mu\text{m}$ ), and stored at 4-10°C in acid washed, pre-flushed PE bottles. Part was directly acidified to pH=1 with ultrapure HNO<sub>3</sub> for ICP-analysis. Analyses were performed in random order using ICP-AES, IC, OC/TOC analyzer (DOC), and spectrometry (NH<sub>4</sub>, PO<sub>4</sub>). After inspecting the raw data from all 244 screens, samples that showed deviating analyses and samples with an ionic unbalance were reanalyzed. Final ion balance calculations are within 2% deviation from zero in 89% of the samples, and 96% within 5% deviation from zero for 1996. In 2002 the same field and field lab methods were used. One portion of the samples was acidified with ultrapure HNO<sub>3</sub> for

cation and sulphate analysis by ICP-AES and ICP-MS; another portion was acidified with sulphuric acid for anion, DOC and TN analysis. Chloride, NH<sub>4</sub>, NO<sub>3</sub>, and PO<sub>4</sub> were measured by auto analyzer and photometry, DOC and TN by TC/TN Analyzer. For 2002 final ion balance is within 2% deviation in 83% of the samples, and 93% within 5% deviation from zero.

#### 4.4.2 Identification of water quality boundaries

Water quality boundaries were identified by examining the ‘chemical contrast’ between vertically adjoining mini screens. A large chemical contrast indicates a boundary caused by differences in input (streamtube boundary), by geochemical processes (geochemical boundary), or by local heterogeneities such as clay layers (hydrological boundary). The chemical contrast is calculated simply as the difference of an element between two miniscreens (Equation 1):

$$\text{SCD} = | [S_{(x)(t)}] - [S_{(x-1)(t)}] | \quad (1)$$

where ( $S_{(x)(t)}$ ) is the concentration of an ion in meq/l in mini screen number x of a boring at time t. In the case of a multivariate groundwater composition, the differences in the combination of elements can be looked at, and the Screen Chemical Difference (SCD) could be defined as a sum parameter. Within a streamtube the SCD will be relatively small, while larger SCD values indicate a streamtube boundary (or chemical or hydrological boundary).

*Hydrological boundaries* were identified through detailed analysis of the boring descriptions and of previous groundwater modelling results (see *chapter 3*). By definition, hydrological boundaries are also streamtube boundaries.

*Geochemical boundaries* were identified for the major processes of buffering and reduction only, based on the pertinent major elements. Assignment of the different redox zones was similar to Lyngkilde and Christensen (1992), and based on a lognormal bimodality in NO<sub>3</sub>, Fe, and SO<sub>4</sub> concentrations. Similarly, the calcite buffering boundary was based on bimodality in the HCO<sub>3</sub> concentration. Geochemical boundaries may or may not be streamtube boundaries as well, depending on the observation of an additional SCD for an element that is not related to the geochemical process identified, e.g. a difference in Cl in addition to a difference in NO<sub>3</sub>.

*Streamtube boundaries* were then identified as those water quality boundaries that are not geochemical boundaries only. The relative horizontal position of each boring within the groundwater flow system was obtained from groundwater modelling results (*chapter 3*). This information, together with the spatial land use pattern, was used to corroborate the number and type of streamtube boundaries identified.

#### 4.4.3 Identification of water quality changes

Similar to the SCD, changes in groundwater quality can be identified by a second parameter, the Temporal Chemical Difference (TCD). The formula is analogous to equation 1:

$$\text{TCD} = \left| [S_{(x)(t)}] - [S_{(x)(t-1)}] \right| \quad (2)$$

This parameter was used to aid in identifying the independent changing of the streamtubes.

Within a vertical cross-section, type 1 changes were identified as a displacement of one or more streamtubes. Type 2 changes were identified as consistent increases or decreases in concentration over the streamtube as a whole (or initially in the upper wells only). Type 3 changes were identified as the progression of a geochemical boundary.

## 4.5 RESULTS

### 4.5.1 Hydrological boundaries

The calculated recharge lines of the well screens are shown in Figure 4.3. Figure 4.5 shows a transit distance map with groundwater flow system boundaries (*chapter 3*). It shows that borings A2, A6, A8, and A11 are situated in upward seepage areas, and that only borings A7 and A8 are possibly situated in the same groundwater flow system. Some boundaries between local and regional groundwater flow systems were modelled in borings A2, A3, A7, and A8 (Figure 4.3). In these wells a shallow local groundwater flow system may be superimposed on a regional, deep groundwater system. Clay layers as identified from the borings are shown in Figure 4.6.

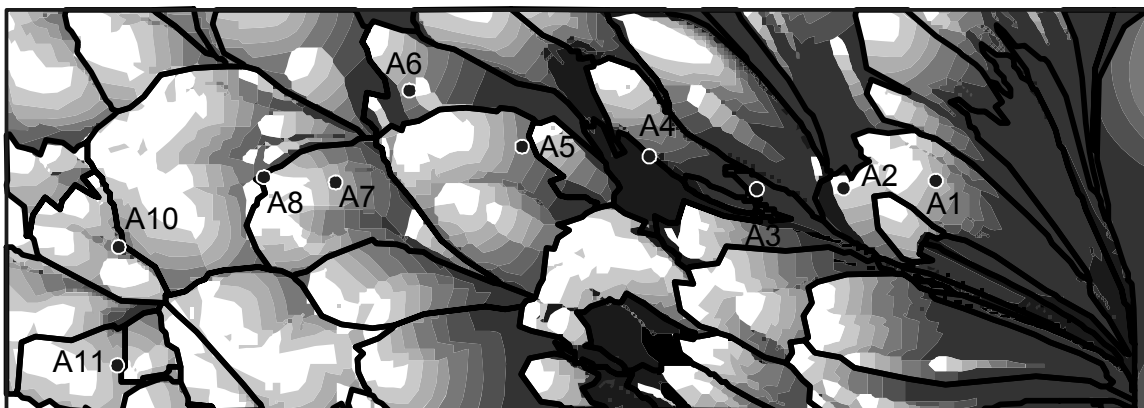


Figure 4.5 Transit time map of the well-section area and groundwater flow system boundaries (*chapter 3*). Groundwater flow system boundaries were obtained by a Monte Carlo simulation (*Chapter 3*). Dark areas have the largest transit distance; white areas have near-zero transit distance, indicating upward seepage. The position of the wells is indicated as well.

### 4.5.2 Geochemical boundaries

Figure 4.7 demonstrates the bimodality in  $\text{NO}_3$ , Fe, and  $\text{SO}_4$  concentrations, indicating the distinct redox stages in the wells. Nitrate concentrations may drop from 200 mg/l to detection limit within a one-meter vertical mini screen distance, confirming high rates of denitrification compared to groundwater flow velocity, also noted by Postma et al. (1991) and Pedersen et al. (1991). In some wells denitrification occurs above the nitrate

reduction boundary, as indicated by decreasing  $\text{NO}_3$  trends with depth combined with decreasing  $\text{Ca}/\text{HCO}_3$  ratios, as well as by grey-coloured sediment pockets in this zone (also identified in another aquifer by Pedersen et al. 1991). Nitrate-reduced samples contain less than 1 mg/l  $\text{NO}_3$ , and Fe and Mn are present above ICP-AES – detection limits (0.03 mg/l). Iron- and manganese reduced samples are thus considered one group. Sulphate reduction is a much slower process (Van Cappellen and Gaillard, 1996, Jakobsen and Postma, 1999), and is indicated by a decreasing  $\text{SO}_4/\text{Cl}$  – ratio in combination with a decreasing  $\text{Ca}/\text{HCO}_3$  ratio with depth. Only fully  $\text{SO}_4$ -reduced samples ( $< 2$  mg/l  $\text{SO}_4$ ) were included in the sulphate-reduced group. The distribution of the three redox zones for the 1996 data is shown in Figure 4.6.

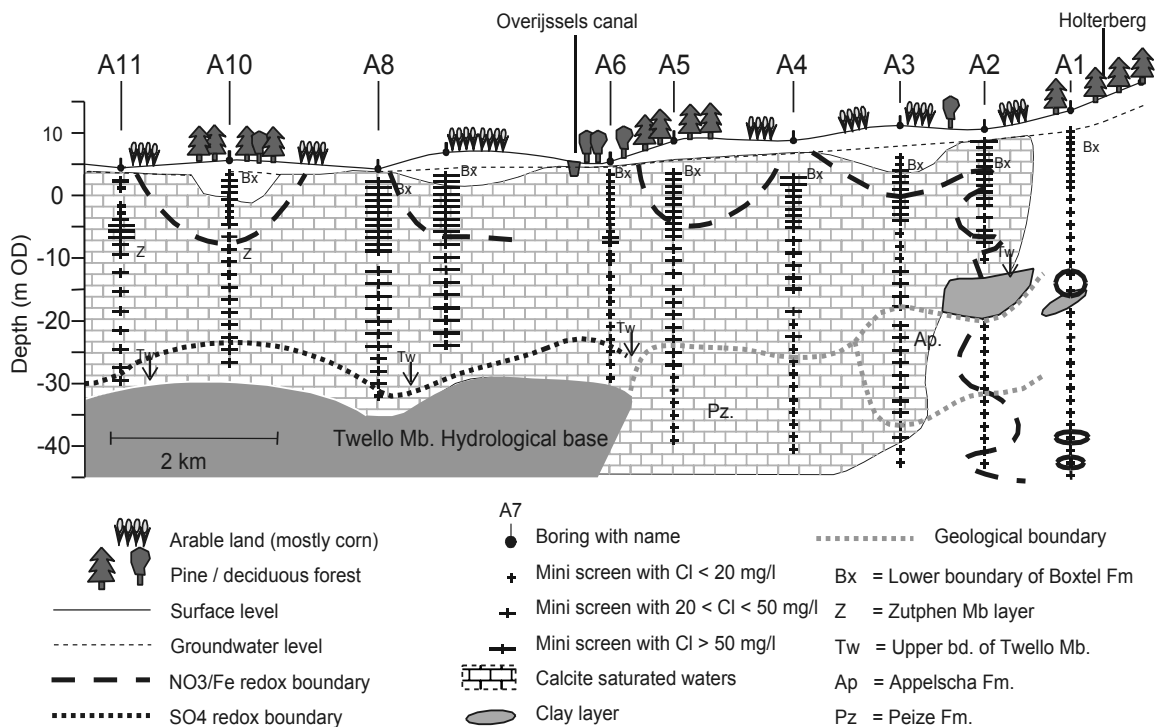


Figure 4.6 Geology, geochemical preconditions, land use, and well design, projected on the general E-W flow-direction

The bicarbonate lognormal multi-modality (Figure 4.7) follows calcite saturation indices as calculated by WATEQ4F (Ball and Nordstrom, 1991). Samples containing less than 50 mg/l  $\text{HCO}_3$  have only passed through calcite-free parts of the aquifer. The resulting calcite-saturation pattern of the 1996 data is also shown in Figure 4.6.

#### 4.5.3 Streamtube boundaries

The identification of streamtubes is illustrated using boring A1, which contains a number of typical hydrological and hydrochemical boundaries. In this case the different streamtubes were distinguished by a sum SCD. The 1989, 1996 and 2002 SCD-lines of boring A1 are displayed in Figure 4.8. Nine water quality boundaries with an average thickness of 5 meters were discerned in boring A1. In this boring the SCD between the

streamtubes is 3-5 times larger than within the streamtubes. The number of streamtubes thus identified conforms to the variation in land use as observed along the calculated recharge line (Figure 4.3).

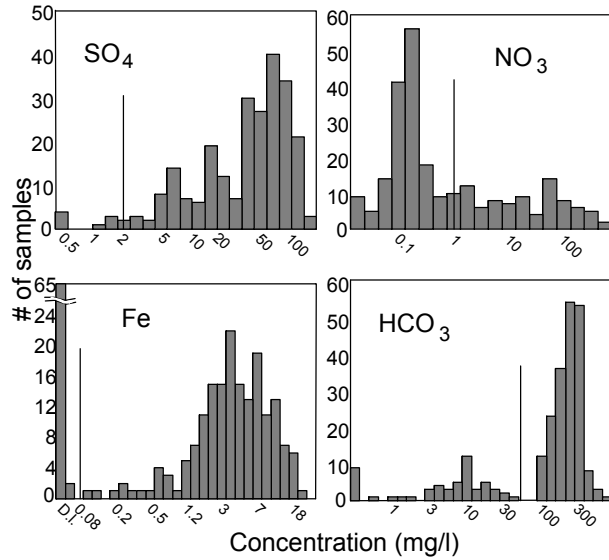


Figure 4.7 Histograms of the lognormalized  $\text{SO}_4$ ,  $\text{NO}_3$ , Fe, and  $\text{HCO}_3$  concentrations in 1996, where spikes indicate concentration levels where groundwater types are subdivided

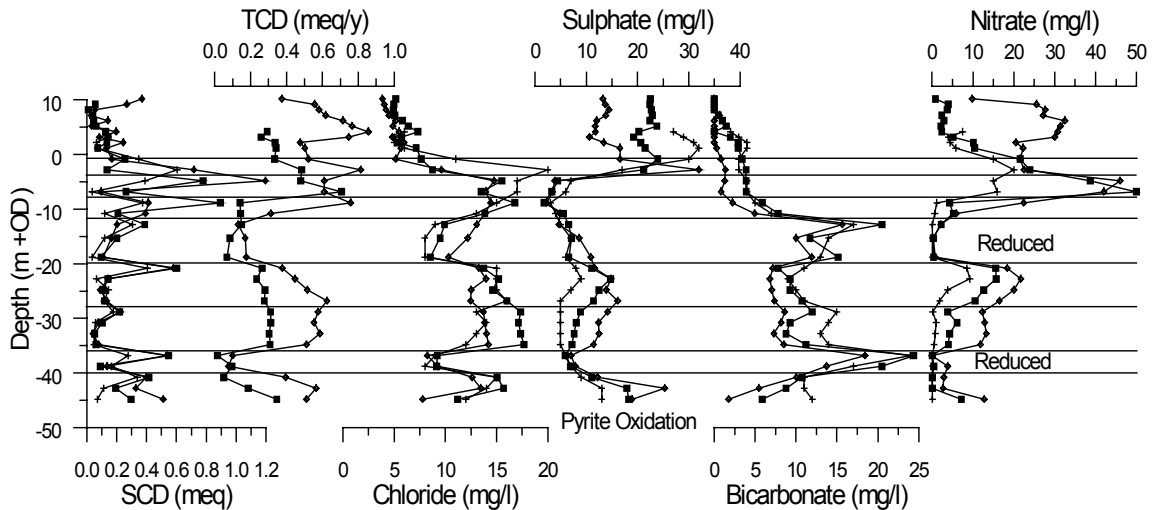


Figure 4.8 SCD, TCD, Cl,  $\text{SO}_4$ ,  $\text{HCO}_3$ , and  $\text{NO}_3$  - depth profiles of boring A1. The streamtubes with reduced groundwater are indicated, as well as the streamtube boundaries. (+ = 1989, ■ = 1996, ◇ = 2002). Both the TCD and SCD are defined as sum parameter of Cl,  $\text{HCO}_3$ ,  $\text{NO}_3$ , and  $\text{SO}_4$  expressed in mmol/l. TCD is calculated as the difference between 1989 and 1996 (■), and between 1996 and 2002 (◇)



#### 4.5.4 Changes

The changes in water chemistry are illustrated by the conductivity profiles, used as a general indicator of groundwater quality. From the Ec – depth profiles of the 1989, 1996, and 2002 sampling rounds we can readily see where the general chemical composition has changed (Figure 4.9).

Type 1 changes (changes in the flow pattern) were identified in borings A1, A4, and A6. However, most SCD peaks in boring in these wells remained positioned at the same depth.

Type 2 changes (changes in the chemical composition of the infiltrating water) occur in all borings, the ones indicated in Figure 4.9 are those where a major shift in overall hydrochemistry has occurred within a streamtube. The example of boring A1 (Figure 4.8) shows that the hydrochemistry within adjacent streamtubes changes independently, which further confirms the identification of the streamtube boundaries. The depth interval between -20 and -36 m OD in boring A1 (Figure 4.8) illustrates how type 2 changes in streamtubes aid in predicting water quality dynamics. The concentrations of  $\text{SO}_4$  and  $\text{NO}_3$  in 1989 are distinctly greater in the shallowest screens of these streamtubes than in the deeper screens. This indicates that the streamtube will contain higher  $\text{NO}_3$  and  $\text{SO}_4$  concentrations in the near future. Analyses from 1996 confirm this; the 1996 depth profile predicted that concentrations would keep on rising, which was observed in 2002. The vertical age difference in these ‘thicker’ streamtubes is probably more than 7 years, because the samples found in the deeper parts in 1996 are similar to those of the shallower samples from 1989. In most streamtubes of boring A1, however, a complete change of chemistry was observed over the 7-year period between sampling.

Type 3 changes (changes caused by geochemical processes) occur in borings A1, A2, and A7. All type 3 changes identified are iron reduced miniscreens that have become nitrate-oxic in the 13-year monitoring period.

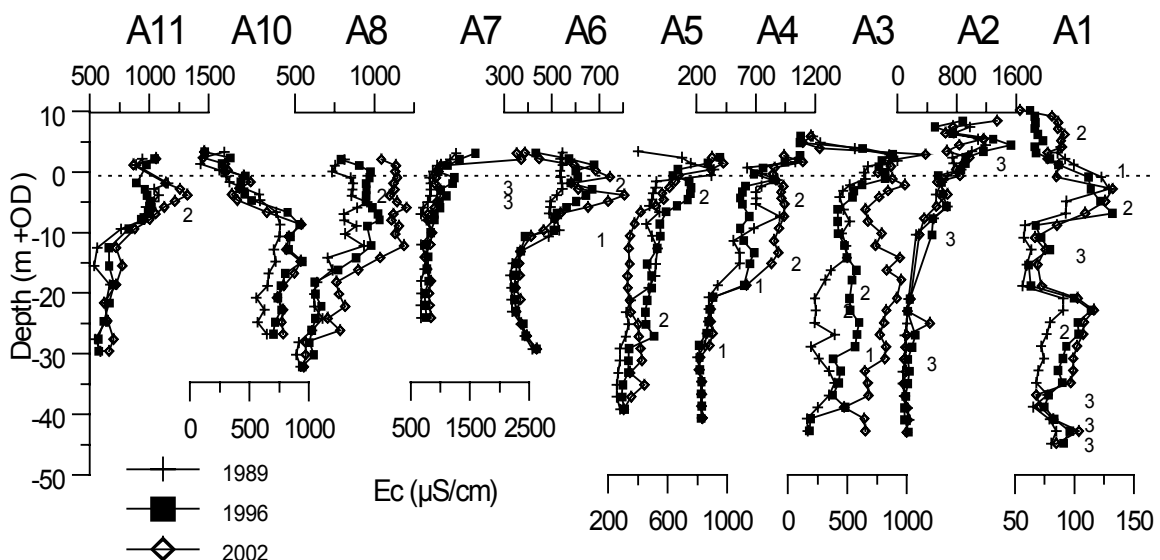


Figure 4.9 Electrical conductivity - depth profiles in the Salland A section, with the type of change indicated as a number. Note the difference in scales used

#### 4.6 DETAILED INTERPRETATION OF PATTERNS AND CHANGES IN THE WELLS

In boring A1 nine streamtubes were discerned (Figure 4.8), which could be linked to its varied landuses along its 1600 m long recharge line (Figure 4.3). Differences between streamtubes are in most cases related to differences in evaporative concentration. Water recharged in forest is approximately four, and water from heathland is approximately 1.7 times concentrated rainwater, as reflected by the Cl difference relative to rainwater (Stuyfzand, 1993). The conductivity profiles show recognizable bands with sharp boundaries between -12 and -20 m OD, and between -36 and -40 m OD. These distinct streamtubes are characterized by low Cl and SO<sub>4</sub> and high Fe contents, and bound a nitrate-free, pristine groundwater type. Clay layers, where the groundwater chemistry is more reduced, owing to stagnation of water flow, form these sharp hydrological streamtube boundaries. The geochemical boundaries are thus related to hydrological boundaries. A type 1 change occurred above the clay layer, where the water from the forest edge at -3 m OD moved downwards. Type 2 changes in this boring are mainly caused by air pollution, reflected by NO<sub>3</sub> and SO<sub>4</sub> increases. From -20m to -36 m OD these components increased while chloride remained constant. In the top 10 meters of the boring, the decrease in sulphate emissions since the 80's is visible (Prechtel et al. 2001), leading to a decrease in SO<sub>4</sub>/Cl. Nitrate shows a sudden increase in 2002 here, which can be linked to the cutting of sods of grass, which is done in order to stop the eutrophication of heathlands (Van Breemen and Van Dijk, 1988). This resulted in a release of both N and P from degrading organic material, which is not taken up by plants anymore. Two mini screens showed a type 3 change in 1996, and two in 2002, as they became nitrate-oxidizing (Figure 4.9).

In boring A2 (of which only conductivities are given in Figure 4.9) the shallowest well screens have conductivities of up to 1600 µS/cm, are high in DOC and K, and are highly variable in redox stage, SiO<sub>2</sub>, and alkalinity, indicating heterogeneity of the sediment. The recharge line from the profile above the thick clay layer starting at -12 m OD is 800 meters upstream; the groundwater is partly recharged on the forested ridge flank, as also indicated by the decrease in Ec with depth, and is buffered by the calcareous Kreftenheye sands. Below the clay layer unbuffered water types are found originating from the ridge. Part of this pristine water is reduced and not calcite-buffered (Figure 4.6). A geochemical boundary can be related to the geological boundary between the Peize and Appelscha formations; the yellow-coloured sands of the Appelscha formation impose oxic conditions. Type 2 changes hardly occurred; the pollution pattern remained the same. In many shallow mini screens type 3 changes occurred, as previously reduced groundwater was found to be nitrate-bearing in later sampling rounds.

In boring A3 (Figure 4.10), the pattern has changed dramatically over time. Until -40 m OD the recharge line is 965 meter long, and crosses a patch of forest and several agricultural fields. The well is situated in a regional infiltration area, and shows a calcite buffering boundary above which high Mn concentrations are found due to the acidic nature, and a redox boundary below which Fe and Mn are reductively dissolved. Both boundaries did not move in the last 13 years. The deeper water that is situated in the calcite-free sediments of the Appelscha and Peize formations is calcite-buffered; it has

passed the calcareous Kreftenheye sediments confirming the local origin. Both the Fe and Mn profiles are clearly influenced by these formations. The pattern in the upper part of the aquifer remained constant, showing a slight increase in pollution. In 1996 groundwater quality was found to be deteriorated from -15 to -30 m OD. In 2002 an even larger depth interval (from -5 m OD downwards) shows dramatic increases of HCO<sub>3</sub>, SO<sub>4</sub>, Ca, and Mg, and large increases of Na and Cl. Since no natural or seminatural change in the groundwater flow pattern can explain such changes (it would take more than 40 years), upstream agricultural pumping is hypothesized to have caused this change.

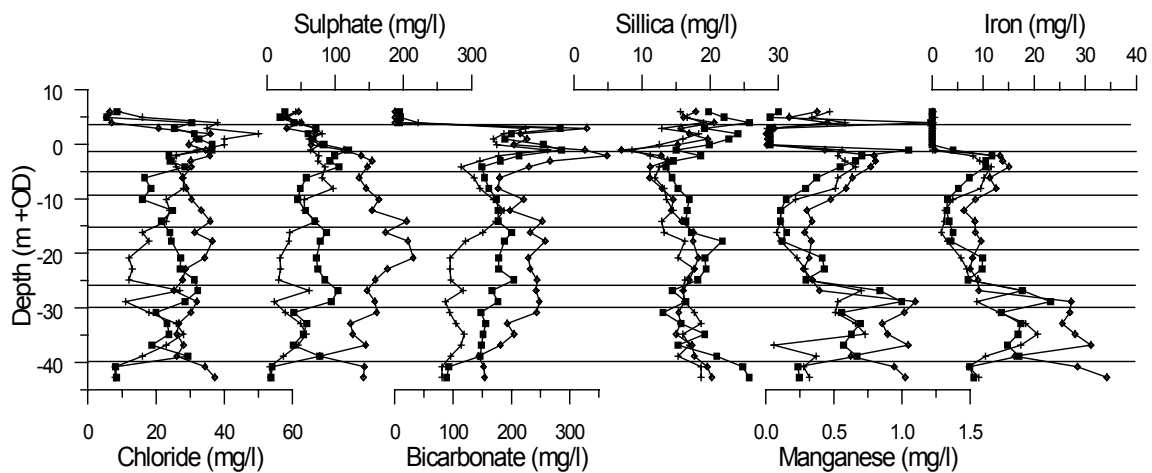


Figure 4.10 Chloride, SO<sub>4</sub>, HCO<sub>3</sub>, Si, Mn, and Fe - depth profiles of boring A3 with streamtube boundaries (legend Figure 4.9)

Boring A4 shows a large SCD at -20 m OD. Above this depth the groundwater is nitrate reduced and polluted (Figure 4.9). Below this depth the Ec is comparable to A1 and the deeper parts of A2 and A3, indicating pristine water of the reduced water type. Reducing conditions are found over the entire length of the boring, indicating upward seepage, although this cannot be inferred from Figure 4.5. The recharge line is 700 meters. A large-scale type 1 change occurred in the deeper part of the boring, as the lowest three streamtubes moved downwards in 1996 and in 2002. The pristine water represents water from more than 100 years old; no non-agricultural land use is near. With very low SO<sub>4</sub>/Cl ratios it consists of two streamtubes, the lowest having Cl = 10 mg/l, indicating heather, and the upper streamtube having Cl = 20 mg/l, indicating forest. No changes occurred over the 13 years observation period. The polluted upperpart of the well consists of 4-5 streamtubes that are iron reduced, with Cl = 30-40 mg/l. The temporal increase in Ec (Figure 4.9) is mainly caused by higher concentrations of SO<sub>4</sub> and Ca.

Boring A5 (Figure 4.11) and its 950m long recharge line (Figure 4.3) is situated in a pine forest. Boring A5 shows distinctive streamtubes, related the clear land use boundaries and management of large patches of forest, and pollution in the upper streamtube. The shallowest groundwater shows clear characteristics of agriculturally polluted water (Frapporti et al. 1995), originating from an agricultural field situated upstream of the boring. In 1989, only the upper mini screen had the characteristics of unpolluted forest-water. In 1996 and 2002, which were relatively dry years, this upper

mini screen was dry due to a drop in water level. Chloride concentrations are high; evapotranspiration factors of more than 10 indicate the difference between this area with a shallow groundwater table and the water recharged pine forest on the ice-pushed ridge found in boring A1. The independent change in chemistry of each streamtube in time is clearly distinguishable.

Boring A6 is the only well situated in a wetland area, and has long been considered as the discharge area of a regional flow system (Hoogendoorn, 1990). It is characterized by its bowl-shaped topography, implying low gradients and thus slow circulation of the groundwater. The area is drained, but always remained too wet for agricultural use. The calculated recharge line is 440 meters; at -11 m OD a streamtube boundary is found, below which the water is of pristine origin. In 1989 the shallowest well screens had relatively high conductivities up to 500  $\mu\text{S}/\text{cm}$  (Figure 4.9), which indicates a contribution from polluted flow systems to the discharge area. The  $E_c$  increased to 700  $\mu\text{S}/\text{cm}$  in 1996, and in 2002 to about 800  $\mu\text{S}/\text{cm}$ .

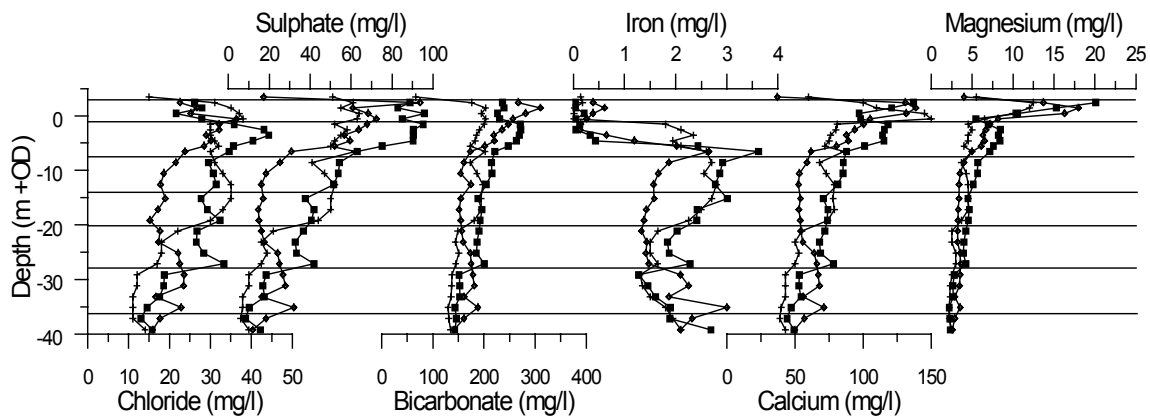


Figure 4.11 Chloride,  $\text{SO}_4$ ,  $\text{HCO}_3$ , Fe, Ca, and Mg - depth profiles of boring A5 with streamtube boundaries. Note the similarities in elemental ratios in the lower streamtubes. (legend Figure 4.9)

Like boring A6, borings A7, A8, A10 and A11 end at the thick Drenthe clay layer at -30 m OD. They all have high conductivities (600 - 1200  $\mu\text{S}/\text{cm}$ , Figure 4.9). Except for boring A10, the shallowest well screens (below -10 m OD) have higher conductivities, which had increased in 1996. This increase is mainly caused by increasing  $\text{SO}_4$  (diffuse pollution); only occasionally higher Cl and  $\text{HCO}_3$  concentrations were found. Like in boring A6, in borings A8, A10 and A11 the influence of sulphate reduction was found. The deepest mini screens have been reduced with respect to  $\text{SO}_4$ ;  $\text{HCO}_3$  concentrations increase slightly by  $\text{SO}_4$  reduction, while calcium concentrations gradually decrease with depth due to lower pollution grade, indicating  $\text{SO}_4$  reduction is a slow gradual process. For these borings, only the deepest samples are completely reduced with respect to sulphate.

Boring A7 is located in an infiltration area, has a recharge line of 900 m, with a small hiatus caused by the Overijssels canal, which was calculated to be at a depth of -16m OD. Till this depth the upper zone is infiltrated in a corn field, displaying high concentrations of Ca, Mg,  $\text{NO}_3$ , K, and DOC. At 0 m OD the calcite dissolution front is found, and at -5 m OD the Fe redox boundary, which shifted downwards 2 meters

between 1989 and 1996. Denitrification starts immediately after infiltration, first by DOC and later by organic material in the sediments.

Boring A8 is situated 3 m from a ditch in a well-drained discharge area; all samples are reduced with respect to nitrate. Modelling indicates a groundwater flow system boundary at -23.5 m OD, and a very short recharge line of 250m, which fits the very few streamtube boundaries found. Potassium concentrations have increased from 2 to 8 mg/l, and subsequently decreased to 7 mg/l over the entire upper 12 meters of this boring, and are remarkably constant, like most components. This indeed cannot be explained by infiltration, in which case input changes should advance approximately 7 m between sampling rounds, and even less when retardation (Ceazan et al. 1989) is taken into account. The change is explained by subvertical discharge flow towards the ditch.

Boring A10 is situated on top of a groundwater flow system boundary, indicating subvertical infiltration. It has a recharge line of 460 meters positioned almost parallel to the groundwater flow system boundary. In the upper streamtube of boring A10 the vertical age difference of groundwater (thickness approximately 10 m: Figure 4.12) is greater than 7 years. The low concentrations of Cl have shifted about 5 meters downward between 1989 and 1996 (0.7 m/yr), and more than 10 meters between 1996 and 2002 (>1.0 m/y). Both hydrology and hydrochemistry indicate the groundwater found in this streamtube originates from the surrounding forest (Figure 4.3), with evaporation factors and subsequent net recharge matching those calculated from meteorological data (KNMI, 1966-2003), displaying evaporative concentration factors of up to 10 times in dry years, and lower than 2 times in wet years. Within this upper streamtube a chemical boundary, the calcite dissolution front, is found. Within mini screen distance (1 m, approximately 1.5 years), the groundwater almost reaches calcite saturation. At -6m OD, a streamtube boundary is found; below it polluted groundwater was detected, above it pristine groundwater. The streamtube boundary in this case also represents a chemical boundary: the NO<sub>3</sub> reduction boundary, which is linked to the Zutphen Member organic rich deposits found at this depth. No type 3 changes occurred in this boring.

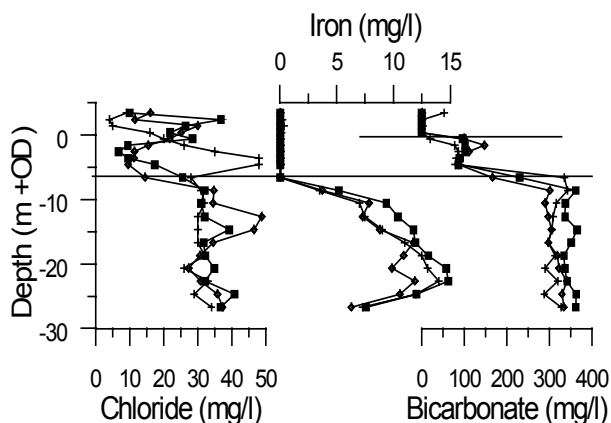


Figure 4.12 Chloride, Fe, and HCO<sub>3</sub> - depth profiles of boring A10 with the two type-3 boundaries indicated, as well as the streamtube boundary. (legend Figure 4.9)

Boring A11 is completely reduced and shows a constant depth profile of polluted water types, indicating no major shifts in land use. The recharge line of the well measures 860

meters, but only 200m to -25m OD. The upper part of the well is recharged in cropland, the lower part in meadows.

#### 4.7 CONCLUSIONS

The conceptual framework presented in this study optimizes the added value that can be obtained from sampling a section of mini screen wells in understanding groundwater quality patterns and the changes therein on a local to regional scale. It does so by explicating the role of groundwater flow, the spatial and temporal pattern of landuse at recharge locations, and the physico-chemical characteristics of the aquifer for the types of groundwater quality boundaries and the types of quality changes observed (1=hydrological, 2=input, 3=geochemical). It therefore integrates hydrological, hydrochemical, geochemical, borehole, historical, and geographical information.

The basic aspect of the conceptual framework is the identification of water quality boundaries, through the chemical differences between adjacent well screens. Being able to identify the causal process behind observed water quality differences is clearly a prerequisite for groundwater quality monitoring and management. Application of the framework predicted that increased pollution first observed in the upper well screens of a streamtube was later extended to the deeper wells, which was demonstrated to occur in the Salland multilevel well section which has been sampled three times since 1989. The average streamtube thickness in the Salland area was identified to be only about 5 m, due to the small scaled land use pattern, and a complete change in water quality was observed in many streamtubes for the given sampling frequency of about once per seven years. When the variability between adjacent streamtubes exceeded the temporal variability, an apparently stable vertical pattern of groundwater quality in a well was observed.

The streamtube concept emphasizes that the relative horizontal position of an observation point within a groundwater flow system must be considered in addition to groundwater age (depth), to interpret or model groundwater quality patterns from point observations.

The Salland section clearly demonstrates that during fifteen years of regional monitoring in a rural area, groundwater quality is not only affected by increased agricultural inputs (type 2), but also by changes in hydrology (type 1), hence the historical development of the area in broad. The observed type 3 changes from reduced to nitrate-oxic conditions are indirectly attributed to agricultural influence as well, but stress the role of sediment reactivity. Even in the deeper parts of the unconsolidated aquifer relatively large changes in water chemistry were observed, indicating the dynamics over a longer time span.

#### 4.8 REFERENCES

- Appelo, C.A.J., Postma, D. (1993), *Geochemistry, Groundwater, and Pollution*, Balkema, Rotterdam
- Ball, J.W. and Nordstrom, D.K. (1991), *WATEQ4F—User's manual with revised thermodynamic data base and test cases for calculating speciation of major, trace and redox elements in natural waters: USGS Open-File Report 90-129*, 185 p

- Barcelona, M.J., Holm, T.R. (1991), Oxidation-reduction capacities of aquifer solids. *Environmental Science and Technology* 25, pp 1565-1572
- Böhlke, J-K. (2002), Groundwater recharge and agricultural contamination. *Hydrogeology Journal* 10, pp 153-178
- Buckau, G., Artinger, R., Geyer, S., Wolf, M., Fritz, P., Kim, J.I. (2000), Groundwater in-situ generation of aquatic humic and fulvic acids and the mineralization of sedimentary organic carbon. *Applied Geochemistry* 15, pp 819-832
- Ceazan, M.L., Thurman, E.M., Smith, R.L. (1989), Retardation of ammonium and potassium transport through a contaminated sand and gravel aquifer: The role of cation exchange. *Environmental Science and Technology* 23, pp 1402-1408
- Champ, D.R., Gulens, J., Jackson, R.E. (1979), Oxidation-reduction sequences in ground water flow systems, *Canadian Journal of earth sciences*, 16, pp 12-23
- Chapelle, F.H. (2003), Geochemistry of groundwater, In: Drever, J.I. (ed), *Treatise on Geochemistry*, Chapter 5: Surface and ground water, weathering, and soils, Elsevier, pp. 425 – 449
- Datta-Gupta, A., King, M.J. (1995), Semianalytic Approach to Tracer Flow Modelling in Heterogeneous permeable Media. *Advances in Water Resources* 18, pp 9-24
- De Mulder, E.F.J., Geluk, M.C., Ritsema, I.L., Westerhoff, W.E., Wong, Th.E. (2003), *De ondergrond van Nederland*. Wolters-Noordhoff bv Groningen/Houten, The Netherlands
- DeSimone, L.A., Howes, B.L. (1998), Nitrogen transport in a shallow aquifer receiving wastewater discharge: a mass balance approach. *Water Resources Research* 34, pp 271-285
- Elburg, H. van, Engelen, G.B., Hemker, C.J. (1987), Een computerprogramma voor de modellering van stationaire stroming en weergave van het net van stroomlijnen en equipotentiaalijnen, alsmede tweedimensionale verticale doorsnede van de ondergrond. Instituut voor Aardwetenschappen, Vrije Universiteit, Amsterdam
- Engelen, G.B. (1981), A systems approach to groundwater quality – Methodological aspects. *The Science of the Total Environment* 21, pp 1-15
- Engelen, G.B., Kloosterman, F.H. (1996), *Hydrological systems analysis, methods and applications*. Water science and technology library 45, Kluwer academic Publishers
- Feyen, J., Jacques, D., Timmerman, A., Vanderborght, J. (1998), Modelling water flow and solute transport in heterogeneous soils: A review of recent approaches. *Journal of Agriculture and Engineering Research* 70, pp 231-256
- Frind, E.O., Duynisveld, W.H.M., Strelbel, O., Boettcher, J. (1990), Modeling of multicomponent transport with microbial transformation in groundwater: The Fuhrberg Case. *Water Resources Research* 26, pp 1707-1719
- Frapporti, G., Vriend, S.P., Van Gaans, P.F.M. (1993), Hydrogeochemistry of the shallow Dutch groundwater: interpretation of the national Groundwater Quality Monitoring Network. *Water Resources Research* 29, pp 2993-3004
- Frapporti, G., Hoogendoorn, J.H., Vriend, S.P. (1995), Detailed hydrochemical studies as a useful extension of national ground water monitoring networks. *Ground Water* 33, pp 817-828
- Griffioen, J. (2001), Potassium adsorption ratios as an indicator for the fate of agricultural potassium in groundwater. *Journal of Hydrology* 254, pp 244-254
- Hansen, B.K., Postma, D. (1995), Acidification, buffering, and salt effects in the unsaturated zone of a sandy aquifer, Klosterhede, Denmark. *Water Resources Research* 21, pp 2795-2809
- Hemker, C., van Elburg, H. (1990), *Micro-Fem user's manual*. Amsterdam
- Hoogendoorn, J.H. (1990), *Grondwatersysteemonderzoek Salland I en II*. DGV-TNO, Oosterwolde
- KNMI (Royal Dutch Meteorological Institute) (1966-2003), *Maandoverzicht van de Neerslag en Verdamping in Nederland (Monthly recharge and Evapotranspiration in the Netherlands)*, De Bilt, the Netherlands
- Jakobsen, R., Postma, D. (1999), Redox zoning, rates of sulfate reduction and interactions with Fe-reduction and methanogenesis in a shallow sandy aquifer, Rømø, Denmark. *Geochimica et Cosmochimica Acta* 63, pp 137-151
- Japenga, J., Harmsen, K. (1990), Determination of mass balances and ionic balances in animal manure. *Netherlands Journal of Agricultural Science* 38, pp 353-367
- Jensen, D.L., Boddum, J.K., Tjell, J.C., Christensen, T.H. (2002), The solubility of rhodochrosite ( $\text{MnCO}_3$ ) and siderite ( $\text{FeCO}_3$ ) in anaerobic aquatic environments. *Applied Geochemistry* 17, pp 503-511

- Kjøller, C., Postma, D., Larsen, F. (2004), Groundwater acidification and the mobilization of trace metals in a sandy aquifer. *Environmental Science and Technology* 38, pp 2829-2835
- Lyngkilde, J., Christensen, T.H. (1992), Redox zones of a landfill leachate pollution plume (Vejen, Denmark). *Journal of Contaminant Hydrology* 10, pp 273-289
- Meinardi, C.R. (1994), Groundwater recharge and travel times in the sandy regions of the Netherlands, RIVM Rep 715501004, PhD thesis, Vrije Universiteit, Amsterdam
- McDonald, M.G., Harbaugh, A.W. (1988), A Modular-Three Dimensional Finite Difference Ground-water Flow Model. *Techniques of Water Resources Investigations of the USGS. Book 6, Chapter A1*
- Pedersen, J.K., Bjerg, P.L., Christensen, T.H. (1991), Correlation of nitrate profiles with groundwater and sediment characteristics in a shallow sandy aquifer. *Journal of Hydrology* 124, pp 263-277
- Portniaguine, O., Solomon, D.K. (1998), Parameter estimation using groundwater age and head data, Cape Cod, Massachusetts. *Water Resources Research* 34, pp 637-645
- Postma, D., Boesen, C., Kristiansen, H., Larsen, F. (1991), Nitrate reduction in an unconfined aquifer: water chemistry, reduction processes, and geochemical modelling. *Water Resources Research* 27, pp 2027-2045
- Prechtel, A., Alewell, C., Armbruster, M., Bittersohl, J., Cullen, J.M., Evans, C.D., Helliwell, R., Kopáček, J., Marchetto, A., Matzner, E., Meesenburg, H., Moldan, F., Moritz, K., Veselý, J., Wright, R.F. (2001), Response of sulphur dynamics in European catchments to decreasing sulphate deposition. *Hydrology and Earth System Sciences* 5, pp 311–325
- Reilly, T.E., Pollock, D.W. (1995), Effect of Seasonal and Long-Term Changes in Stress on Sources of Water to Wells. *USGS Water Supply Paper* 2445
- Rödelsperger, M. (1989), Natural Denitrification processes in the aquifer, In: Kobus H.E., Kinzelbach, W. (eds), *Contaminant transport in groundwater*, Balkema, Rotterdam, pp 159-161
- Schot, P.P. (1990), Groundwater systems analysis of the Naardermeer wetland, the Netherlands, In: Simpson, E.S., Sharp, J.M. (eds), *Selected papers from the 28th International Geological Congress*, Washington, Hannover, 1, pp 257-269
- Smith, R.L., Howes, B.L., Duff, J.H. (1991), Denitrification in nitrate-contaminated groundwater: Occurrence in steep vertical geochemical gradients. *Geochimica et Cosmochimica Acta* 55, pp 1815-1825
- Stollenwerk, K.G. (1996), Simulation of phosphate transport in sewage-contaminated groundwater, Cape Cod, Massachusetts. *Applied Geochemistry* 11, pp 317-324
- Stuyfzand, P.J. (1993), Hydrochemistry and hydrology of the coastal dunes of the Western Netherlands. PhD thesis, Free University of Amsterdam, Amsterdam
- Thiele, M.R. (1994), Modeling Multiphase Flow in Heterogeneous Media Using Streamtubes. PhD dissertation, Stanford University, Dept. of Petroleum Engineering, Stanford, CA
- Tóth, J. (1963), A theoretical analysis of groundwater flow in small drainage basins. *Journal of Geophysical Research* 68, pp 4795-4812
- Van Breemen, N., Van Dijk, H.F.G. (1988), Ecosystem effects of atmospheric deposition of nitrogen in the Netherlands. *Environmental Pollution* 54, pp 249-274
- Van Cappellen, P., Gaillard, J., 1996. Biogeochemical dynamics in aquatic sediments. In: Lichtner, P., Steefel, C, Oelkers, E. (eds), *Reactive Transport in Porous Media. Reviews in Mineralogy* 34, Mineralogical society of America, pp. 335–379, Chapter 8.
- Van Uden, J.G., Vissers, M.J.M. (1998), A hydrochemical study in Salland (in Dutch), M.Sc. thesis, Utrecht University, Department of Geochemistry, Utrecht
- Vissers, M.J.M., Frapporti, G., Vriend, S.P., Hoogendoorn, J.H. (1999), The dynamics of groundwater chemistry in unconsolidated aquifers: the Salland section. *Physics and Chemistry of the Earth (B)* 24, pp 529-534
- Zijl, W. (1999), Scale aspects of groundwater flow and transport systems. *Hydrogeology Journal* 7, pp 139-150



# 5 THE CONTROLS AND SOURCES OF MINOR AND TRACE ELEMENTS IN GROUNDWATER IN SANDY AQUIFERS

M.J.M. Vissers, G. van der Veer, P.F.M. van Gaans, B.J.H. van Os

**Abstract.** From a simple conceptual model, the behaviour and source of trace elements in a sandy aquifer in the Netherlands is explained. Groundwater from multilevel well screens in a sandy fresh water aquifer was analyzed by ICP-MS, resulting in a comprehensive set of trace elements analyses that could be interpreted in terms of saturation, co-dissolution/precipitation, and input and cation exchange. Pure phase equilibrium modelling explained few major and trace elements (Al, P, Ca, Mn, Fe, Ba, and U). Arsenic is explained by codissolution from Fe hydroxides, and Ba and Sr by dissolution of calcite. For Mn coprecipitation with Fe controls concentrations in reduced siderite saturated water. Molybdenum, U, Mn, and possibly Sb are separately controlled by redox conditions. In shallow parts of infiltration areas, weathering of Al-silicates caused by acidification results in anomalous concentrations of Ni, Co, Zn, Be, Cd, Tl, Ga, and REY. Many elements were found to be best explained by source-term limitation from surficial input, where the sorption complex starts acting as the control upon a disturbance. This enabled identification of anomalies related to specific environments or processes: enhanced Co, Ni, and Zn in acid, reduced waters; mobilization of Ni and Co at reduction and buffering boundaries; slow incongruent release of Li, Rb, and Cs; and pollution (e.g. B, Ti, Cu, Rb, Sb, Tl, Pb).

*Keywords: Trace elements, Netherlands, precipitation, codissolution, acidification, cation exchange*

## 5.1 INTRODUCTION

Diffuse pollution of the environment by trace elements (TE) is widespread throughout the world, yet studies on the effects of diffuse pollution on TE concentrations in groundwater are still relatively scarce. There is no doubt, however, that the increased use of metals and their dispersal in the environment must have affected the soil and groundwater compartments. First of all, agricultural diffuse pollution in the form of manure and fertilizers is expected to contribute to metal dispersal in the subsoil. In the Netherlands for instance there is a net import of TE, in the form of constituents of swine and poultry food and food additives (As, Cu, and Zn; Bolan et al. 2004), and of phosphate fertilizers (e.g. Cd, Nicholson and Jones, 1994, and U, Guimond, 1990). Also diffuse atmospheric TE pollution (Nriagu, 1989) will most probably influence groundwater background concentrations. Furthermore, the changes in pH, redox potential, and salinity associated with many forms of pollution are known to indirectly affect TE concentrations in groundwater (Edmunds et al. 1992; Kjølner et al. 2004; Welch et al. 2000).

Most studies on trace metal behaviour in aquifer systems concentrate on sedimentary sources and geochemical processes as explaining factor, which are indeed the dominant factors in many fresh rock aquifers in unpolluted, land climate conditions. Studies concerned with the effects of diffuse agricultural pollution mostly concentrate on major elements or nutrients (Böhlke, 2002). Only in a few cases and for a few TE, rain is accounted for in the explanation of groundwater concentrations, for example for Li (Lyons and Welch, 1997; Edmunds et al. 1987), and 'invariable low As baseline

concentrations in rain' by Smedley and Kinniburgh (2002). Stuyfzand (1984; 1989; 1991) argued that polluted atmospheric deposition may significantly contribute to observed concentrations of Br and probably B, Cr, Cu, F, I, Pb, Rb, Sb, V, and Zn in shallow dune groundwater in the Netherlands. Recently Meinardi (2003) described the similarities between rain and pristine groundwater TE concentrations, and concluded that many trace elements in groundwater may originate from natural atmospheric deposition as well. Johannesson et al. (2000) have shown, using TE-Cl plots, that evaporative concentration may dominantly explain variation in TE such as B, Mo, V, and W in an aquifer in the west of Nevada. Hodge et al (1996) showed similar relationships for Mo, Re, and U with Cl, Na, and SO<sub>4</sub> in oxic groundwater. However, a sedimentary source was suggested as ratios were found to be much too high as compared to seawater. Marques et al. (2004) argue that atmospheric deposition is largely responsible for maintaining the divalent trace element contents in highly leached Brazilian soils.

Under natural conditions, rainwater as a source of TE can be considered a steady-state background input. Steady state sources of TE in the atmosphere consist of seasalt sprays, soil-derived dust, and biogenic sources (Nriagu, 1989). Natural perturbations of the steady state patterns occur by volcanic eruptions and forest fires, as indeed have been observed in polar ice caps (Boutron et al. 1984) and in tree rings (Padilla and Anderson, 2002). In groundwater this type of short-term perturbation is often averaged out through cation exchange and hydrodynamic dispersion, since the time span of these events is small as compared to the residence times in aquifer systems, and the surplus quantities of TE immitted are small compared to the exchangeable pool. Natural TE concentrations patterns in groundwater are therefore expected to be relatively constant in time and space.

Over the last century, atmospheric emission volumes of TE have shown an exponential pattern; mankind has become the key agent in the global atmospheric cycle of trace metals (Nriagu, 1989). Especially in densely populated industrialized areas such as Western Europe, however, large spatial variations in atmospheric emission occur at the km scale. This translates into even larger variability in immisions to the soil-groundwater compartment, because of the relatively short residence times in the atmosphere (Norra and Stüben, 2004), the effects of surface roughness of the soil/land-atmosphere interface (Beier and Gundersen, 1989; Erisman et al. 1998), and land use related diffuse agricultural inputs. This pattern is further complicated as the aquifer sediment may act as a buffer or additional TE source.

The aim of this study is to develop and demonstrate a methodology to identify the sources and controls of TE in groundwater; specifically to better differentiate between sediment interaction and surfacial inputs, because different causes of undesirable enhanced TE concentrations require different mitigating policy approaches. The study area for this demonstration is a 10 km long transect of 10 miniscreen wells reaching -50 m OD, situated in the sandy region of Salland, the Netherlands. The wells were placed in 1988, and have been sampled three times since. Trace element analysis has been included in the latter two sampling rounds. For the current aims, the small size of the study area eliminates the effect of large variations in atmospheric input. The many and detailed previous analyses already provide the necessary background on hydrogeochemical conditions and processes and their development in time and space. Finally the sandy, and hence for many TE relatively inert character of the aquifer, reduces the complexity of the hydrochemical system. These favourable aspects of the research area, together with the

recent advances in analytical techniques that enable low absolute concentrations to be measured in rain and groundwater, formed the preconditions to facilitate the identification of the controls and sources of TE. A process-based sequential approach is used for the interpretation and explanation of the observed TE concentrations in the transect samples. It includes the two-step approach as proposed by Bruno et al. (1998) that combines thermodynamic equilibrium calculations for pure phases (EQ) with the codissolution - coprecipitation (CD-CP) approach. This is then followed by a new step, which is called the sorption equilibrium through steady state input (SEQSSI) approach.

## 5.2 THEORY

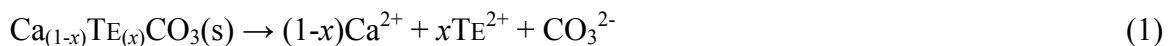
### 5.2.1 Pure phase thermodynamic equilibrium approach (EQ)

The first control on groundwater composition that is to be checked in the sequential approach is true thermodynamic equilibrium (EQ) between pure TE solid phases and solution. Saturation indices of pure phases were calculated by WATEQ4F V2.63 (Ball and Nordstrom, 1991), which includes a large number of phases, and by CHEAQS P2005.1 (Verweij, 2005), as it includes a very wide range of TE. In using these models colloidal transport and organic complexation are not explicitly accounted for. Specific attention was given to redox-sensitive elements. The observed aqueous concentrations were allocated to a single valence state for Co(II), Cr(III), Cu(II), Fe(II), Mn(II), Sn(II), and U(VI). Arsenic and Se were entered as total concentrations, and their speciation into As(III)/As(V) and Se(IV)/Se(VI) was based on the measured redox potential (pE) as entered in the model calculation.

### 5.2.2 Codissolution - coprecipitation approach (CD-CP)

Since saturation control by pure TE phases is rare, the next step in the sequential approach addresses mixed solids, where the TE substitutes for a major constituent. The association of TE with major elements (ME) may also be used as a diagnostic tool to identify the mineral phase and reaction involved, as shown by Magaritz et al. (1990).

Codissolution (CD) of TE simply considers the congruent dissolution of minerals, where the ME and the associated TE dissolve in the same ratio as found in the mineral phase. For calcium carbonate and an associated divalent TE ( $TE^{2+}$ ) this can be described as:



where  $x$  is the mole fraction of the TE in the carbonate. The codissolution hypothesis can be tested in case there is one dominant TE-ME mineral association that acts as the major dissolution source for both ME and TE, and its TE/ME ratio  $x/(1-x)$  should ideally be identified from aquifer sediment data. Codissolution assumes undersaturation with respect to the mineral considered (Pauwels et al. 1989), which can be due to kinetic constraints or source limitation.

In the coprecipitation (CP) approach again thermodynamic equilibrium (saturation) is assumed, but in this case between groundwater and a mixed mineral phase. In this case TE are also related to a major element, but through their solubility products and activities in the mineral phase (Bruno et al. 1998). Coprecipitation has been intensely studied for the carbonate system, the most important buffering system in groundwater. For minor amounts of  $\text{TECO}_3(\text{s})$ , in the host carbonate phase  $\text{CaCO}_3(\text{s})$  ( $x$  less than 5%) the solid solution can be considered ideal, and the thermodynamic activity  $a_{\text{TECO}_3(\text{s})}$  may be equated to its molar fraction  $x_{\text{TECO}_3(\text{s})}$ . Therefore, we can derive a conditional solubility constant  $K_{\text{s}}^*(\text{TECO}_3)$  from the true solubility constant for the pure  $\text{TECO}_3$ ,  $K_{\text{s}}(\text{TECO}_3)$ , as:

$$K_{\text{s}}^*(\text{TECO}_3) = K_{\text{s}}(\text{TECO}_3) \cdot x_{\text{TECO}_3(\text{s})} =_{(\text{at equilibrium})} [\text{TE}^{2+}] \gamma_{\text{TE}} \cdot [\text{CO}_3^{2-}] \gamma_{\text{CO}_3} \quad (2a)$$

with square brackets indicating aqueous concentrations on the molar scale, and  $\gamma_{\text{A}}$  the activity coefficient of ion A. Since we similarly have:

$$K_{\text{s}}^*(\text{CaCO}_3) = K_{\text{s}}(\text{TECO}_3) \cdot (1-x) =_{(\text{at equilibrium})} [\text{Ca}^{2+}] \gamma_{\text{Ca}} \cdot [\text{CO}_3^{2-}] \gamma_{\text{CO}_3} \quad (2b)$$

and assuming the activity coefficient  $\gamma$  for the TE to be similar to that of the ME it replaces, the expected TE/ME ratio in solution at equilibrium would then be  $[xK_{\text{s}}(\text{TEphase})]/[(1-x)K_{\text{s}}(\text{MEphase})]$ , or

$$[\text{TE}^{2+}]/[\text{Ca}^{2+}] = [xK_{\text{s}}(\text{TECO}_3)]/[(1-x)K_{\text{s}}(\text{CaCO}_3)] \quad (3)$$

In addition, a constant undersaturation by a factor  $x$  should be calculated for the pure TE phase  $\text{TECO}_3$ .

In case the solubility of the pure TE phase and the pure major element phase are similar, CD and CP lead to indistinguishable results for the TE/ME ratio in solution. Also, a codissolved TE would then be in equilibrium with the mixed solid phase when saturation is reached for the major element. Often this is not the case. This phenomenon can also be described using a partition coefficient  $K_{\text{d}}$ . Partition coefficients indicate the preference for a TE to enter the solid phase relative to the ME:

$$K_{\text{d}} = \frac{x/[\text{TE}^{2+}]}{(1-x)/[\text{Ca}^{2+}]} \quad (4)$$

As a result of such a preference ( $K_{\text{d}} > 1$ ) net dissolution for the ME may be accompanied by net precipitation for the TE. When for example magnesian calcites dissolve in fresh water environments, the Ca/Mg ratios will evolve along flow paths (Appelo and Postma, 1993; Edmunds et al. 1987). For ideal aqueous and solid solutions  $K_{\text{d}}$  is equal to  $K_{\text{s}}(\text{MEphase})/K_{\text{s}}(\text{TEphase})$  (compare Eq. 3 and 4), but often  $K_{\text{s}}(\text{TEphase})$  is not well defined and  $K_{\text{d}}$  needs to be determined experimentally.

In this study, besides carbonates also iron hydroxides, sulphides, phosphates, the accessory mineral zircon, and the broad category of clay minerals and feldspars, will be considered as potential ME phases controlling TE through CD-CP processes. In practice,

however, distinction between pure phase saturation and CD or CP processes can be rather indeterminate. As these processes can lead to similar TE distributions, mineralogical data should ideally be used to eliminate or support the various hypotheses. Evolution of ratios can be a sign of coprecipitation, but other processes can also be responsible for changing ratios.

### 5.2.3 Sorption equilibrium through steady state input approach (SEQSSI)

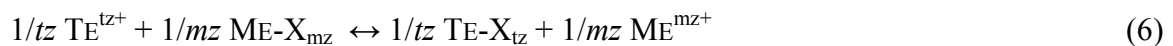
Bruno et al. (1998) already argued that source limitation, sorption, or kinetic effects should be responsible for trace element patterns that cannot be explained by the two above approaches. Kinetic effects can lead to both undersaturation and supersaturation. Source limitation generally leads to undersaturation, but may be of atmospheric / surficial as well as of sedimentary origin.

In our steady state input approach we consider that over pre-industrial times the aquifer must have reached steady-state equilibrium with the long term natural input. For a truly conservative element this simply means that the concentration in the aquifer equals that in the net input. For elements that have no mineral source or sink in the sediment (no EQ or CP-CD) but do participate in exchange reactions (semi-conservative elements, SCE), this comes down to the adsorption complex also being loaded to saturation equilibrium, with aquatic concentrations still equal to the net input, independent of pH and redox conditions. In this natural situation, concentrations in the net input already show spatial variation, primarily through differences in the evapotranspiration factor and possible input of TE in the unsaturated zone by e.g. mineral dissolution.

When such a system reacts to changes, through increased diffuse input or changes in land use, the cation exchange complex becomes an important control of groundwater concentrations. An important aspect of the steady-state input approach is that the conditional distribution coefficient for exchange reactions (Appelo and Postma, 1993; Bradbury and Baeyens, 1997) in dilute water, using a simple single-site sorption model of a SC TE<sup>tz+</sup> competing with a SC ME<sup>mz+</sup> electrolyte, can be described as:

$$K'd = \frac{[TE_{ads}]}{[TE_{aq}]} = \frac{CEC}{tz} \left( K_{TE/ME} \cdot \frac{\beta_{ME}^{1/tz}}{[ME_{aq}]^{1/mz}} \right)^{tz} \quad (5)$$

with CEC the cation exchange capacity,  $\beta_{ME}$  the fraction of the cation exchange complex occupied by the major element, and  $K_{TE/ME}$  the selectivity coefficient between trace and major element, as derived from the exchange reaction (7).



with  $tz$  and  $mz$  the charge of respectively the trace and major element. In fresh water sandy aquifers, CEC,  $K_{TE/ME}$ , and  $\beta_{ME}$  may be taken as constant upon evaporative concentration. Equation (5) can then be simplified as:

$$K'd = [TE_{ads}]/[TE_{aq}] \propto 1/[ME_{aq}]^{tz/mz} \quad (7a)$$

or

$$[TE_{ads}] \propto [TE_{aq}]/[ME_{aq}]^{tz/mz} \quad (7b)$$

or, when  $[TE_{ads}]/[TE_{aq}] \gg 1$ , and hence small adsorptive changes primarily effect the aqueous concentration:

$$[TE_{aq}]/[ME_{aq}]^{tz/mz} = \text{constant} \quad (7c)$$

For TE and ME of equal valence, equation 7b and 7c show that evaporative concentration, leading to equal relative increases for both TE and ME, does not lead to net TE exchange, and thus to seemingly conservative behaviour for the TE. In case of unequal valences, adsorptive competition for a single site will lead to desorption of the TE upon a temporal increase in the evapotranspiration factor if the TE has the highest charge. Such exchange behaviour has indeed been experimentally observed for Cs, as described by Zachara et al. (2002), where partition coefficients show this inverse power relation with electrolyte concentrations. Mutual selectivity depends on the specific TE/ME couple considered. Zachara et al. (2002) found the exchange competition with Cs to be in order of decreasing importance for  $K \gg Na \leq Ca$ .

Changes in the TE/ME *ratio* in the net input, resulting from anthropogenic effects other than changes in evapotranspiration, will be buffered by the adsorption complex both in the case of equal as unequal valences. In the case of equal valences the buffering will initially maintain the TE/ME at the same ‘pristine’ aqueous ratio as before the disturbance, but the new concentrations will be different and fully depend on the new, disturbed, ME concentration (eq. 7c with  $tz/mz=1$ ). In the case of unequal valence also the ratio will change according to Eq. 7c.

A direct check on the presence of steady state is of course a comparison with ratios and concentrations as observed in deposition. Under the steady state input assumption ‘natural’ TE/ME ratios should be analogous to those observed in atmospheric deposition. A drawback here is that no adequate data on pre-industrial TE concentrations in rainwater are available: current rainwater probably contains enhanced amounts of terrestrial dust and anthropogenic inputs. Natural rainwater in the Netherlands is partly determined by the seawater composition, especially in coastal areas, so comparison with seawater ratios offers an alternative.

The above is summarized in Figure 5.1. The pristine rainwater TE/ME ratio is somewhere between the seawater ratio and that in current rainwater. In the natural situation the groundwater composition is expected to be somewhere in the dark grey parallelogram of evapotranspirated rainwater. Upon disturbance, the reaction of the adsorption complex in initial equilibrium with this natural groundwater is either adsorption or desorption, as indicated by the grey vertical arrows. The trajectory of the groundwater composition as observed in a well is worked out for two situations via the dashed lines: a reaction to agricultural pollution (2) for equal valence competitive exchange, and a reaction of a divalent trace element to a monovalent salt shock (3). They show the initial control by the exchange complex, followed by the slow conformation to the new condition. The trajectory observed in case of simply a TE increase (1), only involves the slow conformation to the new condition, its delay depending on the conditional partition coefficient.

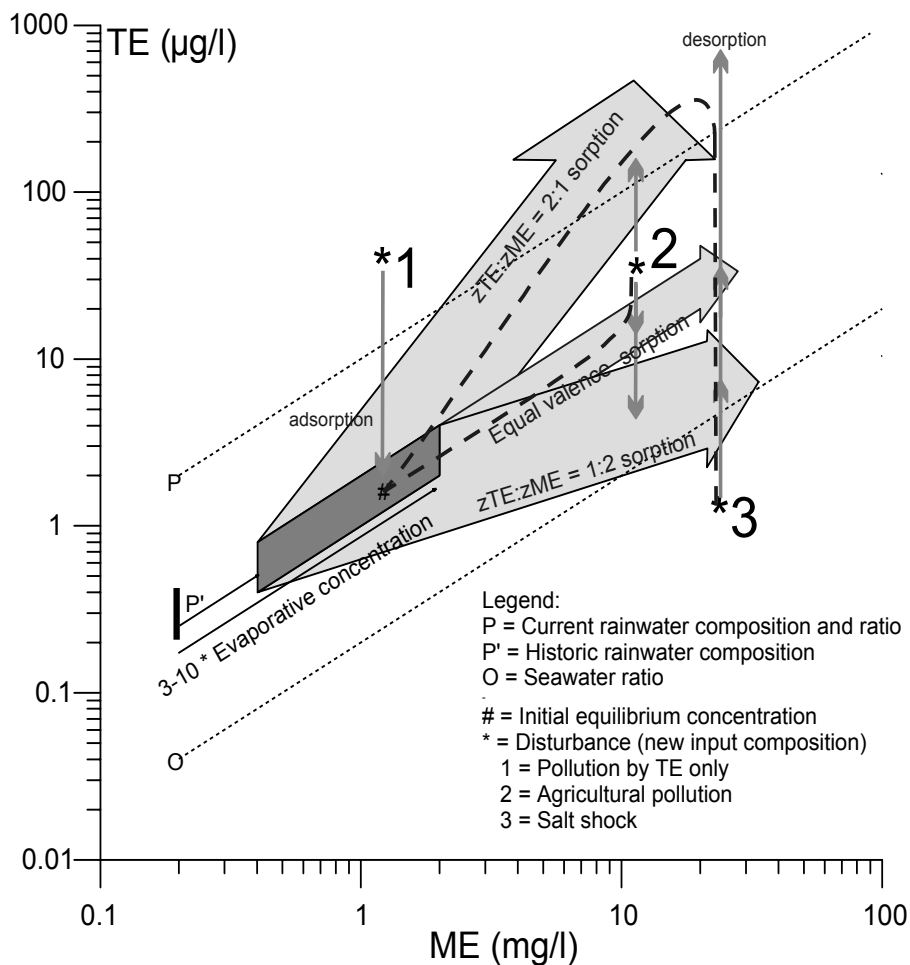


Figure 5.1 Graphical view of the conceptual model of the controls on the groundwater TE as defined in the SEQSSI approach. The dark grey parallelogram shows the natural groundwater composition field. The broad light grey arrows indicate the shift from natural to disturbed groundwater composition. Grey vertical arrows indicate the reaction of the sorption complex upon the disturbance indicated; black dashed lines indicate the concentration development at an observation point.

Depth profiles of TE/ME ratios when both behave as SCE, are also important to reveal for which TE and to what extent the historic steady state situation is still present. The TE/ME ratios should be constant, especially in the deeper aquifer with pre-industrially infiltrated water. Deviations from a steady state TE/ME ratio would indicate saturation / CD-CP processes already identified in the previous steps, yet unidentified sedimentary sources or sinks, unequal-valence buffering by the adsorption complex, or changes in the input ratios that may eventually lead to a new steady state. Sedimentary source-term limitation resulting from slow incongruent dissolution of minerals will be indicated by an increasing TE/ME ratio with age, hence depth. Through the use of the steady state input approach identification of the effects of adsorption / desorption and sedimentary source term limitation is greatly facilitated.

## 5.3 MATERIALS, FIELD AND LABORATORY METHODS

### 5.3.1 Geography, geology and geohydrology

The Salland area, in which the section of multilevel wells was placed, is situated in the east of the Netherlands. The basic geomorphology of the area was shaped during the Saalian (~150 ka ago, De Mulder et al. 2003). The well section starts at the ‘Holterberg’ ice-pushed ridge (ice-displaced local deposits flanking the glacial tongue basin), which reaches +75 m OD (Figures 5.2 and 5.3). Towards the west, the well section runs across an eolian sand plain, with undulating topography. The sand cover (Boxtel Formation, Wierden Member, Lithostragraphy cf. Schokker, 2003) is a few meters thick overlying coarser fluvial sands (Kreftenheye Formation) that contain a significant amount of largely unweathered rock fragments (typically slates and schists). Therefore, the reactivity of this deeper layer might be somewhat higher compared to the upper aquifer sediment. These deposits, that formed in the late Saalian, Eemian, and Weichselian (~150 – 11 ka BP) comprise the studied aquifer with a base typically at - 30 m OD. In the western part of the well section they are underlain by impermeable fluvio-glacio-lacustrine clays that filled the Saalian tongue basin following deglaciation (Kreftenheye Formation, Twello Member; Figure 5.3). In the eastern part the poor sands of the Peize and Appelscha formations are found, which consist of river sands. The Peize formation consists of very poor grey to white coloured sands and gravels from Baltic rivers; the Appelscha formation contains grey or light yellow medium to very coarse sands and gravel, and is of slightly different origin. Active, rain water fed groundwater flow was initiated at the start of the Holocene, when permafrost and depositional river flow conditions ceased to prevail over the area.

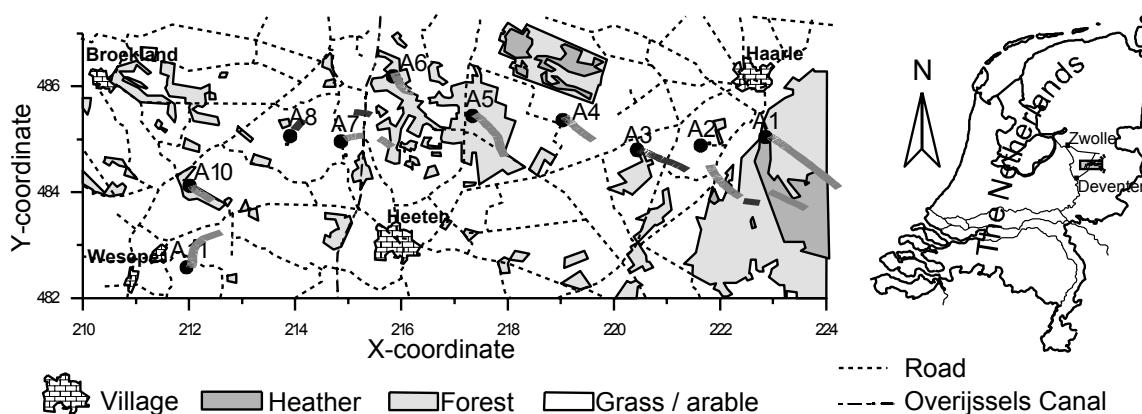


Figure 5.2 Map of the Salland study area, its position in the Netherlands, landuse, the borings and their recharge lines. Coordinates in km RDS

Average annual rainfall in the area is about 770 mm (KNMI, 1966-2003). The climate is temperate, with a precipitation deficit in summer. Based on tritium measurements, Meinardi (1994) calculated a net infiltration of approx. 340 mm/yr on grassland. A dense network of ditches drains the area, to make it suitable for agriculture. Groundwater modelling estimates water ages of up to 120-150 years in the aquifer system (Hoogendoorn, 1990; van Uden and Vissers, 1998; *chapter 3*). The calculated backward



projections on the surface of the vertical well profiles (recharge lines) are shown in Figure 5.2.

The western part of the area was first inhabited in the 13th century, and as the population increased in the 19th century, the poor sandy soils near the ice-pushed ridge were cultivated on a local scale. Most of the sandy soils east of the Overijssels Canal (Figure 5.2) remained vegetated by heath. With the advent of fertilizers, after 1900 much of the heath was rapidly removed and the land was drained and cultivated; forests on the ridge disappeared due to wood felling. By 1970, almost all the heathlands on the ice-pushed ridge had been reforested. With the introduction of intensive indoor cattle breeding in the region at this time, fodder maize became the primary crop, also because it can take high manure doses. The increase in manure production is to a lesser extent applied to grassland. Figure 5.2 shows the present land use. Today 20% of the land consists of forest/heath; of the agricultural land, 75% is used as meadow (dairy farming), and 25% as arable land.

### 5.3.2 Available geochemical information

#### *Geochemistry of the well section*

The well transect was placed in 1988, at which time also sediment samples were collected. Water sampling and analysis took place in 1989 (major elements only; Hoogendoorn, 1990; Frapporti et al. 1995), in 1996 (Vissers et al. 1999), and recently in 2002.

Frapporti et al. (1995) determined the mineralogy of the aquifer formations. The sediments of the aquifer contain mainly quartz (up to 95 mass%) and 0-10 mass% alkali-feldspars, whereas plagioclase is virtually absent (see also Van Baren, 1934). The clay fraction (5-25 mass%) mainly consists of illite, with lesser amounts of smectite and kaolinite. Calcite is absent in the shallow part of the ice-pushed ridge; low concentrations (up to 1 mass%) are found in the deeper parts of borings A2-A5 (Figure 5.3, Peize and Appelscha Fm). The other parts of the well section contain 2 – 20 mass% of calcite (coarse sands 2 – 5 mass%, fine sands 5 – 20 mass%), and may occasionally contain trace amounts of pyrite of up to 0.4 mass%. Organic matter contents are commonly less than 0.05 mass% organic carbon, in some deeper sediments 0.5 mass% organic carbon is found. Accessory minerals identified by microprobe analysis are barite ( $\text{BaSO}_4$ ), rutile ( $\text{TiO}_2$ ), monazite ( $(\text{Ca,L a,N d,Th})\text{PO}_4$ ), zircon ( $\text{ZrSiO}_4$ ), ilmenite ( $\text{FeTiO}_3$ ), titanite ( $\text{CaTiSiO}_5$ ), apatite ( $\text{Ca}_5(\text{F,Cl,OH})(\text{PO}_4)_3$ ), pyrite ( $\text{FeS}_2$ ), dolomite ( $\text{CaMg}(\text{CO}_3)_2$ ), variscite ( $\text{AlPO}_4 \cdot 2\text{H}_2\text{O}$ ), garnet ( $(\text{Ca,Fe,Mg})_3\text{Al}_2(\text{SiO}_4)_3$ ) and gypsum ( $\text{CaSO}_4 \cdot 2\text{H}_2\text{O}$ ). A NaAc –  $\text{NH}_4\text{Ac}$  sequential extraction of carbonates, performed under oxic conditions by van Uden and Vissers (1998), showed that carbonates contain both Mn and Sr in significant amounts, but no significant amounts of Mg.

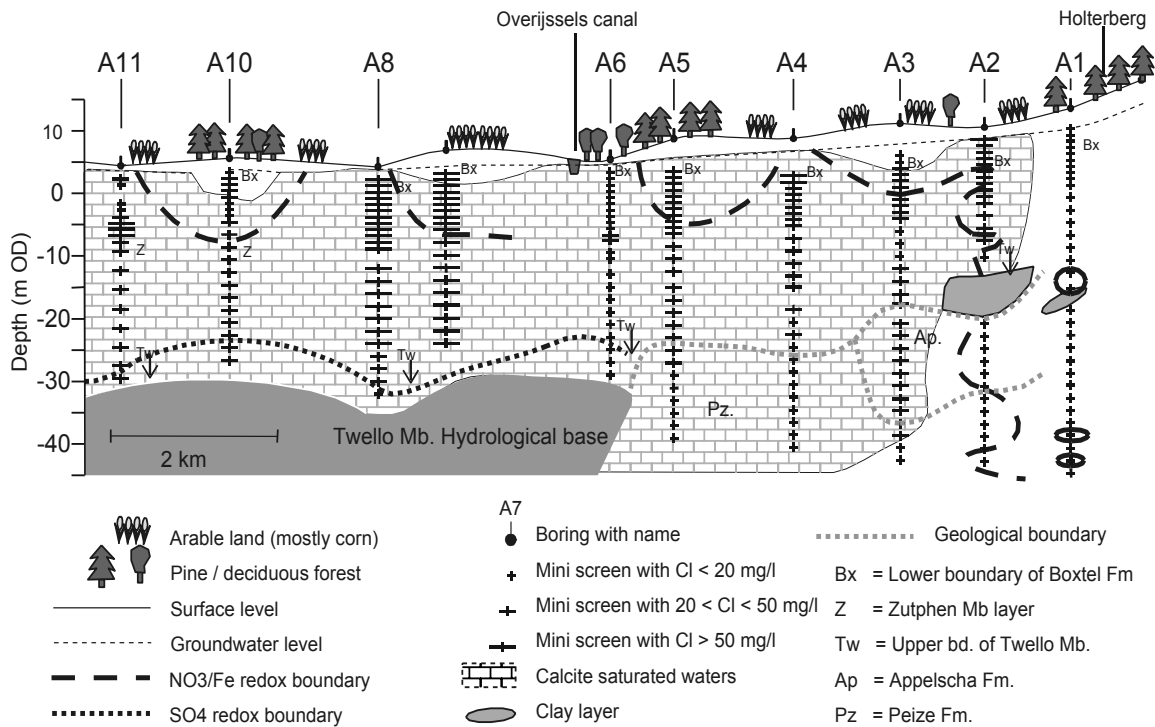


Figure 5.3 Cross section showing the multilevel well transect with major hydrogeochemical zones, pollution grade, geology, and land use. Dutch Ordnance Datum (NAP) is used

The major element geochemistry of the groundwater in the area is controlled by calcite dissolution, redox processes, and pollution, and has been previously described by Frapporti et al (1995) and Vissers et al (1999). Figure 5.3 shows the distribution of the resulting water types in the form of buffering and redox boundaries, and Cl as a general indicator of agricultural influence. The water in the well screens situated in upward seepage areas is calcite buffered and reduced with respect to nitrate, well screens situated in infiltration areas show a general sequence of hydrochemical alteration, which is calcite dissolution followed by nitrate reduction with organic carbon, sometimes followed by sulphate reduction. Altogether, five major water types can be distinguished (Figure 5.3): (1) an unbuffered natural water type occurring mainly in boring A1, the lower part of A2 and the top of borings A3 and A10, a calcite unbuffered, yet nitrate reduced water type is found in some depth intervals in borings A1 and A2; (2) an unbuffered, severely polluted water type in the top of boring A2 and in some screens of borings A5 and A7; (3) an oxic agriculturally influenced and buffered water type in part of the upper screens of borings A2, A3, A5 and A10; (4) a calcite buffered and iron reduced natural water type occurring in the lower parts of borings A4 - A6; and (5) a similarly buffered and reduced, but agriculturally influenced water type, in most of borings A3 and A7-A11 and the upper part of A4. The characteristics of these water types in terms of major cations are depicted in Figure 5.4; relative occupancies of major elements on the sorption complex vary depending on affinities and pH (proton sorption).

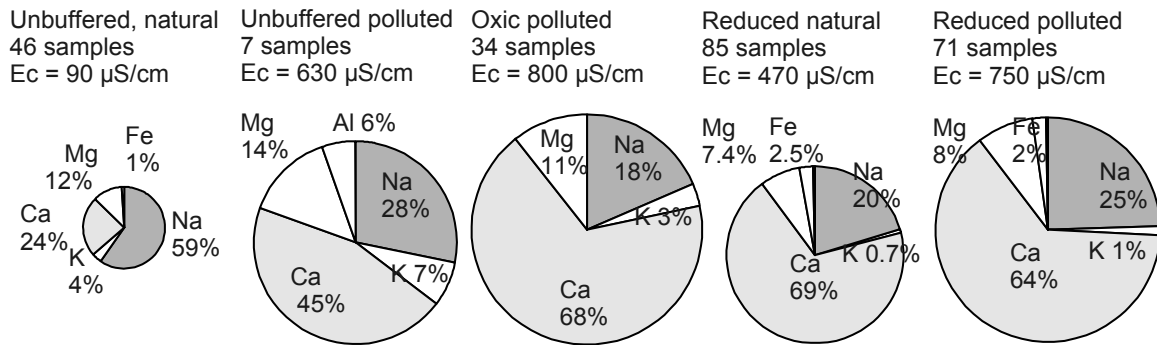


Figure 5.4 Pie diagrams of cations in the average water types found in the well section (mmol/l)

### TE/ME ratios in aquifer minerals

Little is known about the trace element composition of the individual mineral phases in the aquifer sands. In a recent geochemical study of the Dutch subsoil, the relative TE contribution to various mineralogical fractions was determined (Van der Veer, 2006) from bulk geochemical data. For the sandy soils (Boxtel Formation) it was shown that a large part of the TE are concentrated in either heavy minerals (HFSE such as Nb, Hf and Zr, but also Cr, Sb, Th, Ti, U, V, Y and REE) or in alkali-feldspars (Ba, Rb, Tl, and Sr), compared to reactive phases such as micas, clays, and oxihydroxides (Van der Veer, 2006). The TE associated with the more labile fraction, mainly comprising of chlorite, smectites, and Fe-oxihydroxides, are As, Cu, Zn, Bi, and Hg. Beryllium, Cs, Ga, Pb and Sn show less preference for a specific mineralogy and are controlled by Al-silicates in general. For these latter elements TE/Al ratios are relatively constant (Figure 5.5a and 5.5b). For elements that show large fractionation between mineralogical fractions, the ratios in the different mineral fractions in many instances can be estimated from ratios of sedimentary, mineralogically non-pure, endmembers (Figure 5.5c).

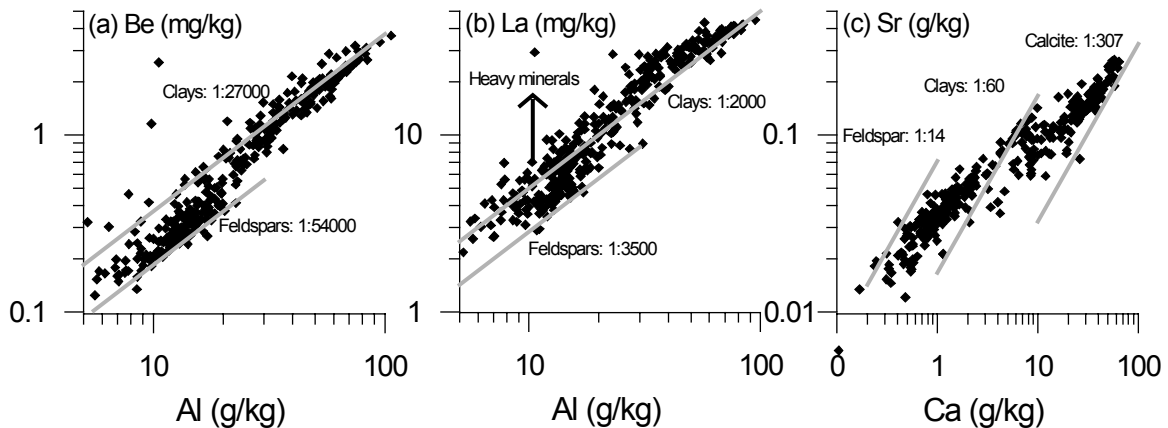


Figure 5.5 Bivariate geochemical relations in the Dutch subsoil (Van der Veer, 2006) (a) Be-Al and (b) La-Al, and (c) Sr-Ca

### Rain and seawater hydrochemical data

Published seawater compositions show a large variation for many TE (Nozaki, 1997), and no nearby data for the North Sea are available. We therefore used the data from both Ball

and Nordstrom (1991) and Nozaki (1997) to estimate the input TE/SCE ratios in seawater.

Estimates for modern rainwater composition were taken from various sources. The Dutch rain monitoring network (RIVM, 1994-2000) consists of 15 stations, equipped with glass wet-only catchers (RIVM, 1994). Samples are collected every two weeks, and combined for monthly analysis. Major elements, and Cd, Cu, Pb, Mn, Fe, and Zn were measured for all stations from the start; As, Cr, Ni, and V initially were analyzed for only two stations, but this was extended to all stations in 1999, at which time also Co was added to the list of analytes. For some elements these data show a large temporal and spatial variability. Nearby stations (#722, #724, and #732) were used to estimate the Salland rainwater composition.

A local rainwater sample was collected in 2002 during a large summer storm. A glass dish was acid washed and rinsed three times with rainwater collected at the start of the storm. Two samples were taken; sample treatment and analysis were identical to that for the groundwater samples.

As only a limited set of elements in the Dutch rainwater is measured, results are also compared to rainwater from a Swedish study (Erikson, 2001), where the 1999 average composition was analyzed from monthly samples of wet deposition. These samples may be considered as being slightly closer to pristine natural conditions than Dutch rain water.

### **5.3.3 Groundwater sampling and analysis, quality control**

The present groundwater study is primarily based on the sampling round of 2002. Sampling was done using vacuum hand pumps, flushing the mini well system with at least 3 volumes (3 liters) before collecting the sample. Ec, Eh (in 1996) and pH were measured during sampling using standard electrodes, while alkalinity (by Gran-titration) was measured within 12 hours at a field lab. Samples were filtered (0.45  $\mu\text{m}$  cellulose nitrate membrane filter), one part was acidified to pH=1 with ultrapure  $\text{HNO}_3$  in new, trice pre-flushed PE bottles, and two other samples were acidified with sulphuric acid in PE test tubes for anion and DOC/TN analysis. A fourth sample was filtered at 100 $\mu\text{m}$  for alkalinity titration. Samples were stored in ice in the field and at 4°C afterwards. A total of 246 well screens were sampled, 26 of which in duplicate to assess the field sampling precision. Four field blanks (sampled on different days from a vessel of deionized water) were prepared as well to ascertain the absence of contamination through the sampling procedure in later analysis. Sampling error and bias may for example arise from short-circuiting in the monitoring wells and particulate mobilization due to pumping, despite the low volume and flow rate of the sampling system.

Analyses were performed in random order to avoid entanglement of spatial and analytical variability. Methods used were ICP-AES for major cations and sulphate, auto analyzer and photometry for major anions and  $\text{NH}_4$ , and ICP-MS for trace and some major elements (see Table 1 for the isotopes used). Samples with ionic imbalance were reanalyzed. Trace element analysis was divided over six separate batches. The duplicate samples were always analysed twice as a pair within randomly selected batches, thus creating 26 sample quadruplets that allowed assessment of both the within batch and field sampling error and the between batch analytical error.

Final ion balance in 2002 is within 2% deviation for 83% of the samples, and within 5% in 93% of the cases. For TE, total duplicate error was found to be dominated by the between batch analytical error, suggesting the main cause of error is in the calibration and instrumental changes between days. The error is proportional to the concentration over the complete range of concentrations for most elements, as evidenced from graphs, due to a constant sensitivity of the apparatus. Lognormalized data were therefore used in the error analysis. The measure used to quantify the precision was the between batch replicate standard deviation (RSD; Table 1), which is defined as:

$$RSD = \sqrt{\{\Sigma(x_1-x_2)^2/(2N_d)\}} \quad (8)$$

where  $x_1$  and  $x_2$  are the logtransformed values in different batches for the same sample and  $N_d$  is the number of between batch duplicate pairs (here 52).

*Table 5.1* Summary statistics (median, standard deviation SD of logtransformed data) and analytical precision of the trace elements analysed as the replicate standard deviation (RSD; Eq. 8), with their isotope mass. The asterisk indicates elements that show inconsistencies with the 1996 data, a grey shading of the cell indicates the element does not comply with the set analytical quality criteria

Elem.	Med. µg/l	SD	DL %	RSD	RSD/ SD %	Elem	Med. µg/l	SD	DL %	RSD	RSD/ SD%
Li 7	2.0	0.30		0.12	40.0	Sb	0.023	0.64	5	0.37	57.8
Be 9	0.084	0.73		0.22	30.1	Cs	0.004	0.39	15	0.14	35.9
B 11	8.2	0.69	5	0.20	29.0	Ba	85	0.47		0.05	10.6
Al 27	2.4	0.87	5	0.32	36.8	La	0.017	0.86	1	0.30	34.9
P 31	49	0.59	30	0.26	44.1	Ce	0.032	0.84		0.42	50.0
Sc 45	0.67	0.21		0.13	61.9	Pr	0.004	0.86		0.32	37.2
Ti	0.56	0.35		0.17	48.6	Nd	0.021	0.85	1	0.29	34.1
V 51	0.22	0.58	16	0.17	29.3	Sm	0.004	0.86	1	0.37	43.0
Cr	0.45	0.67	50	0.41	61.2	Eu	0.001	0.91	6	0.35	38.5
Mn	260	0.80	4	0.07	8.8	Gd	0.006	0.82		0.39	47.6
Fe 57	2400	0.97	2	0.21	21.6	Tb	0.001	0.82	4	0.28	34.1
Co 59	0.083	0.63		0.14	22.2	Dy	0.007	0.79		0.33	41.8
Ni 60	0.66	0.59	2	0.19	32.2	Ho	0.001	0.79	1	0.28	35.4
Cu 65	0.4	0.48	7	0.26	54.2	Er	0.005	0.78		0.42	53.8
Zn 66	4.1	0.51		0.16	31.4	Tm	0.000	0.77	4	0.30	39.0
Ga 71	0.003	0.61	8	0.36	59.0	Yb	0.005	0.76		0.25	32.9
As 75	0.94	0.69	1	0.09	13.0	Lu	0.000	0.73	3	0.21	28.8
Se	0.4	0.41	16	0.44	107.3	Hf	0.003	0.71	49	0.22	31.0
Rb 85	0.58	0.51		0.05	9.8	Ta	0.006	0.95	83	0.07	7.4
Sr 88	290	0.39		0.04	10.3	W	0.10	0.76	77	0.16	21.1
Y 89	0.058	0.74		0.20	27.0	Au	0.009	0.69	74	0.20	29.0
Zr	0.18	0.80	56	0.25	31.3	Hg	0.002	0.67	66	0.46	68.7
Nb	0.023	0.84	77	0.17	20.2	Tl	0.012	0.54	47	0.28	51.9
Mo	0.13	0.61	5	0.17	27.9	Pb	0.18	0.60	10	0.39	65.0
Ag10	0.000	0.62	50	0.40	64.5	Bi	0.000	0.72	41	0.46	63.9
Cd	0.005	0.92	13	0.41	44.6	Th	0.002	0.77	15	0.41	53.2
Sn	0.009	0.78	51	0.50	64.1	U	0.013	1.07	19	0.32	29.9

Like any standard deviation, the RSD is sensitive to large differences between  $x_1$  and  $x_2$ . The replicate median absolute deviation (RMAD) was generally less than half the RSD. Trace elements were discarded from further interpretation if either the RSD was

considered too large with respect to the observed variation in concentrations, or the number of observations below the detection limit was too large. For the RSD, an indicative cut-off value of 40% of the overall population standard deviation (SD, also based on logtransformed data) was used, similar to Farnham et al. (2002; 2003). Evidently this should be considered as only a 'soft' criterion, as TE may also fail for lack of variation within the dataset. Therefore, Ag, Bi, Cr, Er, Ga, Hg, Pb, Sb, Se, Sn, Th, and Tl were eliminated, but Cd, Pb, and Cu were still included because of their environmental relevance, Ga is still incorporated in the CD-CP approach, and relevant anomalies of Sb and Tl will be mentioned briefly. Elements that can be analyzed reasonably precise in only half or less of the samples are Au, Hf, Nb, Ta, W, Zr. Of these, Zr and Hf were still included in the CD-CP approach only. Ti was discarded because serious biases between analytical batches were evident.

## 5.4 RESULTS AND DISCUSSION

### 5.4.1 Pure phase thermodynamic equilibrium approach (EQ)

Of course, the model calculations also provided saturation estimates for ME phases. Since these are relevant for the CD-CP approach they are briefly discussed here as well. ME saturation occurs for calcite, rhodochrosite, and siderite in the carbonate saturated reduced water type (Figure 5.3), where most samples also show vivianite saturation. In the polluted carbonate saturated water calcite plus apatite saturation occur. Based on the observed TEAP (terminal electron accepting process; reduction of O<sub>2</sub>, NO<sub>3</sub>, Mn(IV), Fe(III), or SO<sub>4</sub>) in the groundwater samples, pE values were estimated from measured redox potentials in 1996. Except for the acid waters in boring A1, the larger part of A2, and the top of A3, A7 and A10, near-saturation with ferrihydrite is calculated throughout the aquifer (in oxic as well as reduced conditions), which corroborates the pE values adopted in the calculations.

An overview of the TE pure phases considered and those found to reach saturation is given in Table 2. In line with other studies on TE behaviour in groundwater systems, only few TE are explained by saturation with a pure mineral phase. Barite saturation is found in many of the deeper samples but no distinct boundaries are observed; apparently barite dissolution is a slow process compared to groundwater flow or is source-term limited. Phosphate saturation is observed for the LREE and Y at low pH. Of the redox sensitive elements, U was calculated to be saturated with uraninite in the reduced zone, following the theoretical pattern of lowest concentrations at lowest pE (Cochran et al. 1986; Casas, et al. 1998). From the TE suspected of being controlled by the solubility of their oxyhydroxides, only Al is actually calculated to be saturated with its hydroxide phase Al(OH)<sub>3</sub>, most probably a gibbsite-like mineral (Hansen and Postma, 1995). Again with the exception of the acid waters in the shallow well screens in borings A3-A10, the whole of boring A1, and the deeper part of boring A2, gibbsite saturation occurs throughout the aquifer. For Mn, dissolution of oxyhydroxides explains concentrations found at low pH, and the negative 2:1 log[Mn]:pH relation (Hem, 1978) is observed. Beryllium shows an average 10,000 times subsaturation with respect to Be(OH)<sub>2</sub>. Yet,

like Ga and REE, it shows high concentrations at low pH, indicating pH dependent behaviour.

An inverse relation with pH may also be induced by saturation control by a carbonate phase, or a positive relation when complexation with carbonate occurs. Hence, speciation results of the modelling are also of interest. Most elements are mainly present as free cations (As, Cd, Cs, Co, Li, Ni, Rb, Sr, Ti, Zn) or oxyanions ( $\text{H}_2\text{BO}_3^0$ ,  $\text{MoO}_4^{2-}$ ,  $\text{H}_2\text{VO}_4^-$ ). Carbonate complexation is found at high pH for Cu ( $\text{CuCO}_3^0$ ), the REY (Rare Earth Elements and Yttrium:  $\text{REYCO}_3^+$ ), and U ( $\text{U}^{\text{VI}}\text{O}_2(\text{CO}_3)_2^{2-}$  and  $\text{UO}_2(\text{CO}_3)_3^{4-}$ ). Relevant hydroxide complexation at high pH occurs for Be ( $\text{Be}(\text{OH})_2^0$ ). At low pH, complexation of REY with sulphate ( $\text{TESO}_4^+$ ) may be relevant.

Table 5.2 Possible (+, or associated element) and observed (grey shading) saturation phases of TE

TE	halogenide	(hydr)oxide	silicate	sulphate	carbonate	phosphate	oxyanion-salt
Li	F,Cl						
Be		+					
B							
Al	F	+	+	+		+	
V		+					Ba,Ca,NH <sub>4</sub> ,Sr
Mn		+			+	+	
Fe	Cl	+	+	+	+	+	
Co		+			+		
Ni		+			+		
Cu	Cl	+	+	+	+		
Zn	Cl	+	+		+	+	
As		+					Ba,REY
Rb							
Sr	F			+	+		
Mo		+					Ca,Mg
Cd		+			+	+	
Cs							
Ba	F	+		+	+		
REY	F	+			+	+	
U		+	+		+	+	
Ga		+				+	
Zr		+					
Sb			No data				
Hf		+					
Tl							
Pb	F,Cl	+		+	+	+	

#### 5.4.2 Codissolution - coprecipitation approach (CD-CP)

*Carbonates:* Calcite is the most studied mineral phase with respect to coprecipitation and has been studied for a large number of TE and minor elements (Curti, 1999; Rimstidt et al. 1998; Lakshatnov and Stipp, 2004). CD-CP processes with calcite are generally found

to be important for Sr and Ba (Stuyfzand, 1989, Magaritz et al. 1990), Mg, and other bivalent TE.

In Figure 5.6a the Sr-Ca scatterplot is given. Calcite saturated samples and non-saturated samples are distinguished, based on the previous thermodynamic equilibrium results. Lines of constant Sr/Ca ratio (a log-log slope of 1) are shown for the observed ratios in local rain, local calcite, and endmember ratios of major mineral phases as found in the Dutch subsoil. The larger part of the non-saturated samples shows a Sr/Ca ratio of about 1:150 (mass basis), which is similar to that in local rain. Non-saturated samples originating from the upper screens of borings A1 and A10 have much higher ratios of about 1:75 to 1:35, indicating codissolution from aluminosilicates. The calcite saturated samples follow a pattern of codissolution of Sr from a calcium carbonate with a Sr/Ca mass ratio around 1:250 in the naturally buffered samples, and from a more variable source in agriculturally influenced waters, ranging from ratios similar to those in rain water down to 1:560 in the most heavily polluted samples.

In Figure 5.6b the Mg-Ca scatterplot is given. Calcite saturated and non-saturated samples are distinguished and relevant ratios are indicated. The interpretation appears similar to that for Sr, with a Mg/Ca rain water ratio of about 1:5.0 in the majority of the unbuffered samples and higher ratios towards 1:1 in the upper screens of A1 and A10. These higher ratios are suggestive of codissolution from dolomite (mass ratio 1:1.65), but in view of their unbuffered nature and the analogy with Sr the aluminosilicate source is more likely. In the buffered samples a distinction between the natural (1:18) and agricultural (1:10) ratio is more evident for Mg than it was for Sr. Apparently the carbonate in agriculturally polluted samples (liming) is rich in magnesium compared to the natural background (often dolomitic limestone from the 'Winterswijk quarry' is applied). However, a codissolution model cannot be adopted for magnesium in the non-agricultural water, since it was shown not to be present in significant amounts in calcites in the sediments of the section (Van Uden and Vissers, 1998). Therefore we must assume that only Ca is added upon dissolution of sedimentary calcite, and the observed ratio is controlled by coprecipitation and/or sorption.

In Figure 5.6c the Ba-Ca scatterplot is shown with subdivision in barite saturated and barite undersaturated samples. The groundwater samples give evidence of codissolution of calcium carbonate (Edmunds et al. 1987; Frapporti et al. 1996; Duro et al. 1997); the naturally calcite buffered samples show a Ba:Ca ratio of approximately 1:1500. Barite saturation in calcite undersaturated samples suggests another source for Ba. This source partly consists of aluminosilicates as evidenced by the Mg and Sr anomalous samples indicated, and partly consists of barite, which is also found in the sediments.

From the other bivalent TE considered (Be, Cd, Co, Cu, Mn, Ni, Zn) only Co and Ni show a relation with calcium in the buffered samples (TE/Ca about 1:1400 and 1:160 respectively). However, similarly high Co and Ni concentrations are observed in non buffered water, which excludes codissolution with calcite as a source.

*Iron minerals, iron and manganese (hydr)oxides and siderite:* Iron minerals are often mentioned as a potential source of many TE. Of specific interest are As, and Mo with similar redox behaviour, Co, Ni, Cu, Cd, Pb, Cr, and Zn (Tessier et al. 1996, Manceau et al. 2000; Van der Veer, 2006). As the determination of TE contents in iron hydroxides is highly problematic (McCarthy et al. 1998) and cannot be inferred from



bulk geochemical data, only water data can be used for the deduction of CD-CP processes. As was found in the Eq step, Fe concentrations are controlled by siderite saturation in most reduced groundwaters.

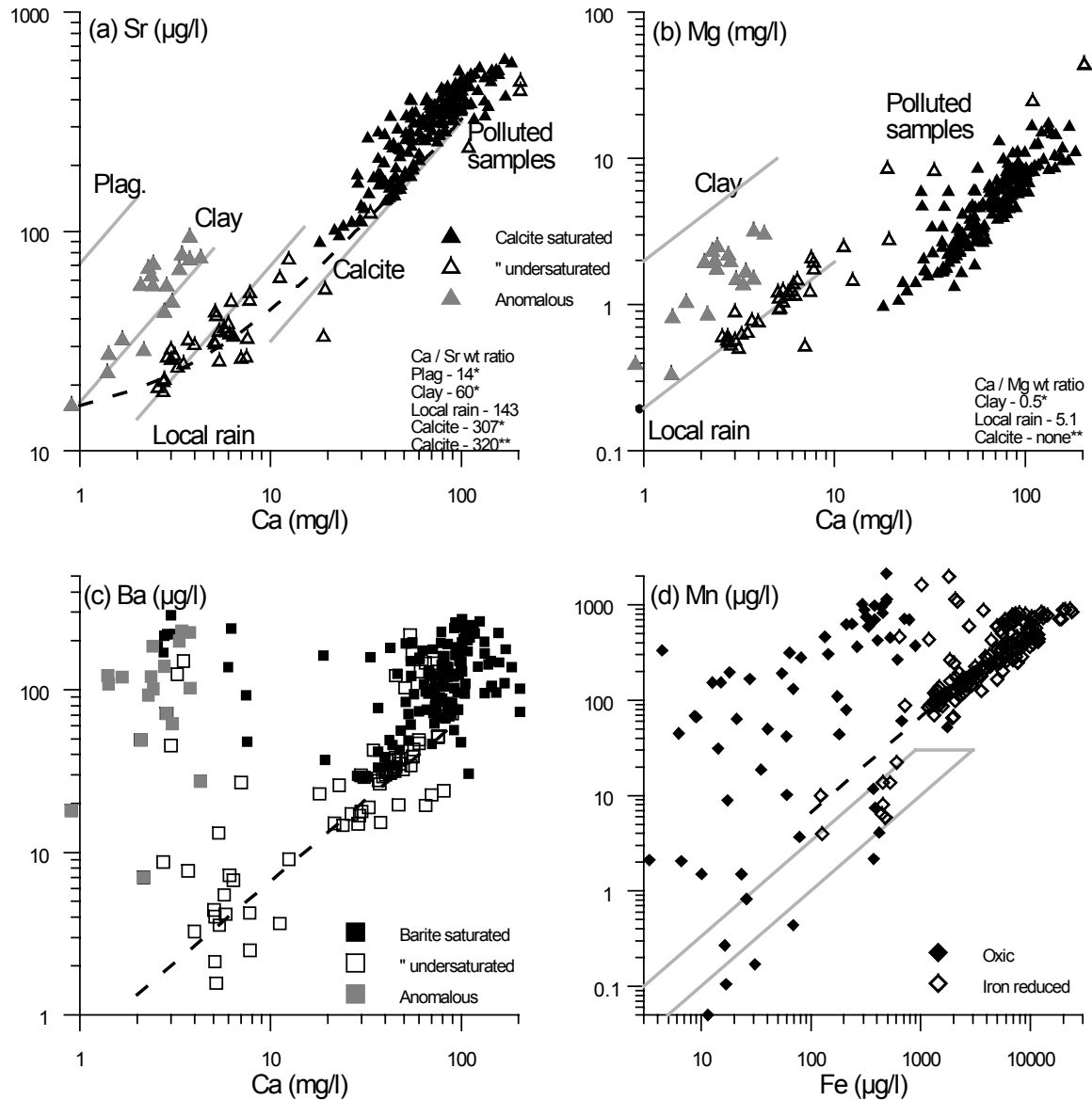


Figure 5.6 (a) Sr-Ca, (b) Mg-Ca, (c) Ba-Ca, and (d) Mn-Fe scatterplot. Percentages given are the axis cut-off values of the manually fitted straight line of codissolution. \* = calculated from Dutch subsoil data; ratio given in graph, \*\* = calculated from sequential extraction (Van Uden and Vissers, 1998). Grey lines indicate observed sedimentary ratios, dashed lines are lines of CD-CP.

Figure 5.6d shows the Mn-Fe scatterplot. As expected from the observed carbonate saturation, there is a clear relation between Mn and Fe for the buffered and reduced groundwater. However, the Mn-Fe relation, around a ratio of 1:18, is even tighter than their individual relations with Ca. Saturation indices of rhodochrosite are around 0, and of siderite around 0.5. Whether or not both siderite and rhodochrosite are precipitating as

individual phases cannot be ascertained. In view of the Fe supersaturation and higher  $Fe > Mn$  aqueous activities, siderite is expected to be the stable phase (Saunders and Swan, 1992), with kinetic hindrance for siderite precipitation (Jensen et al. (2002), Wajon et al. 1985). Mn is then likely to be controlled by coprecipitation (Wersin et al. 1989). Similar to the relation of Ni and Co with Ca in the calcite saturated water, a relation of Co, Ni, and Zn with Fe is found in the iron reduced groundwater. Here too, however, a relation through codissolution with Fe must be ruled out.

For the process of iron reduction towards siderite saturation i.e. from nitrate-free waters to siderite saturated water a vertical distance of several miniscreens is observed. Apparently this process is kinetically constrained and takes several years. A more detailed study of the concentration-depth profiles for those borings in which a clear Fe-reduction front is observed, may shed more light on potential codissolution of TE with reductive dissolution of Fe-(hydr)oxides. Figure 5.7 shows the profiles for Mn, As, Mo, U, Co, Ni, Cu, Na, and P as compared to Fe for borings A3, A5, A7 and A10. Apart from the redox front, an acidification front is also present in most of these borings.

In boring A3 Fe, Mn, As, as well as Mo, follow similar patterns across the profile, differing mainly in depth of reductive dissolution. The sequence is Mo, followed by Mn, Fe and As. The As increase at the iron reduction front suggests codissolution with iron at  $As:Fe = 1:8300$ . Apart from high concentrations in the upper screens, Co, Ni, and U show a distinct concentration peak at the reduction front; Ni and Co also peak at the buffering front. For the buffering front this is suggestive of desorption due to pH lowering, with subsequent adsorption in response to higher pH (Kjøller et al. 2004). For the reduction boundary it suggests pyrite oxidation (Van Beek et al. 1989) or desorption from the oxides being dissolved at the redox boundary (Zachara et al. 2001), followed by re-adsorption.

In boring A5, Mn is mobilized first, followed more slowly by Mo. The increase of As with Fe suggest codissolution ( $As:Fe = 1:2500$ ). A Co desorption peak is also present at the Fe reduction front, and U shows high concentrations in the manganese- but not yet iron-reduced zone. Boring A7 somewhat resembles A5, with Mn and Mo concentrations already high in the upper screens. Uranium again is high in the manganese but not iron-reduced zones. Arsenic increases at the Fe reduction front ( $As:Fe = 1:830$ ). Boring A10 is more similar to A3, with the redox front for Mn and Fe almost coinciding. Both As and Mo more or less follow the Fe pattern ( $As:Fe = 1:1700$ ). The redox boundary in this boring also is a pollution boundary. No desorption peaks are observed in borings A7 or A10. In all these borings (A5, A7, A10), Sb shows similarities with U behaviour.

In summary, As shows consistent signs of codissolution at the iron reduction front but in varying ratios. Manganese reduces earlier, and is sometimes governed by low pH conditions precipitating at the calcite buffering boundary (boring A3 and A10). Molybdenum reduces and mobilises at similar depths, but slower than manganese (boring A3, A5, A7), similar to U (and Sb) that, however, precipitates as soon as siderite saturation is reached. Very similar redox behaviour for Fe, As, Mo, and Mn, as well as mobilization at the redox front for U and Sb was observed in a sandstone aquifer by Smedley and Edmunds (2002). Nickel and Co show local desorption at both buffering and redox boundaries, but concentrations seem to be more linked to pollution considering that the highest concentrations are found in the upper samples.

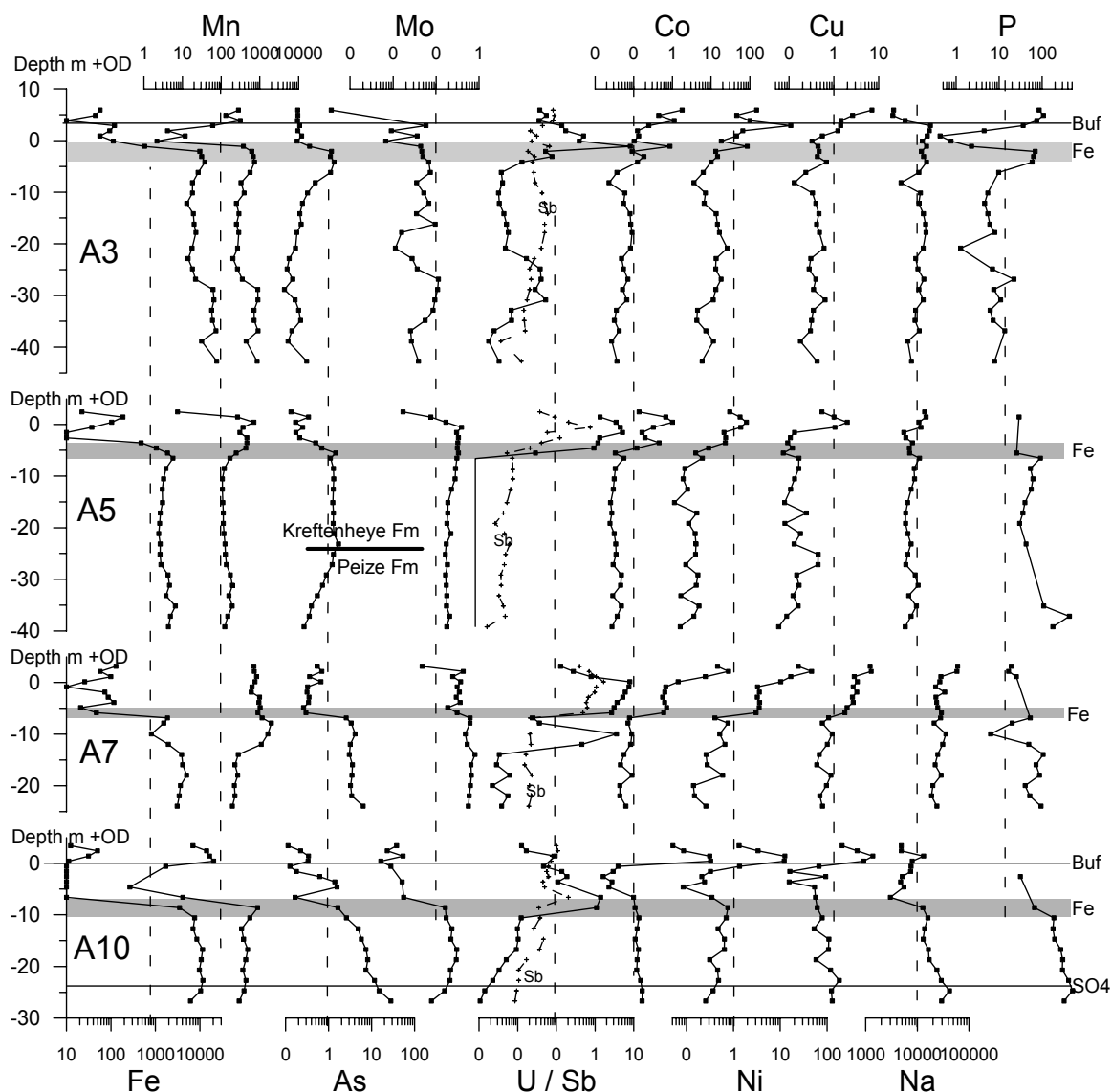


Figure 5.7 Concentration – Depth profiles of Fe, Mn, As, Mo, U, Co, Ni, Cu, Na, and P for borings A3, A5, A7, and A10 in µg/l. Boundaries indicated are: Buf: Calcite buffering boundary, Fe: zone of iron reduction, SO4: Boundary below which samples are completely sulphate reduced

**Sulphides:** Formation of sulphides can be a sink, while oxidation can be a source of TE. Though no  $S^{2-}$  concentrations were measured, both processes can indirectly be deduced from major element hydrochemistry. Pyrite oxidation takes place in the deepest part of boring A1, indicated by anomalously high sulphate concentrations and decreasing pH (see profiles in *chapter 4*). No TE are found to be associated with this process, indicating that the decrease in pH with depth is in steady state with respect to cation exchange, and that the sulphides being oxidized do not contain significant amounts of TE. Sulphate reduction and possible sulphide formation takes place in the deeper parts of boring A4, A6, A7, A8, and A10. Decreasing  $SO_4/Cl$  ratios in combination with increasing  $HCO_3/Ca$  ratios suggest sulphate reduction, while decreasing Fe concentrations falling below siderite saturation indicate pyrite formation. This combination of phenomena is only

found in the deepest; completely sulphate reduced parts of boring A7 and A10, and is not associated with a specific increase or decrease in TE. Only changes in As and Mo appear to be connected to the sulphate reduction process, but in highly variable ways. Both the highest and the lowest measured concentrations of As are found in sulphate-reducing water. The decrease of As with depth in boring A5 (Figure 5.7), which does not show sulphate reduction, suggests another type of kinetic removal of As, linear with age. This, probably sorptive, removal (Bowell, 1994) takes place after the water enters the Peize Formation, and thus indicates that the geology is the governing factor.

*Phosphorus minerals:* Saturation with apatite, vivianite, and some LREE phosphates was calculated in the pure phase equilibrium approach. However, these minerals are not the major control of either Ca or Fe, which are calcite and iron-hydroxide plus siderite respectively. These latter minerals therefore indirectly control phosphate concentrations in the groundwater.

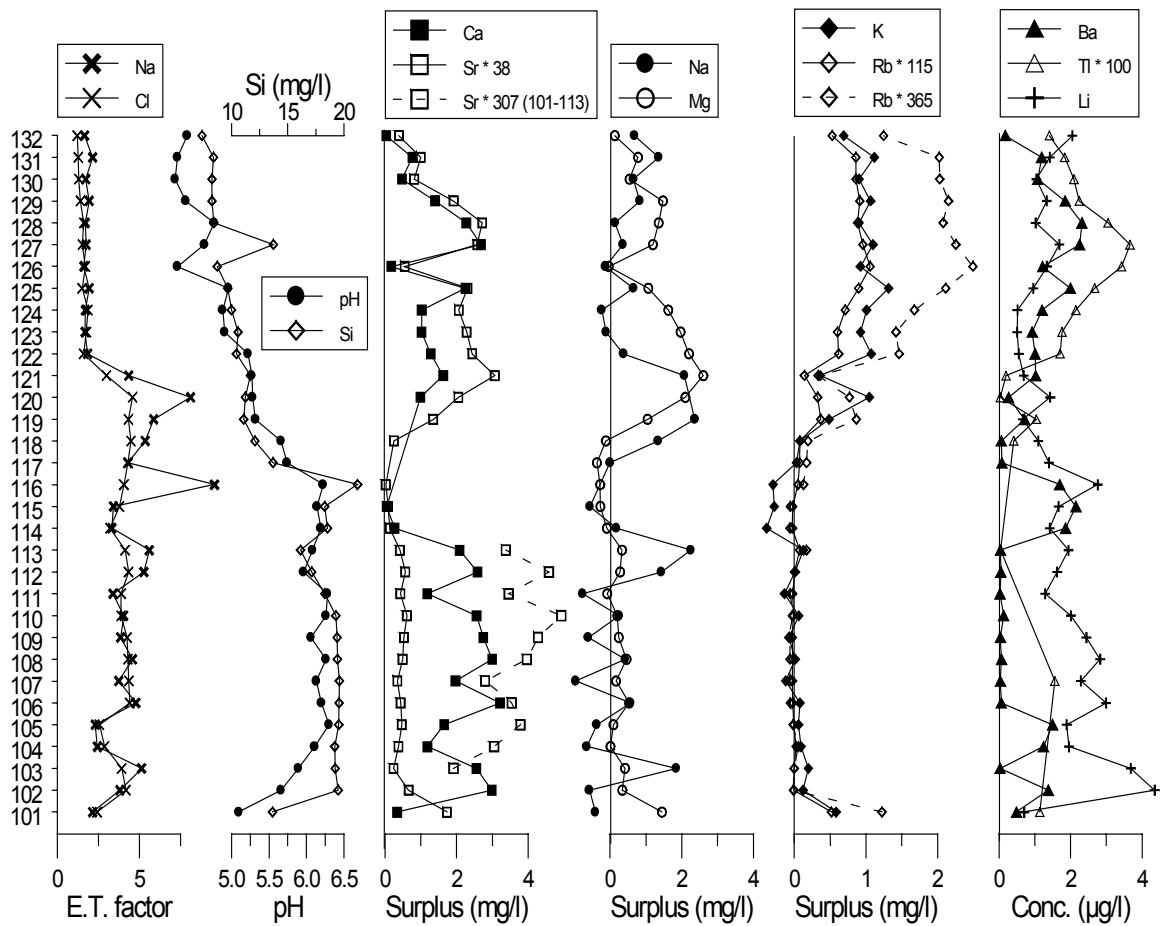


Figure 5.8 Sample profiles in boring A1, showing surplus (rainwater corrected) concentrations of Ca, Sr, Na, Mg, K, Rb, where concentrations of Sr and Rb are multiplied by their respective sedimentary endmember ratios with Ca and K respectively. Furthermore, concentrations of Ba, Tl, Li, Si are displayed, as well pH. Na and Cl evapotranspiration (E.T.) factors are displayed after correction for local rainwater concentrations, and are approx. 1.7 for heather, and 4 for forest areas

*Feldspar and clay minerals:* Weathering of plagioclase and clay minerals is a generally slow and incongruent reaction releasing trace and major elements, and can therefore only indirectly be incorporated in a CD model by its effects on the groundwater composition. The process can be recognized by its release of elements that may occur in seemingly congruent fashion.

For the alkali feldspar group especially Ba, Sr, and Tl are expected to codissolve with K, Ca, and Na (Van der Veer, 2006), and for the clay minerals these and other elements are expected to be released as well, including the ME Mg. K-feldspar is expected to be relatively enriched in Ba, Rb, and Pb as compared to Na feldspars (Nagasawa, 1971). Potassium/Rb mass ratios are 1500 – 3300 for the majority of the groundwater samples, and even higher for potassium-polluted groundwaters that show Rb depletion compared to natural samples. A small group of Rb-enriched samples with a ratio of about 200 is identified as being the same group that was found enriched in Sr and Mg (Figure 5.6a and 5.6b). Evidently, in these samples active weathering has taken place, higher than found anywhere else in the well section. Most of these samples are found in boring A1 that is not agriculturally polluted, and where the absence of calcite causes buffering by aluminosilicates.

Strontium isotopic data might give definite proof of which minerals actually weather (Probst et al. 2000; Bau et al. 2004), but ratios of major and trace elements compared to the ratios found in sediment endmembers (Van der Veer, 2006) give strong indications as well. Relevant element – depth profiles for boring A1 are given in Figure 5.8. In this figure, concentrations are corrected for rainwater input, by multiplying observed rainwater concentrations with the evapotranspiration factor based on Cl, and subtracting this concentration from the groundwater sample concentration. Calculated surplus concentrations are expected to originate from mineral weathering. Effects are probably complicated as the soil exchange complex is not in steady-state equilibrium in acid-disturbed areas.

Yet, different zones clearly can be distinguished. In the upper part of the boring active weathering takes place, resulting in increasing pH and Si concentrations, and high surplus concentrations of Na, K, Mg, and Ca. High Sr/Ca and low Rb/K in the upper zone (#132-127) suggest dominant clay mineral dissolution, while further down (#124-119) the opposite occurs and feldspar dissolution may be more important. Beryllium, Ga, Li, Co (#132-126), Cd, Tl (#132-122), Zn (#132-121), Ba, Ni (#132-119) are also mobilized in these zones, indicating codissolution for these elements, which for Ba and Cd was also noted by Frapporti et al. (1996). Beryllium, Ga, Li, and Co are thus observed to be preferentially released from the clay fraction; Cd, Tl, Ba, and Ni also seem to be liberated from the feldspar fraction. These observations match the observations in sedimentary data (Van der Veer, 2006), which indicate relative enrichments of Be (Figure 5.4), Ga (Figure 5.4), (Co), and Li in clays compared to feldspar and vice versa for Tl and Ba. Only Ni, which is relatively enriched in clay, does not meet expectations, but is known to be mobile in slightly acid water. For Cd no relative enrichments in either two phases can be observed. In the clay dissolution zone, the increased Ca:Mg:Na:K can be approximated by 2:2:1:1, which almost equals illitic ferrous clay,  $\text{Na}_{0.3}\text{K}_{0.4}\text{Ca}_{0.2}(\text{Mg}_{0.2}\text{Fe(II)}_{0.6}\text{Al}_{1.3})(\text{Si}_{3.4}\text{Al}_{0.6})\text{O}_{10}(\text{OH})_2$ , as described by Banwart (1999). In the deeper, buffered zone of the well (#113-101) slight calcite dissolution controls Ca and Sr surplus concentrations.

*Heavy minerals, REY and HFSE (High Field Strength Elements):* Figure 5.9a shows the Hf – Zr scatterplot of the water samples as compared to ratios in the Dutch subsoils (Van der Veer, 2006). Data are in accordance with congruent dissolution of these elements with a Hf/Zr mass ratio of 1:37 (Erlank et al. 1978). As these elements have differing aqueous chemistry, source-term limitation may explain their coherent behaviour. However, as is also the case for Th and REE, the particulate form may also be important (Alaux-Negrel, 1993). This form may in turn be associated with DOC and pH, as is actually observed for Zr – DOC (Spearman  $r^2 = 0.65$ ).

Figure 5.9b shows the Ga – Al scatterplot of water and sediments. Gallium is not related to specific mineralogical phases, and substitutes for Al in aluminosilicates (Goldschmidt, 1954), leading to constant Al/Ga ratios in rocks and sediments. Gallium is less soluble than Al (Shiller and Frilot, 1996); solubility of their hydroxide phases differs by approximately 2 log units. However, since Ga is much less abundant as compared to Al (1:13000 on mole basis; Van der Veer, 2006, Shiller and Frilot, 1996, Burton and Culkin, 1972), source-term limitation for Ga may be expected where for Al saturation is reached in buffered waters. This expected behaviour of both elements can in fact explain the observed patterns, where congruent dissolution of Al silicates explains Ga behaviour. A few samples with higher Al/Ga ratios can indicate buffering with secondary phases poorer in Ga.

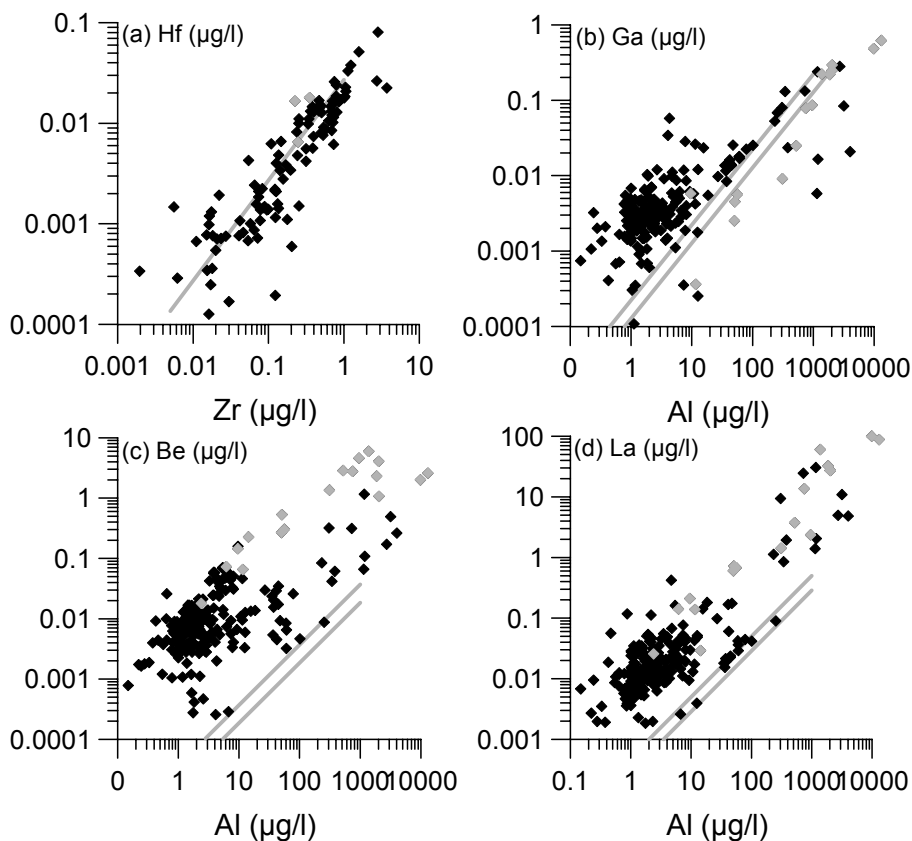


Figure 5.9 (a) Hf-Zr, (b) Ga-Al, (c) Be-Al, and (d) La-Al scatterplots in µg/l. The range of ratios observed in Dutch subsoil is indicated by the grey lines. Anomalous samples as identified in Figure 6 are displayed in grey

Figure 5.9c and 5.9d show the Be – Al and La – Al scatterplots. Beryllium and La show mobilization in sedimentary ratios in the water samples from the upper screens, indicating either codissolution or particulate mobilization in these samples. The latter is more likely, since these samples also show NASC-normalized (Gromet et al. 1984) REE (Rare Earth Element) patterns identical to those observed in the clay fraction of sediments. LREE (Light REE) depletion is observed in the highest  $\Sigma$ REE waters, which may be caused by e.g. phosphate saturation as calculated by equilibrium modelling, coprecipitation with apatite-like minerals (Bruno et al. 2002), or selective scavenging during weathering (Otsuka and Terakado, 2003). Similar to Ga, Al precipitation leads to higher ratios of TE/ME. Beryllium is codissolved with Al and may also be desorbed from ironoxyhydroxides (Krám et al. 1998), and is only indirectly related to pH due to acidification related weathering. Beryllium seems to be bound by an upper limit, possibly due to coprecipitation or competitive sorption with Al. Similar results and significant relations with Mg, Ca, Sr, and Cd were also noted by Navratil et al. (2002), whom suggested pH as important controlling factor.

#### **5.4.3 Sorption equilibrium through steady state input approach (SEQSSI)**

Sodium was selected as the major SCE against which to compare the expected (semi-) conservative behaviour of the TE. As shown in Figure 5.4, Na is the dominant cation in the unbuffered water type whereas Ca, due to calcite dissolution, dominates the buffered water types. Within the buffered water types Na is still the second dominant, and is correlated with the overall Ec. Sodium indeed appears to be controlled by input, evaporative concentration, and adsorption, as evidenced by a high correlation with Cl, apart from the small zone of feldspar dissolution found in boring A1. This also means that TE/Na ratios can still be compared to rain and seawater ratios. A further advantage of using Na as an SCE lies in the sensitivity of ratios to analytical error. Since Na and the TE were both analyzed by ICP-MS, using a combined standard, calibration errors are of less influence.

The controls of evaporative concentration and sorptive adjustment to changes in input are firstly explored simply via TE-Na scatterplots in which also the estimated rainwater and seawater ratios are indicated (Figure 5.10). The samples already identified in the CD-CP approach as resulting from anomalous weathering are indicated separately. Evidently, the scatterplots indicate that for most TE there is currently no steady state equilibrium throughout the aquifer, as TE/Na ratios in recent rain water are generally much higher than those found in the bulk of the samples. Yet, the high ratios found in recent rain are certainly evidence that atmospheric/surficial input can be an important source for TE in groundwater, and that the aquifer may currently act as a sink rather than a source for many TE. However, samples of pre-industrial age and originating of natural land use generally show a fairly constant TE/Na ratio at the base of the data cloud (Co, Ni, B, Rb, Cs), suggesting that these actually might represent the pre-industrial rain water ratio, with which the deeper aquifer is still more or less in steady state. Further confirmation for this lies in the fact that no or hardly any compositions below this base line are observed for these elements. For some TE, the ratio still seems to be the same in current rain (Co, B, Rb). Lithium also shows base line concentrations matching rainwater

ratios very well, but most samples show higher concentrations, indicating a sedimentary source of this element. The lower than base line concentrations are all found in one coherent depth interval in boring A7, and might originate from irrigation with water from the Overijssels Canal. The lower than base line concentrations of Cd and V, in contrast, are not spatially related but are basically from single analytical batches, strongly suggesting analytical artefacts. For many TE, the graphs of Figure 5.10 indicate a drastic increase in rainwater concentrations in recent times (Ni, Cu, V, Cd, Cs).

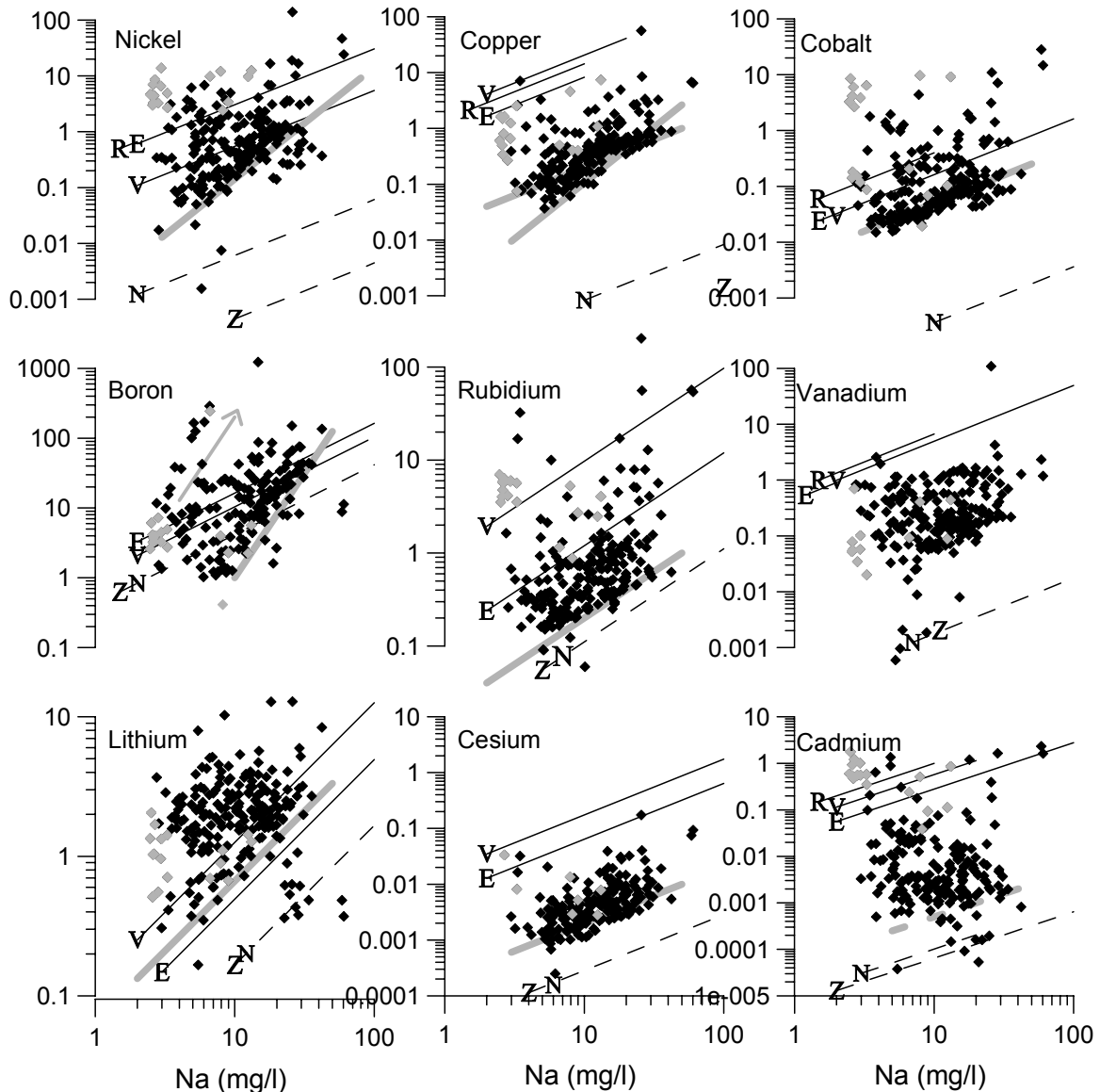


Figure 5.10 Co, Ni, Cu, V, B, Rb, Cd, Li, and Cs scatterplots against Na with seawater and rainwater ratio estimates as lines, (N = Ball and Nordstrom, 1978, Z = Nozaki, 1997), and rain (R = RIVM, 1994-2000, E = Eriksson, 2001, V = this study), With the grey line the observed cation exchange behaviour is shown where evident. Anomalous samples as identified in Figure 5.6 are displayed in grey

The effects of sorptive adjustment is most evident for elements displaying different valence TE-ME exchange, such as Ni, Cu, and B. Boron apparently exchanges trivalently



against  $\text{Na}^+$  as evidenced by the third power slope of the base line in the region of agriculturally influenced waters. In the lower Na concentration range, the dominant effect is evaporative concentration of natural rainwater (linear slope), which equals seawater ratios. The high B concentrations found in some of the unpolluted waters represent either recently infiltrated water (shallow samples in borings A1, A3, and A10) or result from temporal increases in background electrolytes in previously pristine water (complete boring A6, deeper parts of boring A2). Nickel also dominantly shows the evaporative effect for low concentrations, and a quadratic slope upon disturbances, suggesting 2:1 competition primarily with Na. The high Na samples falling beneath this exchange base line all originate from the deepest samples in boring A7 and A10. The behaviour of Cu seems opposite to that of Ni, with a quadratic slope at low Na, and a linear slope at high Na. The latter is interpreted as in fact mimicking a linear Cu-Ca slope and thus equal-valence exchange with Ca. This is also the case for Co, and would imply that the exchange behaviour would be better represented in a TE-Ca plot (Figure 5.11). Indeed for the buffered waters a linear TE-Ca slope is found for Co and Cu whereas for Ni a quadratic slope is found, which now is interpreted as mimicking the true quadratic Ni-Na slope. The quadratic slope at low Na in the Cu plot represents sorptive adjustment in competition with Na to disturbances that are lower in Na than the initial steady state, for example as a result of deforestation and diminished evapotranspiration. This is in accordance with Na being the main cation in the unbuffered waters. Such effects may not be visible for other elements that either do not compete with Na or have low partition coefficients at low pH.

The base lines of Rb and Cs, like Co, show a linear relation with Na, here of course through equal valence cation exchange with Na (Zachara et al. 2002), the dominant monovalent cation. The base line cloud is relatively wide, which may indicate a sedimentary source similar to Li. The V data cloud is also wide, indicating the less strong control of the adsorption complex on the V concentration. Cadmium shows a less clear base line and concentrations of freshly infiltrated water match rainwater ratios.'

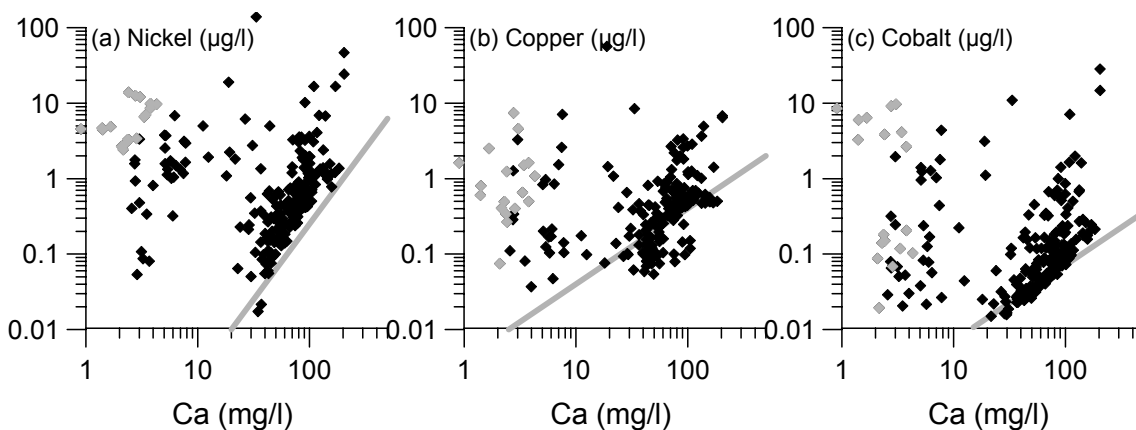


Figure 5.11 Co, Ni, and Cu scatterplots against Ca with seawater and rainwater ratio estimates as lines (for legend see Figure 5.10). In grey the observed cation exchange behaviour is shown where evident. Anomalous samples as identified in Figure 5.6 are displayed in grey

At large the assumptions in the SEQSSI approach appear to be valid for the elements presented in Figure 5.10. We will briefly point out some conditions for which these assumptions are no longer valid.

Firstly, the situation where  $K_{TE/ME}$  (Eq. 5) cannot be considered constant is discussed. Agricultural pollution is often associated with enhanced concentrations of complexing agents such as DOC, F, and  $PO_4$ . Especially for elements with a high affinity for DOC (Benedetti et al. 1996) this may increase solubility. Aluminium is a good example of this feature, as its solubility at neutral pH is determined mainly by its speciation. This may generate induced correlations with Na as a general indicator of pollution (Figure 5.12a). For elements that are not solubility-controlled but source-term limited, an increased solubility through complexation or pH changes will not directly affect aqueous concentrations. However, pH and complexing agents influence the selectivity coefficients and thus the conditional distribution coefficient (Buerge-Weirich et al. 2002), and may thereby lead to increased TE concentrations that deviate from the basic SEQSSI model even in the absence of an increased TE input.

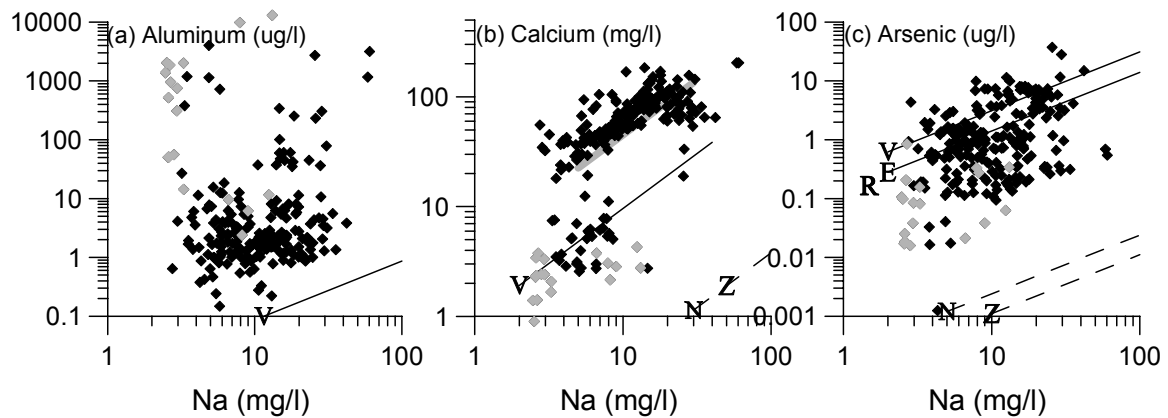


Figure 5.12 Al, Ca, and As scatterplots against Na with seawater and rainwater ratio estimates as lines (for legend see Figure 5.10). In grey the observed cation exchange behaviour is shown where evident. Anomalous samples as identified in Figure 5.6 are displayed in grey

Secondly, the relative occupancies  $\beta_{ME}$  (Eq. 5) of the major cations may change significantly. Figure 5.12b shows the relative aqueous concentrations of the dominant cations Ca and Na that control the exchange complex. Apart from the difference between buffered and unbuffered water types, a small group of Na-rich samples can be distinguished below the bulk Ca/Na ratio in buffered samples. In the case of Ni (Figure 5.10) the higher  $\beta_{Na}$  indeed leads to adsorption and lower aqueous Ni concentrations for this group (See Eq. 5). The inverse effect is shown for Co (Figure 5.11), where a lower  $\beta_{Ca}$  leads to desorption. An apparent effect is visible in the TE-ME plot for the ME that was not identified as the competitor. The Co-Na plot thereby simply mimics the Ca-Na plot (and the Ni-Ca plot a Na-Ca plot).

For the sake of completeness, we also present an example of the SEQSSI approach applied to a redox-controlled element. At first sight, both Mo and As (Figure 5.12c) would appear to be candidates for SEQSSI; concentrations match reasonably well with rain and seawater. However, recently infiltrated waters display the lowest TE/ME ratios, while the older, reduced waters show highest ratios through reductive

(co)dissolution. As a rule, TE – depth (age) plots corrected for exchange effects (Eq. 7c) should be considered as well.

Cesium (not shown) and Rb show consistent depth profiles as expected (Figure 5.13). High relative concentrations are found in the unpolluted boring A1, indicating clay mineral dissolution as discussed previously. The shallow samples of borings A2 and A3 are polluted, as evidenced by the even higher enrichments for K (not shown). A slight overall increase with depth suggests a ubiquitous sedimentary source. This increase is much more pronounced for Li that shows an overall loglinear increase with depth for all borings, equivalent to a linear increase with age and thus indicating zeroth order (incongruent) dissolution. With these assumptions and an infiltration rate of 330 mm/y, porosity of 0.33, and historic Na concentration of 7 mg/l, a Li dissolution rate of 20  $\mu\text{g/ky}$  is estimated (Rb: 1  $\mu\text{g/ky}$ , Cs: 0.02  $\mu\text{g/ky}$ ). This is more than ten times higher than observed in a Triassic sandstone aquifer (Edmunds and Smedley, 2000). The high relative Li concentrations of boring A6 confirm the supposedly more regional or ‘older’ character of the upward seepage present. The polluted water type in the shallow half of this boring indicates a more recent origin, displacing the older water due to a flow pattern change. The lower than base line ratios found in boring A7 were already ascribed to irrigation with water from the Overijssels Canal.

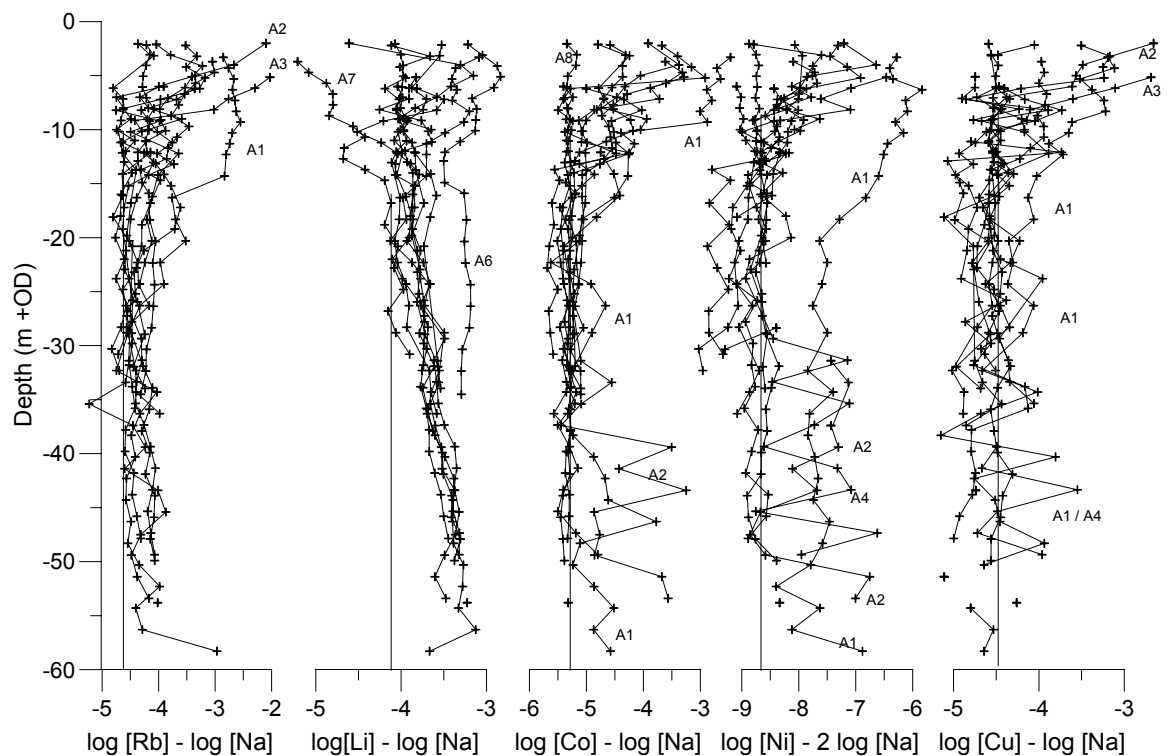


Figure 5.13 Sodium normalized TE-Depth profiles of Rb, Li, Co, Ni, and Cu (weight basis) for all borings, and numbers indicate borings with an anomaly from the base line

The corrected Co and Ni depth profiles show the straight base line as expected. The shallow groundwater samples show high relative concentrations in infiltration wells, and base line relative concentrations in the upward seepage wells. High relative Ni and Co concentrations also occur in the deeper part of boring A2 and a few depth intervals in

boring A1. These intervals are not calcite saturated, and nitrate reduced, which apparently enhances Co and Ni mobility. Ni is clearly more mobile than Co in slightly acidic environments, as is particularly visible in the depth profile of boring A1. Like Ni and Co, Zn is also observed to be mobilized in the unbuffered reduced groundwater samples. These conditions are known to lead to mobilization of adsorbed elements (Zachara et al. 2001; Davranche and Bollinger, 2000); these mobilised elements are either precipitated onto iron oxyhydroxides (Pb, Cr<sup>3+</sup>, Cu: Dzombak and Morel, 1990), or remain mobilized (Cd, Ni, Zn).

The Na normalized Cu-depth profiles show that the large measurement error has adverse effects on the consistency of the profiles. Highest concentrations are found in the upper screens of the polluted A2 and A3 borings, indicating agricultural pollution. This pollution appears also to involve Be, B, Ti, (Cr), Co, Ni, Cu, Zn, Ga, Rb, Cd, Sb, Cs, REY, Tl, Pb, and (Bi), of which some elements may have increased mainly due to increased weathering due to acidification. For B, Ti, (Cr), Cu, Rb, Sb, Tl, Pb, and (Bi) pollution seems more important, while for Co, Ni, and Zn both pollution and weathering seem to be important.

## 5.5 CONCLUSIONS AND SUMMARY

Trace element behaviour in simple systems helps to better understand complex systems (Bau, 2004), as does an integrated interpretation of many trace elements as carried out in this study. The bivariate character of trace element concentrations caused by shared sources, similar behaviour, or common controls, was explored through a three-step approach. This included testing trace element concentrations for pure phase equilibrium (EQ), for codissolution – coprecipitation (CD-CP) processes, and for sorption equilibrium through steady-state input (SEQSSI). Results are summarized in Table 3.

The EQ approach explained few major and trace elements (Al, P, Ca, Mn, Fe, Ba, and U) that are commonly controlled by saturation phases and in most cases have a sedimentary source. The CD-CP approach explains As by codissolution from Fe hydroxides, and Ba and Sr by dissolution of calcite. Magnesium is not related to Ca through codissolution from sedimentary calcite, but is controlled by cation exchange and surficial input. For Mn coprecipitation with Fe controls concentrations in reduced siderite saturated water. Sedimentary sources for Mo, U, Mn, and possibly Sb could not be related to ME release; they were found to be separately controlled by redox conditions. In the shallow parts of infiltration areas, weathering of Al-silicates caused by acidification results in anomalous concentrations of a large set of trace elements associated with Al and base cations. These included enrichments for Ni, Co, Zn, and Be, that are more commonly attributed to acidification (Edmunds et al. 1992), and these as well as Li, Rb, and Cd (Stuyfzand, 1993), and in this study also Tl, Ga, and REY. The major type of source-mineral: feldspar or clay, was identified based on a comparison with ratios observed in the Dutch subsoil.

Many elements, however, were found to be best explained by the SEQSSI-approach (Table 3), which implies source-term limitation from surficial input. In the natural situation rainwater is then the dominant source and control. Upon disturbance, the exchange complex, which has been loaded under the natural conditions, starts acting as

the control. The type of exchange (equal or unequal valence competition with the major electrolytes; Table 3) and the major electrolyte shift together determine the transient TE concentration path. The time needed to reach a new steady state of course depends on the actual soil water distribution coefficient. Surmised pristine conditions were observed in some parts of the aquifer only, but the natural sorption equilibrium is still present throughout most of the aquifer. From this the pristine surficial input Na/TE ratio could be estimated (Table 3). For equal valence competition this ratio also forms the exchange base line in the TE-Na plot.

Table 5.3 Summary of the governing controls of TE concentrations, X indicates the control is identified

Element	EQ	CD-CP <sup>1</sup>	SEQSSI pristine ratio <sup>2</sup>	SEQSSI Compet. <sup>3</sup>	Other <sup>3</sup>	Details
Li		CD	15*10 <sup>3</sup>	Na	X	Low-pH weathering, slow ubiquitous IDIS <sup>4</sup>
Be		CD				Low-pH weathering
B			2.4*10 <sup>3</sup>	Na		
Al	X					Gibbsite
P	X					Apatite, Vivianite
V			28*10 <sup>4</sup>	-		
Mn	X	CP				EQ: Mn(hydr)oxides/rhodochrosite, CP: siderite
Fe	X					Siderite
Co		CD	2*10 <sup>4</sup>	Ca	X	Low-pH weathering, mobilization in reduced acid GW
Ni		CD	5*10 <sup>4</sup>	Na	X	Low-pH weathering, mobilization in reduced acid GW
Cu			5*10 <sup>4</sup>	Na/C		
Zn		CD	3*10 <sup>3</sup>	Ca	X	Low-pH weathering, mobilization in reduced acid GW
As		CD			X	CD: Fe oxyhydroxides; Sedimentary control in #A3
Rb		CD	5*10 <sup>4</sup>	Na	X	Low-pH weathering, slow ubiquitous IDIS <sup>4</sup>
Sr		CD				Calcite and Al-silicates
Mo					X	Redox-control
Cd		CD	12*10 <sup>6</sup>	Ca		Low-pH weathering
Cs		CD	5*10 <sup>6</sup>	Na	X	Low-pH weathering, slow ubiquitous IDIS <sup>4</sup>
Ba	X	CD				EQ: Barite, CD: Calcite and Al-silicates
U	X				X	EQ: Uraninite, S: Mobilisation at Mn redox boundary
RE		CD				Low-pH weathering
Ga*		CD				Low-pH weathering
Sb*						Behaviour similar to U
Tl*		CD				Low-pH weathering
Pb*			1*10 <sup>5</sup>	Ca		
Zr*						Mobilization on organic complexation
Hf*		CD				Zircon

1 CD = Codissolution, CP = Coprecipitation

2 Base line weight ratio Na/TE

3 From SEQSSI – corrected depth profiles, and from concentration – depth profiles for As, Mo, and U

4 IDIS = Incongruent dissolution from Al-silicates

\* = Not complying to set analytical quality criteria, incorporated only briefly in interpretation

Including the SEQSSI approach in depth profiles, by normalizing for the major electrolyte effect, also resulted in identification of anomalies not directly found by applying the EQ and CD-CP approaches. These anomalies can be related to specific environments or processes: enhanced Co, Ni, and Zn in acid, reduced waters;

mobilization of Ni and Co at reduction and buffering boundaries; slow incongruent release of Li, Rb, and Cs; and pollution (e.g. B, Ti, Cu, Rb, Sb, Tl, Pb). Some parallels of trace element behaviour with research in carbonate aquifers and sandstone aquifers (Edmunds et al. 1987; Smedley and Edmunds, 2002) were found. Doubtless, the sorption equilibrium through steady-state input observed in this study will be relevant in many other types of aquifers as well.

## 5.6 REFERENCES

- Alaux-Negrel, G., Beaucaire, C., Michard, G., Toulhoat, P., Ouzounian, G. (1993), Trace-metal behavior in natural granitic waters. *Journal of Contaminant Hydrology* 13, pp 309-325
- Appelo C.A.J., Postma, D. (1993), *Geochemistry, groundwater and pollution*, A.A. Balkema, Rotterdam
- Ball, J.W., Nordstrom, D.K. (1991), User's manual for WATEQ4F, with revised thermodynamic data base and test cases for calculating speciation of major, trace, and redox elements in natural waters. USGS Open File Report 183, 59p
- Banwart, S.A. (1999), Reduction of iron(III) minerals by natural organic matter in groundwater. *Geochimica et Cosmochimica Acta* 63, pp 2919-2928
- Bau, M., Alexander, B., Chesley, J.T., Dulski, P., Brantley, S.L. (2004), Mineral dissolution in the Cape Cod aquifer, Massachusetts, USA: I. Reaction stoichiometry and impact of accessory feldspar and glauconite on strontium isotopes, solute concentrations, and REY distribution. *Geochimica et Cosmochimica Acta* 68, pp 1199-1216
- Beier, C., Gundersen, P. (1989), Atmospheric deposition to the edge of a spruce forest. *Environmental Pollution* 60, pp 257-271
- Benedetti, M.F., van Riemsdijk, W.H., Koopal, L.K., Kinniburgh, D.G., Gooddy, D.C., Milne, C.J. (1996), Metal ion binding by natural organic matter: From the model to the field. *Geochimica et Cosmochimica Acta* 60, pp 2503-2513
- Böhlke, J.K. (2002), Groundwater recharge and agricultural contamination. *Hydrogeology Journal* 10, pp 153-179
- Bolan, N.S., Adriano, D.C., Mahimairaja, S. (2004), Distribution and Bioavailability of Trace Elements in Livestock and Poultry Manure By-Products. *Critical Reviews in Environmental Science and Technology* 34, pp 291-338
- Boutron, C., Leclerc, M., Lorius, C. (1984), Atmospheric trace elements in Antarctic prehistoric ice collected at a coastal ablation area. *Atmospheric Environment* 18, pp 1947-1953
- Bowell, R.J. (1994), Sorption of arsenic by iron and oxyhydroxides in soils. *Applied Geochemistry* 9, pp 279-286
- Bradbury, M.H., Baeyens, B. (1997), A mechanistic description of Ni and Zn sorption on Namontmorillonite. Part II: Modelling. *Journal of Contaminant Hydrology* 27, pp 223-248
- Bruno, J., Duro, L., de Pablo, J., Casas, I., Ayora, C., Delgado, J., Gimeno, M.J., Pena, J., Linklater, C., Perez del Villar, L., Gomez, P. (1998), Estimation of the concentrations of trace metals in natural systems. The application of codissolution and coprecipitation approaches to El Berrocal (Spain) and Pocos de Caldas (Brazil). *Chemical Geology* 151, pp 277-291
- Bruno, J., Duro, L., Grive, M. (2002), The applicability and limitations of thermodynamic geochemical models to simulate trace element behaviour in natural waters. Lessons learned from natural analogue studies. *Chemical Geology* 190, pp 371 - 393
- Burton, J.D., Culkin, F. (1972), Parts 31B-310 - Gallium. In: Wedepohl, K.H. (ed), *Handbook of geochemistry*, Springer-Verlag, Berlin
- Buerge-Weirich, D., Hari, R., Xue, H., Behra, P., Sigg, L. (2002), Adsorption of Cu, Ni, and Cd on goethite in the presence of natural groundwater ligands. *Environmental Science and Technology* 36, pp 328-336
- Casas, I., de Pablo, J., Gimenez, J., Torrero, M.E., Bruno, J. et al. (1998), The role of pe, pH, and carbonate on the solubility of UO<sub>2</sub> and uraninite under nominally reducing conditions. *Geochimica et Cosmochimica Acta* 62, pp 2223-2231

- Cochran, J.K., Carey, E., Sholkovitz, E., Suprenant, L.D. (1986), The geochemistry of uranium and thorium in coastal marine sediments and sediment porewaters. *Geochimica et Cosmochimica Acta* 50, pp 663-680
- Curti, E. (1999), Coprecipitation of radionuclides with calcite: estimation of partition coefficients based on a review of laboratory investigations and geochemical data. *Applied Geochemistry* 14, pp 433-445
- Davranche, M., Bollinger, J-C. (2000), Heavy metals desorption from synthesized and natural iron and manganese oxyhydroxides: Effect of reductive conditions. *Journal of Colloid and Interface Science*, 227, pp 531-539
- De Mulder, E.F.J., Geluk, M.C., Ritsema, I.L., Westerhoff, W.E., Wong, Th.E. (2003), *De ondergrond van Nederland*. Wolters-Noordhoff bv Groningen/Houten, The Netherlands
- Duro, L., Bruno, J., Gomez, P., Gimeno, M-J., Wersin, P. (1997), Modelling of the migration of trace elements along groundwater flowpaths by using a steady state approach: application to the site at El Berrocal (Spain). *Journal of Contaminant Hydrology* 26, pp 35-43
- Dzombak, D.A., Morel, F.M.M. (1990), *Surface complexation Modeling; Hydrous Ferric Oxide*. Wiley-Interscience, New York
- Edmunds, W.M., Smedley, P.L. (2000), Residence time indicators in groundwater: the East Midlands Triassic sandstone aquifer. *Applied Geochemistry* 15, pp 737-752
- Edmunds, W.M., Kinniburgh, D.G., Moss, P.D. (1992), Trace metals in interstitial waters from sandstones: Acidic inputs to shallow groundwaters. *Environmental Pollution* 77, pp 129-141
- Edmunds, W.M., Cook, J.M., Darling, W.G., Kinniburgh, D.G., Miles, D.L. (1987), Baseline geochemical conditions in the chalk aquifer, Berkshire, UK a basis for groundwater quality management. *Applied Geochemistry* 2, pp 251-274
- Erikson, J. (2001), Concentrations of 61 trace elements in sewage sludge, farmyard manure, mineral fertiliser, precipitation and in oil and crops, Swedish Environmental Protection Agency, Report 5159
- Erismann, J.W., Mennen, M.G., Fowler, D., Flechard, C.R., Spindler, G., Grüner, A., Duyzer, J.H., Ruigrok, W., Wyers, G.P. (1998), Deposition monitoring in Europe. *Environmental monitoring & Assessment* 53, pp 279-295
- Erlank, A.J., Smith, H.S., Marchant, J.W., Cardoso, M.P., Ahrens, L.H. (1978), Section 72 – Hafnium, In: Wedepohl, K.H. (ed), *Handbook of Geochemistry*, Springer-Verlag, Berlin
- Farnham, I.M., Singh, A.K., Stetzenbach, K.J., Johannesson, K.H. (2002), Treatment of nondetects in multivariate analysis of groundwater geochemistry data. *Chemometrics and Intelligent Laboratory Systems* 60, pp 265-281
- Farnham, I.M., Johannesson, K.H., Singh, A.K., Hodge, V.F., Stetzenbach, K.J. (2003), Factor analytical approaches for evaluating groundwater trace element geochemistry data. *Analytica Chimica Acta* 490, pp 123-138
- Frapporti, G., Vriend, S.P., Van Gaans, P.F.M. (1996), Trace elements in the shallow ground water of the Netherlands. A geochemical and statistical interpretation of the national monitoring network data. *Aquatic Geochemistry* 2, pp 51-80
- Frapporti, G., Hoogendoorn, J.H., Vriend, S.P. (1995), Detailed hydrochemical studies as a useful extension of national ground-water monitoring networks. *Ground Water* 33, pp 817-828
- Goldschmidt V M. 1954. *Geochemistry*. Oxford University Press, Oxford
- Gromet, L.P., Dymek, R.F., Haskin, L.A., Korotev, R.L. (1984), The "North American shale composite": Its compilation, major and trace element characteristics, *Geochimica et Cosmochimica Acta* 48, pp 2469-2482
- Guimond, R.J. (1990), Radium in fertilizers: the environmental behavior of radium, International Atomic Energy Agency, Technical Reports Series, 310, pp 113-128
- Hansen, B.K., Postma, D. (1995), Acidification, buffering and salt effects in the unsaturated zone of a sandy aquifer, Klosterhede, Denmark. *Water Resources Research* 31, pp 2795-1809
- Hem, J.D. (1978), Redox processes at surfaces of manganese oxide and their effects on aqueous metal ions. *Chemical Geology* 21, pp 199-218
- Hodge, V.F., Johannesson, K.H., Stetzenbach, K.J. (1996), Rhenium, molybdenum, and uranium in groundwater from the southern great basin USA: evidence for conservative behavior. *Geochimica et Cosmochimica Acta* 60, pp 3197-3214
- Hoogendoorn, J.H. (1990), *Grondwatersysteemonderzoek Salland I en II*. DGV-TNO, Oosterwolde

- Jensen, D.L., Boddum, J.K., Tjell, J.C., Christensen, T.H. (2002), The solubility of rhodochrosite ( $\text{MnCO}_3$ ) and siderite ( $\text{FeCO}_3$ ) in anaerobic aquatic environments. *Applied Geochemistry* 17, pp 503-511
- Johannesson, K.H., Lyons, W.B., Graham, E.Y., Welch, K.A. (2000), Oxyanion Concentrations in Eastern Sierra Nevada Rivers – 3. Boron, Molybdenum, Vanadium, and Tungsten. *Aquatic Geochemistry* 6, pp 19-46
- Kjøller, C., Postma, D., Larsen, F. (2004), Groundwater acidification and the mobilization of trace metals in a sandy aquifer. *Environmental Science and Technology* 38, pp 2829-2835
- KNMI (Royal Dutch Meteorological Institute), 1966-2003, Maandoverzicht van de Neerslag en Verdamping in Nederland (Monthly recharge and Evapotranspiration in the Netherlands), De Bilt, the Netherlands
- Krám, P., Hruška, J., Driscoll, C.T. (1998), Beryllium chemistry in the Lysina catchment, Czech republic. *Water, Air, and Soil Pollution* 105, pp 409-413
- Lakhstano, L.Z., Stipp, S.L.S. (2004), Experimental study of europium (III) coprecipitation with calcite. *Geochimica et Cosmochimica Acta* 68, pp 819-827
- Lyons, W.B., Welch, K.A. (1997), Lithium in waters of a polar desert. *Geochimica et Cosmochimica Acta* 61, pp 4309-4319
- Magaritz, M., Brenner, I.B., Ronen, D. (1990), Ba and Sr distribution at the water-table: implications for monitoring ground-water at nuclear waste repository sites. *Applied Geochemistry* 5, pp 555-562
- Manceau, A., Schlegel, M.L., Musso, M., Sole, V.A., Gauthier, C., Petit, P.E., Trolard, F. (2000), Crystal chemistry of trace elements in natural and synthetic goethite. *Geochimica et Cosmochimica Acta* 64, pp 3643-3661
- Marques, J.J., Schulze, D.G., Curi, N., Mertzman, S.A. (2004), Trace element geochemistry in Brazilian Cerrado soils, *Geoderma*, 121, pp 31-43
- McCarty, D.K., Moore, J.N., Marcus, W.A. (1998), Mineralogy and trace element association in an acid mine drainage from oxide precipitate comparison of selective extractions. *Applied Geochemistry* 13, pp 165-176
- Meinardi, C.R. (1994), Groundwater recharge and travel times in the sandy regions of the Netherlands, RIVM Rep 715501004, PhD thesis, Vrije Universiteit, Amsterdam
- Meinardi, C.R. (2003), Basic values of trace elements in the fresh groundwater of the Netherlands (in Dutch). RIVM report 714801028, 43 p
- Nagasawa, H. (1971), Partitioning of Eu and Sr between coexisting plagioclase and K-feldspar. *Earth and Planetary Science Letters* 13, pp 139-144
- Navrátil, T., Skriván, P., Minářík, L., Žigová, A. (2002), Beryllium geochemistry in the Lesní Potok catchment (Czech Republic), 7 years of systematic study. *Aquatic Geochemistry* 8, pp 121-134
- Nicholson, F.E., Jones, K.C. (1994), Effects of phosphate fertilizers and atmospheric deposition on long-term changes in the cadmium content of soils and crops. *Environmental Science and Technology* 28, pp 2170-2175
- Norra, S., Stüben, D. (2004), Trace element patterns and seasonal variability of dust precipitation in a low polluted city - the example of Karlsruhe/Germany. *Environmental monitoring & Assessment* 93, pp 203-228
- Nozaki, Y. (1997), A Fresh Look at Element Distribution in the North Pacific, EOS electronic supplement, may 1997
- Nriagu, J.O. (1989), A global assessment of natural sources of atmospheric trace metals. *Nature* 338, pp 47-49
- Otsuka, M., Terakado, Y. (2003), Rare earth element abundances in high phosphorus and low iron groundwaters from the Nishinomiya district, Japan: Variations in Ce anomaly, redox state and heavy rare earth enrichment. *Geochemical Journal* 37, pp 1 – 19
- Padilla, K.L., Anderson, K.A. (2002), Trace element concentration in tree-rings biomonitoring centuries of environmental change. *Chemosphere* 49, pp 575-585
- Probst, A., El Gh'mari, Aubert, D., Fritz, B., McNutt, R. (2000), Strontium as a tracer of weathering processes in a silicate catchment polluted by acid atmospheric inputs, Strengbach, France. *Chemical Geology* 170, pp 203-219
- Pauwels, H., Zuddas, P., Michard, G. (1989), Behavior of trace elements during feldspar dissolution in near/equilibrium conditions: Preliminary investigation. *Chemical Geology* 78, pp 255-267



- Rimstidt, J.D., Balog, A., Webb, J. (1998), Distribution of trace elements between carbonate minerals and aqueous solutions. *Geochimica et Cosmochimica Acta* 62, pp 1851-1863
- RIVM (1994-2000), Landelijk meetnet regenwatersamenstelling, Meetresultaten (National Rainwater Monitoring Network), RIVM 723101027
- Saunders, J.A., Swann, C.T. (1992), Nature and origin of authigenic rhodochrosite and siderite from the Paleozoic aquifer, northeast Mississippi, U.S.A. *Applied Geochemistry* 7, pp 375-387
- Schokker J. 2003. Patterns and processes in a Pleistocene fluvio-aeolian environment, Roer Valley Graben, south-eastern Netherlands. *Nederlandse Geografische Studies* 314: 142 p
- Shiller, A.M., Frilot, D.M. (1996), The geochemistry of gallium relative to aluminum in Californian streams. *Geochimica et Cosmochimica Acta* 60, pp 1323-1328
- Smedley, P.L., Kinniburgh, D.G. (2002), A review of the source, behaviour and distribution of arsenic in natural waters. *Applied Geochemistry* 17, pp 517-568
- Smedley, P.L., Edmunds, W.M. (2002), Redox patterns and Trace-element behavior in the East Midlands Triassic Sandstone Aquifer, U.K. *Ground Water* 40, pp 44-58
- Stuyfzand, P.J. (1984), Groundwater quality evolution in the upper aquifer of the coastal dune area of the western Netherlands. IAHS Publication 150
- Stuyfzand, P.J. (1989), Factors controlling trace element levels in groundwater in the Netherlands. In: Miles (Ed), *Water Rock Interaction WRI-6*, Balkema Rotterdam, pp 655-659
- Stuyfzand, P.J. (1991), Nonpoint sources of trace elements in potable groundwaters in the Netherlands. *Water Supply* 9, pp SS10-11 - SS10-15
- Stuyfzand, P.J. (1993), Behaviour of major and trace constituents in fresh and salt intrusion waters, in the western Netherlands. In: *Study and modeling of saltwater intrusion into aquifers*, Proceedings 12<sup>th</sup> Saltwater Intrusion Meeting, Barcelona
- Tessier, A., Fortin, D., Belzile, N., DeVitre, R.R., Leppard, G.G. (1996), Metal sorption to diagenetic iron and manganese oxyhydroxides and associated organic matter: Narrowing the gap between field and laboratory measurements. *Geochimica et Cosmochimica Acta* 60, pp 387-404
- Van Baren, F.A. (1934), *Het voorkomen van kali-houdende mineralen in de Nederlandse gronden*. PhD-thesis, Agricultural University Wageningen 120
- Van Beek, C.G.E.M., Hettinga, F.A.M., Straatman, R. (1989), Release of heavy metals in groundwater due to manure spreading. In: Miles (Ed), *Water Rock Interaction WRI-6*, Balkema Rotterdam, pp 703-706
- Van der Veer, G. (2006), (in prep), Trace element contribution of various mineral phases in Late Pleistocene (fluvio-)eolian sediments in the Netherlands.
- Van Uden, J.G., Vissers, M.J.M. (1998), *A hydrochemical study in Salland* (in Dutch), M.Sc. thesis, Utrecht University, Department of Geochemistry, Utrecht
- Verweij, W. (2005), CHEAQS P2005.1
- Vissers, M.J.M., Frapporti, G., Hoogendoorn, J.H., Vriend, S.P. (1999), The dynamics of groundwater chemistry in unconsolidated aquifers: The Salland section. *Phys. Chem. Earth (B)* 24, pp 529-534
- Wajon, J.E., Ho, G-E., Murphy, P.J. (1985), Rate of precipitation of ferrous iron and formation of mixed iron-calcium carbonates by naturally occurring carbonate minerals. *Water Research* 19, pp 831-837
- Welch, A.H., Westjon, D.B., Helsel, D.R., Wanty, R.B. (2000), Arsenic in groundwater of the United States: occurrence and geochemistry. *Ground Water* 38, pp 589-604
- Wersin, P., Charlet, L., Karthein, R., Stumm, W. (1989), From adsorption to precipitation: Sorption of  $Mn^{2+}$  on  $FeCO_3(s)$ . *Geochimica et Cosmochimica Acta* 53, pp 2787-2796
- Zachara, J.M., Fredrickson, J.K., Smith, S.C., Gassmann, P.L. (2001), Solubilization of Fe(III) oxide-bound trace metals by a dissimilatory Fe(III) reducing bacterium. *Geochimica et Cosmochimica Acta* 62, pp 75-93
- Zachara, J.M., Smith, S.C., Liu, C., McKinley, J.P., Serne, R.J., Gassman, P.L. (2002), Sorption of  $Cs^+$  to micaceous subsurface sediments from the Hanford site, USA. *Geochimica et Cosmochimica Acta* 66, pp 193-211



# 6 SYNTHESIS

## 6.1 INTRODUCTION

In this thesis the spatio-temporal distribution of groundwater composition in sandy unconfined aquifers, and the changes therein, were analyzed from the viewpoint of the three principle determinative factors. The three factors, which were introduced in *chapter 1*, are (1) Flow, which determines where and when groundwater of a certain composition will be found, (2) Input, which determines the composition of the infiltrated water, and (3) Geochemical processes, which determine post-infiltration alteration of the chemical composition.

Given these factors, the assessment of groundwater quality evidently required a multidisciplinary approach, combining among others hydrological, geochemical, mineralogical, agricultural, atmospheric, and geographical information. An effective description of the spatio-temporal distribution of groundwater quality was shown to require a proper understanding of the factors and processes, of the spatial and temporal scales at which they operate, and of the uncertainty involved.

The successive studies presented in this thesis were directed by the following research questions:

- What is the spatio-temporal distribution of groundwater quality in phreatic aquifers and how can it best be characterized in terms of groundwater flow, input, geochemical processes, and their interaction?
- What is the influence and impact of the recent environmental changes in these three factors?
- What are the opportunities for using this information to better predict the future distribution of groundwater quality in phreatic aquifers?

In this synthesis, the main findings will be summarized and discussed following the framework given above. First, the answers to research questions 1 and 2 are addressed along the three-factor framework in section 6.2 (spatial aspects) and 6.3 (temporal aspects). Section 6.4 discusses some opportunities for improved prediction and management, and for an improved collection and use of information (question 3).

## 6.2 THE SPATIAL DISTRIBUTION OF GROUNDWATER QUALITY

### 6.2.1 Flow

The role of flow in the spatiotemporal distribution of groundwater quality was explored along the two perspectives as put forth by Falkenmark and Allard (1991). The first perspective questions how the observed water quality in streams, discharge areas, and wells can spatially be related to recharge areas in terms of land-use history. The second perspective questions where and when pollution problems can be expected in terms of future and past pathways of point-source pollution. A set of comprehensible maps was presented (*chapter 2*) that conclusively answers the two complementary questions for

relating groundwater flow to groundwater quality. This core set includes transit time, transit distance, and travel distance maps at specified depths, on which the groundwater flow systems as delineated are superimposed. The maps were derived using high-resolution hydrological modelling with particle-tracking analysis of the resulting flow pattern. Furthermore, the definition of groundwater flow systems (Tóth, 1963) was extended towards three dimensions to enable the delineation of the groundwater flow systems (*chapter 2*).

The main properties of a hydrological system that determine the spatiotemporal distribution of groundwater quality are its age-depth relation (which depends on recharge, porosity, and aquifer thickness) and the groundwater flow system configuration. Whereas the age depth relation was shown to be relatively invariable throughout phreatic aquifers (*chapter 3*), the modelled groundwater flow system configuration was found to be very complex, due to the likewise complexity of topography and drainage. The often-used conceptual representation of the basic groundwater flow system (*chapter 1*) appears to be an oversimplification as compared to the modelled flow pattern. Groundwater flow is mostly at an angle to the overall gradient, as it follows the generally larger transversal gradients towards active parts of streams that flow in the direction of the overall gradient. Such topography, which evolved through the evolution of the stream network, characterizes most sandy areas (De Vries, 1977). The resulting calculated average groundwater flow systems size in the study areas, in the order of a few square kilometres, is very small compared to the Dutch land surface that measures approximately 36,000 km<sup>2</sup>. The groundwater flow system configuration is further complicated due to human interventions, such as artificial drainage networks, groundwater abstractions, and land use change (*chapter 2*).

The stability of groundwater flow systems was assessed through a sensitivity analysis that applied the groundwater flow system theory in three dimensions (*chapter 2*) and used automation of the systems analysis (*chapter 3*). From these analyses, it was shown that the uncertainty in the modelled groundwater flow pattern is mainly determined by the managed drainage levels and the temporal variation in recharge, leading to activation or inactivation of parts of the drainage pattern. Intrinsic (invariable) aquifer parameters, such as anisotropy and drainage resistance, were shown to be of less influence for the configuration. Patterns and uncertainties were shown to be highly variable throughout the areas studied, meaning in certain areas flow direction is more uncertain than in other areas. Within groundwater flow systems, flow directions are highly certain and invariable near discharge areas, whereas near groundwater flow system boundaries flow directions are highly uncertain and variable (*chapter 3*).

### **6.2.2 Input**

The input water composition is controlled by the composition of recharging water (e.g. rain including dry deposition, or surface water), evapotranspiration, added substances (e.g. manure, fertilizers, road salt, organic contaminants), and processes in the unsaturated zone (e.g. buffering and plant uptake). From the collected hydrochemical data it was shown that agricultural landuse and atmospheric deposition directly enhances major constituent concentrations such as NO<sub>3</sub>, PO<sub>4</sub>, K, Mg, Na, Cl, SO<sub>4</sub>, and Ca, but also trace element concentrations (Cu, Pb, and possibly B, Rb, Sb, Tl primarily from manure;

others from atmospheric deposition; *chapter 5*). Some trace elements, however, are not so much added to the groundwater system, but indirectly mobilized (see below).

When spatial differences in input water quality are combined with a groundwater flow pattern, distinct hydrochemical streamtubes are expected to emerge (*chapter 4*). Such streamtubes were identified from detailed sampling of a multilevel well section in the Salland area in the eastern part of the Netherlands. Their patterns were explained by combining hydrological modelling and geographical analysis (*chapters 3 and 4*). Groundwater quality boundaries are also found at the boundaries between local and regional groundwater flow systems, due to the difference in recharge area and age, hence input (*chapter 4*).

### 6.2.3 Geochemical processes

For geochemical processes the sediment is of main importance as it acts as a buffer, due to its acid neutralizing capacity, and oxidation, reduction, and sorption capacity. This buffer capacity is consumed depending on the quantity of acid, reductant, oxidant, or pollutant in the groundwater. In this way the rate of the geochemical processes is related to input and their location also to groundwater flow (*chapter 4*). Calcite buffering and redox boundaries were used in the description of the spatiotemporal distribution of major element groundwater composition (*chapter 4*).

Calcite minerals buffer infiltrating water to near-neutral pH, whereby Ba and Sr are codissolved with Ca, and mobilization of Ni and Co at this boundary can be observed (*chapter 5*). In zones where calcite is leached out, buffering by clay and alkali-feldspar minerals results in anomalous concentrations of a large set of trace elements associated with Al and base cations. These included enrichments for Ni, Co, Zn, and Be, Cd, Tl, Ga, and REY (*chapter 5*). The major type of source-mineral; feldspar or clay, could be identified based on a comparison with ratios observed in the Dutch subsoil (*chapter 5*).

Redox reactions not only affect  $\text{NO}_3$ , Fe,  $\text{SO}_4$ , and  $\text{HCO}_3$  concentrations (*chapter 4*), but also many trace element concentrations. Arsenic is codissolved from Fe hydroxides; Mn is controlled by coprecipitation with Fe in reduced siderite saturated water; mobilization of Ni and Co occurs at the iron reduction boundary. Sedimentary sources were identified for Mo, U, Mn, and possibly Sb, but their mobilization could not be attributed to codissolution with a major element. The concentrations of these elements are separately controlled by redox conditions (*chapter 5*).

Source-term limitation from surfacial input in combination with sorption processes affects the observed concentrations and mobility of many elements. Most major elements behave seemingly conservative, but Mg and K, both minor elements in pristine groundwater, are controlled by cation exchange when affected by pollution (*chapter 4, 5*). Such sorptive control also explains observed concentrations for many trace elements (*chapter 5*). Upon disturbance of the steady state (changes in flow, input, or geochemical changes, see below), the exchange complex, which has been loaded under the natural conditions, starts acting as the control. The major type of exchange was identified as equal valence exchange of Li, Rb, and Cs with Na, and of Co, Cu, Zn, and Cd with Ca, and unequal valence exchange of B and Ni with Na. For Cu, an exception was observed in pristine, unbuffered waters, where it is controlled by exchange with Na (*chapter 5*). The

type of exchange and the major electrolyte shift together determine the resulting trace element concentration.

Another control identified was mineral saturation, which in many cases explains Al, P, Ca, Mn, Fe, Ba, and U concentrations. These elements are commonly controlled by saturation phases and in most cases have a sedimentary source. Enhanced concentrations of Co, Ni, and Zn were related to the specific environment of acid, reduced waters; the slow release of Li, Rb, and Cs was found to be ubiquitous.

### 6.3 THE TEMPORAL DISTRIBUTION OF GROUNDWATER QUALITY

The conceptual framework presented in *chapter 4*, facilitated not only the detection of changes in the groundwater quality, but also the three types of changes could be identified from the hydrogeochemical data obtained from the multilevel well section over a period of 13 years.

The first type of change, due to a change in the groundwater flow pattern, was expected based on hydrological calculations (*chapter 3*), and was identified through hydrochemical analysis (*chapter 4*). Climatic variability and human interventions were the most probable causes. Especially the construction of the artificial drainage network in the early 20<sup>th</sup> century has led to significant changes in the configuration of groundwater flow systems (*chapter 3*). Since then, groundwater flow can be considered relatively stable due to its intimate relation with topography and the drainage network.

Type 2 changes, changes due to a change in input water quality, are the most common type. They include changes in rainwater quality as well as changes in land use that generally result in input water with increased oxidation capacity and mineral and acid loads. The most important changes detected are those related to the cultivation in the early 20<sup>th</sup> century, the introduction of maize in the 1970s leading to highly polluted groundwater, and the decrease in sulphate emissions since the 1990s (*chapter 4*).

Type 3 changes, geochemical changes, are slow compared to groundwater flow rates and can be linked to changed sedimentary characteristics. Observed changes are in most cases related to changes in reduction capacity due to the continuous infiltration of nitrate (*chapter 4*). In the Salland section no changes in the calcite-buffering front are observed in the 15 years of monitoring at the meter-scale. Potassium breakthrough was observed in few miniscreens, while for trace elements, for which a very large retention is expected, no changes were observed in the 7 years of trace element monitoring.

## 6.4 DISCUSSION

### 6.4.1 Modelling and verification of groundwater flow patterns

To accurately describe flow, some scale aspects of the aquifer need specific attention as compared to more conventional modelling aimed at predicting groundwater levels (*chapter 2 and 3*). In topography driven groundwater flow systems anisotropy and topographical wavelength (Zijl, 1999) determine the configuration and penetration depth

of groundwater flow systems. The ‘wavelength’ in a relatively flat topography equals stream distance. The drainage pattern thus largely determines the groundwater flow pattern, as in sandy areas anisotropy is relatively constant. Streams and ditches should explicitly be incorporated in groundwater flow models (*Chapter 2 and 3*).

As diffuse drainage is related to surface level, model discretization should accurately describe topography as well. In areas of low relief decimetre scale differences determine groundwater flow (*chapter 2 and 3*). Large model cell sizes may lead to overgeneralization of the topography (Bryan et al. 2003, *chapter 2*) and in fact determine the minimum wavelength that can be considered (Zijl, 1992), which is twice the cell length. Furthermore, to accurately track groundwater flow, enough cells should represent features of flow convergence and high flow velocities (Haitjema, 2001, Zheng, 1994). This means regional modelling for the purpose of accurately predicting groundwater flow is becoming feasible just now with advances in computer power. For the areas studied in this thesis a model cell-size of 50 m was needed, which is substantially smaller than generally used in previous regional groundwater studies.

The resulting flow paths lengths are therefore much shorter than observed in earlier studies. Furthermore, local flow systems in most cases reach the full depth of the aquifer. More importantly, groundwater flow directions are highly variable, even at the km scale. Validation of such fine-scaled flow patterns is not yet done through hydrological observations, but the expected short flow path length explains the observed hydrochemical patterns (*chapter 4*). For hydrology, very detailed networks would be necessary to verify flow even in a single groundwater flow system. The need for such a detailed network has implications for the conclusions that can be drawn from existing, larger-scaled hydrological networks, as interpolation of head measurements does not describe the actual situation: only the general flow direction that follows the regional gradient will be obtained. Detailed studies, using topographical analysis, hydrological and hydrogeochemical information, of single groundwater flow systems could be used to verify the horizontal extents of groundwater flow systems.

This study therefore not only demonstrates that the modelling of groundwater flow aids in the interpretation and understanding of the spatio-temporal distribution of groundwater quality, but also that groundwater quality data may aid in validating groundwater flow models.

#### **6.4.2 Characterization of groundwater quality patterns**

The management and prediction of groundwater quality nowadays mainly focuses on input as determining factor, and geochemical processes receive much interest as sanitation strategy (*chapter 1*). This thesis shows that flow is very important as well. Both flow and geochemical processes show dynamic behaviour, and thus cannot always be taken as constants. Furthermore, for agricultural contaminants such as nitrate (*chapter 4*) and for many trace elements (*chapter 5*), sediment composition and reactivity are crucial for the observed patterns, and should be taken into account.

In fact, aquifer reactivity and buffer capacity is the missing link for an adequate prediction of the future groundwater quality, for oxidizing, reducing, as well as adsorbing contaminants. Though some studies account for this, they are sparsely founded by data. For the movement of nitrate reduction front this study is among the first to monitor its

progress (*chapter 4*) in semi-natural conditions. For the Salland area, the time span (13 years) and spatial resolution (1-2 m) of the well section monitoring were sufficient to detect such major element changes. For trace elements changes occur much slower (*chapter 5*) and even smaller spatial resolution may be necessary (see also Kjøller et al. 2004).

Information on groundwater flow was also shown to be important when interpreting observations at the point scale and for groundwater quality patterns in general. Taking into account the position in the groundwater flow system and land use at the point of infiltration was shown to improve the characterization of groundwater quality patterns for both trace and major elements (*chapter 4*, Vissers et al. (2004), Schipper and Vissers, 2003).

The small-scale groundwater flow pattern is of special relevance to point-source pollution; an important observation is that pollutants are 'captured' in groundwater flow systems. This 'natural hydrological isolation' can, besides removal and in situ remediation, be used in risk assessment, urban water management, and passive remediation techniques. The techniques presented for groundwater flow systems analysis open new perspectives with respect to the use of groundwater flow and quality in spatial planning. Information on the characteristics (a.o. transit time/distance) and the spatial pattern of groundwater flow systems (*chapter 2*) and their uncertainties (*chapter 3*) can for example improve stream restoration and wetland conservation, because the relevant recharge areas and age distribution of the discharging water can now be adequately assessed.

### **6.4.3 Groundwater sampling and monitoring**

As mentioned earlier in this discussion, the detailed monitoring in Salland proved to be very helpful in the characterization of groundwater quality patterns. This suitability firstly originates from the large number of samples and because biases in sampling and analysis (sampling and analysis equipment and techniques) are consistent within the data set. Secondly, within one miniscreen well the samples are spatio-temporally correlated. This means that already one sampling round represents an analytically consistent statistical sample that is a 2-D time - land use cross section of the 4-D groundwater quality pattern, as compared to the 1D temporal evolution that can be observed after long term monitoring of an isolated screen.

As such this type of sampling design appeared adequate in reducing underdetermination by decreasing the degrees of freedom for the description and explanation of processes, allowing for a detailed process-based interpretation of groundwater quality patterns (*chapter 4 and 5*).

Because the samples are spatially correlated, the types of changes could be identified (*chapter 4*). Furthermore, the progress of the nitrate reduction boundary was monitored (*chapter 4*), and reaction kinetics for incongruent release of trace elements were obtained (*chapter 5*). Reaction kinetics of iron and nitrate reduction, and breakthrough of contaminants might be determined as well from the available Salland data.

Whereas the Salland well section was initially placed with specific research objectives in mind, current findings also prove that this type of monitoring approach is



more helpful in reaching the monitoring goals as generally put forth for both management and policy purposes (Van Duijvenbooden et al. 1985).

## 6.5 REFERENCES

- Bryan, B.A. (2003), Physical environmental modeling, visualization and query for supporting landscape planning decisions. *Landscape and Urban Planning* 65, pp 237-259
- De Vries, J.J. (1977), The stream network in the Netherlands as a groundwater discharge phenomenon. *Netherlands Journal of geosciences* 56, pp 103-122
- Falkenmark, M., Allard, B. (1991), Water quality genesis and disturbances of natural freshwaters, In: Hutzinger, O. (ed), *The handbook of environmental chemistry* 5, part A: Water pollution. Springer-Verlag, Heidelberg-Berlin, pp 45-78
- Haitjema, H., Kelson, V., De Lange, W. (2001), Selecting MODFLOW cell sizes for accurate flow fields. *Ground Water* 39, pp 931-938
- Kjøller, C., Postma, D., Larsen, F. (2004), Groundwater acidification and the mobilization of trace metals in a sandy aquifer. *Environmental Science and Technology* 38, pp 2829-2835
- Portniaguine, O., Solomon, D.K. (1998), Parameter estimation using groundwater age and head data, Cape Cod, Massachusetts. *Water Resources Research* 34, pp 637-645
- Schipper, P.N.M., Vissers, M.J.M. (2003), Ground water quality maps of Hengelo (In Dutch), SKB project report, SV-60, SKB Gouda
- Tóth, J. (1963), A theoretical analysis of ground water flow in small drainage basins. *Journal of Geophysical Research* 68, pp 4795-4812
- Van Duijvenbooden, W., Taat, J., Gast, L.F.L. (1985), Landelijk meetnet grondwaterkwaliteit: eindrapport van de inrichtingsfase (The national groundwater quality monitoring network: final report of the installation), RIVM Report 728820001, Bilthoven
- Vissers, M.J.M., Schipper, P.N., Van Gaans, P.F.M. (2004), Stromingen in grondwaterkwaliteitskaarten. *Stromingen* 10, pp 5-16
- Zheng, C. (1994), Analysis of particle tracking errors associated with spatial discretization. *Ground Water* 32, pp 821-828
- Zijl, W. (1999), Scale aspects of ground water flow and transport systems. *Hydrogeology Journal* 7, pp 139-150
- Zijl, W. (1993), Schaalanalyse met behulp van fourier-analyse: Toepassing op grondwaterstroming ten gevolge van ruimtelijke variaties in de grondwaterspiegel en putonttrekkingen (in English), In: CHO Commissie voor Hydrologisch onderzoek TNO, *Schaalproblemen in de hydrologie, Rapporten en Nota's* 31, pp 51-76



## SUMMARY

In exploring groundwater quality patterns in sandy phreatic aquifers this thesis follows three fundamental tracks, which are of a methodological, of a conceptual, and of a process based kind. First, in chapter 1 the three principle factors that together determine the groundwater quality distribution, which are flow, input, and geochemical processes, are introduced. Also the two perspectives of relating groundwater flow to groundwater quality are presented. The first perspective is in terms of future and past pathways of point source pollution, the second is of a spatiotemporal type, where the water quality in streams, wells, or wetlands is related to the historical landuse within their recharge areas. These concepts form the framework for the following chapters.

In chapter 2 groundwater flow is mapped in terms of the two mentioned perspectives. I show that some powerful 3D aspects of groundwater flow models are underexplored, and that this is due to (1) the lack of adequate visualization methods, and (2) the incompleteness of existing definitions of groundwater flow systems. Both problems are resolved by formalizing groundwater flow systems analysis in three dimensions and by the development of new mapping techniques. This is illustrated for the Hengelo area. Some implications are elaborated upon, both in terms of groundwater flow system and model scale as well as from a conceptual and spatial planning viewpoint.

However, such maps are of limited practical value when the uncertainty of groundwater flow is unknown. In chapter 3 it is shown that existing techniques for estimating uncertainty mainly focus on groundwater levels, whereas in relating groundwater quality to groundwater flow other characteristics of groundwater flow are important. A methodology was developed that assesses the uncertainty in groundwater flow system configuration, and is illustrated for the Salland area. The resulting maps of uncertainty due to anisotropy, drainage resistance, recharge, and drainage level are discussed.

In chapter 4 the often used age-depth relation, as presented in chapter 1, is extended towards an exhaustive framework for groundwater quality patterns. The concept of hydrogeochemical streamtubes is introduced, by which water quality boundaries and changes in their location, as observed in the Salland multilevel well section, are related to flow, input, and processes. Observed patterns are shown to be better explained in this way, especially as the framework presented takes into account groundwater flow system size, position within the groundwater flow system, land use, and land use scale.

In chapter 5 both the sources and controls of trace and major elements are explained using a sequential approach that addresses all known important controls and sources for all trace elements of adequate analytical quality. Advances were made by following two new approaches. First bulk geochemical soil data is used to better explain observed concentrations in terms of codissolution and coprecipitation, and secondly the SEQSSI-approach (sorption equilibrium through steady state input), which explains the behaviour and concentrations of a large set of trace elements is presented.

The thesis concludes with a synthesis in which practical spin-off, in terms of background values, modelling, spatial planning, and monitoring, are further elaborated upon.



# PATRONEN VAN GRONDWATERKWALITEIT IN ZANDIGE AQUIFERS ONDER MILIEUDRUK

## SAMENVATTING

### **Inleiding**

Doel van dit proefschrift is het verkrijgen van beter inzicht in ruimtelijke patronen van grondwaterkwaliteit in zandige aquifers in bevolkte gebieden. Kennis van grondwaterkwaliteit, en van de ruimtelijke patronen hierin, is van groot belang om duurzaam te kunnen omgaan met grondwater. Dit geldt vooral in gebieden met intensief gebruik van de bodem, en met freatische aquifers, d.w.z. watervoerende lagen die direct gevoed worden vanaf het aardoppervlak

In dit proefschrift is de focus op de hydrogeochemie en wordt de grondwaterkwaliteit gedefinieerd als de chemische samenstelling van grondwater. De drie factoren stroming, kwaliteit van het voedende water (input), en geochemische processen vormen het raamwerk voor de bestudering van grondwaterkwaliteitspatronen in dit onderzoek van waaruit ook de onderzoeksvragen zijn geformuleerd:

1. Wat is de ruimtelijke distributie van grondwaterkwaliteit in zandige aquifers, en hoe kan deze het best worden beschreven in de drie termen.
2. Wat is de invloed van recente veranderingen in het milieu op deze ruimtelijke distributie?
3. Wat zijn de mogelijkheden van het gebruik van dergelijke informatie om de toekomstige veranderingen beter te kunnen voorspellen?

Er zijn twee gebieden gekozen om de onderzoeksvragen te beantwoorden; het stedelijk gebied rond Hengelo/ Enschede, en het rurale gebied ten westen van de Sallandse heuvelrug.

### **Stroming van grondwater in relatie tot grondwaterkwaliteitspatronen**

De ondergrondse stroming van grondwater vormt de ruimtelijke schakel tussen de condities en activiteiten aan het aardoppervlak en het onder de grond aanwezige patroon in grondwaterkwaliteit. Wanneer de stroming bekend is, kunnen op de eerste plaats de intrekgebieden worden bepaald van bijvoorbeeld drinkwateronttrekkingen, beken, en natte natuur. De waterkwaliteit in deze objecten kan dan worden beschouwd in het licht van de historische kwaliteit van het in de intrekgebieden infiltrerende water. Op de tweede plaats kunnen de herkomst en de toekomstige verspreiding van puntverontreinigingen worden bepaald. Dit zijn de twee complementaire benaderingen om stroming aan kwaliteit te koppelen (hoofdstuk 1).

In hoofdstuk 2 en 3 van dit proefschrift is grondwater op deze wijze gezien, en is de 3D-kartering ervan uitgewerkt via een beknopte set kaarten die het mogelijk maakt om

waterkwaliteitsvragen vanuit beide benaderingen te beantwoorden. Deze kaarten zijn gebaseerd op een hydrologisch model, daarbij gebruik makend van particle tracking. In hoofdstuk 2 wordt voor de regio rondom Hengelo de volgende set kaarten gepresenteerd:

- Kwel/infiltratie kaart met isohypsen
- Grondwatersystemen met verblijfafstand en stroomlijnen
- Grondwatersystemen met verblijftijd
- Grondwatersystemen met reisafstand op verschillende diepten
- Grondwatersystemen met kwantitatieve aquifer gevoeligheid

Met deze kaarten kan direct worden afgelezen wat de 10 en 25 jaarszone van onttrekkingen, beken, en natte natuurgebieden is, alsmede de verblijftijdcurve, en het (historische) landgebruik. Op deze manier kan een voorspelling worden gedaan van de waterkwaliteit, en van de gevolgen van beleidsmaatregelen en/of landgebruiksveranderingen. Ook kan van puntverontreinigingen direct de herkomst en het 'bedreigd object' worden afgelezen.

In hoofdstuk 3 is een vergelijkbare aanpak gevolgd voor het rurale Salland, waarbij de aandacht vooral was gevestigd op het kwantificeren en karteren van de onzekerheid in grondwaterstromingspatronen. Informatie over dergelijke onzekerheden is bijvoorbeeld nodig om de herkomst van verontreinigingen met meer zekerheid te kunnen achterhalen, of om een betere schatting te kunnen maken van een intrekgebied van een put of natuurgebied: het beantwoordt de twee 'waterkwaliteitsvragen' dus nog beter, en maakt het mogelijk de gevoeligheid en plausibiliteit van verschillende modelconcepten en aannames te testen. Waar de meeste klassieke studies hun aandacht vooral vestigen op intrinsieke parameters van de aquifer, zoals anisotropie, drainageweerstand, doorlaatbaarheid en heterogeniteit, heb ik hier gekozen om de onzekerheid ook te definiëren in termen van condities die daadwerkelijk variëren en daarmee relevant zijn voor de stabiliteit van stromingspatronen en grondwaterkwaliteitspatronen: voeding door neerslag en peilbeheer in de beken. De stromingspatronen in gebieden zoals Salland worden sterk bepaald door het kleinschalige drainagesysteem en zijn daardoor dermate stabiel, dat voor het grootste deel van het gebied met zekerheid is vast te stellen waar het water naar toe stroomt.

### **Kwaliteit van het voedende water**

In hoofdstuk 4 zijn hydrogeochemische patronen in de Salland aquifer onderzocht in termen van stroming, input, en processen. Gebruik makend van zowel geohydrologische als hydrochemische informatie van een minifilterputten raai is een conceptueel raamwerk ontwikkeld gebaseerd op het 'stroombuis' (streamtube) principe. Hydrologische, geochemische, en inputgrenzen zijn onderscheiden, om de patronen te beschrijven en veranderingen hierin te verklaren. Vervolgens zijn deze patronen beschouwd in termen van de positie binnen en de grootte van het grondwaterstromingssysteem, alsmede het landgebruik en de schaal en variabiliteit daarin. De geobserveerde patronen kunnen op deze manier beter verklaard worden dan wanneer enkel de leeftijd-diepte relatie in beschouwing wordt genomen.

## **Geochemische processen**

Hoofdstuk 5 benadert de grondwaterkwaliteit vanuit de geochemische processen, en spitst zich toe op de concentraties sporenelementen. Via een sequentiële aanpak zijn zowel de bronnen als de sturende processen voor een grote groep sporenelementen achterhaald. Allereerst zijn verzadigingen van sporenmineralen berekend, omdat deze de concentraties van metalen kunnen bepalen. Vervolgens is bekeken waar codissolutie en coprecipitatie een rol kunnen spelen door vergelijking met sporenelementgehalten in mineralen, die zijn afgeleid uit bulkgeochemische data van de Nederlandse bodem. Ten derde is bekeken of ‘sorptie-evenwicht door steady-state input’ een rol kan spelen als bron en als sturend proces voor sporenelement concentraties. De belangrijkste conclusie hier is dat de initiële bron van de meeste sporenelementen atmosferische depositie is, en dat onder de invloed van vervuiling het sorptiecomplex voor dergelijke elementen de gehalten aan het grondwater oplegt.

## **Conclusies**

De synthese in hoofdstuk 6 bespreekt de implicaties van de resultaten van deze studie voor een adequate aanpak van de weergave, voorspelling, en monitoring van waterkwaliteitspatronen.

Samenvattend toont dit proefschrift aan dat de hier gepresenteerde, nieuwe manier van karteren van grondwaterstroming, alsmede de hier verbeterde 3D-definitie van grondwaterstromingssystemen, direct inzicht geven in grondwaterkwaliteitspatronen. Dit wordt onderbouwd door actuele waarneming van grondwaterkwaliteitspatronen met behulp van gedetailleerd bemonsteren, en door het karteren en kwantificeren van de onzekerheid in de gemodelleerde grondwaterstroming. De hierbij verkregen inzichten kunnen worden toegepast in ruimtelijke ordening en systeemgericht water(kwaliteits)-beheer. Tot slot is nieuwe kennis op het gebied van sporenelementengedrag ontwikkeld die toepassing kan vinden in het afleiden van achtergrondwaarden, risicobeoordeling, en een beter begrip van diffuse verontreiniging.





## CURRICULUM VITAE

Marc Vissers werd op 27 augustus 1974 geboren te Veghel en groeide op in Uden, op een steenworp afstand van de peelrandbreuk. Na een sprongetje van 4 havo naar 5 vwo slaagde hij in 1992 voor het eindexamen aan het Comenius College te Uden. Vanuit zijn interesse voor tienkampen, het heelal, en het klimaat, en door het hebben van een leuke scheikundeleraar was de studie Geochemie in Utrecht een logische stap. Hij koos voor een afstudeeronderzoek in Salland, omdat de vraagstelling 'iedereen zegt dat er toch niks is veranderd: ga er maar eens kijken' hem zeer aansprak. Dit onderzoek vormde het begin van een nieuwe, langdurige hobby: grondwater. In mei 1998 slaagde hij voor zijn doctoraalexamen, en vervolgens bracht deze hobby hem in het Franse Centraal Massief, in Egypte, bovenop Utrecht CS, en tot slot in Geldermalsen. Vanaf februari 2001 werkte hij als AIO bij de Faculteit Geowetenschappen, Universiteit Utrecht. Maatschappelijke en wetenschappelijke relevantie, bloemenpatronen en scatterplots vormden in deze periode een leidraad.



## DANKWOORD

In dit wellicht door het grootste aantal mensen gelezen stukje proefschrift wil ik een aantal mensen op papier bedanken, en wel in ondefinieerbare volgorde. Als eerste Peter Burrough, voor het mede mogelijk maken van de breedtestrategie en dit project daarbinnen. Paulien van Gaans, voor je professionele en kritische houding, schrijftalent en doorzettingsvermogen. Marcel van der Perk, voor je kritische blik en luisterend oor. Peter Schipper, voor je enthousiasme, je brede blik, en je voorbeeld daarin. Grishja van der Veer, voor je gegevens, samenwerking, discussies, en ideeën. Simon Vriend, Gerard Klaver, Bertil van Os, voor een consistente dataset en het goede contact: mijn eeuwige dank daarvoor. Guiseppe Frapporti als inspirerende voorganger. Joseph Tóth voor het inspirerende gesprek en de ‘short course’ in Mexico. Matthias, Ruth, Mienke, en vele anderen die de congressen zo leuk en aangenaam hebben gemaakt. Ook bedank ik de gemeente Hengelo, Waterschap Regge en Dinkel, de Provincie Overijssel, SKB, en Grontmij, voor de prettige samenwerking en gegevens, Ronald Dubbeldam voor de hulp bij het modelleren, Tebodin en Dolf van der Voort voor een Hengelo-model, het Waterschap Groot Salland, Rijkswaterstaat, en het RIVM voor data, TNO voor de REGIS en DINO data, en Maarten Zeylmans, de mensen van het TNO Lab en FG lab, en ondersteunende diensten.

Breedtestrategen Martin, Paul, Roland, Nicky, Ivo, Anet, Michel, Guido, Cor, collegae Derek Karssenberg, Wiebe Borren, Marc Bierkens, Maarten, Pim, Suzanne, Hans, Raymond, Menno, Reinder, en zeker Daniel Mourad en Hanneke Schuurmans, mijn kamergenoten en trouwste lotgenoten: allen bedankt voor de zonnige sfeer in de kamers van de Zonneveldvleugel en op de 4<sup>e</sup>.

Hester de Boer, Gerard Vissers, José Vissers, Iris van der Cingel, Ivo Thonon, Milan Philipp, Grishja van der Veer, Lennert Pronk, Pieter-Jan van Helvoort, en Japke van Es bedank ik voor de hulp in het veld bij de watermonsters: zo wordt het veldwerk korter dan kort, en leuker dan leuk. Gilles Erkens en Marc Gouw voor de prachtboring en tentoongespreide passie. Kim Cohen voor raad en daad, en Freek Busschers voor zijn virtuele boringen.

Pieter-Jan van Helvoort en Job Spijker als mijn illustere voorgangers: voor de inspiratie. Nabije vrienden Lennert, Milan, de Jantjes, Peter, Grishja, Dirk. Zussen Ingrid en Yvonne, Pa, Ma, familie, de van der Cingels, en met name Iris, voor haar liefde en energie gedurende de promotie.

Tot slot ook nog het platform systeemgericht grondwaterbeheer, bodembreed, NAC, ICG, IAHS, SKB, CSM, AGU, IGWMC, TRIAS, EU, de geochemische kring, en de geochimica actie voor de interessante symposia en congressen: de organisatie en alle goede en minder goede sprekers daarin, en ook alle auteurs van alle artikelen waarnaar ik (soms ook ten onrechte niet) heb gerefereerd: op jullie is het proefschrift mede geïnspireerd.

Marc.



**Appendix 2: Groundwater quality (adapted from Vissers et al, 1999), with median concentrations found in different water types in 1996**

Type	# of sampl.	pH	DOC mg/l	NH <sub>4</sub> mg/l	HCO <sub>3</sub> mg/l	Cl mg/l	NO <sub>3</sub> mg/l	SO <sub>4</sub> mg/l	Si mg/l	Na mg/l
Prec	36	5.6	0.6	< 0.02	8	11	6.6	19	20.0	7.5
PrecR	10	6.1	1.3	< 0.02	11	11	0.34	21	23.5	7.7
PrecP	7	4.3	6.4	0.02	8	37	244	59	11.6	19.3
N-Ox	34	7.1	3.0	< 0.02	228	32	74.4	85	12.8	18.5
Red	43	6.9	1.6	0.06	174	15	< 0.17	17	19.8	7.1
RedP	71	7.0	2.7	0.11	221	32	< 0.17	63	17.6	17.2
RedHP	35	7.0	4.6	0.29	278	62	< 0.17	104	15.7	31.5
SR	7	6.5	5.2	1.17	300	17	< 0.17	0.6	24.1	17.9

Type	K mg/l	Ca mg/l	Mg mg/l	Fe mg/l	Mn mg/l	Al mg/l	Ec μS/cm	Type
Prec	0.9	4.9	1.7	< 0.04	< 0.03	< 0.15	90	Prec = Precipitation type
PrecR	0.6	6.5	1.0	1.37	< 0.03	< 0.15	100	PrecR = Precipitation Reduced
PrecP	8.3	54	10.2	< 0.04	0.97	4.27	630	PrecP = Precipitation Polluted
N-Ox	5.4	118	11.2	< 0.04	0.22	< 0.15	800	N-Ox = Nitrate Oxidizing
Red	0.3	58	2.9	3.31	0.15	< 0.15	350	Red = Reduced
RedP	1.0	88	6.5	4.10	0.28	< 0.15	600	RedP = Reduced Polluted
RedHP	3.3	133	10.5	5.27	0.64	< 0.15	910	RedHP = Red. Highly Poll.
SR	1.5	73	6.4	2.44	0.10	< 0.15	550	SR = Sulphate Reduced

**Appendix 3: Tabular presentation of relevant trace element concentrations in chapter 5 (see chapter 5 for references)**

Element	Ocean (N)	Ocean (Z)	Rain (R) Na = 1	Rain (E) Na = 0.71	Rain (V) Na = 0.404	Median GW	Basic Values (B)
Li	181	180	-	0.047	0.05	2.0	0.7
Be	-	0.00021	-	0.0013	-	0.084	0.02
B	4450	4500	-	1.6	0.41	8.2	2
Al	2	0.03	-	10000	4	2.4	10
P	20	62	-	7	-	49	-
V	1.96	2	0.66	0.43	0.26	0.22	-
Mn	0.2	0.02	-	1.7	0.37	260	-
Fe	2	3.4	-	12	0.6	2400	-
Co	0.40	0.03	0.04	0.017	0.0064	0.083	0.15
Ni	1.7	0.48	0.33	0.29	0.09	0.66	0.6
Cu	0.7	0.15	1.45	0.8	0.83	0.4	0.6
Zn	4.9	0.35	10	10	7.4	4.1	2
As	4	1.2	-	0.13	0.12	0.94	0.6
Rb	117	120	-	0.12	0.39	0.58	0.3
Sr	8140	7800	-	0.72	3.1	290	25
Mo	10.31	10	-	0.03	0.05	0.13	0.03
Cd	0.1	0.07	0.1	0.024	0.023	0.005	0.02
Cs	0.4	0.306	-	0.0067	0.007	0.004	0.0015
Ba	20	15	-	0.79	0.55	85	10
U	3.40	3.2	-	0.0018	0.0008	0.013	0.005
La	-	0.0056	-	0.017	0.01	0.017	0.2
Ga*	0.03	0.0012	-	0.0079	0.0024	0.003	0.09
Sb*	0.34	0.2	-	0.06	0.12	0.023	0.01
Tl*	-	0.013	-	0.0059	-	0.012	-
Pb*	0.05	0.0027	3	1.4	0.45	0.18	0.1
Zr*	0.03	0.015	-	0.025	-	0.18	0.02
Hf*	-	0.0034	-	0.001	-	0.003	0.0005

*N = Ocean (Nordstrom, 1978)*

*Z = Ocean (Nozaki, 1997)*

*R = Rain (estimated from RIVM, 1994-2000)*

*E = Rain (Eriksson, 2001)*

*V = Rain (this study)*

*Median groundwater from Salland section*

*B = Basic values (Meinardi, 2003)*

NGS1

NGS2